Electrochemical Society

Houston Meeting Program Issue

GLC ANODES ARE CUSTOM MADE TO MEET VARYING ELECTROLYTIC CELL NEEDS

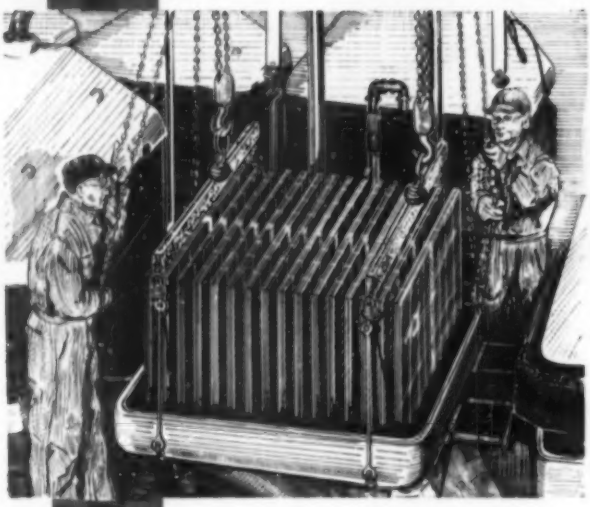

The custom made qualities of GLC Anodes give each cell operator performance characteristics best suited to his particular requirements.

These custom made qualities result from specialized anode production facilities, starting with the raw material mixing chambers and extending through extrusion, baking, graphitizing, oil impregnation and machining.

Equipment, designed exclusively for GLC, controls oil pickup to precise levels, and provides machining of superior accuracy. GLC Anodes are also distinguished for their uniformity of structure.

These factors combine to give GLC Anode customers improved cell operating economies that are a matter of record. May we review this record with you?

PRODUCTS ELECTRODE GLC DIVISION YOU CAN TRUST ®

GREAT LAKES CARBON CORPORATION

18 EAST 48TH STREET, NEW YORK 17, N. Y. OFFICES IN PRINCIPAL CITIES

EDITORIAL STAFF

H. H. Uhlig, Chairman, Publication Committee

Cecil V. King, Editor

Herman Hackerman, Technical Editor

Ruth G. Sterns, Managing Editor

U. B. Thomas, News Editor

H. W. Salzberg, Book Review Editor

Natalie Michalski, Assistant Editor

DIVISIONAL EDITORS

W. C. Vosburgh, Battery

Milton Stern, Corrosion, I

R. T. Foley, Corrosion, II

T. D. Callinan, Electric Insulation

Seymour Senderoff, Electrodeposition

H. C. Froelich, Electronics, I

Ephraim Banks, Electronics, II

Ernest Peskell, Electronics—Semiconductors

Sherlock Swann, Jr., Electro-Organic, I

Stanley Wawzonek, Electro-Organic, II

John M. Blocher, Jr., Electrothermics and Metallurgy, I

A. U. Seybolt, Electrothermics and Metallurgy, II

N. J. Johnson, Industrial Electrolytic

C. W. Tobias, Theoretical Electrochemistry, I

A. J. deBethune, Theoretical Electrochemistry, II

ADVERTISING OFFICE

ECS

1860 Broadway, New York 23, N. Y.

ECS OFFICERS

R. A. Schaefer, President
The Bunting Brass and Bronze Co., Toledo, Ohio

Henry B. Linford, Vice-President
Columbia University, New York, N. Y.

F. L. LaQue, Vice-President
International Nickel Co., Inc., New York, N. Y.

W. J. Hamer, Vice-President
National Bureau of Standards, Washington, D. C.

Lyle I. Gilbertson, Treasurer
Air Reduction Co., Murray Hill, N. J.

I. E. Campbell, Secretary
National Steel Corp., Weirton, W. Va.

Robert K. Shannon, Executive Secretary
National Headquarters, The ECS, 1860 Broadway, New York 23, N. Y.

Manuscripts submitted to the Journal should be sent, in triplicate, to the Editorial Office at 1860 Broadway, New York 23, N. Y. They should conform to the Instructions to Authors, last published in the April 1960 issue, pp. 100C-101C. Manuscripts so submitted become the property of The Electrochemical Society and may not be published elsewhere, in whole or in part, unless permission is requested of and granted by the Editor.

Inquiries re positive microfilm copies for volumes should be addressed to University Microfilms, Inc., 313 N. First St., Ann Arbor, Mich.

The Electrochemical Society does not maintain a supply of reprints of papers appearing in its Journal. A photoprint copy of any particular paper, however, may be obtained by corresponding directly with the Engineering Societies Library, 29 W. 39 St., New York 18, N. Y.

Journal of the Electrochemical Society

AUGUST 1960 **VOL. 107 • NO. 8**

CONTENTS

Editorial

Abstracts 164C

Technical Papers

Investigations on the Reaction Mechanism of the Nickel-Cadmium Cell. *S. U. Falk* 661

Oxidation Properties of Tantalum between 400° and 530°C. *J. V. Cathcart, R. Bakish, and D. R. Norton* 668

Equilibrium Space Charge at the Contact of a Metal and a Pure Highly Insulating Liquid and Its Influence on High-Field Conductivity. *M. J. Morant* 671

The Incorporation of Sulfur in Electrodeposited Nickel, Using Thiourea as a Brightener and Leveler. *G. T. Rogers, M. J. Ware, and R. V. Fellows* 677

(Zn, Hg)S and (Zn,Cd,Hg)S Eectroluminescent Phosphors. *A. Wachtel* 682

Crater Resistance of Submerged Arc Smelting Furnaces Simulated by a Simple Model. *O. C. Bockman* 688

Graphite Anodes in Brine Electrolysis, IV. Effect of Anolyte pH on Corrosion Rate in Chlor-Alkali Cells. *L. E. Vaaler* 691

An Electrochemical Study of Uranium in Fused Chlorides. *D. L. Hill, J. Perano, and R. A. Osteryoung* 698

Electrochemical Study of Metallic Oxides in Fused Lithium Chloride-Potassium Chloride Eutectic. *H. A. Laitinen and B. B. Bhatia* 705

Solutions of Some Alkali Halides in the Pure Liquids and in Mixtures of N-Methylacetamide and Dimethylformamide. *L. R. Dawson and W. W. Wharton* 710

Brief Communications

Electronic Magnetoanalysis of an Iron Single Crystal. *S. Yamaguchi* 714

Stress Corrosion Cracking. *D. van Rooyen* 715

Houston Meeting Program 169C-194C

Current Affairs 196C-208C

Published monthly by The Electrochemical Society, Inc., from Manchester, N. H., **Executive Offices, Editorial Office** and **Circulation Dept.**, and **Advertising Office** at 1860 Broadway, New York 23, N. Y., combining the JOURNAL and TRANSACTIONS OF THE ELECTROCHEMICAL SOCIETY. Statements and opinions given in articles and papers in the JOURNAL OF THE ELECTROCHEMICAL SOCIETY are those of the contributors, and The Electrochemical Society assumes no responsibility for them. Nondeductible subscription to members $5.00; subscription to nonmembers $18.00. Single copies $1.25 to members, $1.75 to nonmembers.

Copyright 1960 by The Electrochemical Society, Inc.

Entered as second-class matter at the Post Office at Manchester, N. H., under the act of August 24, 1912.

Now . . . Du Pont doubles capacity of floating-zone crystal-growing facilities at Brevard, North Carolina plant. You'll have a lower production cost per device when you purchase single crystals from this dependable source, rather than growing them in your own plant.

Now...Du Pont progress in the quantities...diameters...

Du Pont has made great progress with recent and continuing research in silicon development for the growing semiconductor industry. It has expanded production facilities, increased the number of grades available and set up to perform a variety of special services.

These developments are results of Du Pont's continuing silicon research and attention to the specific needs of device manufacturers. For example, now for the first time, Du Pont offers gold-doped single crystals in commercial quantities for high-speed switching devices.

Whatever type silicon you need for production or development, it will pay to consult Du Pont. We have the facilities to produce "special" grades and will be glad to work with you to meet your exact requirements. Du Pont

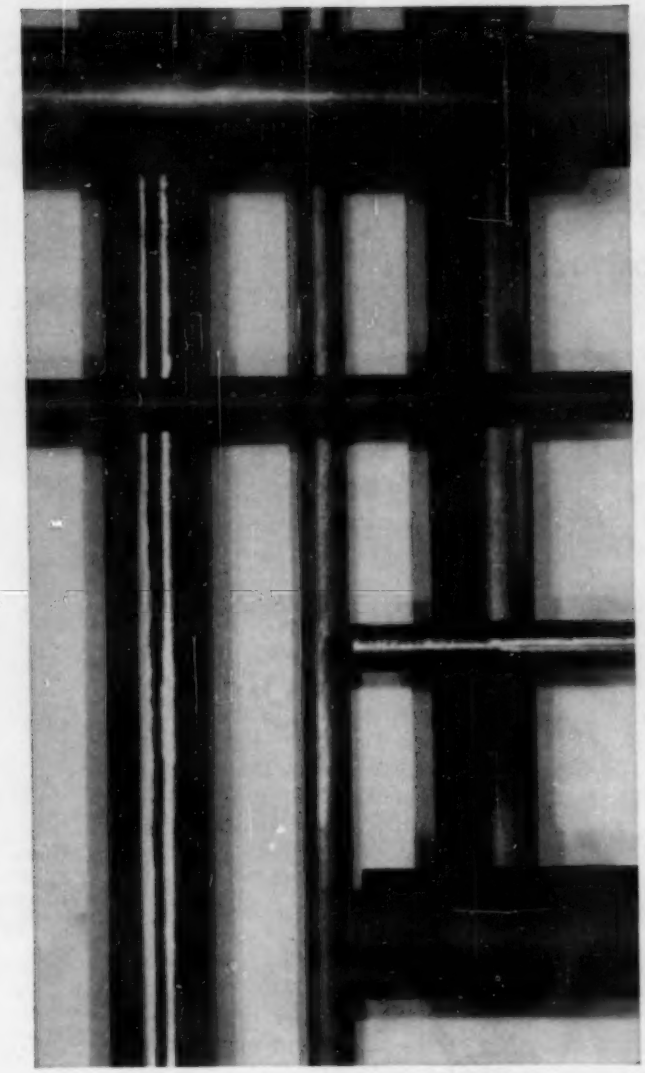

SILANE PROCESS
Single Crystal

"N" type 100 to > 1,000 ohm. cm.

"P" type 300 to > 2,000 ohm cm.

plus polycrystalline rod

ZINC PROCESS
Single Crystal

"N" type .1 to > 250 ohm cm.

"P" type .1 to > 300 ohm cm.

Also grades 1, 2 and 3
in both densified and standard
rod form; solar grade
in densified form.

Now . . . single crystals are available in a wide range of diameters—even greater than one inch. You can specify the diameter crystal that is most efficient and economical for your cutting and dicing operations. Each diameter is available in a wide range of resistivities. Both 1:1:1 and 1:0:0 orientations are available.

Now . . . a Du Pont silane plant is on stream, producing single crystals of high resistivity. This new plant also produces polycrystalline rod for floating-zone crystal growing. Du Pont silane and zinc process plants offer you a complete line of silicon grades and physical forms.

Hyperpure silicon assures and grades you need

is a specialist in the production of silicon—not devices—and will continue in its role of a raw material supplier to the electronics industry.

SEND FOR NEW BOOKLET which gives specifications and prices of all grades of Du Pont *hyperpure* silicon. Write for your copy to E. I. du Pont de Nemours & Co. (Inc.), Pigments Department, 2533 Nemours Building, Wilmington 98, Delaware.

DU PONT

REG. U.S. PAT. OFF.

BETTER THINGS FOR BETTER LIVING . . . THROUGH CHEMISTRY

HYPERPURE SILICON

Editorial

Abstracts

ELSEWHERE in this issue of the JOURNAL (*see* page 195*C*), we publish a "Guide for the Preparation and Publication of Synopses" which is distributed by the International Council of Scientific Unions. Copies of the Guide and also of a small brochure entitled "To Improve the Distribution of Scientific Information" may be obtained (free) by writing to: ICSU Abstracting Board, Bureau des Résumés Analytique due C.I.U.S., 292, rue Saint Martin, Paris 3, France. While study of this literature will not solve all difficulties, and this JOURNAL does not follow all of the policies suggested, we believe that the material deserves serious consideration.

The objectives of the international Abstracting Board have been to induce all science journals to publish author-written (but edited) abstracts or synopses of all technical papers and articles, to urge that the quality be made as high as possible, and to urge that rapid distribution be made. There are two aspects to the quality objective. The abstract which is published with the paper is of primary concern to the reader who is thumbing through the journal; if an article seems to contain information of use to him, he can immediately look further to see the experimental methods, quantitative data, etc. On the other hand, the abstract which appears later in a professional Abstract Journal needs to be as informative as possible about the results of the investigation, perhaps at the expense of descriptive material. It should be made clear to the reader whether he needs to look up the original article, perhaps even go to the trouble and expense of having a translation made.

For this reason, the professional abstractor seldom uses the author's abstract, at least not in full. This is not, as authors may feel, because the abstractor considers the author to be incompetent, but rather because of the differing purposes. In the ideal case, part or all of the author's abstract can be used with the addition of certain material which can be found very quickly when the article is at hand.

This JOURNAL, of course, requires author-written abstracts of all technical papers, containing 100 words or less if practical but up to a maximum of 200 words if it seems really warranted. We realize that the author of a paper has an extremely biased point of view in writing his own abstract; he is too near the background of the problem, the details of the research, and finds it difficult to summarize adequately in a few words, keeping the needs of other readers in mind. The competent author may write three versions of his text, eleven versions of his abstract. Yet, who is better qualified?

We ask our authors to study the problems involved in writing the most useful abstracts for their papers. When you read someone else's abstract, do you feel that it gives a good summary of the paper's content? How might he have improved it? Can you apply these ideas to improve your own abstracts?

—CVK

Germanium *and other semiconductors from* **EAGLE-PICHER**

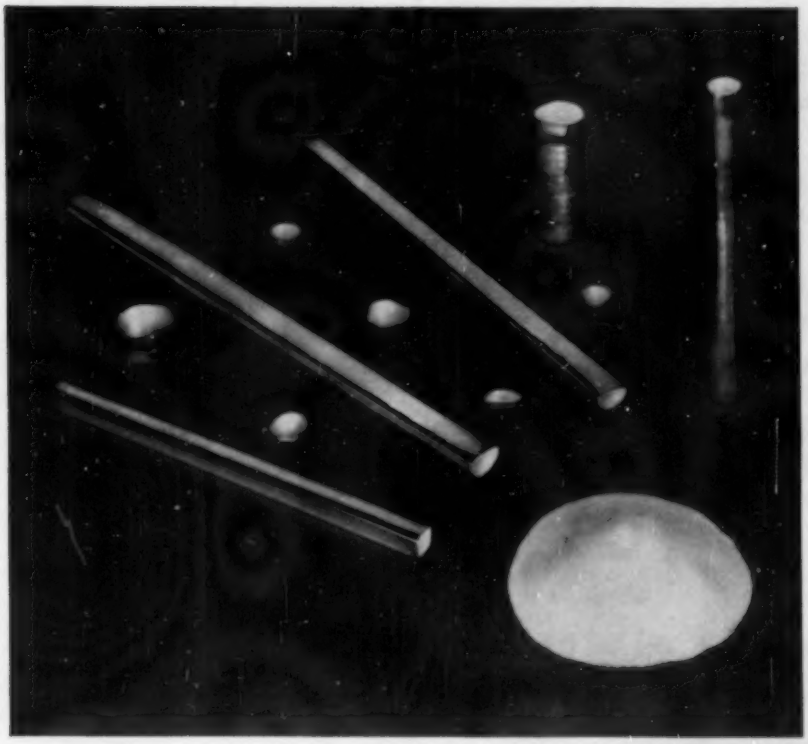

Eagle-Picher Rare Metals and Semiconductors

GERMANIUM DIOXIDE, minimum purity 99.999%.

FIRST REDUCTION GERMANIUM METAL, minimum resistivity 5 ohm-cm.

INTRINSIC GERMANIUM METAL, minimum resistivity 40 ohm-cm.

SINGLE CRYSTAL GERMANIUM [undoped] minimum resistivity 30 ohm-cm.

SINGLE CRYSTAL GERMANIUM [doped] to customers' specified resistivity.

SPECIAL SHAPES, INTRINSIC GERMANIUM METAL, for horizontal or vertical crystal growing. Wide variety in stock, other shapes furnished to customers' specifications.

SCRAP GERMANIUM PLAN, scrap Germanium may be returned for economical reprocessing under a toll arrangement.

—also immediately available

CADMIUM SULFIDE

GALLIUM, ultra pure.
Metallic crystals, minimum purity 99.9999%.
Metallic crystals, minimum purity 99.999%.

GALLIUM SESQUIOXIDE

Eagle-Picher, pioneer in Germanium, is an acknowledged leader in dependable production to meet the precise demands of the semiconductor industry. We offer a complete line of Germanium products and in addition, reprocess customers' *scrap Germanium* under our new low-cost toll arrangement.

FREE! An interesting, new brochure, "EAGLE - PICHER GERMANIUM" is now available. Write for your copy today.

EAGLE EP PICHER

Since 1843

THE EAGLE-PICHER COMPANY

Chemical Division, Dept. JES-860

GENERAL OFFICES: CINCINNATI 1, OHIO

FUTURE MEETINGS OF
The Electrochemical Society

Houston, Texas, October 9, 10, 11, 12, and 13, 1960

Headquarters at the Shamrock Hotel
Sessions will be scheduled on
Batteries, Corrosion, Electrodeposition,
Electrodeposition—Electrothermics & Metallurgy
Joint Symposium on Vapor Deposited Coatings,
Electronics (Semiconductors),
and Electrothermics and Metallurgy

★ ★ ★

Indianapolis, Ind., April 30, May 1, 2, 3, and 4, 1961

Headquarters at the Claypool Hotel
Sessions probably will be scheduled on
Electric Insulation, Electronics (including Luminescence and
Semiconductors), Electrothermics and Metallurgy,
Industrial Electrolytics, and Theoretical
Electrochemistry

★ ★ ★

Detroit, Mich., October 1, 2, 3, 4, and 5, 1961

Headquarters at the Statler Hotel

★ ★ ★

Los Angeles, Calif., May 6, 7, 8, 9, and 10, 1962

Headquarters at the Statler Hilton Hotel

★ ★ ★

Boston, Mass., September 16, 17, 18, 19, and 20, 1962

Headquarters at the Statler Hilton Hotel

Papers are now being solicited for the meeting to be held in Indianapolis, Ind., April 30-May 4, 1961. Triplicate copies of each abstract *(not exceeding 75 words in length)* are due at Society Headquarters, 1860 Broadway, New York 23, N. Y., *not later than January 2, 1961* in order to be included in the program. *Please indicate on abstract for which Division's symposium the paper is to be scheduled, and underline the name of the author who will present the paper.* Complete manuscripts should be sent in triplicate to the Managing Editor of the JOURNAL at 1860 Broadway, New York 23, N. Y.

Presentation of a paper at a technical meeting of the Society does not guarantee publication in the JOURNAL. However, all papers so presented become the property of The Electrochemical Society, and may not be published elsewhere, either in whole or in part, unless permission for release is requested of and granted by the Editor. Papers already published elsewhere, or submitted for publication elsewhere, are not acceptable for oral presentation except on invitation by a Divisional program Chairman.

any way you measure
ANODE PERFORMANCE

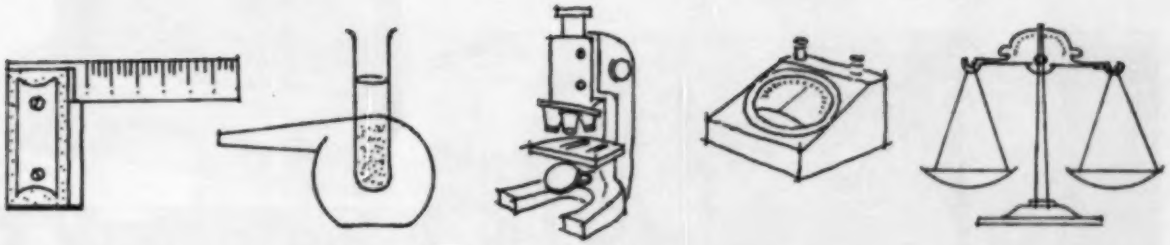

Structural and Dimensional Uniformity? | Chemical Stability of Treatment? | Uniform Texture? | Cell Voltage? | Pounds Consumed per ton of Chlorine Produced?

STACKPOLE
GraphAnode® ANODES
prove second to none for
Economical Chlorine Production

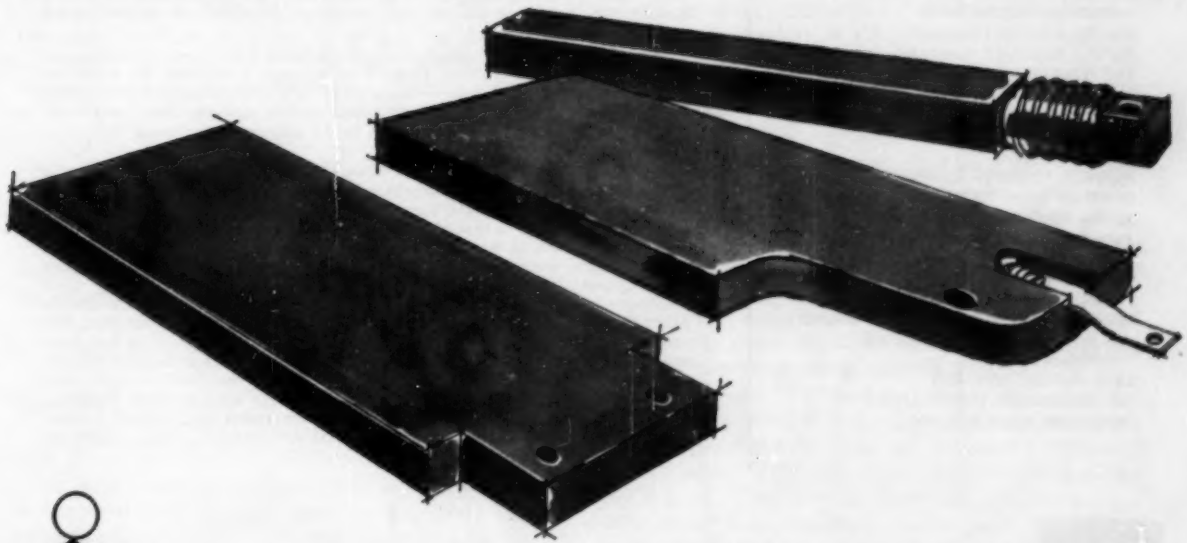

STACKPOLE CARBON COMPANY,
St. Marys, Pa.

CATHODIC PROTECTION ANODES • FLUXING & DE-GASSING TUBES • SALT BATH RECTIFICATION RODS • ROCKET NOZZLES • RISER RODS • GRAPHITE BEARINGS & SEAL RINGS • ELECTRODES & HEATING ELEMENTS • WELDING CARBONS • VOLTAGE REGULATOR DISCS • "CERAMAGNET"® CERAMIC MAGNETS • ELECTRICAL CONTACTS • BRUSHES FOR ALL ROTATING ELECTRICAL EQUIPMENT • AND MANY OTHER CARBON, GRAPHITE AND ELECTRONIC COMPONENTS.

SARGENT-SLOMIN ANALYZERS
are standard equipment in prominent laboratories

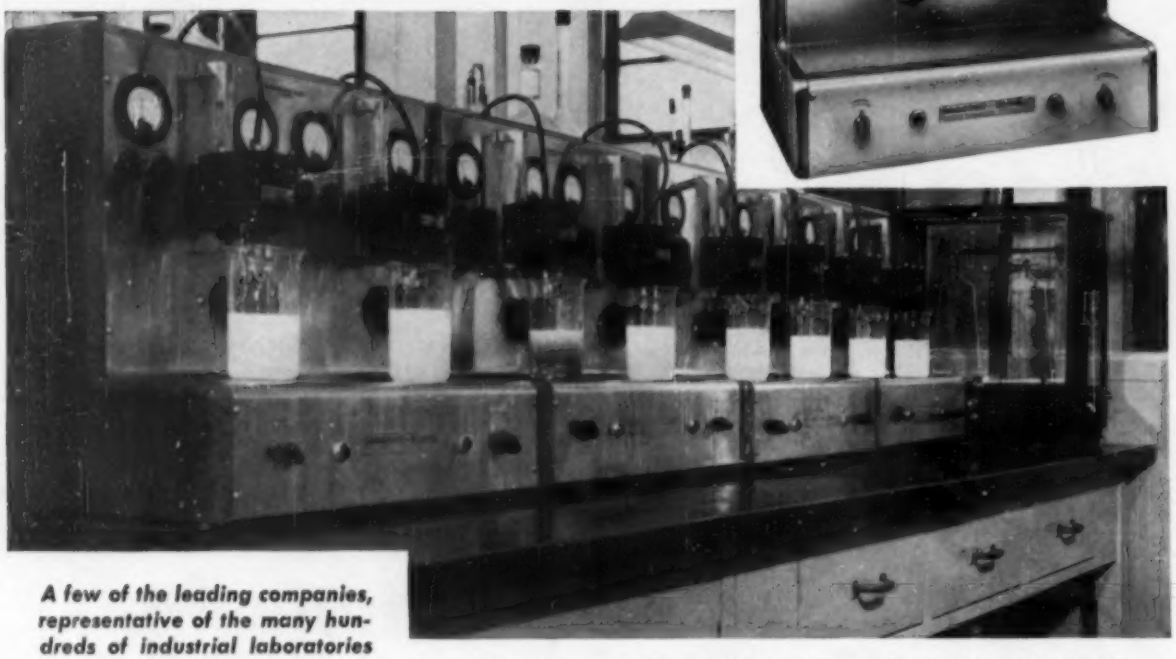

Photo Courtesy INTERNATIONAL HARVESTER COMPANY, Melrose Park, Illinois

A few of the leading companies, representative of the many hundreds of industrial laboratories using the Sargent - Slomin and Heavy Duty Analyzers for control analyses . . .

AMPCO METAL, Inc.
ANDERSON LABORATORIES
CALERA MINING COMPANY
EUREKA WILLIAMS COMPANY
THE FEDERAL METAL CO.
FORD MOTOR COMPANY
THE GLIDDEN COMPANY—Chemical, Metal and Pigment Division
HOT POINT CO.
HOWARD FOUNDRY COMPANY
INTERNATIONAL HARVESTER COMPANY
KENNAMETAL Inc.
McQUAY - NORRIS MANUFACTURING CO.
NATIONAL LEAD COMPANY, Fredericktown, Missouri
PIASECKI HELICOPTER CORPORATION
REVERE COPPER & BRASS INCORPORATED
THE RIVER SMELTING & REFINING COMPANY
SILAS MASON COMPANY
THE STUDEBAKER CORPORATION
THOMPSON PRODUCTS, INC.

Sargent-Slomin Electrolytic Analyzers are recommended for such electro analytical determinations as: Copper in—ores, brass, iron, aluminum and its alloys, magnesium and its alloys, bronze, white metals, silver solders, nickel and zinc die castings. Lead in—brass, aluminum and its alloys, bronze, zinc and zinc die castings. Assay of electrolytical copper, nickel and other metals.

Sargent analyzers are completely line operated, employing self-contained rectifying and filter circuits. Deposition voltage is adjusted by means of autotransformers, with meters indicating volts and amperes and controls on the panel. An easily replaceable fuse guards against circuit overload. Maximum D.C. current capacity is 5 to 15 amperes; maximum D.C. voltage available, 10 volts.

Sargent-Slomin Analyzers stir through a rotating chuck operated from a capacitor type induction motor, having a fixed speed of 550 r.p.m. with 60 cycle A.C. current or 460 r.p.m. with 50 cycle A.C. current. Motors are sealed against corrosive fumes and are mounted on cast metal brackets, sliding on ½" square stainless steel rods, permitting vertical adjustment of electrode position over a distance of 4". Pre-lubricated ball-bearings support the rotating shaft. All analyzers accommodate electrodes having shaft diameters no greater than 0.059 inch. Stainless steel spring tension chucks permit quick, easy insertion of electrodes and maintain proper electrical contact. Special Sargent high efficiency electrodes are available for these analyzers. Illustrated above is one model of the five types of Sargent-Slomin and Heavy Duty Analyzers.

S-29465 ELECTROLYTIC ANALYZER—Motor stirred, Two Position, 5 Ampere. With two adjustable heaters, pilot lights and control knobs. For operation from 115 volt, 50 or 60 cycle A.C. circuits.....**$390.00**

SARGENT *SCIENTIFIC LABORATORY INSTRUMENTS • APPARATUS • SUPPLIES • CHEMICALS*

E. H. SARGENT & CO., 4647 W. FOSTER, CHICAGO 30, ILLINOIS
DETROIT 4, MICH. • DALLAS 35, TEXAS • BIRMINGHAM 4, ALA. • SPRINGFIELD, N. J.

Investigations on the Reaction Mechanism of the Nickel-Cadmium Cell

S. Uno Falk

Svenska Ackumulator AB Jungner, Stockholm, Sweden

ABSTRACT

X-ray diffraction patterns from electrodes submerged in electrolyte have been obtained during charge and discharge by means of a special test cell, and the composition of the active materials has been determined. The question whether CdO or $Cd(OH)_2$ is formed during discharge has been subject to special attention. The low potential reaction of the positive plate has been studied. The emf and the dE/dT have been determined between −40° and +50°C at various states of charge.

The nickel-cadmium cell, the principle of which was patented by Jungner (1) in 1899, has provoked the interest of several investigators ever since, and many theories have been put forward concerning the reactions and thermodynamics of this system. However, opinions still differ in many essentials and this has caused us to publish the results of some investigations carried out to establish the reaction formulas of the nickel-cadmium cell and to elucidate the reaction mechanism.

The Reactants

It is generally agreed that the nickel-cadmium cell works according to the oxygen-lift system, i.e., oxygen (or hydroxyl ion) is transferred from one electrode to the other. This transfer is carried out by the electrolyte.

Opinions have differed appreciably as far as the composition of the compounds constituting the active substances is concerned. Thus, the following formulas have been suggested for the charged material of the positive electrode: $Ni(OH)_2$ (2), NiO_2 (3), $NiO_2 \cdot H_2O$ (4), $NiO_2 \cdot xH_2O$ (5), $Ni(OH)_3$ (6), $2Ni(OH)_3 \cdot 5H_2O$ (7), Ni_2O_5 (8), $Ni_2O_5 \cdot 1.2\ H_2O$ (9), $Ni_2O_5 \cdot 6H_2O$ (10), and β-NiOOH (5) and mixtures or solid solutions of these compounds.

Some of these substances have been referred to in investigations carried out on positive plates of nickel-iron cells, which, however, is of no importance, since the same positive active material is present in these cells.

For the discharged state the following formulas have been suggested: Ni (11), NiO (3), $NiO \cdot 4H_2O$ (4), $2NiO \cdot 9H_2O$ (10), $Ni(OH)_2$ (9), $Ni(OH)_2 \cdot 2H_2O$ (6), $2Ni(OH)_2 \cdot 6H_2O$ (7), Ni_2O_4 (12), and Ni_4O_6 (13).

Cd and CdH_2 (4) have been mentioned as constituents in the charged negative electrode, while CdO (14), Cd_2O (15), $CdO \cdot xH_2O$ (10), and $Cd(OH)_2$ (16) have been suggested for the discharged state.

The first part of these investigations was directed to establishment of the components present in the electrodes at various states of charge. For this purpose x-ray diffraction methods were used primarily.

Several other workers (17-24) used such methods to study different nickel and cadmium compounds. In the cases, however, where electrodes have been investigated, the x-ray exposures have been made on washed and dried samples which obviously may introduce sources of error. Removing the electrolyte may cause hydration changes and, moreover, oxygen may affect the active materials. Therefore, x-ray investigation of an active material in a nickel-cadmium cell should be carried out on a sample completely submerged in the electrolyte and subjected to charge or discharge. Only in that case the spectra obtained may be claimed to represent the true active substances. Application of a charge or a discharge eliminates the risk of decomposition of unstable substances that possibly could be formed when a current is passing, and accordingly otherwise escape detection. These points of view have, as far as we know, been duly taken into account only by Salkind and Bruins (25), who, in an extensive and meritorious investigation of the nickel-cadmium cell have, x-rayed parts of wet electrodes stored in sealed plastic bags and also worked with a Lucite cell, permitting charge and discharge of the electrodes during exposure. Thus, in the first case washing and drying have been avoided and, in the latter, a current is passing. Apparently, the position of the plates in the Lucite cell has permitted free access of the air.

A specially constructed cell was used. It contained one sintered electrode of the kind to be investigated, and one sintered electrode of opposite polarity. Sintered electrodes are used in these investigations, first, because steel ribbons do not screen the active materials and second, because the active materials are not mixed with other substances. Figure 1 shows the set-up. When the desired state of charge has been attained by charge or discharge, the test electrode is pulled sidewise from the counter electrode and is pressed against one of the walls of the plastic bag, making the electrolyte film as thin as possible. The plate is now inserted in the sample holder of the x-ray spectrometer, the part of the bag containing the counter electrode being placed at the side of

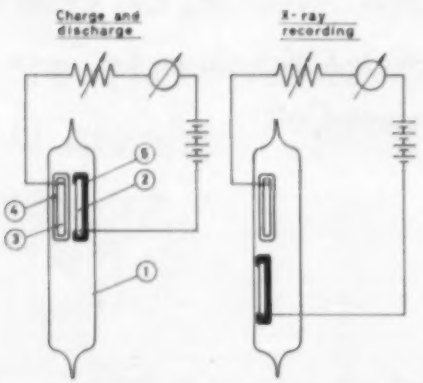

Fig. 1. Polyethylene cell allowing x-ray examination of electrodes without removal from electrolyte and without interruption of current. 1, U-bent very thin polyethylene sheet, welded at the ends and filled with electrolyte; 2, electrode under test; 3, counter electrode; 4, filter paper separator covering the counter electrode; 5, layer of epoxy plastic directing the current exclusively to the plate front.

the holder. The current is not interrupted during these manipulations, nor during the subsequent x-ray exposure. However, the current is sufficiently decreased during the exposure to permit recording the entire diffraction pattern without any appreciable change of the state of charge of the electrode. In this manner, positive as well as negative electrodes have been investigated at various states of charge. For the exposure Ni-filtered Cu K_α-radiation was used. The reflections were registered by means of a Geiger counter and a potentiometer recorder.

The Positive Active Material

Figure 2 shows x-ray patterns of fully charged, 1/3 discharged, 2/3 discharged, and fully discharged positive electrodes. The polyethylene peaks have been omitted from this figure.

The discharged positive material has proved to be $Ni(OH)_2$ of small grain size. This is indicated by the conspicuous broadening of the $Ni(OH)_2$ lines as compared to, for instance, the Ni reflections. Broadening of the reflections may be due to several other causes, such as irregular lattice, mechanical crystal deformation or lacking chemical equilibrium. However, we have found by means of Hahn's emanation method (26, 27) that the broadening in this case is caused by very small crystals. The approximate crystal size may be calculated from this broadening. During charge this $Ni(OH)_2$ is successively transferred into a still more finely divided compound having a spectrum agreeing well with that of β-NiOOH. No traces of higher nickel oxides have been discovered even at strong overcharge. At discharge β-NiOOH is again transferred into $Ni(OH)_2$. These transformations do not imply a decrease of $Ni(OH)_2$ and an appearance of β-NiOOH reflections but instead some $Ni(OH)_2$ peaks decrease while others gradually are displaced toward β-NiOOH. This indicates the presence of a solid solution of β-NiOOH and $Ni(OH)_2$, further supported by the fact that the emf curve varies with the state of charge. This observation will be discussed later.

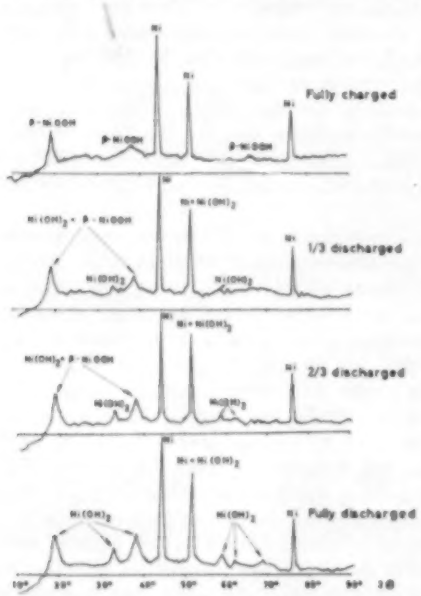

Fig. 2. X-ray diffraction patterns from positive electrode

In our x-ray investigations of the charged positive material β-NiOOH was the highest nickel compound encountered, this being the case also after heavy overcharge. Naturally, this does not necessarily mean that higher compounds like NiO_2 are not present, as these may be amorphous to x-rays. At any rate, a freshly charged positive plate contains more active oxygen than corresponds to the formula founded on trivalent nickel. This was found by Foerster (9), who stated that the charged material consisted of a solid solution of NiO_2 and $Ni_2O_3 \cdot 1.2H_2O$. The opinion has been shared by several others, but Pitman and Work (28) recently considered it to be more likely that the excess of active oxygen is adsorbed by β-NiOOH. This theory is based on an investigation of the concentration of active oxygen in the electrode as related to the open-circuit potential after charge. If Foerster's theory were correct, the potential would vary linearly with the logarithm of the active oxygen concentration. However, Pitman and Work have observed that the potential decreases directly as a straight line with the oxygen concentration, indicating an oxygen adsorption, thus, as far as we can understand, disproving Foerster's theory. The freshly charged state should, according to Pitman and Work, be represented by the formulas $Ni_2O_3(O)_{ads}$ or $(\beta\text{-NiOOH})_2(O)_{ads}$. As we have found that β-NiOOH is present in the charged active material, the latter formula is considered correct.

The capacity available from the adsorbed oxygen is comparatively small: a freshly charged positive plate will yield 10-15% more capacity than a plate having rested some 24 hr after charge.

The secondary discharge reaction frequently appearing at a voltage of about 0.7 v was an object of interest as early as 1905-1910, when Foerster and Zedner performed some experiments. It has been established that the potential step in question originates from the positive electrode. The causes of the reaction have been widely discussed, but the source accepted nowadays seems to be the oxygen adsorbed

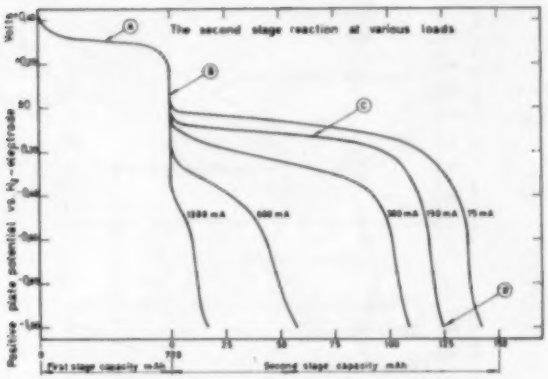

Fig. 3. Second stage reaction at various loads

by the graphite present in positive pocket electrodes, the step not appearing in plates without graphite. This explanation is not correct, as we have been able to find the potential step also in sintered positive electrodes, completely lacking graphite. The duration of the stage can be increased by repeated reversals. The reaction occurring at an anode voltage of about −0.15 v as measured against the hydrogen electrode may correspond to 20% of the total capacity. The step is dependent on the load; its shape at different loads is shown in Fig. 3.

X-ray diffraction patterns have been recorded of sintered positive electrodes, discharged in the polyethylene cell previously described to the points (A), (B), (C), and (D) according to Fig. 3. It was intended to obtain, if possible, the structure of the compounds causing the second stage reaction. However, no new compounds appeared in these patterns, nor were any significant changes of position or intensities of the $Ni(OH)_2$ reflections observed.

The opinion of Glemser and Einerhand (5) that $Ni_2O_2(OH)_2$ is the active compound in this case is not supported by any x-ray investigations carried out by these research workers. The presence of $Ni_2O_2(OH)_2$ should certainly be established by x-rays, but we have found neither this compound nor any other. We believe, therefore, that the step is caused by oxygen adsorbed by the nickel hydroxide. In order to obtain further proof of this theory the relationship between the secondary discharge stage and the ambient air pressure was studied. These investigations, carried out on sintered electrodes, corroborated the statement by Zedner (6) that evacuation will decrease the capacity of this stage. Oxygen is generally liberated with substantially less difficulty in the adsorbed state than when attached chemically to nickel, particularly as the possible nickel compound cannot be very highly oxidized. This circumstance in connection with the negative results of the x-ray diffraction tests substantiates our opinion that the secondary discharge reaction is caused by oxygen adsorbed by $Ni(OH)_2$.

Negative Active Material

Figure 4 shows x-ray diffraction patterns of negative electrodes in fully charged, 1/3 discharged, 2/3 discharged, and completely discharged states.

The discharged material consists mainly of $Cd(OH)_2$. However, a small amount of Cd is always

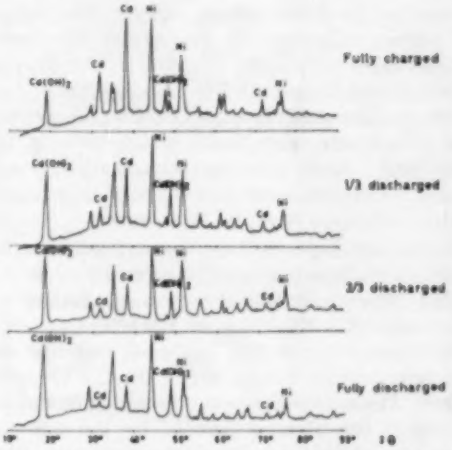

Fig. 4. X-ray diffraction patterns from negative electrode

present. During charge $Cd(OH)_2$ is successively transformed into Cd metal. In this case no solid solution is formed: Cd and $Cd(OH)_2$ spectra may appear simultaneously. This agrees also with the open-circuit voltage measurements carried out at different states of charge. The transformation of $Cd(OH)_2$ into Cd is not complete even after strong overcharge, as indicated by the x-ray pattern at this stage.

According to Troilius (4) a fully charged electrode probably contains a certain amount of CdH_2, which decomposes relatively rapidly after the end of the charge into Cd and H_2. If a discharge is carried out immediately after charge a potential drop appears that might be attributed to CdH_2. However, our x-ray investigations have not revealed any compound corresponding to CdH_2. Comparative tests on negative electrodes and unimpregnated nickel sinter have shown also that the pure nickel sinter after cathodic polarization exhibits a potential "tail" similar to the one noticed on negative electrodes. The value of the potential makes it likely that a pure oxidation of hydrogen adsorbed by the nickel sinter is the cause of this tail. These investigations show that hydrogen may be adsorbed by porous metals, thus giving some extra capacity on discharge. This observation makes it very probable also that the reaction at the negative plate is caused by adsorbed hydrogen. This theory is further corroborated by the fact that evacuation of a negative electrode after a complete charge is accompanied by a substantially less pronounced potential tail when discharged. The capacity excess caused by the adsorbed hydrogen is, however, very slight and in general quite negligible.

The investigations presented here show clearly that $Cd(OH)_2$ is the end product of discharge. However, several writers claim that CdO is formed, this opinion being recently conveyed by Lake and Casey (20) and Winkler (29) among others. According to Lake and Casey, CdO is formed as primary product on anodic oxidation, this oxide subsequently being transformed into $Cd(OH)_2$ in the presence of the alkaline electrolyte. These writers have themselves not been able to establish the presence of CdO, but make this assumption because a dark-colored compound is formed.

Experiments were carried out on charged negative plates, subsequently discharged with various, in some cases very high, currents in the previously described x-ray test cell. The cell has been adjusted on the strongest CdO line, and careful measurements have been made with maximum sensitivity to ascertain the recording of any intensity increase during discharge. All these tests have yielded negative results: in no case has CdO been traced.

Furthermore, plates have been used, the active material of which has been transferred into CdO by heating. After insertion in the sample holder of the x-ray apparatus KOH (sp gr 1.25) was added. The x-ray lines of $Cd(OH)_2$ increase instantaneously from zero to high values, while the CdO reflections weaken. These changes occur within a few seconds. As soon as the plate is touched by the electrolyte, the yellowish brown color changes into grayish white. Thus, it is obvious, that if CdO is the primary product of the discharge, which we by no means have been able to prove, this oxide is immediately transformed by the OH^--ions into $Cd(OH)_2$. Potential measurements indicate, however, as will be discussed later, that Cd is transferred directly into $Cd(OH)_2$.

Winkler's claim that CdO is the end product on discharge is supported by weighing negative plates of different states of charge immersed in the electrolyte, which apparently is a simple and reliable method incidentally used as early as 1904 by Schoop (30). The weight increase on discharge indicates, according to Winkler, the formation of CdO. He found an increase of 0.334 g/amp-hr, adjusted to the dry state, against the theoretical value 0.298 g/amp-hr for CdO. Winkler's paper does not indicate the electrolyte concentration used. If his cells were filled with KOH, sp gr 1.20, calculation shows that the weight increase obtained by Winkler and claimed to agree with formation of CdO, indicates $Cd(OH)_2$ just as well. This coincidence is simply due to the different densities of the two materials. In order to elucidate these matters Winkler's measurements have been supplemented by weighings in KOH of sp gr 1.05 and 1.42, these solutions giving larger differences between the theoretical weight increments. If KOH, sp gr 1.05, is used, the weight increase of the immersed electrode should be 0.245 g/amp-hr for CdO and 0.290 g/amp-hr for $Cd(OH)_2$. For KOH, sp gr 1.42, the corresponding values would be 0.227 and 0.169 g/amp-hr respectively.

Results are shown on Fig. 5.

It was found essential during these measurements that all concentration gradients of the electrolyte across the electrode surface were eliminated before taking the reading. It was also found necessary to remove gas bubbles remaining after the charge. Therefore, the electrolyte was stirred and the container was evacuated after every charge. Weighings were performed at equal intervals of time until constant weight was obtained. The values found on discharge were, in general, more reproducible than those obtained on charge. The diagrams indicated clearly that $Cd(OH)_2$ is the product of discharge. Thus, we consider it established beyond doubt that

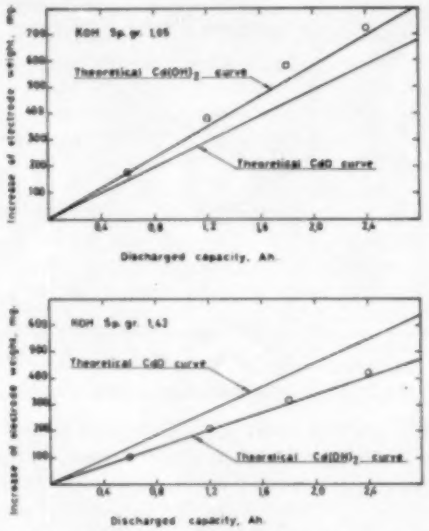

Fig. 5. Weighing of negative electrodes immersed in electrolyte.

$Cd(OH)_2$, not CdO, is the reaction product on discharge of the negative electrode.

The Electrolyte

Opinions on the participation of the electrolyte in the cell reaction have been and still are diverging. Frequently the reaction formula is written in a manner showing that the total concentration of the electrolyte does not change between charge and discharge (7, 31, 32). Condon and Odishaw (2) give a reaction formula according to which the electrolyte is diluted during discharge in a manner similar to the lead cell. According to Troilius (4) and Salkind (25) the total concentration of the electrolyte decreases on charge to regain its original value on discharge.

To clarify this point, potential measurements have been carried out on half charged sintered cells, previously filled with electrolytes of different concentrations. If the over-all concentration does not change in the working cell, then the emf obviously is independent of the electrolyte concentration. The cells were constructed without isolation between the electrodes which, furthermore, were widely separated from each other. Thus the ratio electrolyte/electrodes was substantially higher than is the case in normal cells. These steps were taken, first, to prevent diffusion phenomena on charge and discharge from affecting the measurements, second, to minimize the concentration variations on charge and discharge. Emf and plate potentials were measured. As is shown in Fig. 6, the cell emf increases with decreasing electrolyte concentration. A concentration increase from 5 to 45% causes an emf decrease of about 0.07 v. Consequently, the over-all concentration of the electrolyte is changing in a working cell.

The plate potentials have been measured against a Hg/HgO electrode and the values were corrected for the liquid potentials.

In the negative plate diagram a theoretical curve has been plotted that is based on the equation

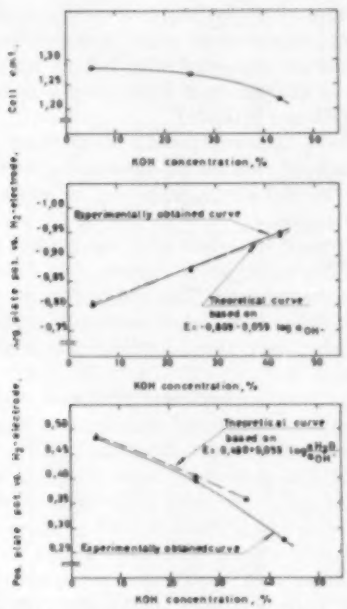

Fig. 6. Electrolyte concentration vs. open-circuit potentials

$$E = -0.809 - 0.059 \log a_{OH^-} \qquad [1]$$

This curve is referring to the electrode reaction

$$Cd + 2OH^- \rightleftharpoons Cd(OH)_2 + 2e \qquad [2]$$

and agrees evidently very satisfactorily with the experimental curve. Thus, this reaction may be considered as definitely established. As indicated by the formula no water participates in the reaction.

The positive electrode is more sensitive to variations of the electrolyte than the negative one, increasing its potential fairly rapidly when the electrolyte concentration is lowered. The formula indicated by the x-ray investigations is as follows:

$$Ni(OH)_2 + OH^- \rightleftharpoons \beta\text{-NiOOH} + H_2O + e \qquad [3]$$

This formula gives the following relationship between electrode potential and electrolyte activities.

$$E = E_0 + 0.059 \log \frac{a_{H_2O}}{a_{OH^-}} \qquad [4]$$

If we asume $E_0 = +0.480$ v and insert the activities of H_2O and OH^- for different electrolyte concentrations, the theoretical curve as shown in Fig. 6 is obtained. The agreement between this curve and the experimental one is clearly not very good. It is obvious, however, that the water activity enters into the equation for the electrode reaction. Water is thus formed on charging the nickel electrode.

Reaction Formulas

The main reaction of the positive electrode may, on basis of the previously given results, be written as follows:

$$2\beta\text{-NiOOH} + 2H_2O + 2e \rightleftharpoons 2Ni(OH)_2 + 2\,OH^- \qquad [5]$$

This equation may, for better understanding, be split up in the following partial reactions:

$$2\beta\text{-NiOOH} + 2H_2O \rightleftharpoons 2Ni^{3+} + 6OH^- \qquad [6]$$

$$2Ni^{3+} + 2e \rightleftharpoons 2Ni^{2+} \qquad [7]$$

$$2Ni^{2+} + 4\,OH^- \rightleftharpoons 2Ni(OH)_2 \qquad [8]$$

Thus, we can make the formal assumption that trivalent nickel ions are formed by dissolution and dissociation of β-NiOOH. On discharge they are transformed into bivalent nickel ions, which rapidly react with the hydroxyl ions of the electrolyte, forming nickel (II)-hydroxide.

However, it is also possible that the reactions take place directly in the interface between the active material and the electrolyte without dissolution and dissociation of β-NiOOH. Therefore, the given reaction steps are not to be considered as definite.

The main reaction at the negative electrode may be written

$$Cd + 2\,OH^- \rightleftharpoons Cd(OH)_2 + 2e \qquad [9]$$

being the summation effect of

$$Cd \rightleftharpoons Cd^{2+} + 2e \qquad [10]$$

$$Cd^{2+} + 2\,OH^- \rightleftharpoons Cd(OH)_2 \qquad [11]$$

Thus, on discharge the cadmium metal is emitting bivalent ions, immediately reacting with the hydroxyl ions of the electrolyte to form cadmium hydroxide. A summation of Eq. [5] and [9] gives the formula of the total cell reaction

$$2\beta\text{-NiOOH} + Cd + 2H_2O \rightleftharpoons 2Ni(OH)_2 + Cd(OH)_2 \qquad [12]$$

In the formulas given above purposely no regard has been paid to the roles of the adsorbed oxygen and hydrogen in the reactions, nor to the secondary discharge stage since all these reactions are of minor importance. The reactions may, however, be written as follows.

$$(\beta\text{-NiOOH})_x(O)_{ads} + H_2O + 2e \rightleftharpoons 2\beta\text{-NiOOH} + 2\,OH^- \qquad [13]$$

$$Cd(H_2)_{ads} + 2\,OH^- \rightleftharpoons Cd + 2H_2O + 2e \qquad [14]$$

$$Ni(OH)_2(O)_{ads} + H_2O + 2e \rightleftharpoons Ni(OH)_2 + 2\,OH^- \qquad [15]$$

Formula [12] for the total cell reaction agrees with the one given by Salkind and Bruins (25).

The EMF and Its Temperature Coefficient

We may assume the emf of the nickel-cadmium cell to be affected primarily by three factors: state of charge, temperature, and electrolyte concentration. The influence of the third factor has been discussed previously.

The emf of the nickel-cadmium cell vs. the state of charge has previously not been subjected to any extensive studies. The relationship between the potential conditions of the nickel electrode and generally rather brief rest periods has on the other hand been investigated by several persons (9, 28, 33, 34).

The results of our x-ray investigations seem to indicate a continuous decrease of the emf with the falling state of charge, because the potential of the positive electrode would fall gradually due to the existence of a solid solution between β-NiOOH and $Ni(OH)_2$, while the negative potential would be

totally independent of the state of charge. In order to obtain a confirmation, measurements were carried out on pocket-type as well as sintered-type cells, which were discharged to different states of charge after previous charging and 5 days of rest. This latter period was introduced to diminish the influence of $(\beta\text{-NiOOH})_x(O)_{ads}$. Emf and electrode potentials were measured after a storage time of 0, 2, 4, and 8 weeks.

These experiments showed that the variations of the electrolyte concentration at various states of charge affected the potentials. The potential of the cadmium electrode, for instance, grew linearly more positive with higher state of charge. Independently of the storage time the potential difference between the 0 and 100% states of charge of the sintered cells amounted to about 11 mv. A check proved this value to agree with the potential change appearing in this type of cell due to the concentration variation of the electrolyte, when formula [12] is applied. Evidently, the magnitude of this difference depends on the ratio volume of active material to electrolyte volume. Naturally, the positive electrode was also similarly affected by the electrolyte variations.

In order to obtain more unaffected values of the relationship between potential and state of charge, tests were carried out as before but on special cells, having a high ratio between electrolyte volume and electrode volume. The specific gravity of the electrolyte in these cells was 1.25. Typical values of emf and electrode potentials as related to the state of charge after 2 weeks' storage at these measurements are shown in Fig. 7.

The curves indicate that the negative electrode potential of the sintered cells is totally independent of the state of charge. This implies the nonexistence of solid solutions of the active compounds. The pocket-type cells have a negative electrode potential which is slightly more negative at higher states of charge. This effect is probably caused by the addition of iron to the negative active material.

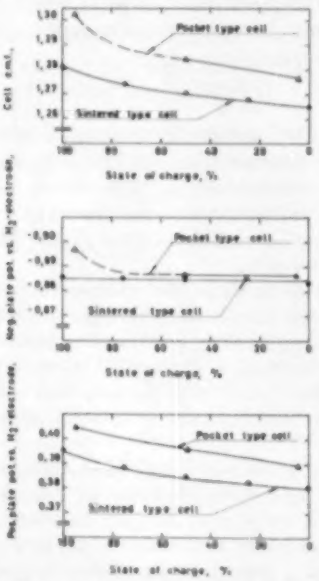

Fig. 7. State of charge vs. open-circuit potentials

The potential of the positive electrode of sintered as well as pocket-type cells is dependent on the state of charge and gradually falling with decreasing state of charge, thus indicating a solid solution of β-NiOOH and $Ni(OH)_2$.

Thus, emf is continuously decreasing with the falling state of charge. In agreement with the collected x-ray data this lowering is caused by the positive electrode.

It is a remarkable fact that the pocket cells consistently display slightly higher emf than corresponding sintered cells. The main part of this effect originates from the nickel electrode, although the cadmium electrode also contributes at higher states of charge.

The relationship between emf and temperature has not yet been subjected to quantitative investigations as far as the nickel-cadmium cell is concerned. This factor has, however, been investigated on the nickel-iron cell, the most extensive work carried out by Hosono and Watanabe (35).

In our investigation cells were tested with pocket as well as sintered electrodes, all discharged to 5, 50, and 95%, respectively, of the capacity after previous full charge. The electrolyte (sp gr 1.25) was covered by paraffine oil in all cells as protection against evaporation. After the discharge the cells were put at rest until the potentials varied only slightly from one day to another. Subsequently, emf and electrode potentials were measured at cell temperatures between about −40° and +50°C. The electrode potentials were all measured with Hg/HgO electrode filled with KOH, sp gr 1.25.

Values for the pocket cells proved to be reproducible at states of charge corresponding to 50 and 95% discharge, while the reproducibility at 5% discharge was less satisfactory and, furthermore, had dE/dT values deviating from the others. This effect indicates an instability and difference in character of the active material at 5% discharge. It is curious in this case that this instability is not dependent on the positive electrode but entirely due to the negative side. It would otherwise have been expected that the positive material would behave differently due to oxygen adsorption. These diverging values of the negative electrode might be due to influence from the iron powder present in the active material.

The sintered cells yielded reproducible values independent of the state of charge. Figure 8 shows typical emf values as related to the temperature on sintered as well as pocket cells. The figures show that all dE/dT values are negative, being more negative for pocket cells than sintered ones at all states of charge. Approximate values of the temperature coefficients of the emf and the electrode potentials are:

dE/dT	dE_c/dT	dE_a/dT
Pocket cells	Sintered cells	Pocket cells
−0.00030	−0.00018	−0.00006
Sintered cells	Pocket cells	Sintered cells
−0.00014	−0.00024	−0.00004 v/°K

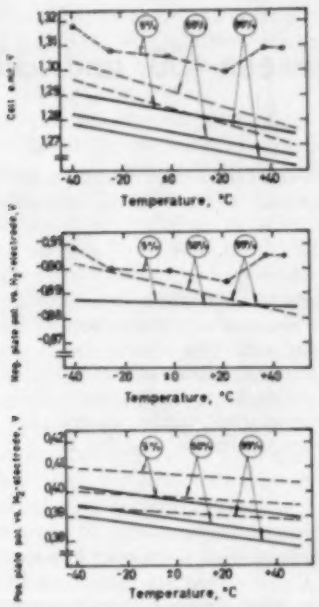

Fig. 8. Emf and electrode potentials vs. temperature. Dashed line, pocket type; solid line, sintered type.

dE/dT is somewhat dependent on the state of charge for pocket cells, of which a 5% discharge yields values disagreeing from the other ones. Otherwise the state of charge does not seem to have any greater influence on the temperature coefficient.

Salkind and Bruins (25) have found that the temperature coefficient of the nickel electrode of sintered cells is negative and decisive in agreement with the values given here.

The differences appearing between sintered and pocket cells as far as emf and dE/dT are concerned are supposed to be due to the presence of graphite in the positive and of iron in the negative pocket electrode.

Summary of Results

1. The main reaction of the nickel-cadmium cell on charge and discharge is
$$2\beta\text{-NiOOH} + Cd + 2H_2O \rightleftharpoons 2Ni(OH)_2 + Cd(OH)_2$$
2. The secondary discharge stage of the positive electrode is probably caused by oxygen adsorbed by $Ni(OH)_2$.
3. The high initial potential of the negative electrode after charge is caused by hydrogen adsorbed by Cd.
4. The emf of the nickel-cadmium cell is dependent on the activity of water in the electrolyte and consequently on the hydroxyl ion activity. An increase of the KOH concentration from 5 to 45% results in an emf decrease of about 0.07 v.
5. The emf of the nickel-cadmium cell depends on the state of charge, falling continuously with lower state of charge. This effect can be attributed to the existence of a solid solution between β-NiOOH and $Ni(OH)_2$ in the positive electrode.
6. The dE/dT value of the nickel-cadmium cell is negative. The magnitude is -0.00018 v/°K for sintered cells and -0.00030 v/°K for pocket cells.

Manuscript received Dec. 10, 1959. This paper was prepared for delivery before the Columbus Meeting, Oct. 18-22, 1959.

Any discussion of this paper will appear in a Discussion Section to be published in the June 1961 JOURNAL.

REFERENCES

1. W. Jungner, Swedish Pat. 10,177, March 11, 1899, and 11,487; Oct. 23, 1899.
2. E. V. Condon and H. Odishaw, "Handbook of Physics," McGraw-Hill Book Co., New York (1958)
3. W. Jungner, Swedish Pat. 15,567, Jan. 22, 1901.
4. C. Troilius, Unpublished paper.
5. O. Glemser and J. Einerhand, *Z. Elektrochem.*, **54**, 302 (1950).
6. J. Zedner, *ibid.*, **12**, 463 (1906).
7. G. W. Vinal, "Storage Batteries," 4th ed., p. 203, J. Wiley & Sons, Inc., New York and London (1955).
8. Allmand and Ellingham, "Appl. Electrochemistry," 2nd ed., p. 256, Longmans, Green and Co., New York (1924).
9. F. Foerster, *Z. Elektrochem.*, **13**, 414 (1907).
10. J. T. Crennell and F. M. Lea, "Alkaline Accumulators," p. 94, Longmans, Green and Co., London (1928).
11. M. DeKay Thompson and H. K. Richardson, *Trans. Electrochem. Soc.*, **7**, 95 (1905).
12. National Educational Association monograph.
13. H. Pender, "Handbook for Electrical Engineers," p. 77, John Wiley & Sons, Inc., New York (1917).
14. A. Hauel, *Trans. Electrochem. Soc.*, **76**, 435 (1939).
15. T. A. Edison, British Pat. 20960, 1900.
16. D. W. T. Kirkman and F. Watson Mann, "Alkaline Accumulators," p. 10, (1932).
17. O. Glemser and J. Einerhand, *Z. Anorg. Chem.*, **261**, 26 (1950).
18. G. W. D. Briggs and W. P. K. Wynne-Jones, *Trans. Faraday Soc.*, **405**, 1272 (1956).
19. K. Huber, *Z. Elektrochem.*, **62**, 675 (1958).
20. P. E. Lake and E. J. Casey, *This Journal*, **105**, 52 (1958).
21. D. P. Bogatskii, *Zhur. Obshchei Khim.*, **21**, 3 (1951).
22. R. A. Baker, Bell Labs Memorandum, Oct. 26, 1955.
23. R. W. Cairns and E. Ott, *J. Am. Chem. Soc.*, **55**, 527 (1933); **56**, 1094 (1934).
24. G. L. Clark, W. C. Asbury, and R. M. Wick, *ibid.*, **47**, 2661 (1925).
25. A. J. Salkind and P. F. Bruins "Investigation of the Sintered Plate Nickel-Cadmium Battery," Final Report: Nov. 1, 1955-Feb. 28, 1958, Polytechnic Institute of Brooklyn.
26. O. Hahn, *Naturwissenschaften*, **17**, 295 (1929).
27. S. Lindroth, *J. Am. Ceram. Soc.*, **32**, 198 (1949).
28. A. L. Pitman and G. W. Work, NRL Report 4845 (1956).
29. H. Winkler, *Dtsch. Elektrotech.*, **11**, 223 (1957).
30. M. U. Schoop, *Electrochem. Ind.*, **2**, 272, 310 (1904).
31. M. Stanimirovitch, *La Revue du Nickel*, April-May-June, 1958.
32. A. B. Mundel, *Direct Current*, Sept. 1954.
33. L. M. Elina, T. I. Borisova, and Ts. I. Zalkind, *Zhur. Fiz. Khim.*, **28**, 785 (1954).
34. E. Jones and W. F. K. Wynne-Jones, *Trans. Faraday Soc.*, **405**, 1260 (1956).
35. T. Hosono and K. Watanabe, *J. Electrochem. Soc. Japan*, **19**, 14 (1951).

Oxidation Properties of Tantalum Between 400° and 530°C

J. V. Cathcart, R. Bakish, and D. R. Norton

Metallurgy Division, Oak Ridge National Laboratory, Oak Ridge, Tennessee; Alloyd Corporation, Cambridge, Massachusetts; and Sprague Electric Corporation, North Adams, Massachusetts, respectively

ABSTRACT

The rate of oxidation of tantalum in 1 atm of purified oxygen was measured at three temperatures between 475° and 530°C. The oxide was initially protective but became nonprotective as oxidation progressed. This kinetic behavior was correlated with metallographic and electron optical studies of oxidized Ta specimens, and it was shown that the oxide films became nonprotective through the formation of microscopic blister-like cracks in the oxide. A comparison between the oxidation characteristics of Ta and Nb is given.

In the course of an investigation of the factors which control the degree of protectiveness of oxide films, a study of the oxidation of tantalum in the range 400°-530°C was undertaken. An attempt was made to correlate the results of kinetic, metallographic, and electron optical studies in order to elucidate the oxidation mechanism for tantalum.

Previous investigations of the gaseous oxidation of tantalum have been limited either to rather low temperatures or to short times at higher temperatures. Thus Waber, *et al.* (1) determined the rate of oxidation of tantalum spectrophotometrically and reported a logarithmic form for the rate equation for temperatures from 320° to 450°C. Gulbransen and Andrew (2) observed rate curves of a parabolic type for the 120-min examination period which they employed at temperatures ranging from 250° to 450°C. Vermilyea (3) studied the oxidation rate of tantalum in the temperature range 50°-300°C, and Fassel and co-workers (4) investigated the effect of high oxygen pressure on the oxidation of tantalum at temperatures from 500°-900°C.

Procedure and Results

In the present research, rates of oxidation of tantalum were determined at 475°, 515°, and 530°C. Oxidation specimens were in the form of coupons 1 x 2 x 0.3 cm. Specimens were carefully mechanically polished and prior to oxidation were annealed overnight at a pressure of 10^{-5} mm Hg at the oxidation temperature.

Oxidation rates were determined from the decrease in oxygen pressure in a closed system as oxidation proceeded. Pressure changes were measured with a sensitive differential manometer similar in design to that previously used in a study of the oxidation rates of the alkali metals (5). Oxidations were performed in purified oxygen at approximately atmospheric pressure. The sensitivity of the manometer was such as to permit the detection of a 5Å change in oxide thickness on the tantalum specimens.

The results of these experiments are illustrated in Fig. 1 and 2 where data from representative experiments are given. The quantity of oxygen consumed per square centimeter is plotted against the time of oxidation. A protective film was formed during the early stages of oxidation, but with increasing time a transition period was reached in which the rate of oxidation increased. Finally, the film became virtually nonprotective, and the oxidation rate curve tended toward linearity. The length of the protec-

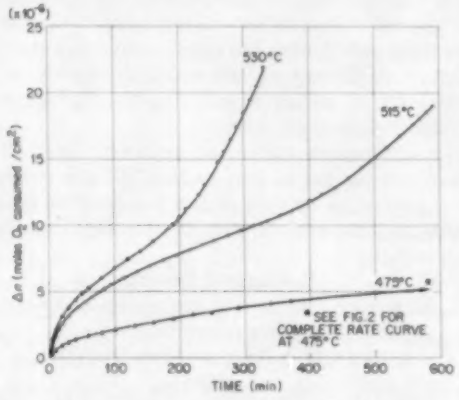

Fig. 1. Oxidation rate curves for Ta at 475°, 515°, and 530°C.

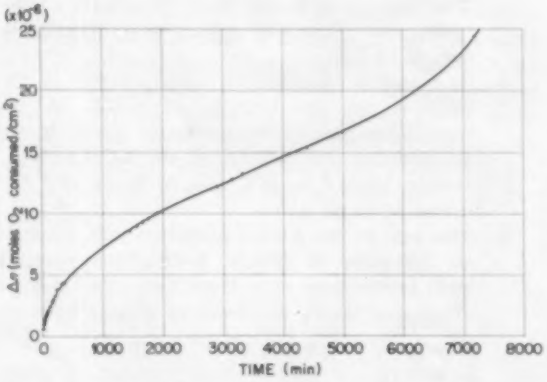

Fig. 2. Oxidation rate curve for Ta at 475°C

tive stage of oxidation varied inversely with temperature. Qualitatively the kinetic behavior of tantalum was very similar to that previously reported for niobium (6).

As a corollary to the rate measurements, the microtopography of the surfaces of oxidized tantalum specimens was examined. Tantalum coupons were prepared in the same manner as described above and oxidized for varying periods of time at temperatures ranging from 400° to 525°C. The oxidized specimens were then preshadowed with gold-manganin and replicated with carbon, and the replicas examined in an electron microscope.

The surfaces of freshly prepared specimens, either chemically or electrolytically polished, exhibited a texture suggestive of bubble-raft dislocation models (see Fig. 3). The origin of this texture is not understood, but it was obtained with a very high degree of reproducibility and persisted during the earliest stages of oxidation. Continued reactions resulted in the superposition on this texture of a pattern of acicular features. As may be seen in Fig. 4, these needle-like structures formed very regular arrays whose orientation varied from grain-to-grain of the substrate metal. This pattern was observed on oxidized specimens which previously had been annealed thoroughly and either chemically or electrolytically polished. On specimens which had been subjected to mechanical polishing only, no such pattern was formed, the oxide film produced under these circumstances exhibiting instead a slight, rather nondescript surface roughening. These results emphasize the relationship between the state of perfection of a metal surface and its oxidation characteristics. Prominent surface features of the oxide film formed on Ta are clearly related to the crystallography of the substrate metal.

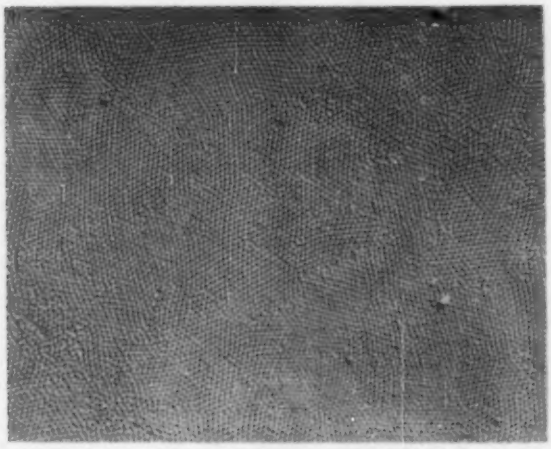

Fig. 3. Electron micrograph of the surface of an electropolished, unoxidized Ta specimen. Indirect carbon replica, Pd shadowed. 33,000 X (All magnifications are before reduction for publication.)

Fig. 4. Electron micrograph of the surface of a Ta specimen oxidized for 24 hr at 400°C. Direct carbon replica, preshadowed with gold-manganin. 7,500X.

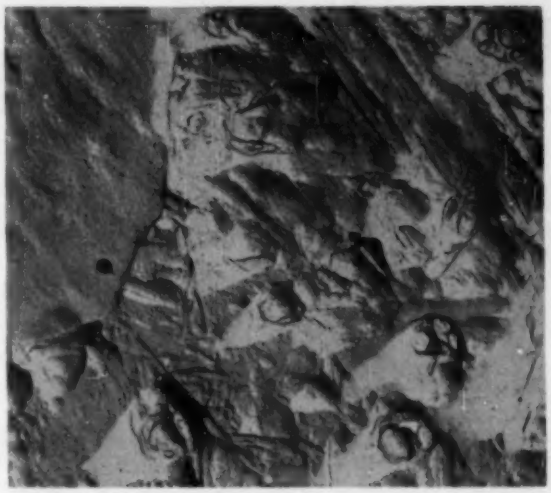

Fig. 5. Electron micrograph of the surface of a Ta specimen oxidized for 10 hr at 515°C. Direct carbon replica, preshadowed with gold-manganin. 12,500 X

At temperatures of 450°C and above, still further oxidation resulted in the formation of numerous cracks and blister-like ruptures in the oxide (see Fig. 5). Such cracks were found after 72, 48, and 4 hr of oxidation at 450°, 475°, and 500°C, respectively.

It was noted that the bubble-raft texture was visible on electropolished Ta specimens before oxidation and that it remained unchanged during subsequent oxidation. Thus the oxidizing of a Ta sample automatically constituted a marker experiment. Since the "markers" receded from the oxide/metal interface, it was concluded that anion diffusion occurred across the Ta_2O_5 film.

Further insight into the oxidation mechanism of Ta was obtained through a metallographic study of taper and cross sections through oxidized Ta specimens. Taper sections such as that shown in Fig. 6 indicated that the oxide film, rather than being confined to a layer parallel to the metal surface, extended into the metal in the form of slightly lenticular platelets parallel to {100} planes of the metal (7). The platelets of oxide appeared to be associated with the needle array observed on the surface of the oxide, and it was thought that the needles represented traces of the platelets on the surface. The formation of similar platelet-like sheets of oxide in

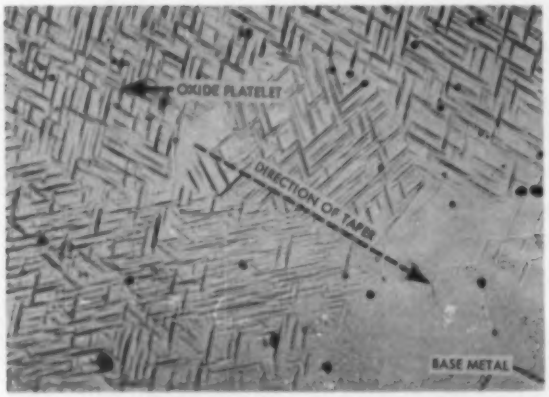

Fig. 6. Low-angle taper section through a Ta specimen oxidized 4 hr at 500°C showing traces of oxide platelets. Depth of cut into specimen increases from left to right. Specimen cathodically etched after polishing. 500 X

Ta was also observed at much higher temperatures and lower pressures of Gebhardt and Seghezzi (8).

Electron- and x-ray diffraction patterns of oxidized tantalum specimens revealed the presence of Ta_2O_5 only. The oxide was crystalline both before and after cracking of the films occurred.

Discussion

The oxidation of Ta proceeded through the formation of a very thin, relatively smooth surface oxide film followed by the production of small platelets of oxide extending into the metal parallel to {100} planes of the metal. The traces of these platelets were visible as acicular forms in the surface oxide. Continued oxidation eventually caused a rupturing of the covering oxide film.

This picture is consistent with the results obtained in the kinetic studies of the oxidation of Ta which indicated an initial protective stage of oxidation followed by a marked increase in the oxidation rate and the on-set of nonprotective oxidation. The increase in oxidation rate was related to the cracking of the oxide film.

It is of interest to compare the oxidation characteristics of Nb and Ta. Important differences exist between the oxidation of the two metals. Two of the major features of oxide films on Ta—the formation of platelets of oxide extending into the metal and the related array of needle-like structures observed on the surface of the oxide—have not been detected in Nb oxide films. On the other hand, striking analogies also have been found in the oxidation properties of the two metals. The oxidation kinetics of both are similar in that at low temperatures both form protective oxide films, for both there is a temperature range in which an initially protective film becomes nonprotective as the time of oxidation increases, and at high temperatures both metals exhibit linear oxidation rate curves. The transition from protective to nonprotective oxidation in both cases is accompanied by similar crack formation in the oxides. Both form analogous series of oxides, and Ta_2O_5 and Nb_2O_5 are crystallographically isomorphous with almost identical lattice parameters (9). Both Ta_2O_5 (10) and Nb_2O_5 (11) are metal-excess semiconductors. These data together with the results of marker experiments indicate that this departure from stoichiometry is due to the presence of anion vacancies in the oxide.

The mechanism of the formation of the oxide platelets is still under investigation; however, the production of the acicular features on the surface of the oxide and the eventual cracking of the oxide films appear to be related at least in part to the mode of diffusion in Ta_2O_5 and to the ratio of the volumes of equivalent amounts of oxide and metal. The model proposed to account for these phenomena is similar to that previously discussed for the oxidation of niobium (6).

If it is assumed, as suggested above, that the oxidation of Ta proceeds via an anion diffusion mechanism, it follows that the new oxide is formed at the oxide/metal interface (or at least that the bottom of the Ta_2O_5 layer if small amounts of the lower oxides are present). A volume increase of approximately 250% is required when Ta is converted to Ta_2O_5. This expansion, however, will be resisted by the already overlying layer of oxide, and the formation of new oxide will be accompanied by the plastic deformation of the existing oxide film. Thus the oxidation process itself continuously produces stresses in the oxide film. In terms of this hypothesis, the stresses resulting from the formation of platelets of oxide in the metal during the oxidation of Ta tend to cause the platelets to press against the layer of covering oxide, deforming this surface film and producing the acicular array already described. Continued oxidation leads to the build up of severe, localized stresses which eventually cause the rupturing of the oxide film.

Manuscript received Dec. 31, 1959.
Any discussion of this paper will appear in a Discussion Section to be published in the June 1961 JOURNAL.

REFERENCES

1. J. T. Waber, G. E. Sturdy, E. M. Wise, and C. R. Tipton, AECU-1355, (1951).
2. E. A. Gulbransen and K. F. Andrew, *J. Metals*, **188**, 586 (1950).
3. D. Vermilyea, *Acta Met.*, **6**, 166 (1958).
4. R. C. Petersen, W. M. Fassell, and M. E. Wadsworth, *J. Metals*, **6**, 1038 (1954).
5. J. V. Cathcart, L. L. Hall, and G. P. Smith, *Acta Met.*, **5**, 245 (1957).
6. J. V. Cathcart, J. J. Campbell, and G. P. Smith, *This Journal*, **105**, 442 (1958).
7. R. Bakish, *ibid.*, **105**, 71 (1958).
8. E. Gebhardt and H. D. Seghezzi, *Z. Metallkde.*, **5**, 248 (1959).
9. N. Schönberg, *Acta Chem. Scand.*, **8**, 240 (1954); S. Lagergren and A. Magneli, *ibid.*, **6**, 444 (1952).
10. W. Hartmann, *J. Physik.*, **102**, 709 (1936).
11. O. Kubaschewski and B. E. Hopkins, "Oxidation of Metals and Alloys," Academic Press, New York (1953).

Equilibrium Space Charge at the Contact of a Metal and a Pure Highly Insulating Liquid and Its Influence on High-Field Conductivity

M. J. Morant

Queen Mary College, University of London, London, England

ABSTRACT

The high-field conduction of a highly purified insulating liquid such as hexane may be largely influenced by electron emission from the cathode. Theoretical interpretations have so far neglected the fact that in equilibrium a space charge layer will probably exist at the contact of a metal and such a liquid, similar to that at a metal-semiconductor contact. The effect of this cannot be calculated without more information, but it does explain the observations that the conduction currents are relatively insensitive to cathode work function. A novel electrostatic method is described which, it is believed, can directly measure the potential of such an electronic double layer at the contact of a metal and a dielectric.

Conduction processes in highly purified insulating liquids are of fundamental interest apart from their value in helping to explain electrical breakdown under extremely high applied fields. A study of the electrical properties of such liquids would ideally give information on the types of charge carrier, their mobilities, trapping and recombination times, etc., and their relationships in determining the actual current and field distribution in a liquid with a given electrode configuration. The variation of the current with the controllable conditions of time, temperature, purity, electrode surface, etc., would follow, electrode processes being particularly important for possible electronic devices. However, little fundamental information is so far available because most of the methods used for investigating gases and solids cannot be used for insulating liquids. In spite of this, the correct interpretation of conductivity measurements alone should be able to provide much information if carried out over a wide enough range of experimental conditions, and particularly as a function of applied field strength. It has recently been shown (1) that with careful technique it is possible to measure the d-c conductivity of a highly purified simple hydrocarbon such as hexane right up to breakdown fields, and this can provide indications of the origins of the current-carrying charges. As field strengths of hundreds of kv/cm are required to obtain currents of about 10^{-10} amp in such liquids, it is not surprising that there have been inconsistencies in the findings of different investigators arising from differences of technique, purity of the liquid, and electrode preparation. Supplementary measurements, not involving conductivity, may therefore be of value in elucidating the critical factors. It is the purpose of this paper to introduce a new type of measurement that can be made on the interface of a highly insulating liquid (or solid) and a metal electrode without applying an external field of any kind. It is believed that this new effect gives the potential difference across an intrinsic space charge layer at the contact of a metal and an insulator.

Before describing the experimental method a brief review is given of the ways in which the electrodes could influence the conductivity, and it is shown that the effects of a double layer between the metal and the liquid must always be included.

Electrode Effects in Liquid Conductivity

Charge transfer in dielectric liquids is more complicated than in either gases or solids. Low energy electrons in a liquid may move in two ways, (i) transferring from molecule to molecule in the field direction, or (ii) trapped permanently to a single molecule which moves as a whole through the liquid. Within each molecule the electron can probably move comparatively freely, but the over-all mobility in the liquid is low whether the electron moves with the whole molecular ion or in a series of jumps between molecules. Charge is probably transferred in both the above ways simultaneously, an electron moving as a large molecular ion until a suitable molecular configuration occurs for the electron to transfer to a neighboring molecule. It may not be possible to distinguish, even theoretically, between the two transport mechanisms. In gases, electron transfer between an ion and a molecule is unlikely because of the low density; also, electrons can move freely between the molecules. In a solid the periodicity leads to a high electron mobility through the lattice, but a trapped electron (i.e., ion) has zero mobility. In both cases it is possible to distinguish between a free electron and an ion. This is not so in a liquid, and a new theoretical background may have to be developed.

Similar reasoning may hold for the transport of positive charge in a liquid. A positive ion may move in the same way as in a gas, but there is the additional possibility that the ion may be neutralized by the transfer of an electron from a neighboring molecule. In this way a positively charged electron vacancy could move through the liquid, corresponding to the movement of positive holes in a semiconducting solid. As for electron transfer it is probably impossible to distinguish between electron vacancies and ion movement. The proportion of the current carried by electrons or electron vacancies as compared with negative or positive ions will depend on the ease with which an electron can be transferred *between* molecules rather than for the whole molecular ion to move.

Any theory of the conduction of dielectrics has, in addition, to account for the origin of the current-carrying charges, and to explain how they are transferred between the insulator and the electrodes. Two distinct types of electrode process exist: (*a*) the electrodes may *emit* all the charged particles required to carry the current; or (*b*) the electrodes may *neutralize* charges which are produced naturally within the dielectric.

The first case includes electron emission from the cathode which is considered further below. Similarly, electron vacancies could be emitted from the anode by the extraction there of an electron, as in a semiconductor. Case (*b*) includes the normal electrolytic effects where the charge originates in the bulk of the liquid due to the dissociation of impurities, absorption of radiation, etc. Both positive and negative ions may be neutralized at the electrodes. When charges originate at the electrodes the conductivity will probably depend greatly on the electrode material, etc., but this is not so if the charge is produced within the liquid.

In general, electrodes can simultaneously perform both functions (*a*) and (*b*) above, e.g., as in a gas discharge where electrons are emitted from the cathode and positive ions neutralize there. Again, in a semiconductor there is a certain naturally occurring charge density (electrons, holes, and charged impurities) and additional charges (minority carriers) may be injected from a contact so that both types of process are operative.

In liquids, as in the other examples, the proportion of the charge carriers originating in the bulk and from the electrodes probably depends on the experimental conditions and on the applied field strength. For example, bulk impurities may account for the low-field conductivity and the emitted charges for the increase of the current with field strength. House (1) has produced evidence for collision ionization in hexane at the highest fields in certain conditions, this being another mechanism by which free charge can originate in the bulk. Whichever source of charge predominates, however, it is important to consider the equilibrium between the charges emitted from the electrodes and those produced within the liquid. It will be shown that one consequence of this is that a space charge layer will always exist in a dielectric liquid close to the electrodes, in the same way as at the contact of a metal and a semiconductor. This layer should greatly influence the charge transfer to the liquid even in cases where the electrode effects predominate.

Theories of the conduction of highly purified liquids have usually either entirely neglected the electrode effects or the presence of charges occurring naturally in the bulk of the liquid. Several authors (1-6) have attempted to explain the high-field conduction in terms of field-aided electron emission from the cathode, but it will be shown that this model must be seriously modified to allow for the production of free charge within the liquid also. The emission theories usually neglect the liquid apart from its dielectric constant, K, and its possible effect in lowering the work function of the metal, so that the conduction current is limited only by the cathode emission, and the electrons are implicitly regarded as being free within the liquid. At the high fields concerned, 10^5-10^6 v/cm, electron emission from the metal may occur by the Schottky process of field-aided thermionic emission, or by Fowler-Nordheim cold emission depending on the conditions. As in the case of electron emission into gases, the former is more likely to give agreement between experimental values and reasonable theoretical estimates of work function, field intensification, and emitting area (7, 8). Even so, the agreement is not perfect, and more elaborate models have been proposed to explain the emission (6, 9).

A serious objection to emission-limited theories of liquid conduction was first raised in 1937 by Plumley (4). Emission should depend on the work function of the cathode, possibly modified from its vacuum value by the presence of the liquid. Plumley showed that, within experimental error, brass and gold cathodes gave the same current in iso-octane up to 175 kv/cm. Thermionic emission (with the vacuum values of the work function) would have given currents in the ratio of 3.10^5:1. More recently, Green (6) has investigated the dependance of conduction currents in hexane on the cathode conditions and has found a variation over a range of about 100:1, but dependant more on the surface layer, as affected by heat treatment, than by the material of the cathode. House (1) found a maximum difference of only 3:1 between silver and chromium electrodes in hexane. Zaki (10), also working in this laboratory, has obtained similar results, and has also shown that differences of up to 100:1 in the high-field currents in hexane may result from the state of oxidation of the cathode. All these results suggest that the conduction is influenced by the cathode, but that it is unlikely to depend simply on the work function. It will be shown that this may be explained by considering the complete surface barrier when some of the free charge is produced within the liquid. But first it is necessary to consider the charge density at the interface of a metal and a dielectric liquid.

Equilibrium Space Charge

The electron density outside the range of image forces of a metal surface of work function ϕ is

$$n_\infty = 2\left(\frac{2\Pi mkT}{h^2}\right)^{3/2} e^{-\phi/kT} \text{ cm}^{-3} \qquad [1]$$

Away from such a metal surface in a vacuum the electron density, $n(x)$, decreases indefinitely, and the electrostatic potential, V, rises as required by the Boltzmann distribution and Poisson's equation

$$n(x) = n_s e^{-eV/kT} \qquad [2]$$

and

$$\frac{d^2V}{dx^2} = -4\pi ne \qquad [3]$$

in the one-dimensional case. This is the "electron atmosphere" that always exists in equilibrium with a metal surface in a vacuum. It is distinct from the denser space charge that occurs when current is drawn. At the contact of a metal and an idealized dielectric, there is a similar electron atmosphere except that the dielectric constant, K, has to be included as a denominator in [3], and the electron density, n_s, may be very much greater than at the vacuum interface due to the lowering of the work function of the metal by the dielectric to a value ϕ^*. The difference $(\phi - \phi^*)$ may be regarded as the potential energy of the lowest electronic conducting level in the dielectric (Fig. 1a and b).

The potential rise in the electron atmosphere outside a plane metal surface is easily calculated from [2] and [3] (11). At room temperature the electron density is very low and in vacuum, for example, the potential rises to only 35 mv at a distance of 32 cm from a metal having a work function of 1 ev. The potential rise is even slower for practical values of ϕ. However, the result is very sensitive to *lower* values of ϕ as may be encountered at the contact with a dielectric. For instance if $\phi^* = 0.5$ ev the same potential rise occurs in $3 \cdot 2.10^{-4}$ cm. For two plane electrodes, solutions of [2] and [3] may also be found giving the potential in the enclosed electron space charge. Von Laue (12) and Fowler (13) have shown that the potential close to each electrode is scarcely affected by the presence of the other. In equilibrium the normal contact p.d. occurs between the electrodes and the potential in the gap reaches a peak at a position determined by the work functions. Skinner (14) has considered the current that would flow in an idealized dielectric, containing an electron atmosphere of this form, on applying an additional potential difference.

There are two respects in which a real dielectric may be expected to differ from this idealized case, and both affect the form of the potential variation. In the idealized dielectric the electron density can decrease continuously toward zero (limited only by the applicability of [2] and [3]), but in any real dielectric a lower limit is set by the naturally occurring charge density which, as explained above, will be formed in a liquid by the dissociation of impurities, absorption of stray radiation, and possibly by thermal excitation. For neutrality equal positive and negative charge densities must be produced in the bulk of the liquid. If an electron density n_i cm^{-3} is formed the potential rise in the space charge between the metal and the bulk of the dielectric must be limited to

$$V_\infty = \frac{kT}{e} \log_e \frac{n_s}{n_i} \qquad [4]$$

as shown in Fig. 1c. This potential difference can be regarded as a first approximation to the contact potential between the metal and the interior of the liquid due to the naturally occurring charge density in the latter. A space charge barrier setting up this potential is required for equilibrium at the interface in the same way as at the contact of a metal and a semiconductor. Equation [4] may in fact be derived from the true equilibrium condition which is the equality of the electrochemical potentials in each phase. Similarly the electron atmosphere in a vacuum is required to try to bring it into equilibrium with the metal.

The second specific effect of the dielectric is to concentrate this "equilibrium space charge" much closer to the interface than in a vacuum. In a real liquid dielectric, the electrons will not be distributed as a perfectly free gas, they will not diffuse far into the liquid, and Eq. [2] will no longer be valid. Any tendency for electrons to become trapped in or between molecules will concentrate the space charge layer even closer to the metal surface as shown in Fig. 1d. With a low effective work function an appreciable part of the equilibrium space charge could be within 10^{-4} cm of the metal.

When considering the emission of electrons into a vacuum the potential of the electron atmosphere is extremely small compared with other surface forces. In liquids, the theories of field-aided electron emission have also neglected the equilibrium space charge, although it now seems probable that it could give appreciable potential changes even within the range of image forces. For this reason the conductivity of liquids is unlikely to be explained by models for the emission of electrons into a vacuum. The above description of the equilibrium space charge applies strictly only when there is no applied field. Much more information about charge carriers, their mobilities, trapping effects, etc., will be required before it is possible to predict the influence of contact space charge on current flow in liquids even with low fields: the methods would be expected to be similar to those developed for metal-semiconductor contacts. The difficulties are even greater for high applied fields. The conductivity increases by anything up to six orders of magnitude between low fields and breakdown. Assuming that this is due to increasing current-carrying charge density in the bulk, the potential across the space charge in the contact region would fall by only 0.6 v (from Eq.

Fig. 1. Potential energy of an electron at the contact of a metal and a dielectric. (a) Vacuum; (b) idealized dielectric; (c) dielectric with bulk charge; (d) dielectric with bulk charge and trapping.

[4]). This emphasizes that the contact space charge rather than straightforward electron emission from the cathode is important up to the highest applied fields.

Although the current flow through the complete surface barrier cannot yet be calculated, the equilibrium space charge has one important consequence which is confirmed experimentally. Electron emission from a cathode to the surface region of a liquid is controlled by the modified work function, ϕ^*, of the metal. The space charge imposes the additional potential barrier, V_∞, which from [4] and [1] is

$$V_\infty = \frac{kT}{e}\left\{\log. 2\left(\frac{2\Pi mkT}{h^2}\right)^{3/2} - \frac{\phi^*}{kT}\right\} - \frac{kT}{e}\log. n_1$$

or substituting numerical values, with $T \sim 300°K$, the total barrier height is

$$\left(V_\infty + \frac{\phi^*}{e}\right) = 1{\cdot}115 - \frac{1}{40}\log. n_1 \text{ v} \qquad [5]$$

That is, the total potential barrier between the Fermi level of the metal and a conducting level in the liquid is independent of the work function of the metal, but it does depend on the liquid charge density. A low work function gives a high electron density at the interface and so a large space charge potential, and vice versa (Fig. 2). Thus the relative insensitivity of conduction currents in simple liquids to the cathode material is not incompatible with emission-limited conduction modified by the equilibrium space charge barrier. This removes the major objection to emission theories first stressed by Plumley and confirmed since. Although the barrier height is constant, a relatively small cathode dependence would still be expected due to differences of the barrier shape with ϕ^* and V_∞.

It must be stressed that this model is highly simplified and that it assumes electronic equilibrium between the metal and the liquid. The presence of either positive or negative ions alters the double layer potential V_∞, but whatever the details, some sort of space charge layer must exist at the interface for equilibrium. The experimental work described below also directly demonstrates the existence of such a space charge layer. At first sight the above model cannot account for the considerable effect of the state of oxidation of the cathode on the conductivity of dielectric liquids. The equilibrium space charge is unaffected by replacing a clean metal surface by an oxide of the same work function so the conduction currents should also be independent

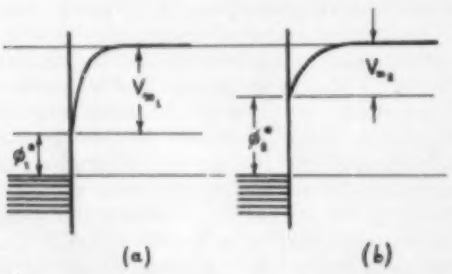

Fig. 2. Potential energy at the contact of a dielectric and electrodes of (a) low, and (b) high work function.

of the oxide work function. However, with current flow across an insulating oxide layer the equilibrium between the solid and the liquid may be seriously disturbed. Electrons may not be able to pass through the oxide layer quickly enough to maintain the equilibrium concentration, n_∞, or the space charge potential V_∞. The emission current would then be partly limited by the potential across the oxide layer. On the other hand, an unoxidized metal surface could always provide sufficient electrons to maintain the contact space charge in equilibrium right up to the maximum currents found in very pure liquids. Much more information is required before it is possible to differentiate between several possible mechanisms at the oxidized cathode.

Experimental Determination of the Space Charge Potential

It is not possible to detect the equilibrium space charge at the contact of a metal and a very highly insulating liquid by any of the classical methods of electrochemistry. However, a new type of electrostatic effect is described below which is believed to measure directly the potential of the double layer formed by the negative space charge and the positive charge induced on the electrode.

The measurement has similarities to the Kelvin method of measuring the contact or Volta potential between dissimilar metals. Plumley (4) and Macfadyen and Holbeche (15) have shown that the contact potential, measured in this way, is changed only slightly by totally immersing both electrodes in an insulating liquid. This would be expected unless the liquid reacted in different ways with each electrode. If there are contact potentials between each metal and the liquid, they cancel out around the circuit, and they cannot be detected by changing the total capacitance between the electrodes as in the Kelvin method. It is believed that this is overcome in the new method by measuring the change of potential of one of the electrodes when its *contact area* with the liquid is changed. The opposite electrode, usually earthed, remains totally immersed. A suitable arrangement is shown in Fig. 3a. An insulated conical electrode just pierces the surface of the liquid held in a metal cup. It is found that the potential of the cone changes reversibly as it is moved in and out of the liquid. Part of this change is due to the contact potential between the metal surfaces detected by the change in the total capacitance as in the Kelvin method, but this may be measured separately, and there is an additional potential change thought to be due to the charge transfer from the metal to the contact region in the liquid. Owing to the high insulation of both the metal and the liquid at the contact, the contact potentials round the whole circuit (including the liquid) cancel out extremely slowly, so that the contact potential across a single interface (where the contact area changes) may be detected. In this way it is a unique type of measurement.

A simplified theory by which the measured potential can be related to the double layer potential will be given. Figure 4 shows the charge distribution on the whole system arising from a double layer at

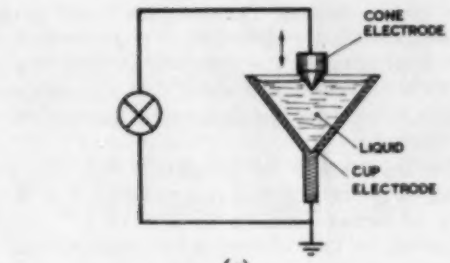

(a)

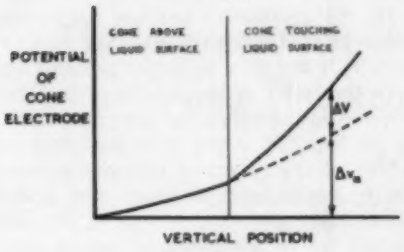

(b)

Fig. 3(a). Experimental arrangement for measuring the equilibrium space charge potential at the contact of a metal and an insulating liquid. Fig. 3(b). Form of the potential variation as the cone electrode touches the liquid surface.

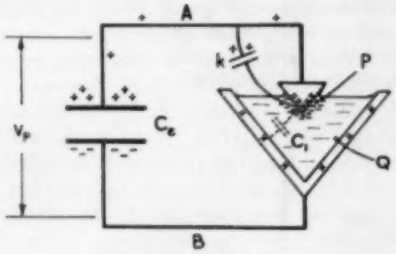

$$V_p = V_l \frac{C_l}{C_l + C_c}$$

Fig. 4. Charge distribution due to double layer of potential v_l at contact P.

the conical electrode, P. The charge at this contact is assumed to be positive on the metal and negative just inside the liquid, the potential difference being v_l. The metal A has lost negative charge as a whole to form this double layer. All this charge is concentrated just inside the liquid at P. Every element of capacitance, such as k, between the contact region of the liquid and the metal A must be charged to the double layer potential. Thus not quite all of the induced positive charge is on the contact surface of the metal. If the insulation of the system (including the liquid) is perfect, there are also induced charges on the electrometer (represented by the capacitance C_c, Fig. 4) and on the opposite metal electrode B. In the external circuit the double layer potential v_l is divided capacitively by C_c and C_l, where C_l is the capacitance between the whole of the cup electrode B and the negative charge layer just inside the liquid at P. Therefore, due to the double layer at P, there exists a potential

$$v_p = \frac{v_l C_l}{C_l + C_c}$$

across the electrometer.

By similar reasoning, a double layer of the same polarity but of potential v_s at the opposite interface of the metal and the liquid gives rise to a potential v_s across the electrometer. The two charge distributions are independent and the electrometer potentials may be added to give the net potential, v, due to the two double layers.

$$v = v_p + v_s = \frac{v_l C_l}{C_l + C_c} - \frac{v_s C_s}{C_s + C_c} \qquad [6]$$

where C_s is the capacitance between the negative charge layer just inside the liquid at Q and the whole of the metal A.

In practice it is not possible to measure the steady potential v as it is swamped by stray charges left by contact potentials, etc., on setting up the system, so a difference method must be used. By slightly moving the cone electrode, the contact area with the liquid at P is changed without greatly changing the total capacitance between the electrodes. Therefore the potential of the spurious charges remains practically constant. However, the electrometer potential, v, due to the double layers is much more sensitive to contact area as the capacitance C_l is due to the field between the negative charge at the contact and the whole of the opposite metal. The corresponding term C_s associated with the opposite double layer of fixed area, at Q, is unaffected, to a first approximation, by the area change at P. Therefore for a small change of contact area at P, the change of the potential across the electrometer is given simply by

$$\Delta v = \frac{v_l \Delta C_l}{C_l + C_c} \qquad [7]$$

and if the capacitances of the system are known, v_l, the potential of a single double layer, may be directly measured.

The above treatment is very simplified, and the full analysis is not given here. The only basic assumptions that have to be made are that the negatively charged layers are thin compared with the dimensions of the apparatus, and that the equilibrium space charge at the contact is set up rapidly, i.e., within a second or two of changing the contact area. The full expression for Δv includes terms due to *both* the metal-liquid interfaces, and for the normal contact potentials between the electrodes (16). The partial and total capacitances of the system have to be examined in detail. Each one is of a few $\mu\mu$farad and of a distributed nature, so that the associated field has to be defined. A measuring technique must be devised for each partial capacitance without deforming the field by the introduction of probes. The analysis eventually gives the potential change, Δv, as a function of the penetration of the liquid surface by the conical electrode, in terms of the potentials v_l and v_s. By initially preparing both electrodes in the same way, the double layers may be assumed to be the same, and they can be found from measurements of Δv by setting $v_l = v_s$. Subsequently the double layer of the single contact between the conical electrode and the liquid may be investigated by keeping constant the surface treat-

ment of the opposing cup electrode. The effect of the preparation and material of the conical electrode may be found in this way.

In practice, measurements of electrostatic potentials of a few millivolts in systems of extremely high resistance and very low capacitance are confused by several spurious effects which may be difficult to eliminate or separate, and the present measurement is one of considerable difficulty. It is hoped to describe experimental details in full elsewhere (17). Our first work on this topic followed the discovery of the effect in solid insulation. In that case, the electrodes in contact with a block of the dielectric consisted of an earthed flat plate and a conical or spherical indenter connected to the grid of an electrometer valve (18, 16). Potentials of up to about 60 mv were obtained for a small change of the spherical contact area, but it is now known that these were largely due to the sensitivity of electrometer valves to the precise value of the external resistance: this varies with the contact area in the same way as the expected electrostatic charging (19). The effect is important for all measurements of small charges. It must be allowed for also in measuring the change of potential associated with the change of area of a metal-liquid contact. Comparatively large indicated potentials may also be due to contact potentials between metals. When the total capacitance, C_{12} between the electrodes is changed by slightly moving one of them, the potential changes instantaneously by

$$\Delta v_{12} = v_{12} \frac{\Delta C_{12}}{C_{12}}$$

where v_{12} is the contact potential. The contact p.d. plus the potential due to stray charges is measured independently by moving the conical electrode just above the liquid surface before making actual contact. The double layer effect, Δv, must then be absent. Figure 3b shows how Δv_{12} is extrapolated by independent measurements of the total capacitance, C_{12}, to separate the spurious and true double layer components of the measured change of potential after contact is made. It can be shown that this extrapolation is justified for nonpolar liquids as the change of C_{12} due to the dielectric constant of the liquid is negligible.

When allowance is made for these and other spurious effects, the reversible change of potential, Δv, is of the order of 1 mv/mm of penetration of a conical stainless steel electrode into hexane. The form of the potential variation agrees with that expected from the full expression for Δv in terms of the partial capacitances. Several other possible side effects that could account for the change in the electrode potential have been eliminated either by features of the experimental results or by experimental precautions, and no alternative can be found to the explanation of the measurements in terms of the interfacial double layer. Most of the work has been concerned with proving that this is so, and tests have so far only been made with stainless steel electrodes and highly purified n-hexane. Results show that the interfacial double layer always has the negative side toward the liquid as required for an electron space charge. The double layer potential, derived from Δv, is found to vary between 0.3 and 0.6 v depending on the electrode surface treatment, but an average value of about 0.42 v is obtained by leaving the electrode immersed in hexane for several days.

This result may be compared with the simple theory of the equilibrium space charge. The conductivity of hexane can be as low as 10^{-20} mho/cm. Assuming, for lack of precise information, that there are no bulk space charge effects, this corresponds to about 10^9 charge carriers per cm^3 for a mobility of 10^{-4} cm^2/v sec [LeBlanc (20)]. As such a low conductivity is found only in highly purified liquids, this may be the order of magnitude of the electron density formed in the liquid by stray radiation, etc. If this is so, Eq. [5] shows that the total height $(V_\infty + \phi^*/e)$ of the potential barrier between the metal and the liquid must be about 0.94 v, so that, if the double layer potential is 0.42 v, the average work function, ϕ^*, of the metal in contact with the liquid is only 0.52 ev. It is difficult to see how the work function of a normal metal surface could be lowered by more than about 0.5 ev by the purely electrostatic effects of a nonpolar liquid (16). The very low value found here for ϕ^* may indicate that there are weakly conducting levels for electrons in the liquid at a depth of about 4 ev, corresponding to the electron affinity of an insulating crystal.

Work on this new electrostatic method of detecting the equilibrium space charge at the contact of a metal and an insulating liquid is continuing, and it is hoped that it will be possible to correlate it with measurements of conductivity carried out on the purest possible samples up to breakdown field strengths.

Acknowledgments

Much of the work described above was carried out in 1951-1954 and was made possible by a maintenance grant from the Department of Scientific and Industrial Research. The current award of the Henley Research Fellowship to the author is also gratefully acknowledged.

Manuscript received March 1, 1960. This paper was prepared for delivery before the Philadelphia Meeting, May 3-7, 1959.

Any discussion of this paper will appear in a Discussion Section to be published in the June 1961 JOURNAL.

REFERENCES

1. H. House, *Proc. Phys. Soc.*, **B70**, 913 (1957).
2. E. B. Baker and H. A. Boltz, *Phys. Rev.*, **51**, 275 (1937).
3. W. R. Le Page and L. A. Du Bridge, *ibid.*, **58**, 61 (1940).
4. H. J. Plumley, *ibid.*, **52**, 140 (1937).
5. D. W. Goodwin and K. A. Macfadyen, *Proc. Phys. Soc.*, **B66**, 85 (1953).
6. W. B. Green, *J. Appl. Phys.*, **26**, 1257 (1955).
7. M. J. Morant, *Proc. Phys. Soc.*, **B68**, 513 (1955).
8. K. Kerner and H. Raether, *Z. Angew. Phys.*, **6**, 212 (1954); also K. Kerner, *ibid.*, **8**, 1 (1956).
9. T. J. Lewis, *Proc. Phys. Soc.*, **B68**, 504 (1955).
10. A. A. Zaki, PhD. Thesis, University of London, (1959).

11. N. F. Mott and R. W. Gurney, "Electronic Processes in Ionic Crystals," p. 171, 2nd ed., Oxford University Press, London (1948).
12. M. von Laue, "Handbuch der Radiologie," 6, p. 460, Leipzig (1925).
13. R. H. Fowler, "Statistical Mechanics," 2nd ed., p. 367, Cambridge University Press, Cambridge (1936); see also M. J. Morant, *J. Appl. Phys.*, **25**, 1053 (1954).
14. S. M. Skinner, *J. Appl. Phys.*, **26**, 509 (1955).
15. K. A. Macfadyen and T. A. Holbeche, *J. Sci. Inst.*, **34**, 101 (1957).
16. M. J. Morant, Ph.D. Thesis, University of London (1955).
17. M. J. Morant, To be published.
18. M. J. Morant and W. K. Mansfield, *Nature* (London), **169**, 499 (1952).
19. M. J. Morant, *J. Sci. Inst.*, **31**, 391 (1954).
20. O. H. Le Blanc, *Bull. Amer. Phys. Soc.*, (II), **4**, 45 (1959).

The Incorporation of Sulfur in Electrodeposited Nickel, Using Thiourea as a Brightener and Leveler

G. T. Rogers[1] and M. J. Ware

Atomic Energy Research Establishment, Harwell, England

and R. V. Fellows

Wilmot Breeden Laboratories, Solihull, Warwickshire, England

ABSTRACT

The amount of sulfur incorporated into nickel electrodeposited from a Watts plating solution containing thiourea as a brightener and leveler has been investigated by radiotracer techniques and autoradiography. The nickel deposit contains sulfur, and the amount of sulfur increases with decreasing current density when the current density is determined by the external electrical circuit or by the geometry of the plating cell. Autoradiographs taken from oblique sections cut through the nickel deposit show the distribution of the sulfur within the deposit. When the nickel is deposited on a surface having a roughness comparable to that encountered technologically incorporation occurs on the peaks of the surface. Thiourea causes leveling which requires the peaks to be regions of lower current density. Therefore the incorporation of sulfur is higher in regions of lower current density when the current density distribution is determined by the behavior of thiourea on a rough surface. Incorporation probably occurs in layers in regions of the deposit which show a laminar structure.

The addition of small quantities of certain organic compounds to solutions used for the electrodeposition of nickel modifies the plating in two ways, brightening and leveling. The mechanisms of brightening and leveling present problems which are relevant to the study of the electrodeposition of metals and which have considerable technological importance. Any investigation of these mechanisms requires data on the extent to which an additive, or compounds derived from it, become incorporated in the nickel plate under various plating conditions. It is also important to know the extent to which anions are incorporated in the plating. Since the amounts of incorporation are too small to be determined conveniently by conventional methods of analysis, radiotracer techniques are very appropriate to these studies because their high analytical sensitivity may be combined with autoradiography to show in detail the distribution of the additive over the area of plating. Recently Beacom and Riley (1) have investigated the incorporation of sulfur compounds from sodium allyl sulfonate using an elegant counting technique and autoradiography to measure the differences between incorporation on the peaks and valleys of grooved cathodes. They found a greater incorporation of sulfur on the peaks than in the valleys, but the scale of their "simulated roughness" was more than two orders of magnitude greater than that which is encountered in practice.

Thiourea is an additive which produces both brightening and leveling, and this paper describes an investigation of the incorporation of sulfur into nickel plating from thiourea labeled with sulfur-35. A study has been made of the distribution of incorporated sulfur within nickel plated on a surface whose roughness is comparable with that of technological interest.

Experimental

The effect of current density on the incorporation of sulfur from thiourea has been studied by plating test cathodes in a Hull cell. The plating baths were supplied with S^{35}—labeled thiourea from a high specific activity stock solution. Plating solutions were prepared by adding labeled thiourea diluted with inactive carrier to a standard Watts' nickel plating solution. A volume of 300 ml of plating solution was used for each cathode which was plated

[1] Present address: United Kingdom Atomic Energy Authority, Wantage Radiation Labs., Wantage, Berks., England.

for 15 min at a total current of 3 amp at 55°C and pH = 4.0. The total concentration of thiourea was 10^{-4} g mole/l and the activity was 517 μc/l. The bath was agitated by a stream of nitrogen introduced along the bottom of the cathode. After plating, the cathodes were washed with cold water and boiled with two changes of distilled water. Autoradiographs were taken from these cathodes by pressing them in close contact with an appropriate photographic emulsion.

Further experiments to determine the effect of current density and thiourea concentration on incorporation were carried out using 1½ in. diameter mild steel disks plated in a cell consisting of an 800-ml beaker with a 1 in. paddle stirrer rotating at 120 rpm between the anode and cathode which were 2¼ in. apart. Four disks were plated at different current densities and thiourea concentrations using 500 ml of fresh plating solution containing 414 μc of S^{35} thiourea for each. All disks were plated at 55°C and pH = 4.0 with a copper coulometer in series with the plating cell. After plating, each disk was washed in the same manner as the Hull cell cathodes. Further boiling of the disks with distilled water caused no change in the incorporated activity.

The β activity of a circle, radius 0.406 cm, at the center of each disk was determined by counting with an end-window Geiger-Muller counter, the geometry of counting being controlled so that the activities of the four samples and a standard source could be compared.

The absorption coefficient for sulfur 35 β particles for the counting conditions used to determine the activities of the disks was determined using one of the disks as a source and nickel absorbers. The absorbers were placed close to the plated disk so that the counting geometry for the external absorbers was as similar as possible to that of the self-absorber. The value of the absorption coefficient in aluminum, the half life, and the absence of any gamma radiation detectable with a scintillation counter showed that all the activity on the disks was due to sulfur 35.

The thickness of the nickel plate at the center of each disk was measured by sectioning. The outside profile of the plating was supported by gluing to it a piece of soft copper sheet with Araldite. The disk was sectioned perpendicular to the plane of the plating, and the section face was polished and etched. The thickness of the plating was measured with a microscope fitted with a reticule eyepiece.

The plating conditions, the plating thicknesses at the centers of the disks, and the activities of the disks are shown in the first six columns of Table II.

To investigate the incorporation of sulfur from sulfate, two brass disks, E and F, were plated in a Watts' solution containing labeled sulfate but not thiourea. 500 ml of the solution contained 16 mc of $(S^{35}O_4)^{2-}$ and the disks were plated for 45 min at a current density of 3.97 amp/dm². The activity of a circle, radius 1.15 cm at the center of each disk, was compared with that of a standard by counting. These activities were very much lower than the activities of the disks plated in the presence of thiourea. Therefore to obtain reasonable counting rates, the counting efficiency was increased by mounting the disks much closer to the counter window. A standard was prepared by diluting 0.1 ml of the plating solution to 100 ml and evaporating 1 ml of the diluted solution onto a counting tray.

Table I

Disk	Surface finish center line avg roughness,* microns	Total conc. thiourea gmole/l	Total act. in bath, μc	Apparent current density, amp/dm²
G mild steel	1.12	10^{-3}	493	4.85
H mild steel	0.19	10^{-3}	493	4.85
K brass	1.17	10^{-3}	407	3.97

* Center line average roughness of length L of the surface equals $\frac{1}{L}\int_0^L |Y|\,dl$ where y is the distance of the surface from the mean center line.

The distribution of the sulfur in nickel plated on a rough surface in the presence of thiourea has been studied by taking autoradiographs of sections cut obliquely through the plating. Disks were prepared on emery to give surfaces with scratches in one direction and various surface roughnesses. 500 ml of solution were used to plate each disk. Details of the surface and the plating conditions are summarized in Table I.

All disks were carefully cleaned before plating. The adhesion of the plating on disk K, which was used for taper sectioning, was further improved by cleaning it cathodically immediately before plating. The plating was sectioned at 5° to the plane of the plating. The outside profile of the nickel plate was supported by gluing to it a piece of soft copper sheet with Araldite. A 5° cut was then made in the brass, the section mounted in Perspex with the brass side outwards, and rubbed down on emery until a suitable profile appeared. The section was polished using normal metallographic techniques and etched with ammoniacal hydrogen peroxide. Autoradiographs were taken on Kodak A. R. 10 emulsion.

Results

Figure 1 shows autoradiographs of a Hull cell cathode (*a*) plated in a nitrogen-agitated bath and (*b*) in a bath without agitation, but in a nitrogen atmosphere. In Fig. 1, the current density increases along the cathode from left to right, and in all the autoradiographs, radioactive areas appear black.

Ratios of sulfur to nickel atoms in the plating can be calculated from the measured count rates. Suppose C counts/min, corrected for background and counter dead time, are obtained from 1 cm² of plating using a given counting geometry. Assume that the plating is of uniform thickness t cm and that it contains a uniform distribution P atoms of sulfur per atom of nickel. The specific activity of the thiourea in the plating bath S millicuries/g mole is equal to the specific activity of the sulfur in the plating in millicuries/g atom, assuming that there is no exchange of sulfur between thiourea, or sulfur in the plating, and sulfate ions during the deposition. A thin layer of plating thickness dx distance x from the free surface contains $(PSp/W)\,dx$ mc S^{35}/cm²

Fig. 1. Autoradiographs of Hull cell cathodes (full size before reduction for publication) (a) (top) plated in a nitrogen agitated bath, (b) (bottom) in a bath without agitation, but in a nitrogen atmosphere. The current density increases along the cathode from left to right and radioactive areas appear black.

where p, W are the density and atomic weight of nickel, respectively. The reduction of the count rate by absorption of S^{35} β particles in thickness x of plating can be calculated approximately by assuming an exponential absorption with an absorption coefficient μ (2).

The thin layer at x contributes $(kPSp/W)e^{-\mu x}\,dx$ counts/min/cm^2 to the measured count rate where k is a constant depending on the geometry of the counting arrangement. Since the distance between the counter and the plating is large compared with the total thickness of the plating, k is independent of x.

Integration over the total thickness of the plating t and rearrangement gives

$$P = \frac{W}{kS}\,\frac{\mu}{p}\,\frac{C}{(1-e^{-\mu t})} \qquad [1]$$

A standard containing m millicuries of S^{35} gave C_m counts/min with the same geometry. This standard was sufficiently thin that the neglect of self-absorption does not introduce a significant error. Then $C_m = km$ and

$$P = \frac{mW}{S}\,\frac{\mu}{p}\,\frac{1}{(1-e^{-\mu t})}\,\frac{C}{C_m} \qquad [2]$$

The results of the nickel absorption measurements; $\log_e$ (count rate) plotted against absorber thickness (mg/cm^2) gave a line which was slightly convex away from the axes for a range of absorbers up to 10.7 mg/cm^2. A mean mass absorption coefficient was calculated from the gradient of the best straight line through the experimental points using the method of least squares. This gave μ/P = 2.303 x 0.132 = 0.304 cm^2/mg. For disks A, B, C, Table II, S = 0.414/0.5 x 10^{-6} = 0.828 x 10^6 mc/mole and for disk D 0.828 x 10^4 mc/mole. For disk A $(1-e^{-\mu t})$ = 0.986. The standard source of 0.104 microcuries of S^{35} gave 1012 counts/min.

$$P = \frac{0.104 \times 10^{-6} \times 58.7 \times 0.304 \times 10^6}{0.828 \times 10^6 \times 0.986}\,\frac{8612}{1012}$$

$$= 19.4 \times 10^{-4} \text{ atoms S/atom Ni}$$

Results for the other disks, Table II, column 7, have been calculated similarly.

The plating on disk H, Table I, was removed from the mild steel disk and the same area of plating counted from both sides. The activities measured from the two sides differed by 5.5%. The error introduced by the assumption that the sulfur is uniformly distributed in the plating is likely to be of similar magnitude.

The activities of disks E, F plated using labeled sulfate were E, 71.5, and F, 53.8 counts/min/cm^2. 16 mc of labeled sulfate were added to 500 ml of plating solution. The plating thickness at the centers of the disks was 27.7 μ and the activity of a standard which contained 0.032 μc of S^{35} was 3865 counts/min. The weight of this standard (0.1 mg/cm^2) showed that the neglect of self-absorption did not introduce a significant error.

These results give sulfur/nickel atom ratios, calculated using Eq. [2], of 0.33 and 0.25 atoms S/10^2 atoms Ni, respectively, taking the total concentration of sulfate in the plating bath as 1M. A nickel deposit plated under the same conditions was analyzed chemically for sulfur and gave a value of 0.37 atoms S/10^2 atoms Ni.

The autoradiographs, Fig. 2 and 4, show the distribution of sulfur incorporated in nickel plated on a rough surface. The plating on disks G and H was bright, and the original scratch lines still showed on G but did not show on H. Figure 2 shows an enlargement of an autoradiograph of disk G.

Table II

Disk	Current density, amp/dm^2	Total thiourea conc., gmole/l	Total wt. of nickel deposited, g	Plating thickness at center of disk, μ	Plating thickness at center of disk, mg/cm^2	Count rate, c/min/cm^2	Atoms S per 10^2 atoms Ni
A	8.6	10^{-3}	0.321	15.8	14.16	8612	19
B	4.3	10^{-3}	0.474	(24.8)*	22.17	16080	35
C	0.86	10^{-3}	0.488	34.7	30.9	30630	68
D	4.3	10^{-4}	0.482	24.3	21.6	18850	4

* Estimated by comparing the thicknesses on disks C, D and the total weights of nickel deposited on disks B, C, D.

Fig. 2. Autoradiograph (5X before reduction for publication) of nickel plated on disk G which had parallel scratches in one direction. Center line average roughness of fine scratches 1.17 μ.

Fig. 3. Micrograph (150X over-all before reduction for publication) of a 5° taper section through nickel plated on a rough surface.

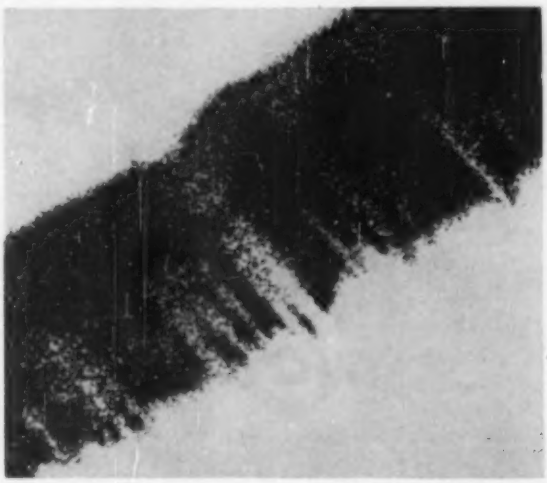

Fig. 4. Micrograph (150X over-all before reduction for publication) taken from an autoradiograph of the taper section shown in Fig. 3.

The taper section was cut from disk K which was plated at an apparent current density of 3.97 amp/dm^2 and its activity corresponded to an incorporation of 44 atoms S/10^6 atoms Ni, in agreement with earlier results (Table II). Figure 3 shows a micrograph of a taper section from disk K, and Fig. 4 is a micrograph at the same magnification taken from an autoradiograph of the section. In Fig. 3 and 4, sectioning at 5° increases the magnification perpendicular to the plane of the plating approximately eleven times. Figure 5 shows the principal features of part of the profile shown in Fig. 3 from which the extra magnification perpendicular to the plane of plating has been removed.

Discussion

Incorporation of sulfur–effect of current density.— The autoradiographs of the Hull cell cathodes show that considerable amounts of sulfur activity are associated with the nickel plated surface, and the cathode plated in the agitated bath shows clearly that the most active areas are those where the current density is lowest. A similar variation of incorporation with current density occurs on the cathode plated in the unagitated bath. High sulfur activity on plated specimens might arise from a uniform thin layer of sulfur-rich metal deposited in the initial stages of plating, which is subsequently covered by nickel containing less sulfur. Then, since the plating is thinner in regions of lower current density, less sulfur β-radiation would be absorbed in these regions, and they would appear to be regions of higher sulfur activity. This possibility was eliminated by plating another Hull cell cathode for 1 min, with the result that very little activity was found on the plate.

Errors in the measurement of the count rate, the volume of stock solution of S^{35} thiourea, and the weight of inactive thiourea added to the bath will introduce errors in the relative values of the sulfur/nickel atom ratios, Table II column 6. These errors are probably less than 10%. The radiochemical

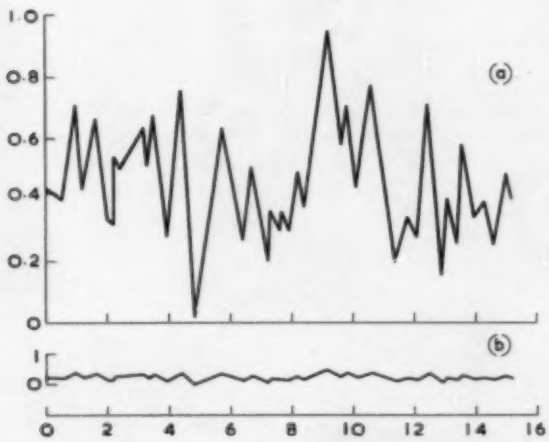

Fig. 5. Scale diagrams of the profile of the surface before plating (a) as seen in the taper section (b) when the additional 11X magnification introduced by the 5° angle of sectioning has been removed. 1 unit = 28 μ.

analysis gives results for a small area at the center of each disk. The plating thickness and therefore the current density decrease from the edge toward the center of a disk, and autoradiographs of the disks show more activity toward their centers. All the results reported in this paper show that incorporation of sulfur varies with current density so differences in current density distribution between disks can affect the relative values of the S/Ni ratios determined at the centers of the disks. The variations in plating thickness, Table II, show that there are appreciable differences in current density distribution between disks, and these differences will introduce errors in the relative values of the S/Ni ratios. The results on the Hull cell cathodes, Fig. 1, show that the amount of incorporation depends on agitation. The conditions of agitation for plating the disks were standardized as far as possible, but differences in agitation between different disks will also introduce errors in the relative values of the S/Ni ratios. It is difficult to assess the total error in the relative values of the S/Ni ratios introduced by differences in current density distribution and agitation, but the error is unlikely to be comparable with the differences in the ratios found for the disks, Table II. Therefore a comparison of the S/Ni ratios provides further qualitative evidence that incorporation of sulfur increases with decreasing current density.

The Hull cell cathodes show that incorporation varies greatly with agitation. Therefore the absolute magnitude of a S/Ni ratio is appropriate only to the particular plating conditions used for the disks.

The results for the incorporation of sulfur from sulfate are less accurate because of the much smaller quantities of sulfur involved.

The S/Ni ratios obtained from the disks show an increase in incorporation with decreasing current density, and autoradiographs of the disks show more activity toward their centers where the thickness of plating shows that the current density was lower than near the edges.

Since in all experiments incorporation was measured by the sulfur^{35} activity, no conclusions may be drawn concerning the chemical form in which sulfur is incorporated.

The deposit on the Hull cell cathode plated in the unagitated bath was much less bright and the general level of incorporation of sulfur much lower than on the cathode plated in the agitated bath. This suggests that brightening and incorporation may both be strongly controlled by the diffusion of thiourea through the solution boundary layer at the metal-solution interface.

Th results obtained using plating solutions containing labeled sulfate anions but no thiourea show that the incorporation of sulfur from sulfate is very much less than from thiourea.

Distribution of incorporation on a rough surface.—The nickel plating on disks G and H showed that thiourea was acting as a brightener and leveler. The scratches on disk G were not completely leveled by the plating, and the corresponding autoradiograph, Fig. 2, shows that, under these conditions, the incorporation of sulfur does not occur uniformly. The finer scratches on disk H were leveled completely, and the incorporation of sulfur showed no fine structure. This suggests that the incorporation depends on the surface profile and is higher either on the peaks or in the valleys. Now leveling requires the time averaged current density to be lower on the peaks than in the valleys, and a comparison of the micrograph and autoradiograph of the taper section (Fig. 3 and 4) shows that incorporation is much higher on the peaks than in the valleys. Therefore high incorporation is again associated with low current density. The dark "tails" to the peaks which show in the micrograph, Fig. 3, may result from the high incorporation of sulfur at these points.

As plating proceeds, the incorporation on peaks becomes weaker and is replaced by a more uniform incorporation which may be layered parallel to the plane of the plating.

Figure 4 suggests a layer of high incorporation immediately above the incorporation on the peaks and one, or possibly two, faint layers above it which appear more clearly when the autoradiograph is examined at a lower magnification. The depth of nickel perpendicular to the autoradiographed surface of the taper section increases linearly from zero at the outside edge of the section to a maximum of ca. 30 μ at the brass-nickel interface. Since the maximum range of S^{35} β-particles in nickel is 35 μ the intensity of radiation per unit area of this surface, and hence the photographic density would decrease monotonically across the autoradiograph of the section for a uniform distribution of sulfur in the plating. Therefore the dark bands which are apparent in the autoradiograph suggest that there are layers of higher sulfur incorporation in the plating. No incorporation of sulfur occurs in the initial filling of the valleys, and at C, where the outside profile of the plating shows that the two large valleys have not been completely leveled, incorporation is lower than at points where leveling is complete. Considerable incorporation of sulfur, showing some layering, occurs in the banded region of the plating. Although the resolution of the autoradiograph is not sufficient in general to show a detailed correlation between incorporation and the banding shown in the micrograph, the three short dark bands at A appear as regions of higher incorporation. At B, curvatures of successive bands and the outside profile of the plating show that local deleveling occurred a short time before the plating was stopped. There is a suggestion in the autoradiograph that the onset of deleveling may have been associated with a local reduction of incorporation.

The results and autoradiographs discussed above show that considerable incorporation of sulfur occurs when nickel is electrodeposited in the presence of thiourea, and that the incorporation increases with decreasing current density in systems where the current density distribution is determined either by the external electrical circuit, or the geometry of the system, as in the Hull cell, or the behavior of thiourea on a rough surface.

When the nickel is deposited on a surface having a roughness comparable to that encountered technologically, the incorporation occurs on the peaks of

the surface, in agreement with Beacom and Riley (1) whose results were obtained on a much larger scale of surface roughness. The layering of incorporated sulfur in regions of the plating where the micrograph shows a laminar structure supports the suggestion by Vanderkooi (3) that layering of the deposit may be associated with the incorporation of additive or compounds derived from it.

Acknowledgments

The authors wish to thank Dr. G. B. Cook and Mr. U. F. Marx for their help and encouragement, and Messrs. Wilmot-Breeden for the provision of experimental facilities and permission to publish this paper.

Manuscript received Aug. 31, 1959.

Any discussion of this paper will appear in a Discussion Section to be published in the June 1961 JOURNAL.

REFERENCES

1. S. E. Beacom and B. J. Riley, *This Journal*, **106**, 309 (1959).
2. E. Bleuler and G. J. Goldsmith, "Experimental Nucleonics," p. 84, Rinehart Publishing Co. (1952).
3. N. Vanderkooi, Doctoral Dissertation, Wayne State University (1958).

(Zn,Hg)S and (Zn,Cd,Hg)S Electroluminescent Phosphors

A. Wachtel

Research Department, Westinghouse Electric Corporation, Bloomfield, New Jersey

ABSTRACT

Solid solutions of (Zn,Hg)S prepared by firing in sealed silica tubes are cubic in structure. With suitable additions of Cu and a coactivator, photoluminescence and electroluminescence are obtained. The coactivators used were halides, Ga, or In. The electroluminescence in the red consists of two emission bands which do not appear to be analogous to the blue and green emission bands of Cu, Cl in ZnS. The quantum efficiency is of the same order of magnitude as that of ZnS:Cu, Cl, but the emission bandwidth is about twice as large and the red electroluminescence consists of emission located to a large extent in the infrared. HgS tends to retain the cubic structure of ternary (Zn, Cd, Hg)S systems provided that the Cd/Hg ratio does not exceed certain limits; until this is so, the introduction of Cd causes increased electroluminescence.

Efforts to prepare EL[1] phosphors emitting at longer wave lengths are usually based on substitution of lattice constituents so as to effect lattice expansion. In ZnS:Cu EL phosphors of Se for S has been investigated by Prener (1) and by Hegyi, Larach, and Shrader (2). Zn(S, Se) and ZnSe constitute good EL phosphors, although the frequency dependence of ZnSe:Cu is large compared to that of ZnS:Cu, so that the low-frequency response is unusually poor.

On the other hand, substitution of Cd for Zn has been shown to result in hexagonal systems with exceptionally poor EL response (3). It is therefore obvious that the effect of substitution of Zn by the next heavier member of the group IIB elements, namely Hg, was of interest. Due to the low sublimation temperature of HgS, its retention in ordinary firing at atmospheric pressure is known to be impossible at temperatures sufficient to cause activator incorporation. Wesch (4) has described a high-pressure furnace by means of which the preparation of pure HgS phosphors was mentioned. Kremheller and Levine (5) prepared (Zn, Hg)S and (Cd, Hg)S solid solutions by aqueous recrystallization under pressure and at temperatures well above the normal boiling point of water, and in a recent publication Kremheller, Levine, and Gashurov (6) describe some of the photoluminescent properties of activated (Zn, Hg)S and (Cd, Hg)S prepared by this method. In the present investigation, the mixed sulfides were prepared by firing in evacuated and sealed silica tubes. Although the pressure developed in the tubes is unknown, the application of hydrostatic pressure from the outside was not found to be necessary.

[1] Electroluminescence or electroluminescent is hereafter abbreviated EL.

Experimental Technique

In addition to the raw materials already described (3), HgS, Ga_2S_3, and In_2S_3 were used. HgS was prepared by reaction of the elements. Ga_2S_3 was prepared by slurrying ZnS with $Ga(NO_3)_3$ solution, drying, and firing in an atmosphere of H_2S. In_2S_3 was precipitated from aqueous solution in the presence of a ZnS carrier, filtered, and dried.

In order to avoid the development of excessive pressure in the sealed tubes, as well as to avoid the influence of gases not normally retained in firings at atmospheric pressure, it was necessary to accomplish complete thermal degassing and decomposition of volatile matter (NH_4-salts, acetate radical) prior to sealing the final mixture into the tubes. All firings were therefore conducted in two stages:

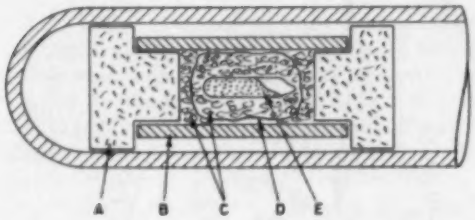

Fig. 1. Technique for firing phosphors with HgS. A, Fire brick; B, mullite tube; C, silica wool; D, silica cloth; E, firing tube.

1. A normal blue or green emitting ZnS:Cu EL phosphor is prepared at atmospheric pressure by known methods (3). The Cu-acetate and NH_4-halides (if any) decompose, and activator incorporation takes place. Traces of H_2O and air are expelled and particle growth of the ZnS facilitates subsequent degassing. The fired phosphor is, however, not washed in NaCN solution since the total amount of Cu added (now partially present as free Cu_2S) is required for the final synthesis of the mixed (Zn, Hg)S EL system.

2. The above product, hereafter referred to as the singly fired phosphor, is mixed with HgS as well as a small amount of S calculated to produce only a few atmospheres of pressure at the subsequent firing. This sulfur addition is necessary since traces of residual air would cause oxidation of S^{2-} and give rise to S-vacancies[2] and poor EL performance of the finished product. The mixture is transferred to a silica tube of 7 mm ID, 9 mm OD, and 40 mm length, closed at one end and provided with a constricted neck at the other end. The tube is evacuated by means of a mechanical oil pump for about 30 min and then sealed at the constriction. The sealed tube is fired at 900°C as shown in Fig. 1.

The thermal insulation afforded by the silica wool packing, as shown in the figure, is necessary to prevent separation of part of the HgS during cooling. The presence of CdS greatly diminishes this effect, and still more homogeneous products may be obtained by allowing the entire assembly to cool in the furnace, although this was rarely done because of obvious considerations of time limitation. Refiring times of 2 hr were found to be sufficient.

The washing procedure in NaCN solution is the same as used for normal green-emitting ZnS:Cu EL phosphors. Because of the small samples (about 2 g) usually prepared, simple grinding in a mortar and pestle was preferred. All figures for Cu and halide in phosphors specifically refer to amounts added before firing, and not to final compositions.

Measurements were performed with a Spectra Brightness Spot Meter,[3] using a demountable castor oil cell. In order to meet the contract requirements as to color, additional measurements were also taken with a red (NBS #3215) filter inserted in the optical path. The ratio between the respective readings served as a sensitive indication of emission color, and it was noted that small differences in this ratio caused large differences in brightness. To enable a valid interpretation of the relative performance of phosphors emitting with different colors, it was therefore necessary to compensate for this effect. The method used consisted of preparing phosphors that differed only in base lattice composition and plotting their relative brightness (based on 100% for the specified color) as a function of the filter ratio. Data on experimental phosphors could then be corrected to yield values hereafter referred to as "normalized brightness."

[2] In the presence of HgS, such reducing conditions result in the formation of metallic Hg, visible as a separate phase.

[3] Photo Research Corp., Hollywood, Calif.

Table I. Unit cell dimensions of cubic (Zn,Hg)S:Cu,NaCl phosphors

Mole % HgS	a (A)
0	5.406
5	5.429
10	5.443
15	5.469
20	5.486
25	5.516
30	5.532
40	5.569
60	5.665
80	5.745

Results

Photoluminescence of (Zn:Hg)S phosphors.—Some basic information was obtained by firing photoluminescent ZnS:Cu (0.01%):NaCl phosphors with increasing additions of HgS at 750°C. Table 1 shows the unit cell dimensions obtained by x-ray powder diffraction. All phosphors (up to 80% HgS) were cubic, although the HgS used was hexagonal. HgS alone similarly fired was also hexagonal. The values can be plotted to give a reasonably good fit to a straight line. Figure 2 shows the emission spectra (3650Å excitation) as obtained on a Perkin-Elmer Universal Spectrometer. Figure 3 shows the diffuse reflection spectra in the near ultraviolet and visible regions obtained by illuminating through a Farrand monochromator and measuring the reflected radiation with a Bausch and Lomb monochromator adjusted to the same wave lengths. It may be noted that the regular manner in which the spectra shift to longer wave lengths is very similar to the effect of Cd substitution. The shift in emission caused by Hg is about four times greater than that caused by similar concentrations (in mole %) of Cd. It was noted that at low Hg concentration (5 mole %) the fluorescence was unusually weak.

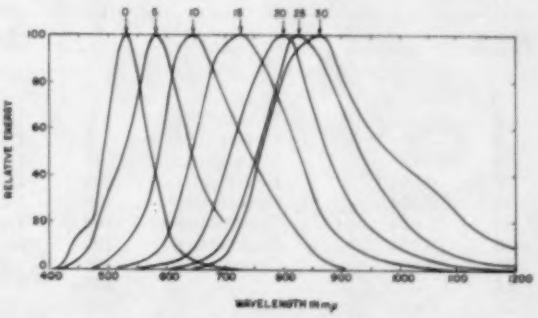

Fig. 2. Emission spectra of (Zn, Hg)S:Cu, NaCl phosphors. Numbers denote mole % HgS in phosphors. Excitation = 3650Å.

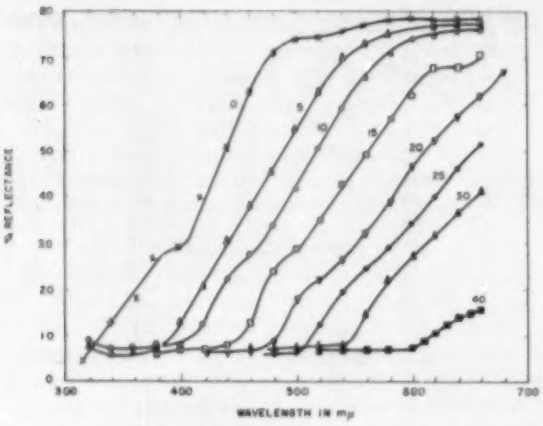

Fig. 3. Diffuse reflection spectra of (Zn, Hg)S:Cu, NaCl phosphors. Numbers denote mole % HgS in phosphors.

The decreasing concentrations of Cu and Cl resulting from increasing additions of HgS were not considered to appreciably influence the shape of the emission and reflection spectra, because Cl was present in excess and only the long wave-length emission band was developed.

Electroluminescent phosphors.—The activator requirements for EL are known to be greater than for photoluminescence. For the systems under investigation, they were also noted to vary with the type of coactivator used. In the case of Cl, additions of the order such as to produce optimum green-emitting singly fired ZnS:Cu, Cl phosphors proved to be too high not only for Cl, but also for Cu. Figure 4 shows the emission spectra of a series of (Zn, Hg)S:Cu(0.2%), Cl(0.075%) phosphors excited at 10,000 cps. The activator additions are such that the ZnS:Cu, Cl phosphor emits predominantly the blue Cu band and are optimum with respect to the orange or red emitting compositions. The emission band gradually shifts to longer wave lengths and broadens until above about 20 mole % Hg, a long wave length emission band increases quite suddenly in relative intensity. It will be shown that this cannot necessarily be identified with the "Cu-green" band emitted in more highly coactivate ZnS-Cu phosphors.

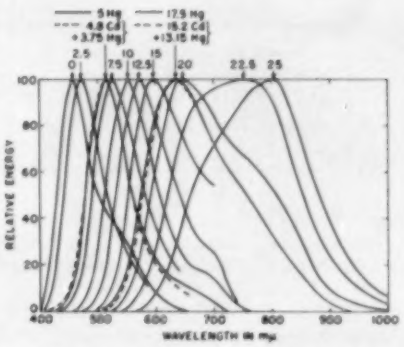

Fig. 4. Emission spectra of (Zn, Hg)S:Cu (0.2%): Cl(0.075%) and two (Zn, Cd, Hg)S:Cu (0.2%:Cl (0.075%) EL phosphors. Numbers denote mole % HgS in samples. Excitation = 10,000 cps.

The effect of Cd on the emission color was determined empirically for orange to deep red emitting (Zn, Hg)S. It was noted that the emission color of [(1 − x)Zn, xHg] S:Cu may be duplicated approximately by firing [(1 − 4n)Zn, 4nCd] S:Cu and refiring this with (x − n)HgS. However, substitutions of more than half of the original concentration of Hg by Cd result in a shift to longer wave lengths. Table II shows the effect on EL brightness of a series of orange-red emitting phosphors based on the original composition (0.8Zn, 0.2Hg)S:Cu (0.2%):Cl(0.075%). The table includes brightness readings of NaCN-washed aliquots of the singly fired (Zn, Cd)S:Cu, Cl phosphors. It also shows measurements by x-ray powder diffraction, so as to illustrate how in both cases the breakpoint in brightness coincides with the appearance of an appreciable percentage of hexagonal phase. These measurements also include values of interlattice spacings (d/n) of the 311 plane. Very similar results are shown in Fig. 5 on deep red emitting phosphors coactivated with Br + I or Ga and excited at 400 cps. This is in agreement with the observation made by Zalm (7), than in ZnS:Cu EL phosphors the cubic phase is preferable.

It can be seen that in all cases Cd increases the emittance of the system until interference by formation of hexagonal material occurs. It can also be

Table II. Effect of Cd/Hg ratio on structure and electroluminescence

First firing					Second firing					
							Brightness			
Mole % Cd used	Brightness 10,000 cps	Emission color	% Hex. phase	d/n, (311)	Mole % HgS added	Mole % Cd in phosphor	400 cps	10,000 cps	% Hex. phase	d/n, (311)
0	6.2	Blue	0	1.630	20	0	0.77	2.4	0	1.653
2	6.8	White-blue	0	1.633	19.5	1.7	0.68	3.5	0	1.653
4	3.5	Green-blue	4	1.634	19	3.2	0.89	3.95	0	1.656
8	1.8	Blue-green	27	1.638	18	6.6	1.10	3.8	0	1.660
16	0.055	Green-blue	100	1.649	16	13.4	1.49	4.9	0	1.665
20	0.024	Green-blue	100	1.654	15	17.0	2.01	5.55	7	1.668
24	0.014	Green-blue	100	1.660	14	20.6	1.16	3.3	43	1.671
28	0.008	Blue-green	100	1.664	13	24.4	0.22	0.17	100	1.677
32	0.006	Green	100	1.668	11*	28.8	0.12	0.25	100	1.679
64	—	—	100	1.707	0	64	—	0.15	100	1.710
72	Faint	Red	100	1.719						
80	Very faint	Red	100	1.728						

* Relationship of 1 Hg = 4 Cd begins to break down. Therefore, only 11 instead of 12 mole % HgS used.

seen that in the presence of HgS a much higher concentration of Cd is permissible before this occurs. The optimum substitution of Hg by Cd appears to be in the neighborhood of 20-25% of the original Hg concentration. Most of the ensuing investigations were therefore performed on such (Zn, Cd, Hg)S:Cu phosphors. The two dashed curves in Fig. 4 represent the emission spectra of (Zn, Cd, Hg)S:Cu, Cl phosphors in which 25% of the Hg was replaced by Cd in the manner outlined above. The compositions are based on original Hg concentrations of 5 mole % (green emission) and 15 mole % (orange emission) and are seen to coincide closely with the emission spectra of the respective (Zn, Hg)S:Cu, Cl phosphors, but the brightness was appreciably higher.

It has been mentioned that optimum additions of Cu and Cl were smaller than those found useful in green-emitting ZnS:Cu, Cl phosphors(3). It was therefore interesting to note that the optimum addition of Br + I [4] was higher, namely similar to that for ZnS:Cu phosphors, although the estimated excess Cu_2S concentration still had to remain smaller than about 0.2 mole %. Such Br + I coactivated phosphors were about two to three times brighter than Cl-coactivated phosphors. In the case of Ga or In coactivation, phosphors were prepared with additions of Cu equal to 0.6 mole % more than the concentration of Ga or In added. Their normalized brightness, excited at 400 cps, increased linearly with coactivator concentration up to 0.125 mole % and then decreased. On the other hand, phosphors coactivated with 0.125 mole % Ga or In showed two brightness maxima with respect to Cu addition, as shown in Fig. 6. It can be seen that the first maximum is very sharp and more pronounced in the case of In coactivation. Prefiring at 1100°C [5] decreases the low Cu maximum. Ga-coactivated phosphors prefired at 1100°C show only a gradual increase in brightness, leveling off at about 1 mole % Cu.

Figure 7 shows the brightness of Br + I and of Ga coactivated (Zn, Cd, Hg)S:Cu phosphors as a function of Cd + Hg concentration. The activator concentrations are not optimized for either system but chosen so that the total Cu addition as well as the green emission color of the ZnS:Cu phosphors are the same. It is interesting to note that in the case of Br + I coactivation there occurs the same initial drop in output at low Hg concentrations as has been observed in the photoluminescent as well as the Cl-coactivated EL phosphors, while, on the other hand, the Ga-coactivated ZnS:Cu is characterized by comparatively poor output, presumably because of the greater trap depth caused by Ga (8, 9). Introduction of Cd + Hg [6] causes an increase in brightness well beyond the point of maximum luminosity (yellow green). This means that, except for the initial drop noted with halide coactivation, the radiant output of the phosphors increases at least up to the point of maximum observed brightness and possibly beyond that. In the case of Ga-coactivation, this might be explained by decreasing trap depth due to lowering of the conduction band, assuming that a similar effect occurs as noted by Klasens for Cd substitution (10). Unfortunately, the

[4] Equimolar mixtures of NH_4Br and NH_4I yielded slightly better results than NH_4Br alone. However, only a very small fraction of the added I^- is retained, so that additions were based on Br^- alone.
[5] To compensate for decreased particle growth in the absence of halides.

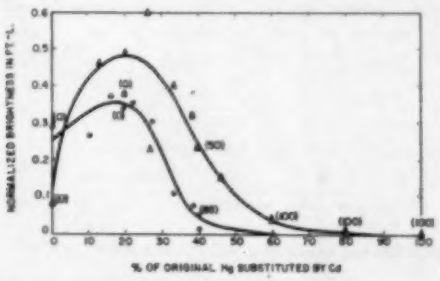

Fig. 5. Normalized brightness of (Zn, Cd, Hg)S:Cu phosphors as a function of Cd/Hg ratio. A, Compositions based on (0.81 Zn, 0.19 Hg)S:Cu(0.4%), (Br + I)(0.46%); B, compositions based on (0.85 Zn, 0.15 Hg)S:Cu(0.9%), Ga(0.13%) Numbers in parentheses denote % hexagonal phase present. Excitation = 400 cps. Groups A and B approximately match in emission color.

[6] The same relationship was noted in the absence of Cd.

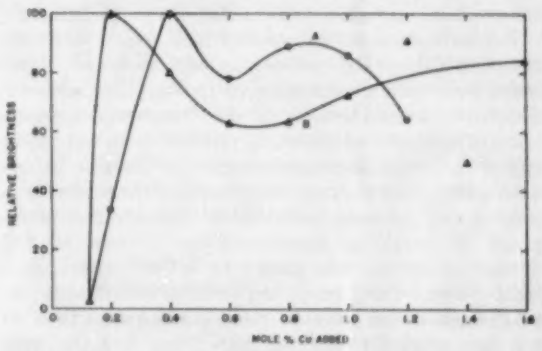

Fig. 6. Normalized relative brightness of red-emitting A:(Zn, Cd, Hg)S: x Cu: 0.125 mole % Ga and B: (Zn, Cd, Hg)S x Cu: 0.125% In phosphors as a function of Cu addition. Excitation = 400 cps.

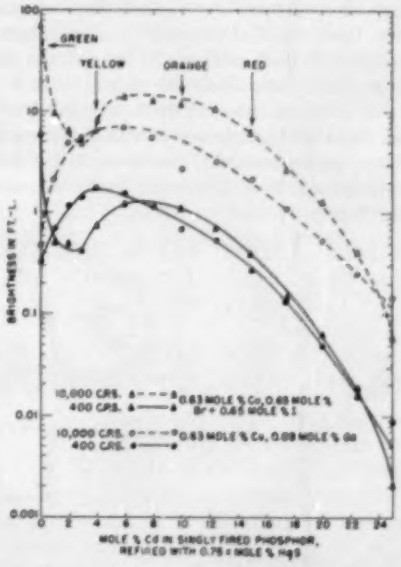
GREEN
YELLOW
ORANGE
RED
BRIGHTNESS IN FT.-L.
10,000 CPS.
400 CPS.
0.63 MOLE % Cu, 0.69 MOLE % Br + 0.65 MOLE % I
10,000 CPS.
400 CPS.
0.63 MOLE % Cu, 0.09 MOLE % Ga
MOLE % Cd IN SINGLY FIRED PHOSPHOR, REFIRED WITH 0.75 MOLE % Hg0

Fig. 7. Brightness and emission colors of (Zn, Cd, Hg)S:Cu phosphors as a function of base lattice composition.

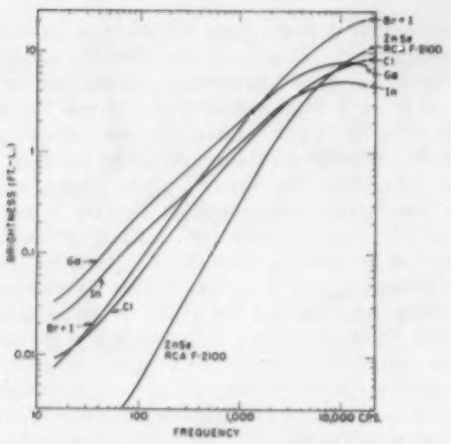

Fig. 8. Brightness of orange-red emitting (Zn, Cd, Hg)S:Cu phosphors with different coactivators and of ZnSe:Cu as a function of frequency.

scope of the present investigation did not permit independent measurements of radiance (such as by thermopile) or glow curves for these samples.

An indication of decreasing trap depth with increasing Cd + Hg concentration was noted, however, by visual observation of thermoluminescence. Similarly, a comparison of the frequency dependence of typical red-emitting phosphors as shown in Fig. 8 indicates decreased output of Ga and In coactivated phosphors at frequencies where no such decrease is evident with halide coactivated phosphors. It should be mentioned that at the red end of the spectrum, the usual variation in emission color with frequency represents variations in brightness which may be more pronounced than in the case of green-emitting phosphors, and that this effect therefore increases the slope of the frequency dependence curves. The phosphors were selected so that at intermediate frequencies their emission color approximately matches that of the ZnSe:Cu phosphor also shown in Fig. 8 for comparison. Therefore they do not necessarily represent specimens suitable for comparison of brightness as a result of optimum conditions of preparation.

It was of obvious interest to determine the actual quantum yield and efficiency of the red phosphor in comparison to a standard green-emitting ZnS:Cu, Cl EL phosphor. The following samples were selected for this purpose:

1. (0.754Zn, 0.133Cd, 0.113Hg)S:Cu, Ga prepared from (0.85Zn, 0.15Cd)S:Cu(0.9%), Ga (0.13%) by refiring with 11.25% HgS. Emission color, red.
2. (0.6945Zn, 0.163Cd, 0.1425Hg)S:Cu, Ga prepared from (0.81Zn, 0.19Cd)S:Cu(0.9%), Ga (0.13%) by refiring with 14.25% HgS. Emission color, deep red.
3. A normal ZnS:Cu, Cl green emitting phosphor.

Each phosphor was operated at 400 cps in the same castor oil cell and the brightness and power consumption measured as a function of applied voltage. In addition, each phosphor while in the same cell was operated at 400 cps and 600 v and the spectral distribution determined, using the same slit width and amplification of the spectrometer. The absolute heights of the resultant curves were therefore comparable. These were corrected for energy, quanta, and luminosity, but not normalized to equal peak heights. Table III gives the integrated values. It is apparent that under similar conditions of excitation the output in energy or quanta for the red phosphors is considerably smaller than for the green phosphor. Nevertheless, the differences in luminosity are much greater and are the main reason for the low brightness presently obtainable with the red-emitting phosphor.

The actual quantum yield was determined according to[7]

$$K = \frac{B\,A\,Q \times 10^{17}}{1.26L}$$

where K is the number of quanta emitted per second, A is the area of the cell in cm², Q is the integrated quantum output, L is the luminosity factor of the spectrum, and B is the brightness in foot-lamberts. Table IV shows the data calculated for each phosphor operating at the voltage where maximum luminous efficiency was observed. It can be seen that the quantum efficiency of the red-emitting phosphor is comparable to that of ZnS:Cu, Cl.

Efforts to increase the brightness without change in emission color appeared to require a narrowing of the spectral distribution with particular emphasis on increasing its slope on the short wave length side. It is well known that in ZnS:Cu phosphors either the blue or the green emission band can be

[7] Let the number of quanta emitted/cm²-sec = $K = \int \frac{C}{h\nu}\frac{dE}{d\lambda}\,d\lambda$, where C is a constant introduced to correct the arbitrary units in which the spectrum is measured to watts/cm². Then,

$$K = \frac{C}{hc}\int \lambda \frac{dE}{d\lambda}\,d\lambda = \frac{CQ}{hc}$$

The constant C may be determined from the measured brightness B (in foot-lamberts) and the spectral distribution as follows:

$$B(\text{ft-L}) = \frac{680\ \text{lpw}}{A\ (\text{ft}^2)}\int Cy\frac{dE}{d\lambda}\,d\lambda = \frac{680 \times 929C}{A\ (\text{cm}^2)}\int y\frac{dE}{d\lambda}\,d\lambda = \frac{680 \times 929CL}{A}$$

Therefore,

$$C = \frac{AB}{680 \times 929L}$$

Since $hc = 1.99 \times 10^{-16}$ erg $= 1.99 \times 10^{-28}$ watt-sec,

$$\frac{Q}{1.99 \times 10^{-28}} \cdot \frac{AB}{680 \times 929L} = \frac{B\,A\,Q \times 10^{17}}{1.26L}$$

Table III. Integrated emission spectra of three phosphors excited in 60μ castor oil cell at 400 cps and 400 v

	Energy $E = \int \frac{dE}{d\lambda}\,d\lambda$	Quanta $Q = \int \lambda \frac{dE}{d\lambda}\,d\lambda$	Luminosity $L = \int y \frac{dE}{d\lambda}\,d\lambda$
Sample No. 1 (red emission)	102.9	77.6	1.36
Sample No. 2 (deep red emission)	166.6	134.8	0.28
ZnS:Cu, Cl (green emission)	472.1	257.0	290.7

Table IV. Output and efficiency of three phosphors excited in 60μ castor oil cell at 400 cps and optimum voltage. Area of cell = 10.8 cm²

	Voltage, V	Brightness, ft-L	Watts	Lumens/watt	Quanta/sec	Quanta/sec watt
Sample No. 1 (red emission)	350	1.1×10^{-1}	6.4×10^{-4}	2.0×10^{-3}	4.3×10^{16}	6.7×10^{20}
Sample No. 2 (deep red emission)	300	7.2×10^{-2}	1.51×10^{-4}	5.6×10^{-3}	2.35×10^{16}	1.55×10^{20}
ZnS:Cu, Cl (green emission)	350	3.66	1.63×10^{-4}	2.6	2.3×10^{16}	1.4×10^{20}

isolated by employing very low or sufficiently high ratios of coactivator to activator. If the broad spectral distribution of the red-emitting phosphors is the result of superimposed emission bands shifted to longer wave lengths but arising from the same centers, then similar variations in activator proportions should also influence the spectral distribution of the red-emitting phosphor in the same manner. Figure 9 shows, however, that this was not observed. The phosphors represented in the figure were prepared in an effort to maintain approximately the same emission color as measured by means of the filter ratio discussed above. This was reasonably successful but required that with increasing coactivator addition, the concentration of Cd+Hg had to be lowered. Nevertheless, the short wave-length emission band increases with such decreasing Cd+Hg concentration and is quite pronounced at a high coactivator concentration such as to result in only the green-emission band in ZnS:Cu phosphors. The increased brightness obtained at higher Br+I addition may now be explained at least partially by the increased slope of the short wave-length side of the emission spectrum.

Discussion

Perhaps the most important question concerning this study is why substitution of Zn by Hg results in good EL at emission colors similar to the photoluminescence emission colors of the respective phosphors, while substitution of Zn by Cd does not. For (Zn, Cd, Hg)S phosphors with a sufficiently high ratio of Cd/Hg so as to effect a decrease in EL, no evidence of a separate (Cu, Cd)S phase (3) could be observed. Therefore, the only clue in this direction is offered by the difference in crystal structure of the two systems.

It has been noted that hexagonal and cubic ZnS:Cu, Cl phosphors prepared with low Cu concentration (such as 0.01 mole %) perform about

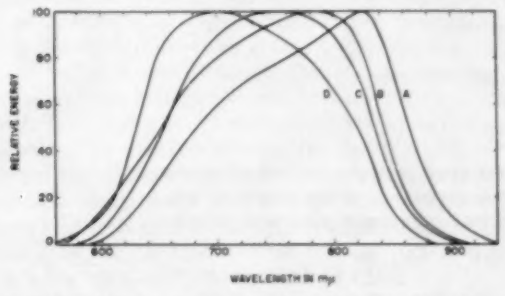

Fig. 9. Emission spectra of (Zn, Cd, Hg)S:Cu phosphors as a function of composition. Excitation = 400 cps. (A), 20.3% Cd, 18.7% Hg, 0.01% Br + 0.01% I; (B), 15.9% Cd, 13.8% Hg, 0.1% Br + 0.1% I; (C), 14.8% Cd, 11.1% Hg, 0.3% Br + 0.3% I; (D), 11.1% Cd, 9.3% Hg, 0.7% Br + 0.7% I.

equally well under artificially induced contact-EL (11). It must therefore be concluded that the better EL performance of cubic (Zn, Hg)S or cubic (Zn, Cd, Hg)S, as compared to the poorer performance of hexagonal (Zn, Cd)S or (Zn, Cd, Hg)S phosphors, results from differences in the means of EL excitation only. In the former case, the field intensifying Cu_xS inclusions are present and active. If in the latter case they are also present, then they are not active, possibly as a result of the different electrical nature of the barrier represented by the nonisomorphic junctions.

The sharp minimum in EL noted at low concentration of Hg is accompanied by a similar minimum of photoluminescence. At present, its appearance can not be explained. Inspection of Fig. 3 shows, however, that the weakly emitting (0.95 Zn, 0.05 Hg)S:Cu, Cl phosphor lacks the secondary hump in reflectivity near the absorption edge. According to an investigation by Froelich (12) the introduction of small amounts of Cu causes just such a hump in the diffuse reflection spectrum of ZnS. This suggests the possibility that at such critically low concentration of Hg, the incorporation of Cu is somehow hindered.

The identity of the long wave-length emission band is questionable since it is favored not by high coactivator concentration (as in ZnS:Cu) but by high Hg concentrations. Bowers and Melamed (13) proposed that the blue emission in ZnS:Cu, Cl may be identified with the "self-activated" blue caused by Zn-vacancies. It now appears that introduction of a sufficient concentration of Hg results in increasing probability that the vacancy becomes a Hg-vacancy. The decreased population of Zn-vacancies would result in the disappearance of the short wave-length band in favor of a different emission band as shown to occur quite abruptly in Fig. 4 and 9. Figure 2 shows that there is also slight evidence that a similar phenomenon occurs with low-Cu photoluminescent phosphors which are sufficiently coactivated so as to give rise to predominantly green (long wave-length band) emission in ZnS.

According to this mechanism, a similar phenomenon should occur on substitution of Zn by Cd. This, however, has not been reported. Instead, Van Gool (14) noted the opposite, namely, a relative increase in the short wave-length emission band of (Zn, Cd)S:Ag phosphors occurring with increasing Cd concentration. These measurements, however, were taken at 77°K while, with increasing temperature, the short wave-length emission band was more rapidly quenched. It is therefore also possible that the increase of relative intensity of the long wave-length emission band with increasing concentration of Hg is caused by increasing thermal quenching of

the short wave-length emission band. The characteristics of the two emission bands in red-emitting (Zn, Hg)S:Cu phosphors are such that at present, no definite conclusions can be drawn as to their origin.

Summary

Introduction of Hg into ZnS:Cu phosphors causes a shift in emission to longer wave lengths which, for moderate substitutions, is about four times as high as that caused by similar molar concentrations of Cd. At sufficient activator concentrations, EL is observed. For compositions emitting in the red end of the spectrum, the quantum efficiency of the EL was found to be of the same order of magnitude as that of green-emitting ZnS:Cu, Cl. This is attributed to the cubic modification of the system, as favored by the presence of HgS, even in ternary (Zn, Cd, Hg)S composition whose concentration of Cd would, in the absence of Hg, result in hexagonal and non-EL systems.

Procedures for the preparation of (Zn, Hg)S and (Zn, Cd, Hg)S EL phosphors have been described. All procedures involve firings with HgS in sealed tubes, using only prefired raw materials. Especially for low-frequency excitation, the substitution of Hg for Zn enables the use of Ga or In as coactivators, presumably due to a decrease in trap depth caused by lowering of the conduction band. For phosphors emitting in the red end of the spectrum, the relative heights of the two emission bands are primarily dependent on Hg concentration. Their identity cannot necessarily be assumed in terms of an analogy with the blue- and green-emission bands in ZnS:Cu phosphors.

From a practical point of view, the (Zn, Hg)S:Cu and (Zn Cd, Hg)S:Cu EL phosphors are preferable to the ZnSe:Cu EL phosphors, mainly because of their better response at low frequencies of excitation, the extent of which can be estimated roughly from Fig. 8. At higher HgS concentrations, EL emission occurring entirely in the infrared has been obtained; the writer does not know to what extent this can be accomplished with (Zn, Cd)Se:Cu EL phosphors. A serious disadvantage is, however, the high volatility of HgS which necessitates special techniques of phosphor preparation.

Acknowledgments

The writer wishes to thank Miss I. Walinski for preparation and brightness measurements of the phosphors, Mr. I. Meister for determinations of spectral distributions, Dr. C. K. Lui-Wei for x-ray diffraction measurements, and Dr. W. Lehmann for determinations of luminous efficiencies. Thanks are also due to Dr. H. F. Ivey for reading and suggesting improvements of the original manuscript.

Manuscript received March 11, 1960. This paper was prepared for delivery before the Chicago Meeting, May 1-5, 1960. This work was supported by Contract AF33(616)-5811 from the Wright Air Development Center.

Any discussion of this paper will appear in a Discussion Section to be published in the June 1961 JOURNAL.

REFERENCES

1. J. S. Prener, U. S. Pat. 2,731,423, Jan. 17, 1956.
2. I. J. Hegyi, S. Larach, and R. E. Shrader, *This Journal*, **104**, 717 (1957).
3. A. Wachtel, *ibid.*, **107**, 602 (1960).
4. L. Wesch, Reichsamt Wirtschaftsausbau Chem. Ber. Investigation No. 15 (PB 52016) pp 487-501 (1942).
5. A. Kremheller and A. K. Levine, *Sylvania Technologist*, **10**, No. 3 (1957).
6. A. Kremheller, A. K. Levine, and G. Gashurov, *This Journal*, **107**, 12 (1960).
7. P. Zalm, *Philips Research Repts.*, **11**, 353 (1956).
8. W. Hoogenstraaten, *This Journal*, **100**, 356 (1953).
9. C. Haake, *J. Opt. Soc. Am.*, **47**, 881 (1953).
10. H. A. Klasens, *This Journal*, **100**, 72 (1953).
11. W. Lehmann, *ibid.*, **104**, 45 (1957).
12. H. C. Froelich, *ibid.*, **100**, 496 (1953).
13. R. Bowers and N. T. Melamed, *Phys. Rev.*, **99**, 1781 (1958).
14. W. Van Gool, *Philips Research Repts.*, **13**, 157 (1958).

Crater Resistance of Submerged Arc Smelting Furnaces Simulated by a Simple Model

Oluf Chr. Bockman

Elektrokemisk A/S, Oslo, Norway

ABSTRACT

An electrolytic trough technique has been used to study the effect of size and shape of the smelting crater on the ohmic resistance of the crater of submerged arc smelting furnaces. The ohm-inch rule is demonstrated, and the correct use of this rule is discussed.

In designing submerged arc smelting furnaces, the anticipated ohmic crater resistance of the projected furnace is the key to the specification of the electrical circuit. Naturally, many workers have devoted themselves to the study of this problem. In 1933, Andrea pointed (1) out that the product of electrode diameter D and crater resistance R of electric smelting furnaces is fairly independent of furnace size. He defined a "peripheral ohm inch factor" r by

$$r = \pi DR \qquad [1]$$

Values of r for different smelting processes have been given by Udy [2] and by Kelly [3]. This factor has proved useful for calculating operating data in designing new furnaces and in scaling up results obtained by pilot tests.

Andrea apparently arrived at this rule empirically. He referred the crater resistance to the electrode periphery by introducing π in Eq. [1], presumably assuming that 1 in. of electrode periphery makes the same contribution to the conductance of the crater in small as well as in large furnaces.

Recently Morkramer (4) derived Eq. [1] by making the following simplifications. The current radiates hemispherically from the tip of the electrode; the charge has a uniform electrical resistivity; the distance from the tip of the electrode to the furnace bottom is very large. On making these assumptions, he demonstrates the r of Eq. [1] actually is the electrical resistivity of the charge.

The simplifications made by Morkramer are drastic. Equation [1] may, however, be derived by making quite a few much more realistic assumptions. This derivation is based on dimensional analysis as applied in the theory of models. Such a derivation may be of value in pointing out the limitations of Eq. [1].

Dimensional Analysis

The conditions prevailing in the smelting zone of an electric furnace are very complex. Actually, the physical properties of the zone and the variation of these properties within the zone are but little known. Probably, temperature and electrical resistivity vary within wide limits. Any calculation of crater resistance by classical methods therefore is bound to fail.

If it is assumed, however, that differently sized furnaces working on the same raw materials form geometrically and electrically similar systems, the theory of models may be used. These assumptions imply that the smelting craters of the furnaces compared have the same shape and the same size relative to electrode diameter and that corresponding points in the two furnaces show the same electric resistivity. Since electric resistivity depends on temperature and composition, corresponding points must also agree in these respects.

The electric current, on passing from the electrode to the charge, may form arcs. Even in submerged arc smelting furnaces the arcs may consume a part of the tip to hearth voltage. The arcs do not obey Ohm's law, the voltage varying in a complex manner which it is difficult to include in the dimensional analysis. The present derivation, therefore, is restricted to the cases where arcing is insignificant. It must also be assumed that the contact resistance between electrode and the charge is negligible. By the passage of the electric current through the charge, Ohm's law may safely be considered valid.

On these assumptions the ohmic voltage drop from the tip of the electrode to the furnace bottom may in principle be found by integrating along a current path according to

$$E = \int \rho i ds$$

where ρ is electric resistivity and i is current density at the increment ds of the path. The variation of ρ and i along the path is however not known. Similarly the electrode current may be found by integrating over any equipotential surface

$$J = \int i dA$$

where i is current density at the surface increment dA. The ohmic crater resistance then is

$$R = E/J = (\int \rho i ds)/(\int i dA)$$

On increasing the size of the system at constant electric resistivity and current density in the various parts of the system, it is seen that E increases with first power and J with second power of linear dimensions. The R therefore is inversely proportional to linear dimensions, which is the basic content of Eq. [1]. The assumption of equal current density in the two sizes of the system is not necessary, however, because E and J are affected in the same way by a change in the level of current density.

The same result may be obtained by a formal dimensional analysis. Since the systems in question are considered as geometrically similar, with corresponding points having equal electrical resistivity, the problem of the shape of the smelting zone and of the variation of resistivity within the zone drop out of the analysis. The only quantities entering the analysis, then, is ohmic crater resistance, R, a representative value ρ for the electric resistivity of the charge in the smelting zone, and electrode diameter D representing the size of the system. By the theory of dimensional analysis (5) these quantities have to be arranged in dimensionless groups, which are arguments in the causal relationship. It turns out that only the group RD/ρ is formed. The relationship sought, therefore, is

$$F(RD/\rho) = 0$$

or

$$RD/\rho = \text{constant} \qquad [2]$$

which is equivalent to [1]

A different form of [2] has been reported previously (6).

$$P\rho/DE^2 = \text{constant} \qquad [3]$$

where E is ohmic voltage and P is power input. By the relation

$$E^2/P = R \qquad [4]$$

it is seen that [3] is equivalent to [2]. Solving [3] for E gives

$$E = \text{const.} \sqrt{P/D} \qquad [5]$$

Similarly, the electrode current J is found to be

$$J = \text{const.} \sqrt{PD} \qquad [6]$$

Different formulas have been proposed for relating power input to electrode diameter (1, 7, 8). Whatever relation is used, [5] and [6] are valid within the same range as [2].

Model Experiments

The validity of [2] may be demonstrated for the case of a simple model, where the smelting crater

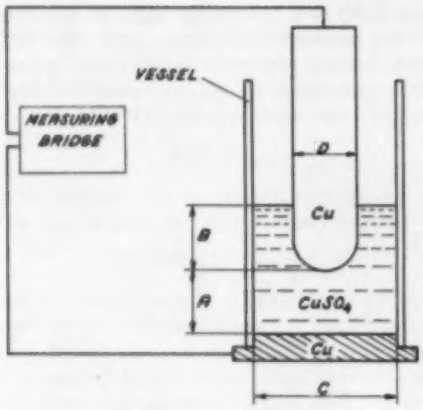

Fig. 1. Model arrangement

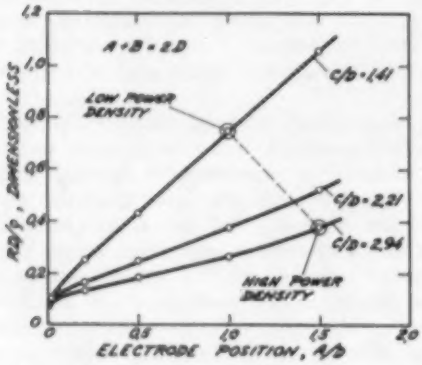

Fig. 2. Effect of electrode position and of size of smelting zone.

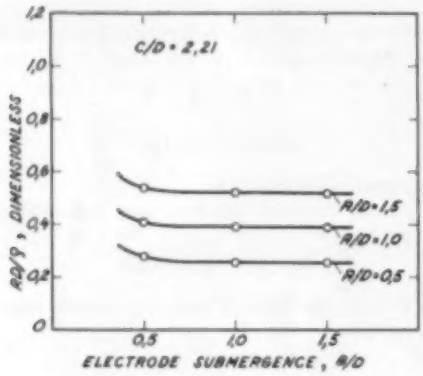

Fig. 3. Effect of electrode submergence

has been simulated by an electrolytic trough as shown in Fig. 1. Between the bottom plate and the electrode, both of copper, is filled an aqueous solution approximately 0.4M $CuSO_4$ and 0.1*N* H_2SO_4. The resistance is measured by a Philips conductivity measuring bridge PR 9500 at a frequency of 1000 cps. The system is made in two sizes, with 1 in. and 2 in. diameter of the electrode, respectively.

In Fig. 2 is shown results obtained for different values of the distance between bottom plate and electrode and for different ratios of vessel to electrode diameters, both at constant liquid level. In Fig. 3 the effect of electrode submergence into the liquid is shown. Corresponding measurements on the two sizes of the system are shown in Table I.

Table I. Values of RD/ρ for 1- and 2-in. electrodes

A/D	B/D	C/D	RD/ρ D = 1 in.	RD/ρ D = 2 in.
0.5	0.5	2.21	0.289	0.278
0.5	1.0	2.21	0.260	0.256
0.5	1.5	2.21	0.256	0.254
1.0	0.5	2.21	0.408	0.414
1.0	1.0	2.21	0.383	0.392
1.0	1.5	2.21	0.380	0.390
1.5	0.5	2.21	0.550	0.543
1.5	1.0	2.21	0.525	0.522
1.5	1.5	2.21	0.522	0.520

Discussion

The model used for simulating the smelting crater is simple and do not reflect all the complexities encountered in actual furnaces. The results, therefore, must be used with caution in interpreting actual furnace behavior. It is seen, however, that within the precision of the measurements Eq. [2] is verified for this simple system.

Within the assumptions made, however, the derivation of Eq. [2] by dimensional analysis is valid also for the complex system of actual furnaces. It is equally valid for three-phase furnaces as for the single electrode furnace simulated by the simple model, as the derivation is not restricted to any definite pattern of electric current. The basic requirement for the derivation is that the smelting zones of the furnaces compared are geometrically and electrically similar. Geometrical similarity implies equal relative electrode position and equal shape and relative size of the smelting zone. Electrical similarity implies that corresponding points of the two smelting zones have equal electric resistivity. The furnaces compared, then, will obtain identical patterns of electric current. This is a less restricting requirement than specifying any definite pattern of electric current and seems to allow a more realistic comparison of different-sized furnaces.

The general trend of measurements on the simple model agrees with everyday experience with smelting furnaces. The resistance increases when electrodes are raised. The shape of the curves on Fig. 2 may indicate the extent to which the voltage drop is concentrated at the tip of the electrode. The slopes of the straight parts of the curves of Fig. 2 correspond exactly to uniform current distribution in the cylindrical vessel. The resistance decreases with increasing diameter of the smelting zone. Most interesting, it is seen from Fig. 3 that the current is found by the model experiments to flow mainly from the very tip of the electrode to the charge. In actual furnaces, the high temperature and good electric conductivity of the smelting zone, as compared with the top of the charge, probably will make this effect still more pronounced.

The derivation of Eq. [2] assumes that the furnaces compared operate at the same relative electrode position and with the same relative size of the

smelting zone. For this to be true, the power input to the furnace must be related to electrode size in a definite manner. Actually, according to Kelly (3), the ohm-inch factor varies with the power density of the electrode. According to his data, furnaces operating at the same power density will show the same value of the ohm-inch factor. By increasing the power density, however, this factor will decrease markedly. By increasing the power input to a given furnace, however, the electrode has to be raised to maintain proper temperature of the metal pool. The size of the smelting zone will in turn increase, which more than offsets the increased distance between electrode and metal. The net result then will be a reduction in the crater resistance. These considerations are illustrated in Fig. 2 by the operating points for low and high power density of the furnace.

For the proper use of the ohm-inch factor, it is important to note that the conditions of the smelting zone may also be affected by the method of attending the furnace. The furnaces to be compared, therefore, must be charged, stoked, and tapped in the same way as far as these operations will influence the furnace performance. When the furnaces operate with substantial arcing of the electrodes, the derivation of Eq. [2] is not valid and the ohm-inch rule should be used with caution.

Most important, the resistivity of the charge depends on the nature of the raw materials used, especially on the nature of the reducing agent. The furnaces to be compared, therefore, must operate on the same raw materials, or at least on the same type of raw materials, if the ohm-inch rule shall apply.

Furnace operation practice differs widely between different works, and the raw materials quality may be highly different in different parts of the world. Two furnaces, operating the same process, picked out at random from different parts of the world most probably will not agree by the ohm-inch rule. In order to use the rule profitably, one has to see that the furnace operations agree with the assumptions underlying the rule. Most profitably the rule may be used internally within the works, when bigger furnaces have to be built, or when scaling up pilot plant results.

Acknowledgment

The author is grateful to Mr. H. Natvig and to Mr. T. Baasen for their helpful comments and discussion of the work. The experimental part has been done by Mr. B. Hogdahl.

Manuscript received Nov. 6, 1958. This paper was prepared for delivery before the Ottawa Meeting, Sept. 28-Oct. 2, 1958.

Any discussion of this paper will appear in a Discussion Section to be published in the June 1961 JOURNAL.

REFERENCES

1. A. Weynarth, *Trans Electrochem. Soc.*, **63**, 309 (1933). F. V. Andrea, *ibid.*, (discussion) 345-347.
2. M. J. Udy, *Can. Chem. Processing*, **35**, 626 (1951).
3. W. M. Kelly, *Metal Progr.*, nr. 5, 73 (1958).
4. M. Morkramer, Paper presented at convention in Stresa, May (1959).
5. R. E. Johnstone and M. W. Thring, "Pilot Plants, Models, and Scale-up Methods in Chemical Engineering," McGraw-Hill Book Co., Inc., New York (1957).
6. O. C. Bockman, *This Journal*, **101**, 493 (1954).
7. F. V. Andrea, *Trans. AIEE*, **69**, 557 (1950), *J. Four Electr.*, **46**, 92 (1937).
8. N. A. Curtis, *This Journal*, **100**, 81C (1953).

Graphite Anodes in Brine Electrolysis

IV. Effect of Anolyte pH on Corrosion Rate in Chlor-Alkali Cells

L. E. Vaaler

Research Laboratories, National Carbon Company, Division of Union Carbide Corporation, Cleveland, Ohio

ABSTRACT

The effect of anolyte pH on cell efficiency and anode corrosion rate was studied in an experimental chlorine cell. With increasing pH, the expected decrease in current efficiency was observed with a resultant increase in the amounts of oxygen and carbon dioxide evolved. The relative increase in oxygen evolution is far greater than the carbon dioxide evolution. The results can be explained by a mechanism whereby the oxygen is formed from physically adsorbed oxygen, while carbon monoxide is formed from chemisorbed oxygen and oxidized to carbon dioxide by oxygen or dissolved chlorine. The increased corrosion resistance of impregnated graphite as compared to plain graphite may be due to the fact that filling of the voids decreases the effective area to one-third of the initial value.

A study of the behavior of graphite anodes in brine electrolysis, and in particular a determination of the rate at which they corrode, requires that the pH of the anolyte be well defined. In some cases pH is well defined by close control of such conditions of electrolysis as current density, temperature, and flux of electrolyte through the cell, and need be measured only occasionally. This is often true in cells without diaphragms. Janes (1) found that pH in an experimental chlorate cell was reproducible

under controlled conditions of electrolysis and proper adjustment of the acidity of the feed brine.

The situation is less satisfactory with diaphragm cells. Part of the hydroxide ion formed in the catholyte leaks through the diaphragm into the anolyte, and the amount of leakage is a function of the method of preparation and age of the diaphragm. It is difficult to obtain negligible leakage or even a reproducible leakage, with the result that pH is not closely maintained. Johnson (2) designed a very useful chlor-alkali diaphragm cell for the laboratory, and it has been used to evaluate various anode materials for many years. However, it has some limits as to precision, and variations in pH from cell to cell probably have an important bearing on this. This relates back to the difficulty in preparing the wrapped asbestos diaphragms used in these cells so that reproducible properties are obtained. This problem is also present in commercial cells with deposited diaphragms.

A mercury cathode cell contains no diaphragm but may act in an analogous manner because of hydrogen discharge at the cathode. The discharge produces sodium hydroxide, and it is difficult to maintain this constant, due to the many variables affecting it.

Chlorine cells operate in the pH range of 3 to slightly over 4 with current efficiencies of 90% or better. The pH is maintained in this range by the buffering action of the anode, which on discharge of oxygen and/or carbon dioxide forms sufficient acid to neutralize sodium hydroxide leaking through the diaphragm. The rate of graphite corrosion is determined to a large extent by the formation of carbon dioxide. The cell efficiency is determined largely by the formation of carbon dioxide plus oxygen. Thus, both the corrosion rate and current efficiency are sensitive functions of the pH.

The excellent and comprehensive work of Foerster (3) and others in the early 1900's was, nevertheless, limited because there were no suitable methods of measuring pH in the desired range. Some attempts to titrate the very dilute acid in the anolyte gave only approximate answers. The work most closely allied to the present study is that of Murray and Kircher (4), who measured the effect of several variables in a commercial Hooker Cell. Chloride concentrations were not the same at the various pH levels tried, but an empirical correction was made to relate directly current efficiency and pH. However, corrosion rate and pH were not similarly studied and only commercial oil-impregnated graphite anodes were used. Barr (5), using existing fundamental and practical data, developed useful relationships relating cell performance to pH and obtained good agreement with the results of Murray and Kircher. However, no prediction could be made of corrosion rate. Okada, Yashida, and Shiragami (6) studied pH in a Krebs-type mercury cell under production conditions, but close control was not possible. When the pH deviated upward to a significant degree from a statistical average, a drop in current efficiency was noted. Lacheisserie (7) plotted his experimental data on a pH-potential diagram showing stability regions for chloride, chlorine, and the various chlorine-oxygen compounds. One-molar solutions were electrolyzed at ambient temperature and an anode current density of 1 ma/cm^2. Thus, conditions were far different from those in a commercial cell.

The purpose of the work reported here was to determine the behavior of three anode materials in anolytes of known pH. The materials were plain graphite, impregnated graphite, and platinum; pH values ranged from 3.0 to 4.2. The porosity of a graphite anode increases as it is corroded, and the extent of porosity can influence the results of electrolysis. To eliminate variables due to porosity, anodes were used for only a few hours during which time corrosion was slight. The corrosion rate was calculated from the composition of the anodically formed gas rather than from weight loss, since the latter was very small over the period of an experiment. Rates calculated in this manner do not take into account loss of graphite due to the formation of sludge.

Experimental

Electrolysis cell.—Figure 1 is a diagram of the experimental cell. It is of the Wheeler type, with diaphragm and wire-screen cathode in the center, and is a modification of the laboratory cell described by Johnson (2). The anolyte was contained in a 6-in. diameter x 12-in. high glass jar. A polymethylmethacrylate cover sealed the cell and held all of the electrolysis and control apparatus. This included the cathode-diaphragm assembly, two opposed anodes, a resistance heater sealed into glass, thermometer, thermistor temperature-control bead, glass and calomel electrodes, brine inlet, a funnel containing acid or alkali for pH control, and orifices for sampling anolyte and anodic gas. These units were pushed through rubber stoppers that fitted in turn into the cell cover. The cover was sealed to the glass jar with a fluorinated paraffin.

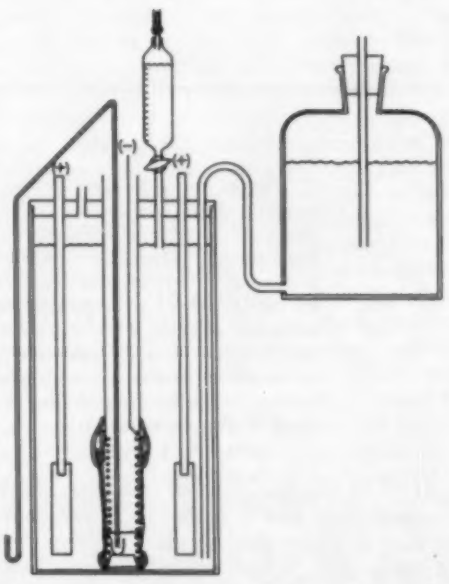

Fig. 1. Experimental chlorine cell

The cathode-diaphragm unit was assembled by partially inserting the end of a 1-in. diameter circular wire-gauze cathode into a glass tube. A rubber sleeve held the two units together and sealed the bottom of the glass tube from anolyte. A 3-in. length of the cathode projecting out of the tube was wrapped with a single layer of asbestos paper, held on with a further wrapping of permeable asbestos tape. Several turns of electrician's rubber tape held the ends of the asbestos tape in place, and a rubber stopper sealed the bottom of the cylindrical cathode. Catholyte was siphoned out of the cathode compartment through a glass tube of sufficiently small diameter to entrain gas bubbles and prevent their collection at the upper bend. A constant head was maintained in the electrolytic cell by means of the feed bottle design shown in Fig. 1.

Platinum sheet anodes 3 x 1¼-in. were bent lengthwise at right angles and positioned so that the bend projected toward the cathode. Graphite anodes were solid specimens ⅝ x ⅝ x 3-in.[1] The average current density for a cell current of 7.2 amp was 0.4 amp/in.^{2}. Independent experiments with an electrode whose front and back halves were separated by a thin strip of insulation showed that about 60% of the current is carried by the front half and 40% by the back half.

For the purpose of experiments at controlled pH, a simple diaphragm or partition to separate cathodic hydrogen from the anode gas may have been sufficient. However, the degree of manual control that can be obtained is much improved by use of an efficient diaphragm, since the frequency and amounts of additions that must be made are reduced. The diaphragm in the experimental cell was submerged under an anolyte head of several inches to minimize back-migration of hydroxide. In a Wheeler cell the diaphragm extends to the surface of the anolyte, at which point there is no flow of anolyte into the cathode chamber. Therefore, back migration is extensive at the anolyte surface and is most noticeable in small cells of limited depth.

Analysis.—Anode gas was collected and analyzed by a method used for production control (8). This involves absorption of chlorine and carbon dioxide into alkaline-arsenite solution and analysis of the unabsorbed gas for oxygen, carbon monoxide, hydrogen, and nitrogen in an Orsat apparatus.

A portion of the arsenite solution is acidified and carbon dioxide distilled over into 0.1*N* caustic solution. Barium chloride is added to precipitate the carbonate, and the amount of carbonate present is determined from the amount of acid needed to decompose it. Carbonate in brine was determined by the same distillation procedure, and carbonate in the caustic used for adjusting pH was analyzed by adding barium chloride and proceeding as above.

Chlorine (as chloride) in the absorbing mixture was determined by the Volhard procedure, but the simpler Mohr method was suitable for chloride in the anolyte after reducing dissolved chlorine with hydrogen peroxide. Active, or dissolved chlorine in the anolyte was determined by pipetting a sample directly out of the cell into a known amount of acidified ferrous ammonium sulfate, boiling for 7 min and titrating with permanganate. The analysis included chlorine, hypochlorite, chlorate, and any other oxidized chlorine compounds.

Experimental procedure.—The cell was operated continuously at 80°C and 7.2 amp, using platinum anodes. The feed rate was about 100 ml/hr. Under these conditions the anolyte pH approximated 3.8, and the catholyte caustic concentration was 110-120 g/l. When graphite anodes were to be studied, they were substituted for platinum at the beginning of an experiment. The pH was immediately adjusted to and held at the desired value for 1 hr. Analysis was made for chloride and dissolved chlorine in the anolyte and anode gas was collected for 1-2 hr. Dissolved chlorine was determined again after gas collection. The rate of flow of catholyte out of the cell was generally determined during gas collection.

Calculations.—The amount of dissolved chlorine generated per hour was calculated from a materials balance:

$$\text{Net chlorine dissolved: } = \left[\begin{matrix}\text{Anolyte through}\\ \text{diaphragm}\end{matrix}\right] \times \left[\begin{matrix}\text{Average dissolved}\\ \text{chlorine concentration}\end{matrix}\right] + \left[\begin{matrix}\text{Anolyte}\\ \text{volume}\end{matrix}\right] \times \left[\begin{matrix}\text{Change in dissolved}\\ \text{chlorine concentration}\end{matrix}\right] + \left[\begin{matrix}\text{Dissolved chlorine}\\ \text{removed by sampling}\end{matrix}\right]$$

This amount was expressed as the per cent of the current required to produce it or in cc of STP gas/hr. The flow of anolyte through the diaphragm was estimated to be 10% greater than the flow of catholyte out of the cell. The reduction in volume is due mainly to the decomposition of water into hydrogen and alkali. At pH 3.0, the amount of chlorine dissolved was found to be less than the experimental error in the above material balance and was neglected. An experiment at this pH was carried out using platinum anodes and stopping the flow of feed brine so that generation of dissolved chlorine could be detected simply by a change in concentration in the anolyte. No change in concentration could be detected over a period of 2 hr.

The amount of air in the sample was determined from the nitrogen present, and the total oxygen corrected for the amount in the air. The evolved Cl_2, CO_2, CO, and corrected O_2 were expressed as volume percent, assuming ideal gases. Further corrections were required for the CO_2 fed into the cell by the brine and by the alkali used for adjusting pH. The evolution of about 3 cc of CO_2 per hour could not be accounted for when platinum anodes were used, and a correction for this amount was made when graphite anodes were employed.

Since the corrections are on a volume per hour basis, it is convenient to know the volumes of gases generated per hour. Due to interruptions during gas sampling, leaks, etc., the gas sample could not be considered the total generated during the collection period.

[1] The two grades of graphite used were National Carbon Co. grades AGLR (unimpregnated) and AGLR-58 (linseed oil impregnated). The unimpregnated graphite had a bulk density of about 1.55 g/cc, corresponding to a porosity of about 30%.

The following calculation yielded the corrections, knowing the relative composition of the gas and amount of dissolved chlorine, including hypochlorite and chlorate. The symbols Cl_2, CO_2, CO, and O_2 denote volume per cent values in the sample and Cl_2' CO_2', CO', and O_2' gas produced by electrolysis in cc/hr. The gases requiring 2 and 4 Faradays per mole, respectively, are added so that:

$$x = Cl_2' + CO' \quad [1]$$

$$y = CO_2' + O_2' \quad [2]$$

then

$$\frac{2x + 4y}{1000} = 22.4 \times F \times E/100 \quad [3]$$

where F is Faradays per hour and
E is nonchlorine current efficiency.

$$x + 2y = 112\,FE = K_1 \quad [4]$$

A second equation in x and y is the following:

$$\frac{CO_2 + O_2}{100} = \frac{y + K_c}{x + y + K_c} = K_2 \quad [5]$$

where K_c is the carbon dioxide corrected for in cc/hr and is a positive value.

All of the K's are experimental quantities, so [4] and [5] may be solved simultaneously for x and y.

$$y = \frac{K_2(K_1 + K_c) - K_c}{1 + K_c} \quad [6]$$

since:

$$\frac{CO_2' + K_c}{O_2'} = \frac{CO_2}{O_2} \quad [7]$$

substitution from [2] gives

$$CO_2' = \frac{y - K_c(O^2/CO_2)}{1 + (O^2/CO_2)} \quad [8]$$

Therefore, CO_2' can be determined from the value of y calculated from [6] and the ratio of O_2/CO_2 in the gas evolved. O_2' is then calculated from [2].

x can be determined from Eq. [4], and CO' related to it by a derivation similar to the above:

$$CO' = (CO/Cl_2 + CO)\,x \quad [9]$$

Cl_2' is then determined from [1].

Results

Data and calculations for the experiments are summarized in Table I. Each pH value represents an average of many readings taken during an experiment, most of which did not vary more than 0.1 unit from the mean. The change in dissolved chlorine during an experiment was not always determined, and values in parentheses are estimated. Regardless of the values shown for dissolved chlorine generated at pH 3, this was assumed to be zero. The gas composition shown is that after correction for CO_2 as described above and after inclusion of dissolved chlorine. The small values for carbon dioxide listed for platinum at pH 4.2 indicate a reasonably good materials balance for this gas, when none is generated at the anode. The value of 100 minus the chlorine current efficiency is that due to generation of CO_2, CO, and O_2.

Figure 2 is a plot of the nonchlorine current efficiency for the three anode materials which indicate the following order for pH 3 to 4:

Plain AGR > Impregnated Graphite > Platinum

At pH 4.2 the nonchlorine efficiency with the impregnated graphite is the same as or higher than that with plain graphite. According to the result the pH should drop when graphite anodes are substituted for platinum, since the chlorine current efficiency, controlled mainly by the diaphragm leakage, will remain approximately constant. A slight drop has been observed.

Table I. Effect of anode material and anolyte pH on cell performance

Anode	pH	Anolyte sodium chloride, g/l	Average dissolved chlorine, meq/l	Dissolved chlorine, generated, % of current	Composition of gas generated				100-Cl_2 current efficiency, %	Calculated anode wt loss, g/1000 amp hr
					Cl_2, %	CO_2, %	CO, %	O_2, %		
Plain graphite	3.01	248	40.2	—0.2	99.09	0.82	0.02	0.06	1.76	1.86
	2.98	251	56.7	1.49	98.99	0.84	0.04	0.11	1.92	1.95
	3.82	270	111	(5)	97.86	1.46	0.08	0.62	4.15	3.38
	3.79	271	80.5	4.9	97.68	1.29	0.09	0.91	4.39	3.02
	4.20	252	120.7	7.4	94.90	2.02	0.12	2.97	9.62	4.56
	4.19	259	144.1	11.8	95.74	1.85	0.11	2.30	8.07	4.21
Impregnated graphite	2.99	252	120	2.4	99.19	0.41	0.03	0.35	1.54	0.98
	3.00	254	113	—	99.36	0.33	0.02	0.30	1.27	0.78
	3.80	258	128	(7)	98.31	0.65	0.06	1.00	3.30	1.56
	3.80	262	135	7.2	98.03	0.66	0.06	1.27	3.85	1.58
	4.18	259	141	26.1	95.16	1.03	0.07	3.74	9.17	2.41
	4.23	243	249	38.4	96.05	0.69	0.07	3.17	7.50	1.63
	4.20	262	276	21.0	95.45	1.05	0.07	3.43	8.64	2.39
Platinum	2.99	275	204	(0)	99.72			0.28	0.56	
	3.00	260	20	(0)	99.71			0.29	0.58	
	3.85	268	76	(5)	98.54			1.46	2.88	
	3.97	260	169	(5)	98.79			1.21	2.39	
	4.19	270	144	13.4	97.54	—0.04		2.52	4.91	
	4.19	244	279	11.5	97.05	—0.06		2.98	5.79	

Temperature 80°C. 7.2 Amp on two ¾ × ¾ × 3 in. blocks or 1¼ × 3 in. sheets.

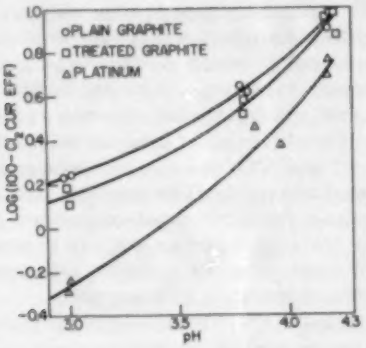

Fig. 2. Effect of pH on current efficiency

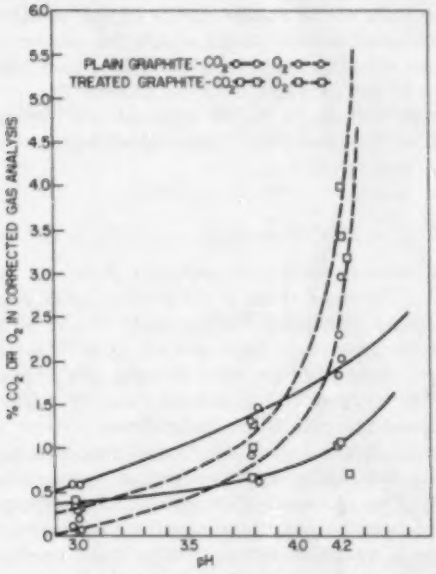

Fig. 3. Effect of pH on per cent O_2 and per cent CO_2

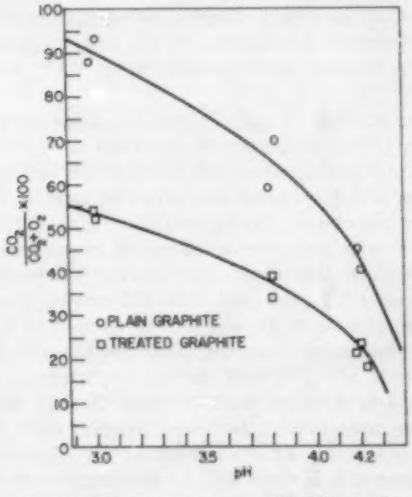

Fig. 4. Effect of pH on ratio $CO_2/CO_2 + O_2$

Figure 3 shows the marked contrast between oxygen and carbon dioxide variations with pH. The oxygen curves undergo a much larger change in slope over the pH range than do the carbon dioxide curves. This means that the slope of a CO_2/O_2 vs. pH plot becomes more negative with increasing pH, as shown in Fig. 4.

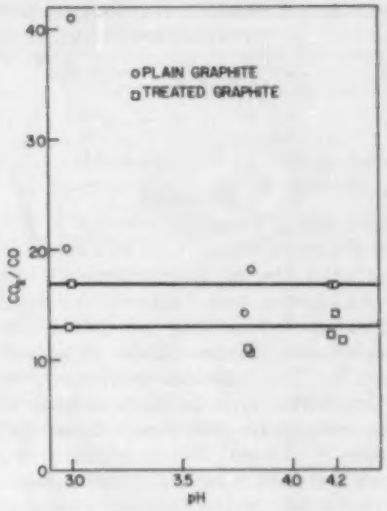

Fig. 5. Effect of pH on ratio CO_2/O_2

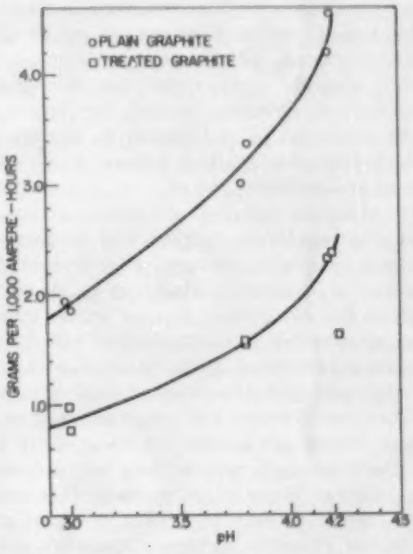

Fig. 6. Effect of pH on anode consumption

On the other hand, the ratio CO_2/CO is probably constant over the pH range. The ratios at pH 3.0 are uncertain, because the amounts of CO in the gas were too small to more than approximate. Figure 5 is a plot of the data and indicates a higher ratio for plain graphite than for impregnated graphite.

Figure 6 shows the variation in carbon consumption as calculated from the gas composition. The curve has the same trend as that for nonchlorine current efficiency, but is less steep because of the compensating effect of the decreasing CO_2/O_2 ratio.

The ratios of consumption for plain graphite compared to impregnated graphite for the three pH values are shown in Table II. The ratio of 2 is unaffected by pH.

Table II. Ratio of consumption of plain graphite relative to impregnated graphite

pH	Weight ratio
3.0	2.2
3.8	2.0
4.2	2.1

Discussion

The amounts of dissolved chlorine in the laboratory cell are much higher than in a commercial cell. With the latter, the amount corresponds to less than 5% of the current under normal operating conditions. This low value may be due to the higher temperature and greater degree of agitation used commercially. The agitation minimizes the formation of an alkaline layer in the anolyte in the vicinity of the diaphragm and thus reduces the amount of chlorate formation. The chemical formation of chlorate is the most reasonable explanation for high chlorine solubility in the laboratory cell, since it is favored by the large ratio of anolyte volume/anode surface. A large anolyte volume means a long hold time for chemical chlorate formation to take place. Electrochemical chlorate formation appears to be no more than expected as evidenced by the amounts of carbon dioxide and oxygen evolved. The very high dissolved chlorine values for impregnated graphite anodes at pH 4.2 appear to involve a further mechanism for solution beyond those operable for the other conditions.

When chlorine current efficiency is based on evolved plus dissolved chlorine, the laboratory and commercial cells compare favorably. This method of comparison is justified in studying anode performance, since the chlorine is formed at the anode regardless of whether it is evolved or dissolved. Results with impregnated graphite anodes in the experimental cell and the Hooker Cell investigated by Murray and Kircher (4) are compared in Table III. Their values are picked off of a curve of hydroxyl ion discharge, which does not include dissolved chlorine. These authors found that chemical chlorate formation was insignificant up to pH 4.2.

The higher chlorine current efficiencies indicated for platinum as compared to graphite reflect a higher overvoltage of oxygen relative to chlorine for the metal. The slightly higher chlorine current efficiency for impregnated as compared to plain graphite is probably related to the less extensive chemical attack by hypochlorite as a result of filling the pores.

The decrease in chlorine current efficiency with increasing pH is expected from the increase in concentration of substances that form oxygen (or CO and CO_2) by anodic oxidation or chemical decomposition. The equilibria and kinetics involved have been discussed in detail by Barr (5) and Murray and Kircher (4). The laboratory data, in confirming the effect of pH on current efficiency, point up the practical attractiveness of using an acid feed to keep anolyte pH low. The decrease in anode consumption is an added advantage. The practical considerations of providing corrosion-proof-containers and conduits for the acid brine as well as a possible decrease in diaphragm life must be balanced against the benefits of operating at lower pH.

Table III. Comparison of current efficiency losses in Laboratory and Hooker Cell

pH	Current efficiency loss	
	Lab. cell	Hooker cell*
3.0	1.4	1.0
3.8	3.6	3.2
4.2	9	6.0

* Values estimated from hydroxyl discharge curve in Ref. (4).

The change in CO_2/O_2 ratio with pH could be due to heterogeneous reactions taking place on the surface of the anode, with or without homogeneous reactions taking place in the vicinity of the anode or in the bulk of the solution. Any of the possible discharge mechanisms could result in adsorption of oxygen directly onto the anode, as could chemical attack of the graphite by hypochlorite. The over-all reaction for discharge of hypochlorite ion, postulated by Foerster (3) from experimental evidence in alkaline solution is:

$$6(OCl)^- + 3H_2O + 6e \rightarrow 6H^+ + 2ClO_3^- + 4Cl^- + \frac{3}{2}O_2$$

Since several steps are probably involved in this over-all reaction, there is the possibility of some intermediate product diffusing away from the anode and homogeneously decomposing to give molecular oxygen. Hypochlorous acid decomposes homogeneously to oxygen and hydrochloric acid. Lister (9) has found the rate to be insignificant except in the presence of a catalyst. Hydrogen peroxide can be formed anodically and decompose to oxygen and water. The question that arises when oxygen is formed from homogeneous reactions is whether such oxygen is available either to attack the anode or to oxidize carbon monoxide formed at the anode or whether it escapes as molecular oxygen and is unavailable as an oxidizing agent. Nevertheless, a mechanism can be proposed, based on the physical and chemical adsorption of all the oxygen supposedly formed, that agrees fairly well with the data.

If, by analogy to mechanisms proposed for air oxidation (10-12), oxygen is adsorbed as a first step, desorption-combination can take place to form oxygen, or a carbon bond can break to form a carbon-oxygen compound. Eyring and Blyholder (10) found that CO was the primary product of air oxidation and ascribed this to its low energy of desorption. Sihvonen (11) proposed that CO comes from desorption of keto or ketene groups formed as a result of oxygen adsorption. He also maintained that α keto acids are obtained during electrolysis, which give rise to a mixture of CO and CO_2. In electrolysis, the presence of adsorbed oxygen need not be the direct result of adsorption of the element, but more probably is the result of oxidation of hydroxyl or hypochlorite ions already present on the surface which then dehydrate or dehydrohalogenate to leave adsorbed oxygen behind. Furthermore, hydroxyl radicals could desorb directly to form hydrogen peroxide which then decomposes to oxygen. This

mechanism is suggested by the fact that Sihvonen found that practically no oxygen was formed at a graphite anode in sulfuric acid solution where peroxide decomposition is slow, while in strong alkali, which readily decomposes peroxide, oxygen was the preponderant anodic gas.

The process for electrolytic oxidation will be assumed to involve the rapid physical adsorption of oxygen on the anode surface, a conversion of a part of this oxygen to desorbed molecular oxygen by a second order reaction and a conversion of the rest to chemisorbed oxygen by a first order reaction followed by rapid desorption of carbon monoxide. The monoxide is then oxidized almost completely to carbon dioxide either by the oxygen desorbed or by dissolved chlorine. The desorption of hydroxyl radicals to form hydrogen peroxide and then oxygen is also a second order reaction, provided the peroxide formation is the rate-determining step.

The following scheme represents the mechanism:

Oxygen source (OH^-, OCl^-, etc)

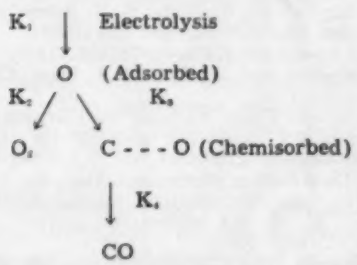

Volume percentages of oxygen and carbon dioxide in the evolved gases are proportional to their rates of formation. In accordance with the assumed mechanism, the volume percentage of carbon monoxide, which is the primary anodic product, is calculated from the volume percentage of carbon dioxide. These rates are proportional to the fraction of active surface sites covered by physically adsorbed and chemisorbed sites, respectively, so that by proper choice of units for the rate constants the following equations hold for the steady state:

$$C_{O_2} = K_2 \theta^2 \qquad [10]$$

$$C_{CO} = K_4 \phi = K_3 \theta \qquad [11]$$

where C_{CO} is volume per cent CO, C_{O_2} is volume per cent O_2, θ is fraction of active sites covered by physically adsorbed oxygen, and ϕ is fraction of active sites covered by chemisorbed oxygen.

$$C_{CO} = K_3 \sqrt{CO_2}/K_4 \qquad [12]$$

which is the obvious relation for competing first and second order reactions leading to carbon monoxide and oxygen, respectively.

To test these assumptions it is necessary to recalculate the data to give CO and O_2 concentrations prior to oxidation of the CO and CO_2. Either oxygen or dissolved chlorine has been assumed to be the oxidizing agent. The results are plotted in Fig. 7, which shows C_{CO} vs. $\sqrt{C_{O_2}}$. Reasonable linearity within the accuracy of the data was obtained for all of the plots. Where it was assumed that oxygen oxidizes carbon monoxide, the lines came closer to the origin. A straight line through the origin indicates rate constants independent of the amount of surface covered with adsorbed atoms, a situation that is not apt to be strictly true. The rate of chemisorption (K_3) when θ and ϕ are very small would probably be higher than when the fractions covered are larger, because only the most active sites on the graphite would be reacting. More exactly, the curves should start at the origin with a slope that decreases with increasing C_{CO} due to a continual decrease in K_3. The Elovich equation [12], or other function with changing slope can be fitted to the data in such a manner that the line passes through the origin, but adds little to a further understanding of the reaction mechanism.

The difference in the results with plain and treated graphite can be explained on the basis of the decrease in area available for electrolysis resulting from the impregnation with oil. The curves in Fig. 7 may be represented as:

$$C_{CO} = A \sqrt{C_{O_2}} + B \qquad [13]$$

A similar equation can be written in which the amount of gas evolved per unit area is used rather than the total

$$C_{CO}/a = A' \sqrt{C_{O_2}}/a + B' \qquad [14]$$

where

$$A' = A/\sqrt{a} \qquad B' = B/a$$

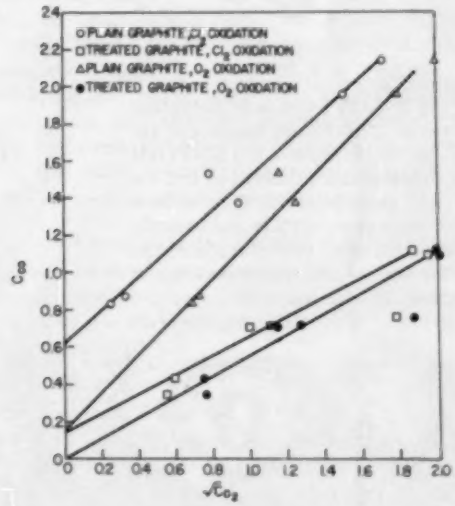

Fig. 7. Plot according to Eq. [12]

Table IV. Relative areas of plain and treated graphite

Graphite	Oxidizing agent	A	B	A_p^2/A_t^2	B_p/B_t
Plain	HOCl	0.89	0.62	3.0	4.1
Treated	HOCl	0.51	0.15		
Plain	O_2	1.02	0.15	3.5	
Treated	O_2	0.55	0		

Thus, in comparing two curves obtained in the same manner:

$$a_1/a_2 = A_p^2/A_T^2 = B_p/B_T \qquad [15]$$

where subscripts p and T refer to plain and treated graphite, respectively. Results are shown in Table IV. The area ratio based on the squares of the slopes is probably much more accurate than that based on the intercept ratio, since the intercept is more uncertain, particularly when it is in the vicinity of the origin. Treatment appears to reduce the effective anode area 3 to 4-fold. This seems reasonable, although the possibility that additional oxygen is formed with treated graphite by the catalyzed decomposition of HOCl cannot be discounted. Cobalt is a suitable catalyst and is contained in the impregnating oil. Joost (13) considered that chemical attack by hypochlorite was an important factor in graphite corrosion, since the addition of cobalt was effective in inhibiting corrosion.

The proposed adsorption mechanism, while giving a reasonable explanation of events in the brine solution, would probably need to be modified to account for results in other media. However, Sihvonen's (14) results, in which he obtained more oxygen than CO_2 in strongly alkaline solution and much more CO_2 than oxygen in strong sulfuric acid solution, exhibit the same trend as the brine data.

In commercial cells the corrosion rate of plain graphite is about double that of impregnated graphite, in agreement with the experimental results in which the corrosion was not allowed to proceed to any extent. It remains to be determined whether such a short test is useful in determining practical corrosion resistances of various anode materials.

Acknowledgment

The author acknowledges the help of Nick Zacharias and Paul Lennon in carrying out the experimental work, and helpful discussions with Charles Lowe, N. J. Johnson, M. Janes, M. S. Kircher, and H. Eyring.

Manuscript received Feb. 4, 1960. This paper was prepared for delivery before the Chicago Meeting, May 1-5, 1960.

Any discussion of this paper will appear in a Discussion Section to be published in the June 1961 JOURNAL.

REFERENCES

1. Milton James, *Trans. Electrochem. Soc.*, **92**, 23 (1947).
2. N. J. Johnson, *ibid.*, **86**, 127 (1944).
3. Fritz Foerster, "Electrochemie Wassriger Lösungen," 4th ed., Barth (1923).
4. R. L. Murray and M. S. Kircher, *Trans. Electrochem. Soc.*, **86**, 83 (1944).
5. Lars Barr, *This Journal*, **101**, 497 (1954).
6. S. Okado, S. Yashida, and O. Shiragami, *J. Electrochem. Soc. Japan*, **22**, 672 (1954).
7. H. de Lacheisserie, *Bull. Soc. Franc. Electriciens*, **7**, 499 ((1957).
8. M. S. Kircher, H. R. Engle, B. H. Ritter, and A. H. Bartlett, *This Journal*, **100**, 448 (1953).
9. M. W. Lister, *Can. J. Chem.*, **34**, 465 (1956).
10. G. Blyholder and H. Eyring, *J. Phys. Chem.*, **61**, 682, (1957).
11. V. Sihvonen, *Trans. Faraday Soc.*, **34**, 1062 (1938).
12. L. Bonnetain, X. Duval, and M. Letart, *Compt. rend.*, **246**, 105 (1958).
13. Joost, Dissertation, Dresden (1910). In A. J. Allmand, "The Principles of Applied Electrochemistry," p. 152, 2nd Impression, Longmans Green, New York (1920).
14. V. Sihvonen, *Acta Chemica Fennica*, **7A**, 25 (1934). Also: Uber Die Oxydation Des Graphits, Suomalainen Tiedeakatemia, Helsinki, 1934.

An Electrochemical Study of Uranium in Fused Chlorides

Derek L. Hill, Jeanne Perano, and Robert A. Osteryoung

Department of Chemistry, Rensselaer Polytechnic Institute, Troy, New York

ABSTRACT

The U(III)-U(O) and U(IV)-U(III) standard potentials in $MgCl_2$-NaCl-KCl eutectic, and the U(IV)-U(III) and UO_2(VI)-UO_2(IV) standard potentials in LiCl-KCl eutectic have been measured at 450°C. The values found are respectively, −2.25, −1.30, −1.25, and −0.285 v vs. the standard Pt(II)-Pt(O) reference electrode on the mole-fraction scale. Polarographic studies of the behavior of U(III), U(IV), and UO_2(VI) in LiCl-KCl eutectic at 450°C have been performed. The significance of the results with respect to certain industrially important processes is briefly noted. A coulometric titration procedure utilizing electrogenerated Pt(II) has been developed for an *in situ* determination of U(III) in LiCl-KCl and $MgCl_2$-NaCl-KCl eutectics.

Recent activity in the use of fused salt baths for the electrodeposition of pure uranium (1, 2) and for the extraction of fission products from a liquid metal fuel reactor (3) and other studies (4, 5) involving this metal suggested that an investigation of certain aspects of the electrochemical behavior of uranium in such solvents would be of interest.

Two chloride eutectic solvents were chosen for for study: (*a*) the binary LiCl (59 mole %)-KCl (41 mole %), mp 355°C, because it has been widely used in electrochemical investigations and would enable direct comparison of uranium electrode potentials to be made with those of other metals, and (*b*) the ternary $MgCl_2$ (50 mole %)-NaCl (30 mole

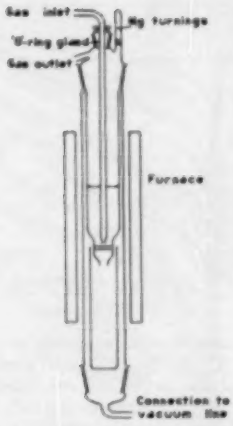

Fig. 1. Pyrex cell for melt purification

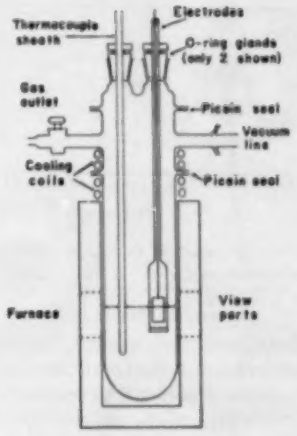

Fig. 2. Pyrex cell assembly

%)-KCl (20 mole %), mp 396°C, because of its suitability for the fission product extraction process.

Experimental and Results

Melt Purification

The apparatus for the dehydration and filtration of the eutectic solvents is shown in Fig. 1. Eutectic components of reagent grade and anhydrous magnesium chloride were mixed in the appropriate ratios and placed in the tube above the fine porosity frit, with the opening of the gas bubbler tube at the lower end, just above the frit. Anhydrous HCl gas was passed through the mixture for 30 min to displace air, and the nichrome-wound tubular furnace was then slowly heated over a period of about 3 hr, HCl passing all the while, until the mixture melted. After HCl had been passed through the melt for a further 30 min, it was replaced by a pure argon stream for 20 min, to remove dissolved HCl. At this point, clean magnesium turnings of Grignard quality were added from the side-tube, and stirred by the argon stream to react with residual impurities. The lower portion of the apparatus was then evacuated, and the melt was filtered into the crucible where it solidified. Finally the apparatus was filled with argon, the crucible was removed, quickly stoppered and transferred to a dry-box by way of a vacuum tunnel, and stored. As required, the weighed solid eutectic, usually about 160 g, was slipped out of the crucible and into the cell assembly, which fitted into a nichrome-wound Vycor tube furnace packed in an insulated container provided with a rear-lighted view-port at the melt level.

Cell Assembly and Related Apparatus

The cell assembly is shown in Fig. 2, the reference electrode and auxiliary cathode fritted compartments, and the titration electrode in Fig. 3 (a) and (b), respectively.

After the solidified eutectic had been placed in the cell and the flanged head carrying the electrodes, etc., had been placed in position, the whole assembly was evacuated overnight at about 10^{-5} mm Hg. It was then slowly warmed until the salt melted under vacuum, after which the temperature was controlled at 450°C by a chromel-alumel thermocouple con-

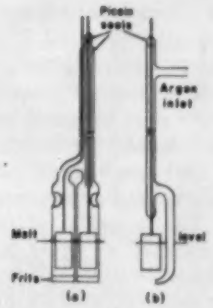

Fig. 3(a). Reference electrode and auxiliary cathode. Fig. 3(b). Argon-stirred titration electrode.

tained in an immersed glass sheath, acting through a Barber-Coleman Wheelco furnace regulator.

The fritted compartments were then lowered till the frits were just above the surface of the melt, where they were kept for 30 min to aid their outgassing. They were then immersed in the melt to a depth of about 2 cm, the cell was filled with pure argon which was then maintained at a steady flow through the cell; the melt filtered up into the compartments and reached its equilibrium level. The compartments each had a small hole above the melt level to avoid pressure differentials and to facilitate the insertion of the electrodes during the assembly of the cell. The reference electrode was then prepared coulometrically by the anodization at ~5 ma cm^{-2} of the Pt foil or Ag wire in one compartment, using the Pt foil in the other as cathode. The generation of Pt(II) and Ag(I) at 100% current efficiency under these conditions has been well established (6). Anodization was generally continued for a time sufficient to bring the mole fraction of Pt(II) or Ag(I) in the compartment to about $1 - 2 \times 10^{-4}$. The exact concentration was determined at the end of each experiment by the weight of eutectic contained in the compartment and the number of coulombs passed. The Nernst relation was then used to refer the potential of the reference electrode to the standard state of unit mole fraction.

Cylinder argon (99.995%) was passed through P_2O_5 and over titanium sponge at 900°-1000°C. Po-

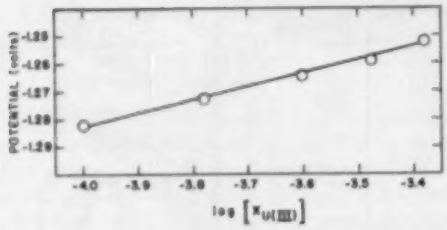

Fig. 4. U(III)-U(O) potential in $MgCl_2$-NaCl-KCl at 450°C. Ag(I)-Ag(O) reference electrode, 3.02×10^{-4} mole fraction of Ag(I).

larograms were recorded with a Sargent XXI recording polarograph. A Rubicon Model 2700 precision potentiometer was used to measure cell potentials. A Sargent coulometric current source was used in all constant current anodization or titration procedures.

U(III)-U(O) *Potential In* $MgCl_2$-NaCl-KCl

To a known weight of ternary eutectic, successive quantities of U(III) were introduced coulometrically by the anodization at about 10 ma cm^{-2} of a carefully outgassed pure uranium rod (analysis: Fe 0.003%, Mg 0.0008-0.003%, Si 0.0008%, Cu 0.0008%, Al 0.0005%). Current efficiency of 100% for this process is demonstrated in the present work and is discussed later. The potential of the uranium rod was measured against a Ag(I)-Ag(O) reference electrode after each addition, insuring uniform concentration in the deep red solution by argon stirring.

A plot of this potential against log [U(III)] at 450°C is shown in Fig. 4 and indicates that the Nernst relation is obeyed, the slope of the line (0.0470 v) being in close agreement with that calculated (0.0478 v) for a 3-electron transfer. Extrapolation to unit mole fraction of U(III) yields a value of -1.61 ± 0.01 v against a standard Ag(I)-Ag(O) reference electrode. Using the data of Laitinen and Liu (6) this value becomes -2.25 ± 0.01 v against a standard Pt(II)-Pt(O) reference electrode.

Polarography of U(III) *and* U(IV) *in* LiCl-KCl

The polarographic behavior of U(III) and U(IV) in the binary eutectic was studied using a Pt needle microelectrode prepared by sealing a length of 14 mil diameter Pt wire into 6 mm Pyrex tubing so that about 1.5 mm^2 projected from the seal. Measurements were made with respect to a Pt(II)-Pt(O) reference electrode. Again, U(III) was added coulometrically by the anodization of a pure uranium rod, which was raised out of the melt after each period of anodization. Current efficiency of 100% was found for this process also, and is discussed later.

By restricting the potential range in which the microelectrode was used to less than 1.5 v negative to the reference electrode, reproducible and well-defined waves for the oxidation of U(III) to U(IV) were observed. Figure 5 illustrates the polarograms obtained after successive additions of U(III). As the U(III) concentration was increased, the potential at which the polarographic current attained the residual value became increasingly negative, but, although the magnitude of the shift was of the right order, exact quantitative agreement with that calculated from the Nernst relation was not obtained. At a fixed potential, the polarographic currents due to successive additions of U(III) showed a linear relation to concentration, as illustrated in Fig. 6.

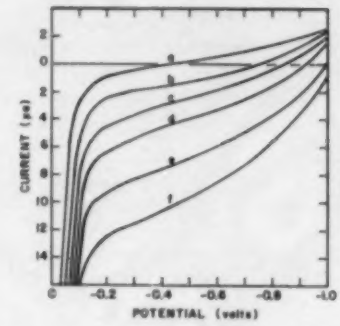

Fig. 5. Polarograms for the oxidation of U(III) to U(IV) in LiCl-KCl at 450°C. Pt(II)-Pt(O) reference electrode, 1.14×10^{-4} mole fraction of Pt(II); microelectrode area 1.65 mm^2; melt weight 160 g; additions of U(III): a:0; b:12; c:28; d:44; e:68; f:92 mg. The current below the zero-axis is anodic.

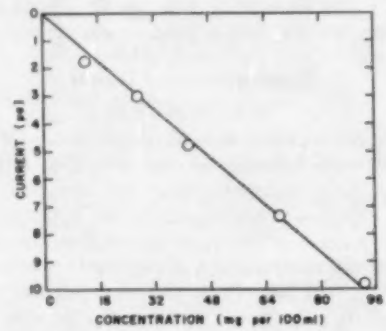

Fig. 6. Relation between U(III)—oxidation polarographic current and U(III) concentration in LiCl-KCl at 450°C (from Fig. 5, at −0.43 v).

Starting with a given concentration of U(III) in the melt, U(IV) could be added to the system by the reaction

$$2U(III) + Pt(II) \rightarrow 2U(IV) + Pt \qquad [1]$$

using Pt(II) generated coulometrically from an immersed Pt foil anode. On making successive additions of U(IV) in this manner, accompanied of course by the equivalent successive removals of U(III), the potential at which the polarographic current attained the residual value became less negative again, and the steady development of the U(IV) reduction wave was observed along with the simultaneous steady disappearance of the U(III) oxidation wave. With equal concentrations of U(III) and U(IV) in the melt, the point of zero current occurred at a potential very close to that found in the potentiometric titration procedure for the determination of the U(IV)-U(III) redox potential described below. The development of the combined U(IV)-U(III) polarograms is shown in Fig. 7.

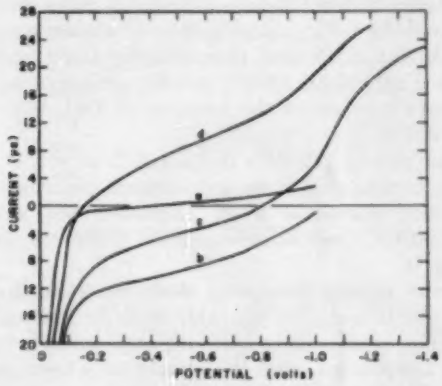

Fig. 7. Development of combined U(III) and U(IV) polarograms in LiCl-KCl at 450°C. Pt(II)-Pt(O) reference electrode, 1.14 × 10^{-3} mole fraction of Pt(II); microelectrode area 1.65 mm^2; a, residual current; b, U(III) oxidation (92 mg U(III) per 100 ml melt); c, U(III) oxidation, U(IV) reduction; d, Pt(II) reduction, U(IV) reduction. Current below the zero-axis is anodic.

Only indistinct waves for the reduction of U(III) to uranium metal were observed, at about −2.2 v, and it appeared that alloying occurred, both from the subsequent appearance of the microelectrode, and also because it was not found possible to obtain unequivocal anodic stripping curves corresponding to the dissolution of the uranium metal which should have been electrodeposited on the microelectrode. The use of a Pt microelectrode at such a negative potential, which is close to that corresponding to the deposition of lithium on Pt (~ −2.4 v), was detrimental to the reproducibility of subsequent polarograms, due to the difficulty of completely dissolving out the electropositive alloying elements from the Pt. The problem was accentuated by the decrease in the separation of the deposition potentials of the two metals by the alloy formation. Attempts to avoid this difficulty by the use of a tungsten or graphite microelectrode were not successful. Immersed, finely polished, flush-ground tungsten microelectrodes were attacked at the glass-metal seal and also gave irreproducible results, while a finely pointed, spectroscopic grade graphite rod immersed just in the surface of the melt gave very unsteady waves and appeared to disintegrate slowly.

A similarly surface-immersed graphite microelectrode was used to examine the behavior of approximately equal concentrations of U(III) and U(IV) at potentials more positive than can be reached with a Pt microelectrode. The U(IV)-U(III) combined wave was clearly shown, but no further waves were found between the potential at which this occurred and that at which chlorine was evolved.

Determination of the U(IV)-U(III) *Redox Potential*

In both the binary and ternary eutectics, when Pt(II) was electrolytically generated from an immersed Pt foil, reaction [1] occurred, and it was found that the potential of the Pt foil, measured against a Pt(II)-Pt(O) reference electrode at intervals between successive periods of anodization, followed typical potentiometric titration curves such as that shown in Fig. 8.

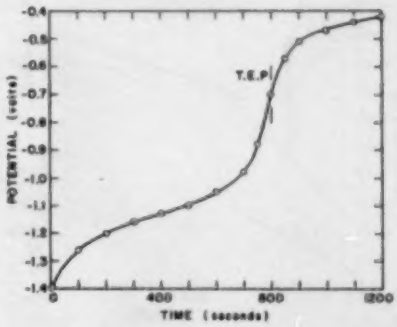

Fig. 8. Coulometric titration of U(III) with Pt(II) in $MgCl_2$-NaCl-KCl at 450°C. Pt(II)-Pt(O) reference electrode, 1.83 × 10^{-3} mole fraction of Pt(II); constant current, 48.25 ma, 1.2 × 10^{-3} equivalents U(III). T.E.P., theoretical end-point.

Titrations were performed with the argon-stirred Pt foil electrode shown in Fig. 3(b). During the course of the titration the initially dark red color of the melts due to U(III) gradually lightened, and just before the end points became light green in color, due to U(IV). Black, finely divided Pt was also seen in the melts. At the end of a titration the immersion of a uranium rod caused the melt to become red again due to the reaction

$$U + 3U(IV) \rightarrow 4U(III) \qquad [2]$$

Since both U(III) and Pt(II) were generated coulometrically, a theoretical end point could be calculated. In experiments with melts having very low residual impurity concentrations, as demonstrated by polarographic residual currents of considerably less than 1 $\mu a\ mm^{-2}$ at −1.0 v against the Pt(II)-Pt(O) reference electrode, the agreement between the amount of U(III) taken and the amount found was very close, as in Fig. 8. In many other experiments, the titration end points fell somewhat short of those calculated. As the initial concentration of U(III) in the melts was less than 600 ppm, it can readily be seen that in the case of a low molecular weight impurity such as oxygen, which reacts very readily with U(III) as described below, less than 10 ppm would be required to oxidize more than 10% of the initial U(III) concentration, and so the occurrence of low titration values is easily understood. Fortunately, this did not interfere too seriously with the determination of the U(IV)-U(III) redox potential which was taken from the relatively flat midportion of the lower branch of the curve. On the mole fraction scale the standard redox potentials found were −1.30 ± 0.01 v in $MgCl_2$-NaCl-KCl eutectic, and −1.25 ± 0.01 v in LiCl-KCl eutectic, with respect to the Pt(II)-Pt(O) couple at 450°C.

For a given experiment the shape of the lower branch of the curve can be calculated from the redox potential by means of the Nernst relation, and in general, good agreement was found with the shape obtained experimentally. Usually the initial potential, before any addition of Pt(II), corresponded to a U(IV) to U(III) ratio of ½% or less.

In view of the polarographic behavior of U(III), U(IV), and Pt(II) it was to be expected that amperometric end-point detection, using a Pt microelectrode at about −0.5 v vs. the working Pt(II)-

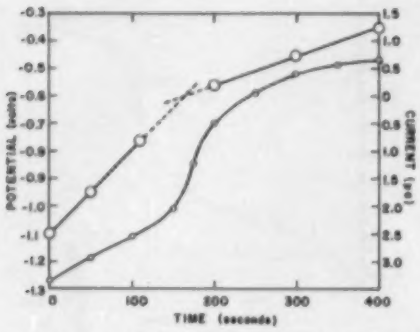

Fig. 9. Coulometric titration of U(III) with Pt(II) in $MgCl_2$-NaCl-KCl at 450°C, with amperometric end-point detection. Pt(II)-Pt(O) reference electrode, 1.75 × 10^{-3} mole fraction of Pt(II); constant current, 48.25 ma, 2.5 × 10^{-4} equivalents U(III). Microelectrode area 1.35 mm^2.

Pt(O) reference electrode, would be a convenient adjunct to the titration. In practice however, it usually presented difficulties, due in part to the necessity of waiting a considerable period of time after argon-stirring the melts for the current to become sufficiently steady to enable a reading to be taken, and in part due to the formation during the titration of finely divided Pt, which tended to become attached to the Pt microelectrode, and which was difficult to dislodge. A successful attempt to use this method of end-point detection is shown in Fig. 9 which also demonstrates that the polarographic behavior in the two eutectics was similar.

Preparation, Polarography, and Potentiometry of Uranyl Species

Solutions of the uranyl species were prepared in both eutectics at 450°C by bubbling dry oxygen (7) through the green solutions obtained by the addition of pure anhydrous uranium tetrachloride. The resulting solutions were clear yellow in color at low concentrations, and reddish-orange at high concentrations. The absorption spectrum in LiCl-KCl eutectic at 400°C was very similar to that observed for uranyl species in this solvent at the same temperature by Gruen (8), showing no evidence of the presence of U(IV), and x-ray patterns of the powdered yellow solid, obtained by grinding this solidified eutectic, showed lines characteristic of uranyl chloride. The reaction appeared to proceed smoothly and rapidly to completion with the evolution of chlorine. It was not possible to determine whether it proceeded directly, or through intermediate stages.

In other experiments it was observed that U(III) in solution in these melts also yielded clear yellow solutions rapidly when dry oxygen was bubbled in, but if moist air were used instead, partial precipitation, probably of oxides, also occurred.

To prepare for the polarographic and potentiometric work on the uranyl species, samples of a known weight of LiCl-KCl eutectic containing UO_2(VI) prepared directly in the melt from a known weight of UCl, were drawn up into several lengths of 6 mm glass tubing, quickly cooled to prevent the formation of concentration gradients, and sealed off to exclude moisture. Weighed samples of this solidified salt were later tapped out and added to LiCl-KCl solvent for study. This procedure provided a more convenient method for the introduction of known amounts of UO_2(VI) to the melt than does the direct addition of pure anhydrous UO_2Cl_2 powder prepared by the standard method of the reaction of UCl, with dry O_2 at 350°C.

Solutions of UO_2(VI) in LiCl-KCl at 450°C prepared in this way gave well-defined polarographic reduction waves at a Pt microelectrode with a Pt(II)-Pt(O) reference electrode; these are shown in Fig. 10.

If the process occurring were the reduction of UO_2(VI) to uranium dioxide, then by holding the potential of the microelectrode at a suitable value along the plateau, solid UO_2 should have been plated onto the electrode. At this point the microelectrode could be disconnected from the polarograph and its potential determined with the potentiometer. By repeating this procedure at various UO_2(VI) concentrations, a Nernst plot should have been obtained if a true equilibrium existed between the oxide and the uranyl species.

This postulate was tested and verified experimentally, and such a Nernst plot is shown in Fig. 11. The slope of the line (0.07166 v) is in good agreement with that calculated for a 2-electron process (0.07174 v). By extrapolation, the standard potential on the mole fraction scale for the UO_2(VI)-UO_2(IV) couple was found to be −0.285 ± 0.005 v against the standard Pt(II)-Pt(O) reference electrode.

Furthermore, a UO_2-plated Pt microelectrode should have produced a large anodic stripping current at potentials more positive than that for the

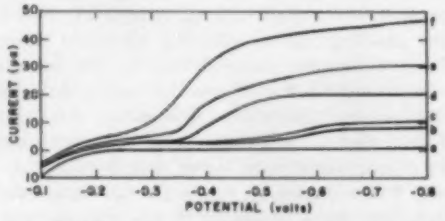

Fig. 10. Polarograms of UO_2(VI) reduction in LiCl-KCl at 450°C. Pt(II)-Pt(O) reference electrode, 1.05 × 10^{-3} mole fraction; microelectrode area, 1.35 mm^2; mole fractions UO_2(VI) × 10^{-4}: a, 0; b, 0.23; c, 0.63; d, 2.42; e, 3.60; f, 4.80

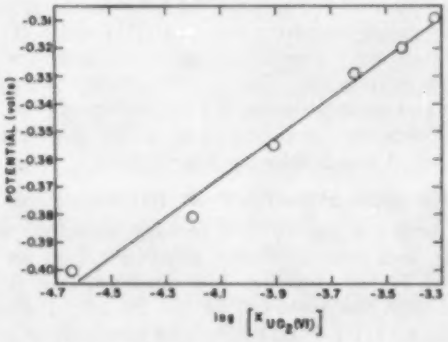

Fig. 11. UO_2(VI)-UO_2(IV) potential in LiCl-KCl at 450°C. Pt(II)-Pt(O) reference electrode, 1.05 × 10^{-3} mole fraction of Pt(II).

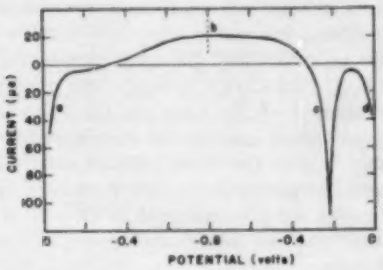

Fig. 12. Combined deposition and anodic dissolution waves for UO_2 in LiCl-KCl at 450°C. Pt(II)-Pt(O) reference electrode, 1.05×10^{-4} mole fraction of Pt(II); mole fraction UO_2(VI), 2.42×10^{-4}; a, Pt dissolution; b, UO_2 deposition, reversal of direction of change in polarization; c, UO_2 dissolution; d, Pt dissolution. Microelectrode area 1.35 mm^2. Current below zero-axis is anodic.

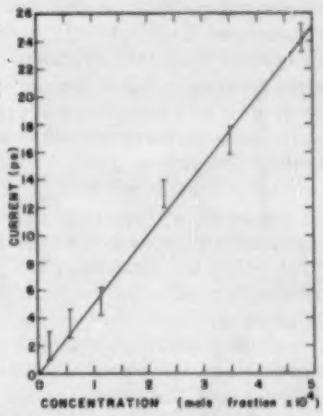

Fig. 13. Relation between wave height for UO_2(VI) reduction and UO_2(VI) concentration in LiCl-KCl at 450°C (from Fig. 10, at −0.7 v).

UO_2(VI)-UO_2(IV) equilibrium if its potential were slowly shifted from a value on the plateau toward less negative values. This effect also was observed, and a typical combined deposition and stripping curve is shown in Fig. 12. The relation between wave height and UO_2(VI) concentration is shown in Fig. 13.

Discussion

Results of the coulometric titration establish that U(III) was electrogenerated at 100% current efficiency in both eutectics. The value of the U(III)-U(O) potential in $MgCl_2$-NaCl-KCl eutectic is virtually identical to that found by Gruen and Osteryoung (9) in LiCl-KCl eutectic at the same temperature. Close correspondence of electrode potentials in different melts is not uncommon (10). The U(IV)-U(III) redox potentials observed in the present work provide a similar example. This correspondence of electrode potentials in different melts suggests that in many cases the behavior of the potential determining solute species is not dependent primarily on the nature of the solvent cationic species.

For the cell

$$(-)\mathrm{U}\left\{\begin{matrix}\mathrm{U(III)}\\ \text{binary or ternary}\\ \text{chloride eutectic}\end{matrix}\right\}\left\{\begin{matrix}\mathrm{Ag(I)}\\ \text{binary or ternary}\\ \text{chloride eutectic}\end{matrix}\right\}\mathrm{Ag}(+) \qquad \text{(I)}$$

the measured emf is in close agreement with that calculated from the established thermodynamic data for the pure compounds. This indicates that the free energies of solution of U(III) and Ag(I) are not very different, and are much smaller than the free energy change for the overall cell reaction, so that only the difference between two minor quantities is included in the calculation. For the cell

$$(-)\mathrm{Pt}\left\{\begin{matrix}\mathrm{U(IV),U(III)}\\ \text{binary or ternary}\\ \text{chloride eutectic}\end{matrix}\right\}\left\{\begin{matrix}\mathrm{Pt(II)}\\ \text{binary or ternary}\\ \text{chloride eutectic}\end{matrix}\right\}\mathrm{Pt}(+) \qquad \text{(II)}$$

a difference considerably greater than can be attributed to experimental error is found on making a similar comparison between measurement and calculation. Since for the cell

$$(-)\mathrm{Ag}\mid \mathrm{Ag(I)\ LiCl\text{-}KCl} \parallel \mathrm{Pt(II)\ LiCl\text{-}KCl}\mid \mathrm{Pt}(+) \qquad \text{(III)}$$

the same comparison leads to good agreement, it would appear that the difference between the measured and calculated values for the emf of cell (II) may be due to a comparatively large term involving the free energy of solution of U(IV). A possible interpretation of this is that U(IV) forms a chloro-

Table I. Comparison of measured cell potentials with those calculated from thermodynamic data[a] for the pure compounds at 450°C

Cell	Solvent eutectic	Potential measured	Potential calculated
(−)U|U(III)||Ag(I)|Ag(+)	Binary	+1.61[b]	+1.619
(−)U|U(III)||Ag(I)|Ag(+)	Ternary	+1.61	+1.619
(−)Ag|Ag(I)||Pt(II)|Pt(+)	Binary	+0.637[c]	+0.612
(−)U|U(III)||Pt(II)|Pt(+)	Binary	+2.25	+2.231
(−)U|U(III)||Pt(II)|Pt(+)	Ternary	+2.25	+2.231
(−)Pt|U(IV), U(III)||Pt(II)|Pt(+)	Binary	+1.25	+0.835
(−)Pt|U(IV), U(III)||Pt(II)|Pt(+)	Ternary	+1.30	+0.835
(−)U|U(IV)||Pt(II)|Pt(+)	Binary	+2.00[d]	+1.882
(−)U|U(IV)||Pt(II)|Pt(+)	Ternary	+2.01[d]	+1.882

[a] W. Hamer, M. Malmberg, and B. Rubin (16).
[b] D. M. Gruen and R. A. Osteryoung (9).
[c] H. A. Laitinen and C. H. Liu (6).
[d] Calculated from present measurements.

complex of sufficient stability in the chloride melts to shift the measured U(IV)-U(III) potential to a value more negative than that calculated from the thermodynamic formation data.[1] Similar considerations have been used by Flengas and Ingraham (11-15) to explain such differences between experimental and calculated values. Table I lists the comparisons made in the present work.

The U(III) oxidation waves are somewhat drawn out and do not conform quantitatively in respect of either log $[i/(i_d - i)]$ vs. potential plots, or potential at the intersection with the residual current vs. log [U(III)] plots, probably due to the difficulties inherent in recording polarograms at a stationary solid microelectrode. Nevertheless, the polarographic behavior otherwise and the potentiometric titration of U(III) demonstrate clearly that the reaction

$$U(IV) + e^- \rightleftharpoons U(III) \qquad [3]$$

behaves in a electrochemically reversible manner in both melts. In addition, the linear relation between wave height and concentration of U(III), and especially the coulometric titration, provide useful *in situ* analytical procedures. This titration is unique in that it uses an oxidant electrogenerated directly from a metal. Coulometric titration with amperometric end-point detection in fused LiCl-KCl using electrogenerated Fe(III) as oxidant has been the subject of a recent paper (17).

The absence of further oxidation waves at a graphite microelectrode in the potential range between U(III) oxidation and chlorine evolution indicates that U(V) and U(VI) are unstable in the melt, and confirms the observation by Gruen (7) that no reaction occurs when chlorine is bubbled into a solution of UCl_4 in the binary eutectic.

It has long been known (18) that pure molten uranyl chloride can be electrolyzed to produce UO_2 at the cathode and Cl_2 at the anode. The present work with the uranyl species clearly demonstrates that the equilibrium

$$UO_2(VI) + 2e^- \rightleftharpoons UO_2(IV) \qquad [4]$$

can be established in the melt LiCl-KCl, and the movement of the UO_2 deposition potential toward less negative values as the $UO_2(VI)$ concentration is increased is readily understood. This work also confirms and extends the observation by Smirnov and Ivanovsky (19) that anodes of compacted UO_2 could be dissolved anodically in LiCl-KCl eutectic at 650°C, with the production of uranyl ions, and that it was possible to obtain weakly adherent electroplates of UO_2 on molybdenum cathodes. In the present work it was noticed that argon stirring of the melt drastically altered the potential of the UO_2-plated microelectrode in the direction consistent with the physical removal of the plate. Smirnov and Ivanovsky also studied the potential of a UO_2 anode at various current densities, and by extrapolation to zero current density obtained a potential of −0.57 v against a chlorine-chloride reference electrode at 550°C in a dilute but undefined concentration of $UO_2(VI)$. Using the value (20) of −0.216 v for the difference between the standard potentials of the Pt(II)-Pt(O) and Cl_2-Cl^- couples, the present work yields a value of −0.501 v for the $UO_2(VI)$-$UO_2(IV)$ standard potential against the standard Cl_2-Cl^- reference electrode on the mole fraction scale. That this is less negative than the value found by Smirnov and Ivanovsky is to be expected in view of the lower temperature and the use of unit mole fraction as the standard state.

The heights of the $UO_2(VI)$ reduction waves are seen to be an approximately linear function of concentration, but it is difficult to determine them accurately because they are not too steady, and the plateaus are not smooth lines. In this case the difficulties associated with the use of stationary solid microelectrodes are probably accentuated by uneven or rough growth and poor adherence of the oxide plate, and straight line plots of log $[(i_d - i)]$ vs. potential do not have the slope expected for a 2-electron process.

With regard to the electrodeposition of pure uranium from fused salt baths, the present work shows clearly that, in the preparation of uranium by the reduction of U(IV) in a chloride melt, the primary process proceeds stepwise, first to U(III), then to the metal. In view of the measured value of the U(IV)-U(III) redox potential, the majority of metal ion impurities in the melt can oxidize U(III) to U(IV), and this is the probable cause of the presence of U(IV) in the melts deduced from the initial potential of the indicator electrode in the coulometric titrations. Further, since both U(III) and U(IV) react rapidly with oxygen to form $UO_2(VI)$, the reduction of either U(III) or U(IV) from a melt contaminated by oxygen must result in the inclusion of UO_2 with the uranium deposit, and from the measured potentials, both U(III) and uranium metal should be capable of reducing $UO_2(VI)$ to $UO_2(IV)$. For the same reasons, the reversible redox equilibrium between uranium dissolved in a liquid metal and U(III) in a molten chloride solvent will be upset by oxygen impurities in the melt.

Acknowledgment

This work was performed under Contract No. AT 30-2-GEN-16 Subcontract No. S-348 with the U. S. Atomic Energy Commission through Brookhaven National Laboratory.

Manuscript received Jan. 6, 1960. This paper was presented, in part, at the 136th Meeting of the American Chemical Society.

Any discussion of this paper will appear in a Discussion Section to be published in the June 1961 JOURNAL.

REFERENCES

1. L. W. Niedrach and A. C. Glamm, *This Journal*, **103**, 521 (1956).
2. L. W. Niedrach and B. E. Dearing, *ibid.*, **105**, 353 (1958).
3. W. S. Ginell, *Ind. Eng. Chem.*, **51**, 185 (1959).
4. G. Meister, *Metal Progr.*, **53**, 515 (1948).
5. D. Inman, G. J. Hills, L. Young, and J. O'M. Bockris, *Trans. Faraday Soc.*, **55**, 1904 (1959); *Ann. N. Y. Acad. Sci.*, **79**, 803 (1960).

[1] This conclusion is in contrast to that of Inman, *et al.* (5) who conclude that complexing of U(III) occurs. However, it appears that the calculations from which this conclusion was drawn are in error, and that their data do not show significant evidence of complexing of U(III), a result in accord with the present work and with that of Gruen and Osteryoung (9).

6. H. A. Laitinen and C. H. Liu, *J. Am. Chem. Soc.*, **80**, 1015 (1958).
7. D. M. Gruen, *Private communication.*
8. D. M. Gruen, S. Fried, P. Graf, and R. L. McBeth, *Proc. Intern. Conf. Peaceful Uses Atomic Energy, 2nd Conf., Geneva, 1958*, **28**, 112 (1958).
9. D. M. Gruen and R. A. Osteryoung, *Ann. N. Y. Acad. Sci.*, **79**, 897 (1960).
10. S. N. Flengas and T. R. Ingraham, *This Journal*, **106**, 714 (1959).
11. S. N. Flengas and T. R. Ingraham, *Can. J. Chem.*, **35**, 1139 (1957).
12. S. N. Flengas and T. R. Ingraham, *ibid.*, **35**, 1254 (1957).
13. S. N. Flengas and T. R. Ingraham, *ibid.*, **36**, 780 (1958).
14. S. N. Flengas and T. R. Ingraham, *ibid.*, **36**, 1103 (1958).
15. S. N. Flengas and T. R. Ingraham, *ibid.*, **36**, 1063 (1958).
16. W. Hamer, M. Malmberg, and B. Rubin, *This Journal*, **103**, 8 (1956).
17. H. A. Laitinen and B. B. Bhatia, *Anal. Chem.*, **30**, 1995 (1958).
18. W. Hampe, *Chem. Ztg.*, **12**, 106 (1888).
19. M. V. Smirnov and L. E. Ivanovsky, *J. Gen. Chem. U.S.S.R.*, **27**, 329 (1957).
20. H. A. Laitinen and J. W. Pankey, *J. Am. Chem. Soc.*, **81**, 1053 (1959).

Electrochemical Study of Metallic Oxides in Fused Lithium Chloride-Potassium Chloride Eutectic

H. A. Laitinen and B. B. Bhatia

Noyes Chemical Laboratory, University of Illinois, Urbana, Illinois

ABSTRACT

The oxygen electrode does not behave reversibly in LiCl-KCl at temperatures of 400°-500°C, and at oxide ion concentrations of 0.1-0.2M. The following electrode systems behave reversibly as electrodes of the second kind: $Cu/Cu_2O,O^=$; $Pt/PtO,O^=$; $Pd/PdO,O^=$; $Bi/BiOCl,O^=$. The $Ni/NiO,O^=$ and $Bi/Bi_2O_3,O^=$ electrodes did not show reversible behavior. Because of the relatively high solubilities of the metal oxides, the applicability of the metal oxide electrodes to the measurement of oxide ion activity is limited to solutions containing oxide ion in concentrations comparable with, or greater than, that contributed by dissolution of the oxides. This limit is 10^{-4}M or higher, depending on the system. The relatively high solubility of heavy metal oxides in this solvent is attributed to the great complexing tendency of chloride ion. It is probable that these oxides would be much less soluble in nitrate and sulfate melts and thus their utility as acidity electrodes could be extended to lower oxide concentrations.

A molten alkali metal chloride solvent may be said to be "buffered" with respect to the addition of Lewis acids such as $AlCl_3$ because of the presence of a large excess of the weakly basic chloride ion. On the other hand, such a solvent can be rendered basic by the addition of substances such as oxide ion which are more strongly basic than chloride ion.

The purpose of the present investigation was to determine the feasibility of using the oxygen-oxide ion electrode or metal-metal oxide-oxide ion electrodes for the electrochemical measurement of oxide ion activity in molten lithium chloride-potassium chloride eutectic at 450°. A secondary objective was to determine the solubilities of metal oxides from emf measurements.

There is considerable evidence for the reversibility of the oxygen-oxide ion electrode at temperatures of the order of 1000°C in various melts containing oxyanions. The early work of Baur and Ehrenberg (1) on borates, silicates, etc., and of Treadwell (2) on metal oxides, using quartz or porcelain as an electrolyte and silver as the indicator electrode, had indicated that the oxygen-oxide ion was exhibiting reversible behavior.

Csáki and Dietzel (3) reported on emf measurements in cells involving platinum indicator electrodes in borate melts, but their interpretation of the results has been criticized by Flood, Forland, and Motzfeld (4). Antipin (5) used a graphite electrode, which had been anodized to make it behave as an oxygen electrode, as a reference electrode in cryolite at 1050°C. The investigations of Lux (6) largely in sulfate and phosphate systems at 950°C were the first which clearly showed the feasibility of oxide ion activity measurements using a platinum electrode with oxygen gas. Similar measurements were made by Flood and co-workers (4, 7, 8) who demonstrated that the dependence of the potential on oxide ion activity obeyed the Nernst equation.

Work at lower temperatures has been much more limited in scope. Rose, Davis, and Ellingham (9) made measurements involving oxygen electrodes in molten NaOH containing small concentrations of tin or lead at 400°-700° and found that the cells behaved reversibly. Hill and co-workers (10) measured emfs of cells of the type

$$M/MO/CaO \text{ in } Li_2SO_4\text{-}K_2SO_4/Pt,O_2 \qquad [A]$$

at 550°-750°C and concluded that for iron, copper, and (at temperatures below 658°C) nickel, the cell emf agreed with that calculated from the free energy of formation of the metal oxide. Since both of the electrodes used by Hill, *et al.* theoretically responded equally to oxide ion activity, the cell emf data did not show whether the potentials of the two types of oxide ion electrodes individually varied properly with oxide ion activity. Selis and co-workers (11) in interpreting the galvanic behavior of a Mg-Ni cell in moist lithium chloride-potassium chloride eutectic, considered that the potential-determining systems were $Mg/MgO,O^=$ and either $Ni/NiO,O^=$ (at temperatures of 445°-535°C) or H_2, $Ni/OH^-,O^=$ (at temperatures of 390°-440°C). Once again, the individual electrode behavior against a reference electrode that was invariant with oxide ion activity was not determined.

In the present investigation, a platinum(II)-platinum electrode (12) was used as a reference for the measurement of the potentials of the oxygen-oxide ion electrode and of various metal-metal oxide-oxide ion electrodes as a function of the concentration of oxide ion.

Previous attempts to measure reversible oxygen potentials, using a platinum foil or graphite rod as an indicator electrode, had been unsuccessful (13). In the present study, a porous graphite electrode was used, again with unsuccessful results, as will be seen below.

For an electrode of the second kind, composed of a metal M, its sparingly soluble oxide $MO_{n/2}$, and free oxide ion, the Nernst equation is given by

$$E = E^\circ_{M^{n+},M} + RT/n\mathbf{F} \ln a_{M^{n+}} \quad [1]$$

$$= E^\circ_{M^{n+},M} + RT/n\mathbf{F} \ln (K_{sp}/a_{O^=})^{n/2} \quad [2]$$

$$= E^\circ_{M^{n+},M} + RT/2\mathbf{F} \ln K_{sp} - RT/2\mathbf{F} \ln a_{O^=} \quad [3]$$

where $E^\circ_{M^{n+},M}$ is the standard electrode potential[1] for the metal ion-metal electrode, and $K_{sp} = a_{M^{n+}}{}^{2/n} a_{O^=}$, is the activity product of the sparingly soluble oxide. The first two terms on the right hand side of Eq. [3] can be combined to give the standard potential of the electrode of the second kind, or

$$E = E^\circ_{ox|Ox} - RT/2\mathbf{F} \ln a_{O^=} \quad [4]$$

which is the Nernst equation for the electrode reaction

$$MO_{n/2} \text{ (solid)} + ne^- \rightleftharpoons M + \frac{n}{2} O^= \quad [5]$$

From previous work on the electromotive force series in LiCl-KCl (12) it may be inferred that activities may be replaced by concentrations in Eq. [1]-[4] if a very dilute solution is chosen as the standard state, at least if the mole fraction of added solute is in the range 10^{-6} to 10^{-4}. For analytical purposes it will be convenient to adopt the molarity scale of concentration, although simple conversion factors to molality or mole fraction may be applied if desired. The formal potential E^{ov}, written to describe the electrode with soluble reactants at a concentration of 1M, will therefore be written as E°, the standard potential. At 450°C the Nernst factor $2.303RT/\mathbf{F}$ becomes 0.1434 v, so that the theoretical slope of the plot of potential against log C, the logarithm of molar concentration of oxide ion, becomes 71.7 mv if a solid uncharged oxide is formed, regardless of the valence of the metal. Deviation from this slope implies a different course of the reaction.

The metals in this study were chosen to have stable oxides at the operating temperature and to be comparatively noble, in order that the electrode potentials would not become excessively negative and therefore subject to interference by traces of reducible impurities in the presence of excess oxide.

Experimental

The eutectic mixture of 41 mole % potassium chloride and 59 mole % lithium chloride (melting point 352°C) was used as a solvent system at 450°C, the working temperature in this investigation. The technique of preparation and purification as described in a detailed form earlier (15, 27) was followed. The reference electrode was a platinum plate immersed in a platinum(II) solution prepared in a fritted glass compartment by anodic dissolution with a known quantity of electricity. After each experiment the reference electrode compartment was analyzed by titration for chloride to determine the amount of solvent, and the potential was corrected to a Pt(II) concentration of 1M by calculation using the Nernst equation.

The associated apparatus and equipment used in fused salt methodology has been described elsewhere (16-19).

The oxygen electrode was a porous graphite electrode, of a type described by Senderoff and Mellors (20), which was held in an oxygen atmosphere at 400°C for 5 hr before use.

In the study of metal oxides the solvent was compartmented into medium porosity fused alumina or zirconia tubes. Prior to their actual use the tubes were soaked in hydrochloric acid for a few days in order to remove any basic oxides incorporated as binding agents in the tubes. After this treatment, the tubes were washed thoroughly with distilled water and dried at 500°C before they were inserted in the melt. There was no evidence for the presence of any objectionable species in the melt due to the use of these tubes. The residual current was found to be the same whether alumina or zirconia tubes or fritted glass compartments were used. Glass frits were used only when the study was purely qualitative in nature, for instance, when it was desired to observe color changes in the system. The solutes, generally anhydrous metallic salts, were added to the compartmentation tubes with the aid of a small platinum scoop which was mounted on a glass handle. At times, coulometric generation of metal ions by anodic oxidation of pure metal foils or wires was employed. At the conclusion of each experiment, the chloride content of each compartment was determined by an argentometric titration as described elsewhere (12). Thus, knowing the volume of the solution in the compartment, the concentration of solute at the time of measurement could be calculated.

[1] The IUPAC sign convention (14), in which half-reactions are written as reductions and the sign refers to the sign of the charge on the metal, is used.

The anhydrous metallic oxides were prepared as follows: Calcium oxide, platinum(II) oxide, and bismuth(III) oxide were made by vacuum desiccation of commercially available anhydrous samples. Lithium oxide was prepared from an analytical grade sample of lithium hydroxide monohydrate according to a procedure outlined by Brauer (21). Nickel(II) oxide (22), copper(I) oxide (21), palladium(II) oxide (23), and bismuth(III) oxychloride (21) were prepared according to available procedures.

Results and Discussion

The oxygen electrode, when dipped into solutions 0.09M to 0.21M in lithium oxide, was found very slow to reach equilibrium at temperatures of 400°-500°C. After 6-7 hr, the potential usually had reached a constant value, the final potentials at 450°C being −0.212, −0.328, and −0.407 v against a 1M Pt(II) reference electrode, at oxide ion concentrations of 0.094, 0.167, and 0.21M, respectively. These data do not yield a linear semi-logarithmic plot, and the rate of change of potential with concentration is much greater than predicted by the Nernst equation. The slope of the "best" straight line is about 0.6 v rather than the theoretical 0.0717 v. Similar behavior was observed at 400° and 500°C. It is concluded that reversible behavior could not be achieved under the conditions of the present study. It is likely that carbon takes part in the potential-determining reaction, in view of the finding by Smirnov, *et al.* (24) that at 800°C in KCl-NaCl saturated with CaO, the potential-determining reaction of a carbon electrode is

$$2Ca^{++} + CO_2 + 4e^- \rightleftharpoons C + 2CaO$$

Consequently, the drifting potentials and nonequilibrium character in the present study are probably due to mixed electrode processes.

The following metal oxides were studied in this investigation: copper(I) oxide, nickel(II) oxide, platinum(II) oxide, palladium(II) oxide, bismuth(III) oxide. In addition, bismuth oxychloride was compared with bismuth(III) oxide. The general procedure was to add a weighed amount of an anhydrous metal oxide to the melt collected in a zirconia tube and to measure the potential after each addition, a metal rod or foil serving as the indicator electrode. A different procedure was followed with bismuth oxide and bismuth oxychloride since metallic bismuth is a liquid at the operating temperature in this investigation (450°C). A tungsten rod in contact with a bismuth pool was used as a bismuth electrode. After each addition of metal oxide, the solution was well stirred and left for 15-20 min before a potential measurement was made. In almost all cases studied, the melt was saturated with the first addition of oxide and no change in potential was observed on subsequent additions of oxide. For following the reversibility of these electrode systems, varying amounts of lithium or calcium oxide were added to establish the oxide ion concentration. These oxides are known to be fairly soluble in lithium chloride-potassium chloride eutectic.

To calculate the equilibrium concentration of oxide ion, it was necessary to take into account the contribution from the solubility of the metal oxide. To illustrate the procedure, the measurements on the Pd-PdO system are given in Table I. The measured emfs of cells of the type

Pt|Pt(II), (A molar)||CaO (B molar), PdO (solid)|Pd [B]

were first calculated to a platinum(II) concentration of 1M, to give the figures in the last column. From the standard potential of the Pd(II),Pd electrode (−0.214 v vs. 1M Pt(II)), estimates of the solubility product of PdO were made, using the stoichiometric concentrations of calcium oxide added (column 2). The two values (6.63 and 6.49 × 10^{-6}, respectively) estimated from the higher added oxide concentrations were averaged to give 6.56 × 10^{-6}. From the solubility product, using a quadratic solution, the corrected oxide ion concentrations were calculated. The oxide ion concentration of a saturated solution of PdO without added CaO would be expected to be equal to the square root of the solubility product, or 8.1 × 10^{-3}M. From the standard potential of palladium and the measured emf, a Pd(II) concentration of 9.38 × 10^{-3}M is calculated. This suggests that some initial oxidation of Pd, promoted by the presence of oxide ion, had occurred before the oxygen had been completely flushed from the system. A better estimate of initial oxide concentration is given by $K_{sp}/9.38 \times 10^{-3} = 7.0 \times 10^{-4}$M.

Table I. Potential of Pd, PdO Electrode at Various Concentrations of Added Oxide Ion

Total CaO added, mg to 8.3 ml cell	CaO added, stoichiometric molar conc.	[O=] corr, molar	E (Cell[B]), volt measured	E, volt, versus 1M Pt reference
0	0	7.0×10^{-6}	−0.2371	−0.3594
7.8	0.0168	2.06×10^{-3}	−0.2700	−0.3923
15.9	0.0342	3.60×10^{-3}	−0.2862	−0.4058
23.0	0.0494	5.07×10^{-3}	−0.2992	−0.4215

The solubility of each metal oxide was estimated by three procedures: (*a*) from the measured potential of the metal in a solution saturated with its oxide, (*b*) from measurements of the voltammetric (polarographic) diffusion current of a solution saturated with the oxide, and (*c*) from $E^\circ_{M|M^{++}}$, defined as the standard potential of the metal, metal oxide electrode obtained from the experimental curve of electrode potential against logarithm of oxide ion concentration extrapolated to a concentration of 1M (Eq. [4]).

Two alternate procedures were used to prepare half-cells. In the first, a metal was dissolved anodically in the melt and lithium or calcium oxide was subsequently added. In the second, a weighed amount of anhydrous metal chloride was added to the melt containing the soluble calcium or lithium oxide. A brief discussion of each metal-metal oxide system studied will now be given. For each electrode system, a plot of logarithm of molarity of oxide vs. potential against 1M platinum reference electrode has been made. These plots are depicted in Fig. 1, 2, and 3. In each figure the points are connected

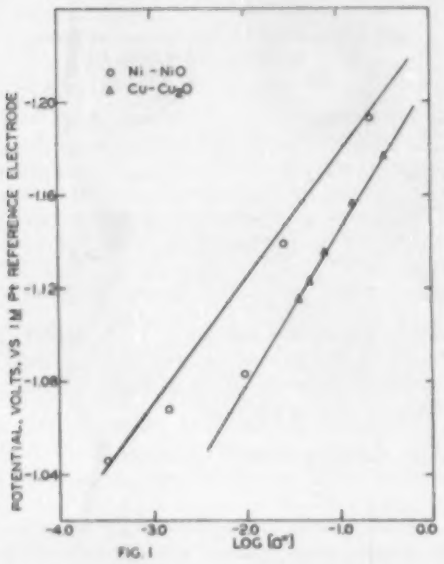

Fig. 1. Experimental behavior of $Ni/NiO,O^=$ and $Cu/Cu_2O,O^=$ electrodes. For comparison with theory, see text.

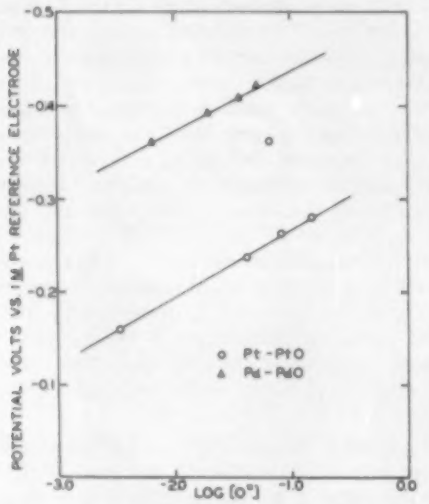

Fig. 2. Experimental behavior of $Pt/PtO,O^=$ and $Pd/Pd,O,O^=$ electrodes. For comparison with theory, see text.

by the best straight line. The experimental and theoretical slopes are compared in the text.

Nickel(II) oxide.—The nickel-nickel oxide couple, $NiO + 2e^- = Ni + O^=$, was the first to be studied. Nickel is known to form NiO as a stable oxide and no oxychloride of this metal is known. The concentration of nickel calculated from the potentials is 3.3×10^{-4} mole liter^{-1}. The concentration found from a polarogram taken of a saturated solution of NiO in the melt was 3.2×10^{-4} mole liter^{-1}. A plot of log $[O^=]$ vs. E, shown in Fig. 1, showed a considerable departure from the theoretical slope and therefore indicated irreversibility of the system. The slope calculated by the least squares method is 53 mv as compared to a theoretical slope of 71.7 mv for a reversible half reaction. The E°_{oxide} value can approximately be quoted as −1.23 v which corresponds to

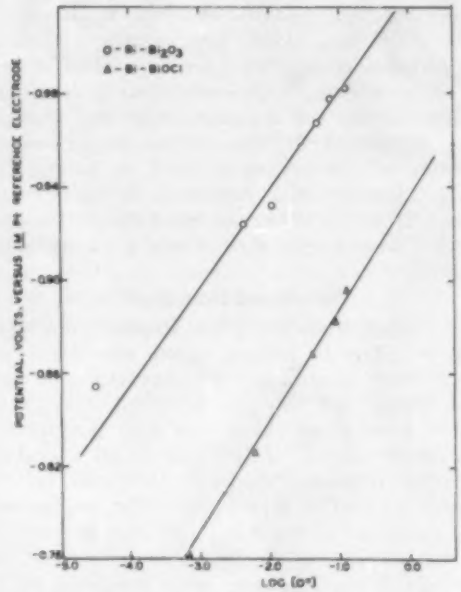

Fig. 3. Experimental behavior of $Bi/Bi_2O_3,O^=$ and $Bi/BiOCl, O^=$ electrodes. For comparison with theory, see text.

solubility of *ca.* 10^{-5} moles/liter, calculated from the theoretical slope. The experimental points on the figure are scattered and thus very little theoretical significance can be attached to the E°_{oxide} value. The value −1.23 v is more positive than expected from $E^\circ_{Ni^{++}-Ni}$ and solubility of NiO estimated polarographically (−1.297 v).

Two reasons may be advanced for the discrepancy between theory and experiment. First, the Ni(II)-Ni system may act irreversibly in the presence of excess oxide ion. This explanation is implausible because of the high exchange current of the Ni(II)-Ni electrode (24) and the moderate solubility of NiO in LiCl-KCl. Second, a higher nickel oxide, e.g., Ni_2O_3, may be formed. In this instance the measured potentials would be mixed potentials due to the presence of NiO and Ni_2O_3. This explanation appears to be more plausible, particularly because the formation of the latter oxide has been shown to be promoted by the presence of lithium oxide (25). Evidence for the existence of Ni_2O_3 at temperatures of 660°C and higher in molten lithium sulfate-potassium sulfate eutectic has also been published recently by Hill and co-workers (10).

Copper(I) oxide.—The solubility of Cu_2O, as determined from potential measurements and from a current-voltage curve, was 3.8×10^{-5} moles liter^{-1} and 5.8×10^{-5} moles liter^{-1}, respectively. A plot of log $[O^=]$ vs. E shown on Fig. 1 gave a slope of 66.2 mv and the E°_{oxide} value, −1.207 v. The solubility calculated from the E°_{oxide} value was 6.95×10^{-5} moles liter^{-1} which is in agreement with the values obtained directly. Corresponding to the electrode reaction $Cu_2O + 2e^- \rightleftharpoons 2Cu + O^=$, the system $Cu/Cu_2O,O^=$ acts as an electrode of the second kind, but the application of this electrode as an indicator electrode for oxide ion is limited by the high solubility of Cu_2O.

Platinum(II) oxide.—A saturated solution of PtO in equilibrium with solid oxide when brought in contact with the platinum foil electrode registered a potential of −0.0546 v vs. a 3.28×10^{-6} M Pt(II) reference. This potential was stable over a long period (4-5 hr). From the potential the solubility of PtO was calculated to be 3.32×10^{-6} moles liter^{-1}. The effect of additional increasing amounts of CaO on the potential was also followed. A plot of log [$O^=$] vs. E is shown in Fig. 2. The slope of the plot is 72.5 mv and $E^\circ_{PtO/Pt}$ is −0.3385 v. The solubility calculated from the $E^\circ_{PtO/Pt}$ value is 4.36×10^{-6} moles liter^{-1} which is in good agreement with the measured value.

In some experiments PtO was generated internally by anodizing platinum foil in the melt in the presence of an excess of CaO. Although the measurements agreed with those obtained by direct addition of PtO, the establishment of equilibrium was so slow that it took almost 24 hr to make four measurements. Stirring of the solution or passing of small current (*ca.* 1 μa), while the measurements were made, did not speed the attainment of equilibrium appreciably

Palladium(II) oxide.—Following the procedure explained above, the solubility of PdO from potential measurements was calculated as 9.4×10^{-6} moles liter^{-1}. The plot of log [$O^=$] vs. E shown on Fig. 2 gives a slope of 74.2 mv and $E^\circ_{PdO/Pd}$, −0.514 v. The solubility calculated from $E^\circ_{PdO/Pd}$ is 8.1×10^{-6} moles liter^{-1}. The attainment of equilibrium in this system was also extremely slow. From the experimental data, however, the electrode system appears to behave as a reversible electrode of the second kind.

Bismuth (III) oxide.—In studying the Bi/Bi_2O_3,$O^=$ system, a re-evaluation of the standard potential of the Bi(III)/Bi electrode was made. Using a tungsten electrode in contact with a molten Bi pool, a value of −0.63 v vs. 1M Pt(II)/Pt on the molarity scale was found. This value is in agreement with the value of −0.64 ± 0.01 v reported elsewhere (24), using a tungsten contact, rather than the previous value of −0.553 v originally reported (12), using a platinum contact. The disagreement may be attributed to alloy formation between platinum and liquid bismuth.

Experimental values of the potential of a bismuth electrode in the presence of sufficient solid Bi_2O_3 to form a solid phase, and with varying concentrations of oxide ion, added as CaO, are given in Fig. 3. The electrode potential followed the empirical equation

$$E = -1.023 - 0.042 \log [O^=] \qquad [6]$$

from which $K_{sp} = 3.2 \times 10^{-4}$ using Eq. [3]. The slope of the logarithmic plot (42 mv), however, does not agree with the theoretical value of 71.7 mv given in Eq. [4]. The value of K_{sp} can also be estimated from the potential of the bismuth pool in the presence of Bi_2O_3 but in the absence of added CaO (−0.8543 v vs. 1M Pt), from which [Bi^{+3}] = 2.06×10^{-2}M. If it is assumed that [$O^=$] = 3/2 [Bi^{+3}] = 3.09×10^{-2}, a value of $K_{sp} = [Bi^{+3}]^2[O^=] = 5.0 \times 10^{-6}$ is estimated, differing by almost an order of magnitude from the estimate made from the intercept.

From the fact that the theoretical Nernst slope is not observed, however, it can be inferred that the simple solubility equilibrium of Bi_2O_3 is not reached. If Bi_2O_3 dissolves through the intermediate formation of BiO^+, the theoretical Nernst slope would not be affected as long as solid Bi_2O_3 were present at equilibrium. If Bi_2O_3 interacts to form a new solid phase of BiOCl and is present in excess so that both solid phases exist, then the equilibrium

$$Bi_2O_3(\text{solid}) + 2Cl^- \rightleftharpoons 2BiOCl(\text{solid}) + O^= \qquad [7]$$

would correspond to a fixed oxide ion (and therefore bismuth ion) activity. Addition of excess oxide would merely change the relative amounts of the two solid phases. On the other hand, if *all* the Bi_2O_3 were converted to a new solid phase of BiOCl, then, in accordance with the half reaction

$$BiOCl\ (\text{solid}) + 3e^- \rightleftharpoons Bi + O^= + Cl^- \qquad [8]$$

a Nernst slope of 2.3 $RT/3\mathbf{F}$ (47.8 mv) would be expected. The concentration of oxide ion, however, would depend on the amount of Bi_2O_3 as well as CaO which had been added. To clarify this point, a separate study of the Bi/BiOCl,$O^=$ electrode was made.

Bi(III) *oxychloride.*—The bismuth electrode in the presence of solid BiOCl and added CaO was found to obey the equation

$$E = -0.935 - 0.045 \log [O^=] \qquad [9]$$

in good agreement with the theoretical equation

$$E = E^\circ_{Bi^{+3},Bi} + RT/3\mathbf{F} \ln K_{sp} - 0.0478 \log [O^=] \qquad [10]$$

where $K_{sp} = [Bi^{+3}][O^=]$.

From the intercept, $K_{sp} = 4.2 \times 10^{-7}$. From the potential in the absence of added oxide (−0.782 v vs. 1M Pt), a bismuth ion concentration [Bi^{+3}] = 6.6×10^{-4} and $K_{sp} = 4.4 \times 10^{-7}$ are calculated, in good agreement with the value calculated from the intercept. Moreover, from the polarographic wave height for saturated BiOCl, a solubility of 6.9×10^{-4}, corresponding to $K_{sp} = 4.8 \times 10^{-7}$, was estimated.

It may be concluded that the electrode Bi/BiOCl,$O^=$ is behaving reversibly and that the above estimates of the solubility are therefore valid. It is interesting to note that these data indicate no appreciable interaction between Bi^{+3} and $O^=$ to form a complex such as BiO^+.

Returning now to the behavior of Bi_2O_3, it is clear from a comparison of Eq. [6] and [9] that, at the same added oxide ion concentration, the Bi_2O_3 electrode showed a more negative potential than the corresponding BiOCl electrode. If Bi_2O_3 were to interact according to Eq. [7] to produce BiOCl and oxide ion, the oxide ion concentration would be increased and qualitatively the electrode potential would be shifted in the negative direction as actually observed. The slope, however, would be affected because the oxide appearing from reaction [7] would exert more influence at low concentrations than at high concentration of added oxide ion. It appears probable that some interaction occurs between solid Bi_2O_3 and the melt, but that either the reaction is not as simple as represented by Eq. [7] or the system is slow to come to equilibrium, or

both. In an event, the $Bi/Bi_2O_3O^=$ electrode cannot be regarded as a reversible oxide ion electrode.

Acknowledgment

The porous graphite used in the fabrication of the oxygen electrode was kindly provided by Dr. Seymour Senderoff, of the National Carbon Company. The authors extend their appreciation to the Office of Ordnance Research and the Diamond Ordnance Fuze Laboratory for the financial support of this project and for the research assistantship held by one of them (B. B. Bhatia).

Manuscript received Dec. 17, 1959. This paper was prepared for delivery before the Chicago Meeting, May 1-5, 1960.

Any discussion of this paper will appear in a Discussion Section to be published in the June 1961 JOURNAL.

REFERENCES

1. E. Baur and H. Ehrenberg, *Z. Elektrochem.*, **18**, 1002 (1912).
2. W. D. Treadwell, *ibid.*, **22**, 414 (1916).
3. P. Csáki and A. Dietzel, *Glastechn. Ber.*, **18**, 33, 65 (1940).
4. H. Flood, T. Forland, and K. Motzfeldt, *Acta Chem. Scand.*, **6**, 257 (1952).
5. L. N. Antipin, *Zhur. Fiz. Khim.*, **29**, 1668 (1955).
6. H. Lux, *Z. Elektrochem.*, **45**, 303 (1939); **52**, 220 (1948); **53**, 41 (1949).
7. H. Flood and T. Forland, *Acta Chem. Scand.*, **1**, 592 (1947).
8. H. Flood and T. Forland, *Faraday Soc. Discussions*, No. 1, 302 (1947).
9. B. A. Rose, G. J. Davis, and H. J. T. Ellingham, *ibid.*, No. 4, 154 (1948).
10. D. G. Hill, B. Porter, and A. S. Gillespie, Jr., *This Journal*, **105**, 408 (1958).
11. S. M. Selis, G. R. B. Elliott, and L. P. McGinnis, *ibid.*, **106**, 134 (1959).
12. H. A. Laitinen and C. H. Liu, *J. Am. Chem. Soc.*, **80**, 1015 (1958).
13. H. A. Laitinen and J. W. Pankey, Unpublished investigations.
14. T. S. Licht and A. J. de Bethune, *J. Chem. Education*, **34**, 433 (1957).
15. D. K. Roe, Ph.D. Thesis, University of Illinois (1959).
16. W. S. Ferguson, Ph.D. Thesis, University of Illinois (1956).
17. H. A. Laitinen and W. S. Ferguson, *Anal. Chem.*, **29**, 4 (1957).
18. H. A. Laitinen, R. A. Osteryoung, and W. S. Ferguson, *This Journal*, **104**, 516 (1957).
19. B. B. Bhatia, Ph.D. Thesis, University of Illinois (1959).
20. S. Senderoff and G. W. Mellors, *Rev. Sci. Inst.*, **29**, 151 (1958).
21. G. Brauer, "Handbuch der präparativen anorganischen Chemie," Ferdinand Enke Verlag, Stuttgart (1954).
22. J. R. Tomlinson, *et al.*, *J. Am. Chem. Soc.*, **77**, 909 (1955).
23. R. L. Shriner and R. Adams, *J. Am. Chem. Soc.*, **46**, 1683 (1924).
24. H. A. Laitinen, R. P. Tischer, and D. K. Roe, *This Journal*, **107**, 546 (1960).
25. M. V. Smirnov, S. F. Pal'guev, Y. N. Krasnov, and L. A. Lyapina, *Zhur. Priklad. Khim.*, **30**, 1687 (1957).
26. R. L. Tichenor, *Ind. Eng. Chem.*, **44**, 973 (1952).

Solutions of Some Alkali Halides in the Pure Liquids and in Mixtures of N-Methylacetamide and Dimethylformamide

Lyle R. Dawson and Walter W. Wharton

Department of Chemistry, University of Kentucky, Lexington, Kentucky

ABSTRACT

Dielectric constants, densities, and viscosities of N-methylacetamide, dimethylformamide, and of mixtures of these liquids have been determined at five temperatures. Conductances, densities, and viscosities of solutions of sodium and potassium bromides and potassium iodide in various mixtures of these solvents have been measured at ten-degree intervals from 20° to 50°C. Variations in the dielectric constant of the solvent over the range 35-165 showed no influence on the degree of dissociation of these salts; they are essentially completely dissociated in all of the solvent mixtures studied. Differences in mobilities of the ions are explained in terms of various specific types of solute-solvent interactions.

During the past few years Dawson and co-workers have published from This Laboratory several papers describing the properties of solutions of electrolytes in solvents having high dielectric constants. Very large degrees of dissociation and correspondence with the theoretical Onsager (1) conductance relationships to concentrations much greater in these solutions than in water are attributable to a considerable extent to the high dielectric constants.

The investigation reported in this paper was designed to study the influence of large changes in dielectric constant on the degree of electrolytic dissociation and the mobilities of the ions of some univalent bromides and iodides. It was expected that

some insight into the comparative solute-solvent effects might be obtained also from the results of these studies.

Experimental

Apparatus and procedure.—The bridge assembly and procedures for conductance measurements as well as viscosity and density determinations have been described adequately in earlier papers (2-4). No significant change in the cell constants of the conductance cells could be detected over the temperature range for which they were used. The cells were held in a thermostated oil-bath maintained at a constant temperature to within ±0.1°.

Solvents.—The preparation and purification of N-methylacetamide (NMA) and dimethylformamide (DMF) has been described previously (5, 6). The solvents used in this work had specific conductances in the range 1 to 4×10^{-7} ohm^{-1} cm^{-1} at 30°.

Electrolytes.—The best obtainable commercial grades of sodium and potassium bromides were recrystallized twice from water and alcohol mixtures, fused, then stored in a desiccator over magnesium perchlorate.

Analytical grade potassium iodide was recrystallized twice, dried at 60° in a vacuum oven, then stored over magnesium perchlorate.

Solutions.—Solutions were prepared and dilutions made on a weight basis. All transfers were made in a dry atmosphere.

Dielectric constants of the solvents were measured (7) at 20°, 25°, 30°, and 40°. Extrapolated values were used for 50°.

Results and Discussion

All conductances were corrected by subtracting the conductance of the solvent from that of the solution. Limiting equivalent conductances were obtained by empirical extrapolation of plots of Λ vs. $\sqrt{C}$. Although there is some uncertainty in the Λ_0 values, they are believed to be accurate generally to well within 1%.

In the mixed solvent dimethylformamide (DMF)-N-methylacetamide (NMA) there are brought together isomeric components having approximately equal densities but widely differing viscosities and dielectric constants (Fig. 1). At 40°, the range of dielectric constants from 35 to 165 is spanned. Viscosities vary from 0.67 for DMF to 3.02 centipoises for NMA. Earlier work (4) has shown that sodium and potassium bromides and iodides are completely dissociated in pure NMA.

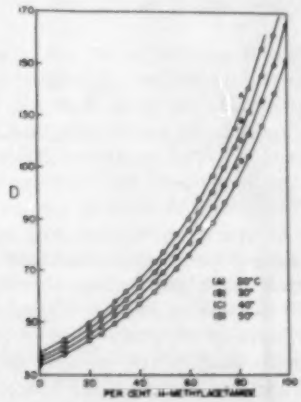

Fig. 1. Dielectric constants of the mixed solvents N-methylacetamide-dimethylformamide.

Table I. Summary of data for solutions of NaBr, KBr, and KI in DMF, NMA, and in the mixed solvent DMF-NMA

% NMA	% DMF	Salt	Temp	Λ_0	η_0	$\Lambda_0\eta_0$
0.0	100.0	KBr	20	78.2	0.00845	0.6604
			30	90.1	0.00746	0.6723
			40	99.8	0.00664	0.6626
			50	111.5	0.00598	0.6670
		NaBr	20	78.6	0.00845	0.6640
			30	89.2	0.00746	0.6654
			40	100.6	0.00664	0.6679
			50	111.8	0.00598	0.6688
90.0	10.0	KBr	20	16.7	0.03765	0.6269
			30	21.3	0.02924	0.6214
			40	26.4	0.02336	0.6172
			50	32.0	0.01907	0.6095
		NaBr	20	16.4	0.03765	0.6186
			30	20.9	0.02924	0.6105
			40	25.9	0.02336	0.6060
			50	31.4	0.01907	0.5988
0.0	100.0	KI	20	77.6	0.00845	0.6552
			30	88.3	0.00746	0.6586
			40	99.4	0.00664	0.6596
			50	110.4	0.00598	0.6604
48.67	51.33	KI	20	39.9	0.01564	0.6234
			30	47.2	0.01314	0.6201
			40	54.9	0.01125	0.6177
			50	63.1	0.00976	0.6159
90.0	10.0	KI	20	18.0	0.03765	0.6777
			30	23.0	0.02924	0.6728
			40	28.5	0.02336	0.6653
			50	34.4	0.01907	0.6575
95.13	4.87	KI	30	20.4	0.03310	0.6759
			40	25.5	0.02635	0.6730
			50	31.3	0.02120	0.6631
98.0	2.0	KI	30	19.1	0.03615	0.6905
			40	24.1	0.02830	0.6823
			50	29.7	0.02274	0.6754
100.0	0.0	KI	30	18.1	0.03888	0.7053
			40	23.0	0.03021	0.6945
			50	28.5	0.02413	0.6875

A summary of pertinent data for the solutions studied is presented in Table I.

Raman spectra and infrared studies (8) have shown that in NMA there exists a trans disposition of the oxygen atom and the amino hydrogen. Hydrogen bonding at these two points produces long chains of molecules leading to extremely high dielectric constants. In an unsubstituted amide such as formamide random associated forms occur which partially cancel contributions made by additional molecules and the dielectric constant is lower. If both amino hydrogens are replaced by alkyl groups, as in DMF, hydrogen bonding is not possible and the dielectric constant is relatively low.

Addition of a small amount of DMF to NMA greatly reduces both the dielectric constant and the viscosity by disrupting the long chains of molecules.

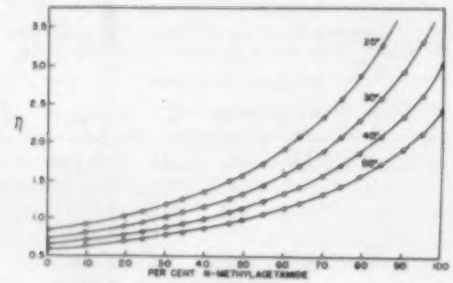

Fig. 2. Absolute viscosities of the mixed solvents N-methylacetamide-dimethylformamide.

Since the densities of the two pure components are so nearly equal, the degree of molecular association has little influence on the density of the mixture.

In all of the solutions studied the viscosity increases as the concentration of added electrolyte becomes greater (Fig. 2). This effect is more pronounced in mixtures richer in NMA. Increased viscosity may result from solvation of the ions by attachment of separate solvent molecules which are available in DMF or which may be produced in NMA by disruption of molecular chains. In addition, the viscosity of NMA solutions may become greater because of other changes in the solvent structure around the ions. In pure NMA the molecules are arranged in long chainlike groups. These linearly disposed molecular chains move past one another without great interference as the liquid flows. Nonelectrolyte solute particles which exert little influence on the solvent molecules encounter resistance which is not abnormally great as they move through the medium. Ionic solute particles at lower concentrations exert pronounced electrostatic attractive forces on various points along the solvent molecular chain but probably disrupt extensively relatively few of the solvent molecular groups. Under the influence of the electrostatic fields of these ions most of the molecular chains around them are only distorted so that they become serrated and curved. Then movement of the solvent units past one another or of solute particles through this medium is greatly hindered. It seems logical that this effect may be largely responsible for the unusual increase in viscosity with increasing concentration of added electrolyte which is observed in NMA solutions.

The absence of a maximum or minimum in the densities, viscosities, or dielectric constants of the solvent mixtures is an indication that compound formation between the components does not occur. The fact that on cooling a solvent mixture, essentially pure NMA crystallizes out, lends additional evidence that interaction between the solvent components is comparatively slight and primarily physical in nature.

Solutions of sodium and potassium bromide.—Plots of the equivalent conductance as a function of the square root of the concentration for sodium and potassium bromides (typical plots shown in Fig. 3-5) at ten degree intervals from 20° to 50° in both the pure components and in the 90-10 NMA-DMF mixtures are typical of highly dissociated electrolytes. Slopes of the KBr plots are slightly less

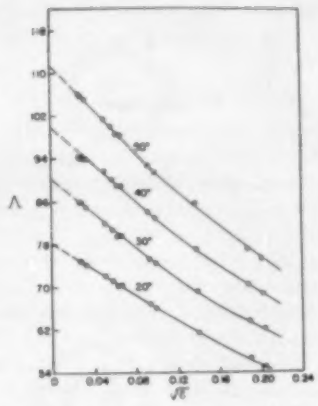

Fig. 3. Kohlrausch plots for solutions of potassium bromide in dimethylformamide.

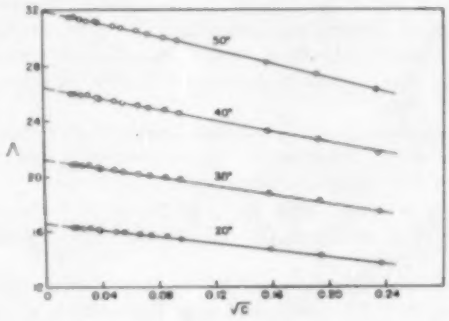

Fig. 4. Kohlrausch plots for solutions of potassium bromide in 90% NMA-10% DMF.

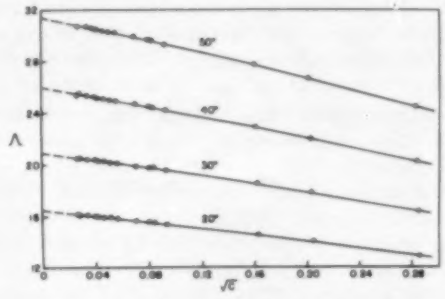

Fig. 5. Kohlrausch plots for solutions of sodium bromide in 90% NMA-10% DMF.

negative while those for NaBr are slightly more negative than the theoretical (Onsager) slopes. The higher charge density on the sodium ion would produce greater ion-solvent interaction than in the case of the potassium ion. This leads to a greater effective viscosity in the immediate environment of the sodium ion although the two alkali ion solvodynamic units may be of nearly equal sizes with equal limiting conductances. The greater solubility of the sodium compound lends support to this supposition.

Solutions of potassium iodide.—Potassium iodide is essentially completely dissociated in both of the pure constituents and in the various solvent mixtures (Fig. 6 and 7). In pure DMF the Λ_o value for KI is about 1% less than for sodium and potassium bromides (Table I); in the 90-10 DMF-NMA mix-

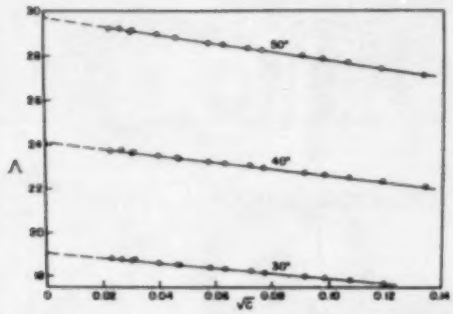

Fig. 6. Kohlrausch plots for solutions of potassium iodide in 98% NMA-2% DMF.

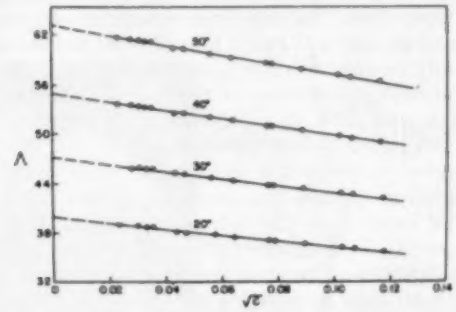

Fig. 7. Kohlrausch plots for solutions of potassium iodide in 48.67% NMA-51.33% DMF.

ture Λ_o for KI is several per cent greater than for the other two salts.

Speculation concerning the possible mechanisms of solvation of bromide and iodide ions in NMA and DMF may be useful. Because of its smaller size and greater electronegativity, the bromide ion would be more likely to undergo hydrogen bonding through the amino hydrogen of NMA. Hydrogen bonding with DMF would not occur. In DMF solvation of an electron-donor ion could proceed through the electrophilic nature of the carbon atom in the carbonyl group (9). Solvation through electrostatic phenomena as ion-dipole or ion-induced dipole effects would be greater with the bromide ion because of its greater charge density. However, the more easily deformable electron atmosphere of the iodide ion makes it more susceptible to dipole-induced dipole attraction.

A comparison at 40°C of 22.99 for the limiting equivalent conductance of potassium iodide in NMA with the value of 21.04 for potassium bromide obtained by Dawson, Sears, and Graves (11) shows the bromide less conducting by about 10%. At 40°, the Λ_o value for potassium iodide in NMA is less by a factor of 4.32 than it is in DMF. Λ_o for potassium bromide, on the other hand, has been reduced by a factor of 4.74 at the same temperature. At this temperature NMA is 4.55 times as viscous as DMF. Thus it is seen that potassium iodide is about 5% more conducting and potassium bromide is about 5% less conducting than would be expected from viscosity effects alone. These data, in addition to the fact that the greater crystallographic diameter of the iodide ion would tend to make it less mobile than the bromide ion, constitute strong evidence that in NMA the bromide ion is solvated to a greater extent than the iodide ion. Similar results are obtained by comparing sodium bromide and potassium iodide.

The results of this investigation emphasize the differences in the behavior of the two halide ions in DMF and in NMA.

Acknowledgments

The authors are indebted to Dr. H. C. Eckstrom for valuable suggestions and to Mr. Murrell Pruitt for some confirmatory experimental work.

Financial support for part of this work was received from the National Science Foundation.

Manuscript received Dec. 31, 1959.

Any discussion of this paper will appear in a Discussion Section to be published in the June 1961 JOURNAL.

REFERENCES

1. L. Onsager, *Physik. Z.*, **28**, 277 (1928).
2. L. R. Dawson, A. Tockman, H. K. Zimmerman, Jr., and G. R. Leader, *J. Am. Chem. Soc.*, **73**, 4327 (1951).
3. C. Berger and L. R. Dawson, *Anal. Chem.*, **24**, 994 (1952).
4. L. R. Dawson, P. G. Sears, and R. H. Graves, *J. Am. Chem. Soc.*, **77**, 1986 (1955).
5. L. R. Dawson, E. D. Wilhoit, and P. G. Sears, *ibid.*, **78**, 1569 (1956).
6. P. G. Sears, E. D. Wilhoit, and L. R. Dawson, *J. Chem. Phys.*, **23**, 1274 (1955).
7. G. R. Leader, *J. Am. Chem. Soc.*, **73**, 856 (1951).
8. S. Mizushima, *et al.*, *ibid.*, **72**, 3490 (1950).
9. A. E. Remick, "Electronic Interpretations of Organic Chemistry," John Wiley & Sons, Inc., New York (1949).

December 1960 Discussion Section

A Discussion Section, covering papers published in the January-June 1960 JOURNALS, is scheduled for publication in the December 1960 issue. Any discussion which did not reach the Editor in time for the June 1960 Discussion Section will be included in the December 1960 issue.

Those who plan to contribute remarks for this Discussion Section should submit their comments or questions in triplicate to the Managing Editor of the JOURNAL, 1860 Broadway, New York 23, N. Y., *not later than September 1, 1960.* All discussion will be forwarded to the author(s) for reply before being printed in the JOURNAL.

Brief Communications

Electronic Magnetoanalysis of an Iron Single Crystal

S. Yamaguchi

The Institute of Physical and Chemical Research, Tokyo, Japan

A piece of iron single crystal about 2 mm in diameter and 10 mm long was used for the experiments described below. One end of this rod was sharpened to a truncated wedge by grinding and then etching with hydrochloric acid. A small permanent magnet (coercive force about 300 Oersted) was attached to the other end of the specimen as indicated in Fig. 1. In this way the magnetic induction of the sample was kept saturated.

To study electron diffraction, an electron beam about 0.05 mm in cross section was allowed to graze the edge of the specimen (Fig. 1). The magnetic deflection of the incident beam can be measured by observing the shift in position of the diffraction pattern. The pattern from the iron crystal was measured with respect to the invariant position of the pattern from a nonferromagnetic gold foil. The patterns from the crystal and the foil were superimposed by means of a double exposure technique (1).

The pattern obtained from an unmagnetized sample (the same iron crystal with the permanent magnet removed) is shown in Fig. 2. The spots from the iron crystal fall on rings which are concentric with rings due to the gold foil. Most of the spots are actually located on rings produced by the gold, due to the near coincidence of the interplanar spacings of iron and gold; this indicates that the specimen contains no major internal stresses.

Figure 3 shows the pattern obtained from the magnetized sample. The spots due to the iron have shifted relative to the reference gold pattern; the shift shows the magnetic Lorentz effect.

Orientation—Figures 2 and 3 show that the incident beam was perpendicular to the (111) plane of the iron single crystal as well as to the magnetic induction $B_{[0\bar{1}1]}$ perpendicular to the $(0\bar{1}1)$ plane. The relations existing between the incident beam, the

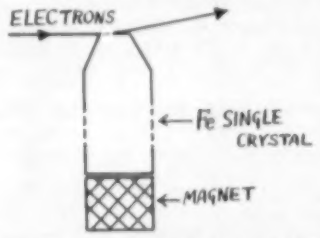

Fig. 1. Arrangement of the specimen relative to the incident beam.

Fig. 2. Double diagram from the nonmagnetized specimen and from a gold foil; no Lorentz effect.

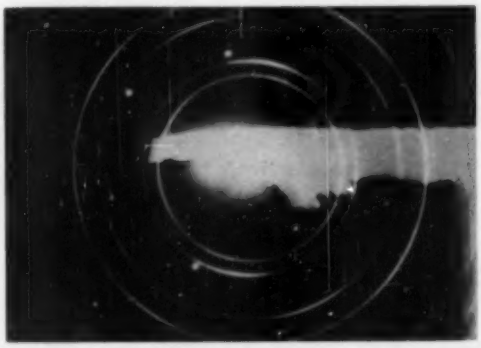

Fig. 3. Double diagram from the magnetized specimen and from a gold foil, showing the Lorentz effect. Wave length, 0.0288Å; camera length; 495 mm; positive enlarged 2.3 times.

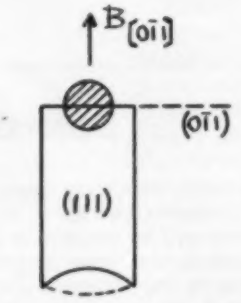

Fig. 4. Relation between the orientation of the specimen and the incident beam.

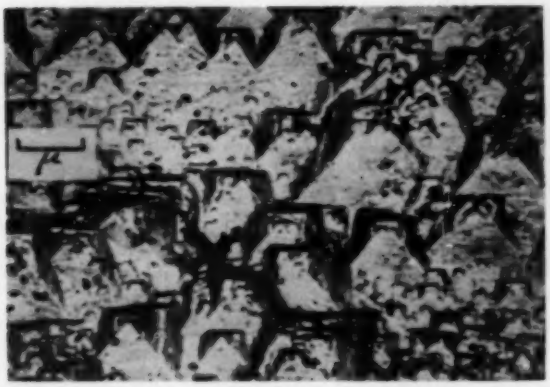

Fig. 5. Electron micrograph of the oxide film on and separated from the specimen.

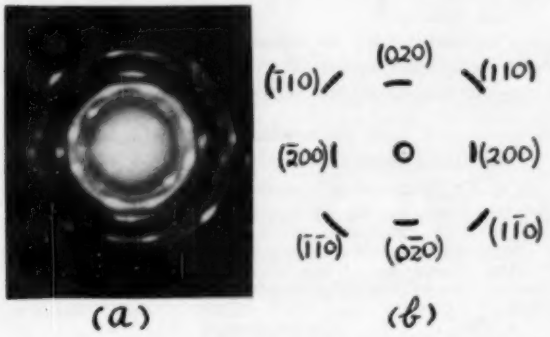

Fig. 6. (a) Diffraction pattern from the oxide film of Fig. 5 (Fe_3O_4). In (b) the Miller indices are assigned to the corresponding oriented diffraction arcs.

orientation of the specimen, and the direction of induction are illustrated in Fig. 4. Here the shadowed circle represents the cross section of the incident beam.

Electron microscopy.—An oxide replica film (thickness: about 200Å) formed on the stem surface of the specimen and then separated from it was enlarged by means of electron microscopy (Fig. 5).[1] Figure 5 pictures the octahedral (111) figures with regular orientation. This confirms the orientation of the specimen as determined by the diffraction process.

An electron beam running perpendicular to the oxide film face of Fig. 5 gave the diffraction pattern shown in Fig. 6(a). This pattern is characteristic of Fe_3O_4 crystals (magnetite, spinel type) oriented as illustrated in Fig. 6(b). In the case of Fig. 6 the incident beam was parallel to the (110) planes of the Fe_3O_4 crystals. It is therefore concluded that the (111) plane of the iron substrate is oriented perpendicular to the (110) planes of the Fe_3O_4 crystals. It is known empirically that there is a regular crystallographic orientation between a ferromagnetic substrate and the ferromagnetic oxide formed on it (2). The result obtained in the present experiment, $(111)_{Fe} \perp (110)_{Fe_3O_4}$, could serve for estimating the position of the iron crystal axis by means of the oxide replica process.

Magnetoanalysis.—The double diagram of Fig. 3 makes it possible to calculate the magnetic induction B of the specimen as a function of its crystal axis. We have a relation between the magnetic deflection of the incident beam readily measurable in Fig. 3 (ΔZ), and B. That is

$$\Delta Z = \frac{eL\lambda}{h} \int_0^l B\, dl \qquad [1]$$

where e is the electron charge (1.6×10^{-20} emu), L is the camera length (495 mm), λ is the wave length of the electrons, h is Planck's constant (6.6×10^{-27} erg sec), and l is the magnetic field traversed by the electron beam.

It is difficult to estimate the magnetic path l in the present experiment. The following process was employed to estimate the value of l. Since the magnetic induction of the specimen under the conditions in Fig. 3 is at saturation induction [B = 20000 gauss (3)], we can calculate the mean value of l according to Eq. [1]. Here it is assumed that B is homogeneous. We thus obtain $\bar{l} = 4\ \mu$, where $\lambda = 0.0288$ A and $\Delta Z = 0.27$ cm. This $\bar{l}$ —value can then be used for the further measurement of the B-H curve of the iron single crystal.

Manuscript received March 16, 1960.

Any discussion of this paper will appear in a Discussion Section to be published in the June 1961 JOURNAL.

REFERENCES

1. S. Yamaguchi, *This Journal*, **106**, 268 (1959); **107**, 55 (1960).
2. R. D. Heidenreich and E. A. Nesbitt, *J. Appl. Phys.*, **23**, 352, 366 (1952).
3. E. M. Mahla and N. E. Nielsen, *ibid.*, **19**, 378 (1948).
4. R. M. Bozorth, "Ferromagnetism," p. 870, D. Van Nostrand Co., Princeton, N. J. (1956).

[1] This oxidation was carried out in an eutectic bath of KNO_3-$NaNO_3$ at about 300°C. The oxide film was isolated from the substrate with a CH_3OH-Br solution [cf. (3)].

Stress Corrosion Cracking

D. van Rooyen

Research Laboratories, Westinghouse Electric Corporation, Pittsburgh, Pennsylvania

A mechanism in which stress corrosion cracks initiate and propagate in austenitic stainless steel in purely electrochemical stages was postulated by Hoar and Hines (1-5). Such a mechanism is supported by recent work (6) which demonstrated that no steps of mechanical fracture could be detected at any stage of the cracking process of 18-8 type stainless steel in boiling magnesium chloride solutions.

In order to account for observed rates of crack propagation, it was calculated that selective dissolution of the highly stressed advancing edge of a crack takes place at current densities of the order of 1 amp/cm^2. Hoar and West (7) demonstrated that 18-8 stainless steels can dissolve at such high current densities without much polarization, provided that the surface is yielding rapidly and provided that concentration polarization is avoided. They concluded that anodic dissolution is highly stimulated by the mechanically induced movement of the surface metal atoms. They further reported that similar tests on pure nickel gave no indication of such a mechanical effect in hot aqueous magnesium chloride.

While it is known that nickel and high nickel alloys do not suffer chloride stress corrosion cracking (8-13), it is uncertain whether their immunity arises in the initiation or in the propagation stage. It is important to know this, since the whole correlation made by Hoar and West between stainless steel and nickel is based on the assumption that cracks actually would not propagate into nickel under their conditions.

Studies on this mechanism of cracking are under way. Attempts are being made to compare the resistance of various alloys to crack propagation with their electrochemical behavior while corroding at high current densities in boiling magnesium chloride solutions. Specimens are prepared by arc depositing a layer of a susceptible material, such as 304 stainless steel, onto a strip of the material to be tested. The compound sample is then alternately rolled and vacuum annealed at 1065°C until the final thickness of about 0.045 in. is reached. The sample is given a final annealing treatment after machining the edges and is placed under direct load while in contact with the test solution which is contained in a glass cell. The load is high enough to cause cracks to start in the susceptible alloy, and their behavior is then studied at the boundary by subsequent metallographic examination. Parallel tests are next carried out in the way described by Hoar and West (7).

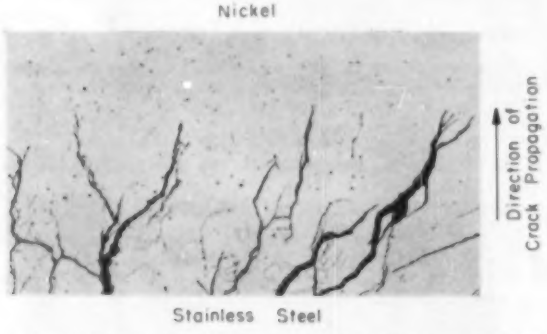

Fig. 1. Cracks stopping at steel-nickel boundary. Magnification 150X before reduction for publication.

Results so far on nickel have confirmed the absence of mechanical stimulation of its anodic dissolution. Furthermore, stress corrosion cracks, which start in the 304 type stainless steel of a bonded specimen, proceed to the nickel boundary where they stop, Fig. 1. It can be seen that the cracks penetrate a short distance into the thin intermediate layer that exists between the sensitive alloy and the nickel. After crack information and penetration in this particular experiment, the stress on the nickel was 43,000 psi, not allowing for any stress-raising effect at the tips of the cracks. Results to be reported later show that it is unlikely that a galvanic effect between the metals could account for the stopping of cracks at the boundary.

The results are in agreement with the electrochemical mechanism of cracking (1-5), although they do not directly constitute further proof.

Acknowledgment

The work reported was partly supported by the Navy Department, administered under the direction of the Office of Naval Research, Washington, D. C.

Manuscript received April 8, 1960.
Any discussion of this paper will appear in a Discussion Section to be published in the June 1961 JOURNAL.

REFERENCES

1. T. P. Hoar and J. G. Hines, *J. Iron Steel Inst.*, **182**, 124 (1956).
2. J. G. Hines and T. P. Hoar, *ibid.*, **184**, 166 (1956).
3. T. P. Hoar and J. G. Hines, Symposium on Stress Corrosion Cracking and Embrittlement, p. 107, John Wiley & Sons, Inc., New York (1956).
4. T. P. Hoar and J. G. Hines, International Committee for Electrochemical Thermodynamics and Kinetics (CITCE), 8th Meeting (Butterworths, London).
5. J. G. Hines and T. P. Hoar, *J. Appl. Chem.*, **8**, 764 (1958).
6. D. van Rooyen, To be published in *Corrosion*.
7. T. P. Hoar and J. M. West, *Nature*, **181**, 835 (1958).
8. C. Edeleanu, "Stress Corrosion Cracking and Embrittlement," p. 129, W. D. Robertson, Editor, John Wiley & Sons, Inc. (1956).
9. O. B. J. Fraser, Symposium on Stress Corrosion Cracking of Metals, A.S.T.M., A.I.M.E. (1945).
10. H. R. Copson, *Corrosion*, **10**, 124 (1954).
11. H. R. Copson, *Welding J.*, **32**, 75S (1953).
12. M. G. Fontana, *Ind. Eng. Chem.*, **46**, 99A (March, 1954).
13. J. T. Waber and S. Waber, U. S. A. E. C. Report LA1313, Los Alamos Scientific Laboratory, Los Alamos, N. M. (1950).

Houston Meeting

THE ELECTROCHEMICAL SOCIETY

One Hundred and Eighteenth Meeting

October 9, 10, 11, 12, and 13, 1960

Sunday through Thursday

CONDENSED TECHNICAL PROGRAM

Monday, Oct. 10, 1960

Battery (Abstracts 1-12) 9:30 A.M.-12:15 P.M.; 2:00-5:00 P.M. (Azalea Room, Exhibit Hall)
Corrosion (Abstracts 34-53) 9:00 A.M.-12:00 M.; 2:00-5:10 P.M. (Continental Room, Shamrock Hilton); 2:00-4:50 P.M. (El Shiro Room, Shamrock Hilton)
Electrodeposition—Electrothermics and Metallurgy (Abstracts 119-128) 9:30-11:40 A.M.; 2:00-4:10 P.M. (Grecian Room, Shamrock Hilton)
Electronics-Semiconductors (Abstracts 129-140) 9:15 A.M.-12:00 M.; 2:00-4:30 P.M. (Emerald Room, Shamrock Hilton)

Tuesday, Oct. 11, 1960

Battery (Abstracts 13-23) 9:00 A.M.-12:00 M.; 2:30-4:40 P.M. (Azalea Room, Exhibit Hall)
Corrosion (Abstracts 54-63) 9:00 A.M.-12:00 M.; 2:00-5:00 P.M. (Continental Room, Shamrock Hilton)
Electrodeposition (Abstracts 89-100) 9:00 A.M.-12:00 M.; 2:00-5:00 P.M. (Grecian Room, Shamrock Hilton)
Electronics-Semiconductors (Abstracts 141-157) 9:00 A.M.-12:00 M.; 2:00-5:05 P.M. (Emerald Room, Shamrock Hilton)
Electrothermics and Metallurgy (Abstracts 169-173) 9:30-11:40 A.M. (El Shiro Room, Shamrock Hilton)

Wednesday, Oct. 12, 1960

Battery (Abstracts 24-33) 9:00 A.M.-12:00 M.; 2:00-4:10 P.M. (Azalea Room, Exhibit Hall)
Corrosion (Abstracts 64-75) 9:00 A.M.-12:00 M.; 2:00-5:00 P.M. (Continental Room, Shamrock Hilton)
Electrodeposition (Abstracts 101-112) 9:00 A.M.-12:00 M.; 2:00-5:00 P.M. (Grecian Room, Shamrock Hilton)
Electronics-Semiconductors (Abstracts 158-168) 9:00-11:30 A.M.; 2:00-4:45 P.M. (Emerald Room, Shamrock Hilton)

Thursday, Oct. 13, 1960

Corrosion (Abstracts 76-85) 9:00 A.M.-12:00 M.; 2:00-4:45 P.M. (Continental Room, Shamrock Hilton)
Electrodeposition (Abstracts 113-118) 9:00 A.M.-12:00 M. (Grecian Room, Shamrock Hilton)

GENERAL INFORMATION

Convention Headquarters is the Shamrock Hilton Hotel, Main at Holcombe Boulevard, Houston 1, Texas; Teletype No. 533, Telephone, Madison 3-9211.

Special rates per day secured only by PREREGISTRATION are: single rooms, $8.00, 10.00, 12.00, 14.00, 15.00; twin-bed rooms, $12.00, 14.00, 16.00, 18.00, 19.00; two rooms with connecting bath only on request. Suites, parlor with one bed room, $25.00, 30.00, 35.00, 40.00; parlor with twin-bed room, $55.00, 60.00, 65.00, 70.00.

Requests for room reservations should be mailed to the Shamrock Hilton Hotel, Main and Holcombe, Houston 1, Texas.

BE SURE to state that you will be attending The Electrochemical Society Meeting. If your wife will be attending, be sure to indicate this on your request for reservation.

The Office of the Secretary is in Room 337, Shamrock Hilton Hotel, 3rd floor, turn right.

The Local Committee Office and Press Headquarters on Sunday, Monday, and Tuesday, Oct. 9, 10, and 11, are adjacent to the Registration Area, Hall of Exhibits; on Wednesday and Thursday, Oct. 12 and 13, they are in the Walnut Room, 3rd floor, Shamrock Hilton.

REGISTRATION

The registration desk will be in the Hall of Exhibits directly connected to the Main Hotel Lobby on Sunday, Monday, and Tuesday, Oct. 9, 10, 11; on Wednesday and Thursday, Oct. 12 and 13, it will be located in the Venetian Room, 3rd floor, Shamrock Hilton, turn right.

The registration schedule is:

Hall of Exhibits

Sunday, October 9—12:00 M. to 9:00 P.M.
Monday, October 10—7:00 A.M. to 4:00 P.M.
Tuesday, October 11—8:00 A.M. to 4:00 P.M.

Venetian Room, 3rd floor, Shamrock Hilton

Wednesday, October 12—8:00 A.M. to 4:00 P.M.
Thursday, October 13—8:00 A.M. to 12:00 M.

Registration fees are:

Technical Session Registration (Men and Women)	
Member	$ 7.00
Nonmember Speakers and Coauthors	7.00
Nonmember	13.00*
Student Members	Complimentary
Student Nonmembers	2.00
Thursday Only	5.00
Ladies Registration Fee for Social Events	5.00

* If a nonmember fills out an application form and subsequently is elected to membership in the Society, the difference between the nonmember and member registration fee will be applied to his first year's dues.

INFORMATION ABOUT HOUSTON

Information about places of interest and other attractions will be available at the Local Committee Office adjacent to the Registration Area, Hall of Exhibits, Sunday through Tuesday, and in the Venetian Room, 3rd floor, Shamrock Hilton, Wednesday and Thursday, where a designated official will be on hand to assist you, be it concerning airline schedules, restaurants, sight-seeing buses, theaters, etc.

SYMPOSIA

The Battery Division has scheduled a lead-acid storage battery symposium in honor of the 100th anniversary of the invention of the lead-acid battery by Gaston Plante, devoted to papers dealing with the processes involved in the corrosion of lead and the formation of active materials. The Division has also scheduled symposia on: Primary Cells; Solid Electrolyte, Secondary Battery Characteristics, and Silver/Silver Oxide Electrodes; and Nickel-Cadmium.

The Corrosion Division has scheduled symposia on: Can Corrosion; Oxidation; Unusual Valence States and the Difference Effect; Certain Properties of the Interface Related to Corrosion; Passivity; Dissolution of Metals and Semiconductors; and a General Session.

The Electrodeposition Division has scheduled symposia on: Electroless and Immersion Plating; Electrophoretic Deposition; Metal Deposition; Alloy Plating; and a General Session.

The Electrodeposition and **Electrothermics and Metallurgy Divisions** have scheduled a Joint Symposium on Vapor Deposited Coatings.

The Electronics Division-Semiconductor Group has scheduled symposia on: Crystal Growth; Compound Semiconductors; Technology; and Surfaces.

The Electrothermics and Metallurgy Division has scheduled a session on Vacuum-Evaporated Films; Refractory and Reactive Metals.

GENERAL FUNCTIONS

Symposia Chairmen Breakfasts

On Monday, Tuesday, Wednesday, and Thursday, Oct. 10, 11, 12, and 13, special breakfasts will be held for symposia chairmen. On the day on which he presides at a session, each chairman should be in the Castillian Room A, 3rd floor, Shamrock Hilton, **at 7:45 A.M.**

Sunday Deep Sea Fishing Trip

The party will leave Freeport, Texas (weather permitting) aboard safe chartered boats **very early** Sunday morning, Oct. 9, for a day of fishing 12 to 60 miles out in the Gulf, re-

turning to the Freeport dock about 5 or 6 P.M. Red snapper, ling, and warsaw will be the probable catches. A grub stake, tackle, bait, and transportation to and from Houston are all part of the package.

Sunday Evening Mixer

There will be a Sunday Evening Social get-acquainted gathering in the Grecian Room just off the Hotel Lobby from 6:00 to 8:00 P.M. All those registered for The Electrochemical Society Meeting are invited to attend. Beer, soft drinks, and snacks will be served on a complimentary basis. Mixed drinks may be purchased at the bar. Admission is by registration badge.

Monday Cocktail Party and Texas Style Barbecue

Arrangements have been made with the Shamrock Hilton Hotel to provide a traditional Texas Barbecue on and around the Hotel's triangular adjoining lawns. Soft drinks and cocktails will be served at 5:00 P.M. The famous Texas local Sheriff's Mounted Posse and their horses will perform for the entertainment of the guests, this being the featured attraction of the evening. Be on the Shamrock Hilton triangular lawns promptly at 5:00 P.M., Oct. 10, for this event. Barbecue and other food will be served at 6:00 P.M. Tickets for this function will be available at the Society's registration desk. This event starts early to prevent the early fall darkness in this locale from interfering with your pleasure.

Tuesday Acheson Medal Reception and Banquet

A reception honoring Dr. Henry B. Linford, the Acheson Medalist, will be held at 6:30 P.M. on Tuesday, Oct. 11, in the Grecian Room, Shamrock Hilton Hotel, just off the Lobby Promenade. Cocktails and soft drinks will be served from 6:30 to 7:30 P.M. The banquet, in the connecting Emerald Room, will begin at 7:30 P.M. Dr. Linford will deliver the Acheson Medal address.

Wednesday Student Round Table and Reception

On Wednesday, Oct. 12, at 3:00 P.M. in the Normandy Room, 3rd floor, Shamrock Hilton, representatives of the various divisions of the Society will discuss the nature of technical activities of interest to each division for specially invited students (seniors and early graduates) and their sponsoring professors from colleges and universities in the Houston area. The object of this function, sponsored by the Society, is to inform students of the opportunities and future in electrochemistry. Following the round-table discussion, a reception and mixer for this group will be held in the Castillian Room, 3rd floor, at 5:00 P.M. Refreshments will be served on a complimentary basis.

PLANT TRIPS

Tuesday—Diamond Alkali Corp.

A tour of the Houston Ship Channel and the Deer Park Plant of the Diamond Alkali Corporation has been arranged. Buses will depart promptly from the main entrance of the Shamrock Hilton Hotel at 1:30 P.M. on Tuesday, Oct. 11, and proceed to the Houston Channel Turning Basin where the party will board the Navigation District's Inspection Boat "Sam Houston." The boat will proceed down the channel for about 15 miles, passing many chemical plant sites. The group will leave the boat at the Diamond Alkali Plant for an inspection of their diaphragm and mercury cell chlorine facilities and utility department. At the completion of the tour, buses will return to the hotel, about 5:45 P.M. The cost per person for the tour is $2.50. The boat trip is provided through the courtesy of the Port of Houston. Attendance will be limited to 50.

Wednesday—Dow Chemical Co.

Buses will depart at 1:30 P.M. on Wednesday, Oct. 12, for a tour of The Dow Chemical Company magnesium reduction plant at Freeport, Texas. This will include a general tour of the chemical plant and an inspection of the operating magnesium cells. Following the tour, a barbecue dinner will be served courtesy of The Dow Chemical Company at the Company Park. Buses will return to the Hotel by 8:00 P.M. Attendance will be limited.

LADIES' PROGRAM

All the ladies are invited to make the Nile Room (turn right on 3rd floor from the elevators), Shamrock Hilton, their headquarters during their stay in Houston. Members of the Ladies' Committee will be there to give information and assist in making your stay a pleasant one. Due to the isolated nature of the Shamrock Hilton Hotel our functions will be mainly in the morning to allow freedom in the afternoon either to relax by the magnificent Shamrock Hilton pool or to make shopping trips to downtown Houston. The Nile Room will be our Hospitality Headquarters.

Sunday, Oct. 9—Start out on the right social foot. Attend the Sunday Evening Mixer in the Grecian Room (take right Promenade, then turn left) from 6:00 to 8:00 P.M. Admission by registration badge.

Monday, Oct. 10—Coffee hour at 9:30 A.M. The ladies are free for the day but are urged to attend the Cocktail Party, Barbecue, and typical Texas-type entertainment of the Sheriff's Mounted Posse that evening at 5:00 P.M. on the front lawn of the hotel.

Tuesday, Oct. 11—Continental breakfast at 9:30 A.M., followed by a talk and demonstration by Mrs. Veberly Nixon, Adult Homemaking teacher for the Brazosport Schools, entitled "Millinery Made at Home" at 10:30 A.M. The ladies are invited to attend the Acheson Medal Reception and Banquet that evening at 6:30 P.M.

Wednesday, Oct. 12—Coffee hour at 9:30 A.M. followed by a sightseeing trip by air-conditioned bus, with a hostess to describe the Rice Institute Campus, the world-known Texas Medical Center, etc., and then on to the Gulfgate Shopping Center for souvenir and other shopping; the trip starts at 10:00 A.M. and return should be about 3:00 P.M.

Thursday, Oct. 13—Coffee hour at 9:30 A.M. followed by a talk at 11:00 A.M. by Mrs. Betty Smith of the John Robert Powers modeling school. If you can stay through luncheon, there will be the regular Thursday Styles Show and Luncheon in the Emerald Room at 12:30 P.M.

BOARD AND COMMITTEE MEETINGS

Sunday, Oct. 9, 2:00 P.M.—Meeting of the **Board of Directors,** Castillian Room B and C, 3rd floor, Shamrock Hilton.

Monday, Oct. 10, 2:00 P.M.—Meeting of the **Convention Advisory Committee,** Room 335, Shamrock Hilton.

Monday, Oct. 10, 12:15 P.M.—Luncheon Meeting of the **Membership Committee,** Castillian Room B and C, 3rd floor, Shamrock Hilton.

Tuesday, Oct. 11, 5:00 P.M.—Meeting of the **Editorial Staff of the Journal,** Castillian Room B and C, 3rd floor, Shamrock Hilton.

Tuesday, Oct. 11, 5:00 P.M.—Meeting of the **Council of Local Sections,** Normandy Room, 3rd floor, Shamrock Hilton.

Wednesday, Oct. 12, 12:00 M.—Luncheon meeting of the **General Chairmen of Future Meetings** in Castillian Room A, 3rd floor, Shamrock Hilton, at 12:00 M.

1961 SPRING MEETING
at the
Claypool Hotel
INDIANAPOLIS, INDIANA
April 30, May 1, 2, 3, and 4, 1961

Sessions probably will be scheduled on:
Electric Insulation
Electronics (including Luminescence and Semiconductors)
Electrothermics and Metallurgy
Industrial Electrolytics
Theoretical Electrochemistry

Abstracts for the Indianapolis Meeting (*not exceeding 75 words in length*) must reach Society Headquarters, 1860 Broadway, New York 23, N. Y., *not later than* January 2, 1961 to be included in the Program.

Please *indicate* on the abstract *for which Division's symposium the paper is to be scheduled* and *underline the name of the author who will present the paper* at the Indianapolis Meeting.

Presentation of a paper at a technical meeting of the Society does not guarantee publication in the JOURNAL. However, all papers so presented become the property of The Electrochemical Society, and may not be published elsewhere, either in whole or in part, unless permission for release is requested of and granted by the Editor. Papers already published elsewhere, or submitted for publication elsewhere, are not acceptable for oral presentation except on invitation by a Divisional program Chairman.

LUNCHEONS AND BUSINESS MEETINGS OF DIVISIONS

Battery Division Luncheon and Business Meeting, **Tuesday,** Oct. 11, 12:30 P.M., on the Terrace, Shamrock Hilton.

Electronics Division, Semiconductor Group Luncheon, **Tuesday,** Oct. 11, 12:30 P.M., in the Castillian Room, 3rd floor, Shamrock Hilton.

Corrosion Division Luncheon and Business Meeting, **Wednesday,** Oct. 12, 12:30 P.M., in the Castillian Room, 3rd floor, Shamrock Hilton.

Electrodeposition Division Luncheon and Business Meeting, **Wednesday,** Oct. 12, 12:30 P.M., on the Terrace, Shamrock Hilton.

COST OF VARIOUS FUNCTIONS

(other than registration)

Please buy tickets at time of registration, if possible.

Deep Sea Fishing Trip	$25.00
Symposia Chairmen Breakfasts	Menu prices
Sunday Evening Mixer	Complimentary
Monday Cocktail Party and Barbecue	7.50
Tuesday Plant Trip to Diamond Alkali Corp.	2.50
Tuesday Acheson Medal Reception and Banquet	8.00
Division Luncheons	3.50
Wednesday Ladies' Shopping Tour	1.00
Wednesday Plant Trip to Dow Chemical Co.	2.50

JOURNALS

Copies of the June, July, August, and September issues of the "Journal of The Electrochemical Society" will be available at the Registration Desk on Sunday, Monday, and Tuesday in the Hall of Exhibits' entrance, and on Wednesday and Thursday in the Venetian Room, 3rd floor, Shamrock Hilton. The price of a single copy of the **Journal** is $1.25 to members and $1.75 to nonmembers.

EXTENDED ABSTRACTS

The Battery Division is making available an extended abstract booklet containing 1000-word abstracts of most of the papers presented at the Division's Houston Meeting. Copies of the booklet may be obtained from C. H. Clark, 34 Pleasant Way, Deal, N. J., after Sept. 15 for $2.00 each.

EMPLOYMENT POSTERS

Companies which desire to recruit employees at the Houston Meeting will have posters to this effect on a Bulletin Board adjacent to the Registration Desks (see Registration for location). Companies are requested to confine their announcements to this Bulletin Board.

DISCUSSION

No recordings will be made of oral discussion. Those contributing to the discussion of a paper and desiring their remarks to be published will be supplied by the symposium chairman with a printed form on which any discussion may be written. These forms should be given to the symposium chairman or to the Managing Editor of the **Journal** after the session; or they can be mailed to the Managing Editor of the **Journal,** 1860 Broadway, New York 23, N. Y. The discussion will then be referred to the author for reply. Publication of the discussion and the comments of the author depends on publication of the article in the **Journal.**

Written discussion of a published paper should be submitted within two months following publication of the article in the **Journal.** A Discussion Section is published semiannually in the **Journal.**

NOTE

Photographing of lantern slides, charts, etc., will be permitted unless specifically prohibited by the speaker. Photo flash and photo floods are prohibited.

Technical Program—Houston Meeting

MONDAY, A.M., Oct. 10, 1960

BATTERY

G. W. Vinal, Honorary Chairman. Primary Cells with W. S. Herbert presiding

(AZALEA ROOM, Exhibit Hall, entrance on Holcombe Blvd.)

9:30 A.M.—"Ambient Temperature Fuel Cells" by H. F. Hunger (Abstract No. 1)

10:00 A.M.—"Electrode Kinetics of Various Redox Couples for Fuel Cell Use" by A. P. Bond and D. Singman (Abstract No. 2)

10:30 A.M.—"Investigation of the Electrochemical Characteristics of Organic Compounds, VIII. Hydrazine and Hydroxylamine Compounds" by R. Glicksman (Abstract No. 3)

11:00 A.M.—"Factors Affecting the Discharge Characteristics of Thermal Cells" by C. W. Jennings (Abstract No. 4)

11:25 A.M.—"Recent Studies on Ammonia Battery Systems" by Otto Adlhart and H. R. Knapp (Abstract No. 5)

11:50 A.M.—"The Photogalvanic Effect in Inorganic Oxidation-Reduction Systems, I. The Iodine-Iodide System" by H. N. Seiger and R. A. Marcus (Abstract No. 6)

CORROSION

Can Corrosion, with E. L. Koehler presiding

(CONTINENTAL ROOM, Shamrock Hilton, off Main Lobby)

9:00 A.M.—"A Hypothesis for the Uncoupling Shift Observed in the Iron-Tin System in Citric Acid" by W. R. Buck, III, A. N. J. Heyn, and Henry Leidheiser, Jr. (Abstract No. 34)

9:30 A.M.—"Effect of Tin Ion Complexing Substances on the Relative Potentials of Tin and Steel in Oxygen Free Acid Media" by A. R. Willey (Abstract No. 35)

10:00 A.M.—"Oxide Films on Tin Plate" by M. Falkenhagen and J. D. Bode (Abstract No. 36)

10:25 A.M.—Ten-minute intermission

10:35 A.M.—"Some Factors Affecting the Surface Chromium Content of Electrochemically Treated Tin Plate" by P. R. Carter (Abstract No. 37)

11:00 A.M.—"Use of Polarization Methods in the Determination of the Rate of Corrosion of 3003 Aluminum in Anaerobic Acid Media" by S. Evans and E. L. Koehler (Abstract No. 38)

11:30 A.M.—"Use of Polarization Methods in the Determination of the Rate of Corrosion of Aluminum Alloys in Anaerobic Food Media" by E. L. Koehler and S. Evans (Abstract No. 39)

ELECTRODEPOSITION and ELECTROTHERMICS AND METALLURGY

Joint Symposium on Vapor Deposited Coatings, with J. M. Blocher, Jr. presiding

(GRECIAN ROOM, Shamrock Hilton, take right Promenade, then turn left)

9:30 A.M.—"Prepurification Techniques: Their Role in Metal Production" by R. G. Bourdeau and E. Rose (Abstract No. 119)

MEETING ROOM SCHEDULE

Meeting	Monday		Tuesday		Wednesday		Thursday	
	AM	PM	AM	PM	AM	PM	AM	PM
Battery	E	E	E	E	E	E		
Corrosion	B	BD	B	B	B	B	B	B
Electrodeposition			C	C	C	C	C	
Electrodeposition—Electrothermics and Metallurgy	C	C						
Electronics—Semiconductor	A	A	A	A	A	A		
Electrothermics and Metallurgy			D					

Shamrock Hilton
A = Emerald Room, Lobby floor.
B = Continental Room, Lobby floor.
C = Grecian Room, Lobby floor.
D = El Shiro Room.

Exhibit Hall
E = Azalea Room.

9:55 A.M.—"Mass and Heat Transfer during the Vapor Deposition of Metals" by J. H. Oxley and J. M. Blocher, Jr. (Abstract No. 120)
10:20 A.M.—"Mechanism of Hydrogen Reduction of Cuprous Iodide Vapor" by C. R. Morelock and G. W. Sears (Abstract No. 121)
10:50 A.M.—"Tungsten Coatings by Gas Phase Deposition" by W. E. Reid, Jr., and Abner Brenner (Abstract No. 122)
11:15 A.M.—"Fluidized-Bed Coating of Uranium Dioxide Powder Particles with Niobium and Other Elements" by J. M. Blocher, Jr., N. D. Veigel, J. H. Oxley, V. M. Secrest, and E. E. Rose (Abstract No. 123)

ELECTRONICS—SEMICONDUCTORS

Crystal Growth, with H. E. Bridgers presiding

(EMERALD ROOM, Shamrock Hilton, off main Lobby)

9:15 A.M.—"Growth Steps on the Surfaces of Germanium, Silicon, and III-V Compound Dendrites" by G. R. Booker (Abstract No. 129)
9:40 A.M.—"Silicon Dendrite Studies" by S. N. Dermatis and J. W. Faust, Jr. (Abstract No. 130)
10:00 A.M.—"Investigations of Crystal Perfection of Semiconductor Crystals by X-Ray Diffraction Microscopy" by G. H. Schwuttke (Abstract No. 131)
10:20 A.M.—"Germanium Structural Defects—Their Cause and Effect" by D. H. Lyon (Abstract No. 132)
10:45 A.M.—"Horizontal Growth of Germanium Single Crystals Using a Silicon Nitride Receptacle" by J. L. Porter (Abstract No. 133)
11:05 A.M.—"Simple Method of Determining Crystal Perfection, II" by H. K. Herglotz (Abstract No. 134)
11:25 A.M.—Recent News Papers. Titles and short abstracts will be available at the Registration Desk.

MONDAY P.M., Oct. 10, 1960

BATTERY (Cont'd)

Primary Cells with C. H. Clark presiding

(AZALEA ROOM, Exhibit Hall, entrance on Holcombe Blvd.)

2:00 P.M.—"Investigation of the Electrochemical Characteristics of Organic Compounds, VII. Organic Positive Iodine and Aliphatic Azo Compounds" by R. Glicksman and C. K. Morehouse (Abstract No. 7)
2:30 P.M.—"Stability and Solubility of Silver Oxide Electrodes in Alkaline Electrolytes" by R. F. Amlie and Paul Ruetschi (Abstract No. 8)
3:00 P.M.—"The Magnesium-m-Ditnitrobenzene Cell" by G. S. Lozier, R. Glicksman, and J. B. Eisen (Abstract No. 9)
3:30 P.M.—"The Influence of the Active Surface on the Cathodic Reduction of MnO_2" by N. C. Cahoon and M. P. Korver (Abstract No. 10)
4:00 P.M.—"Impedance of Dry Cells and Batteries" by R. J. Brodd (Abstract No. 11)
4:30 P.M.—"Recharging of Leclanche Dry Cells" by W. S. Herbert (Abstract No. 12)

CORROSION (Cont'd)

Oxidation, with A. Dravnieks presiding

(CONTINENTAL ROOM, Shamrock Hilton, off Main Lobby)

2:00 P.M.—"The Oxidation of Tin, II. Morphology and Mode of Growth of Oxide Films on Pure Tin" by W. E. Boggs, P. S. Trozzo, and G. E. Pellissier (Abstract No. 40)
2:25 P.M.—"The Oxidation of Tin, I. Kinetics of Oxidation of Pure Tin and the Effects of Temperature and Oxygen Pressure" by W. E. Boggs, R. H. Kachik, and G. E. Pellissier (Abstract No. 41)
2:40 P.M.—"The Oxidation of Tin, III. Mechanisms of Oxidation of Pure Tin" by W. E. Boggs (Abstract No. 42)
2:55 P.M.—"Microtopography of Oxide Films Formed on Tantalum" by R. E. Pawel, J. V. Cathcart, and J. J. Campbell (Abstract No. 43)
3:20 P.M.—Ten-minute intermission
3:30 P.M.—"Interaction between Copper and Gas Discharge Products Condensed at Very Low Temperatures" by Jerome Kruger and W. J. Ambs (Abstract No. 44)
3:55 P.M.—"Copper Oxides on the Surface of Gold Plate" by M. S. Frant and R. Rajaraman (Abstract No. 45)
4:20 P.M.—"Oxidation of Copper between 250° and 450°C and the Growth of CuO 'Whiskers' " by E. A. Gulbransen, T. P. Copan, and K. F. Andrew (Abstract No. 46)
4:45 P.M.—"Corrosion Rate of Fe in High-Temperature H_2O by an Electrical Resistance Method" by A. J. Panson (Abstract No. 47)

CORROSION (Cont'd)

Unusual Valence States and the Difference Effect, with R. T. Foley presiding

(EL SHIRO ROOM, Shamrock Hilton, take right Promenade, then turn left)

2:00 P.M.—"Unusual Oxidation States Encountered in Corrosion Processes" by E. C. Pitzer (Abstract No. 47A)
2:20 P.M.—"Evidence for One-Electron Oxidation as Primary Electrode Reaction in Anodic Dissolution of Bivalent Metals" by A. W. Davidson (Abstract No. 48)
2:50 P.M.—"The Relative Stabilities of Oxidation States of Transitional Metals" by G. W. Watt (Abstract No. 49)
3:20 P.M.—Ten-minute intermission
3:30 P.M.—"Valency of Ions Formed during Anodic Dissolution of Metals in Acids" by M. E. Straumanis (Abstract No. 50)
4:00 P.M.—"The Difference Effect and Anodic Behavior of Zirconium Dissolving in Hydrofluoric Acid" by M. E. Straumanis, W. J. James, and W. C. Custead (Abstract No. 51)
4:30 P.M.—"The Difference Effect and the Chunk Effect" by G. A. Marsh and E. Schaschl (Abstract No. 52)

ELECTRODEPOSITION and ELECTROTHERMICS AND METALLURGY (Cont'd)

Joint Symposium on Vapor Deposited Coatings (cont'd) with J. M. Blocher, Jr., presiding

(GRECIAN ROOM, Shamrock Hilton, take right Promenade, then turn left)

2:00 P.M—"Vapor Deposition of Carbon onto Sintered UO_2 Reactor Fuel" by E. G. Wintucky and E. H. Layer (Abstract No. 124)
2:25 P.M.—"Oxidation Resistant Silicide Coatings for Columbium and Tantalum Alloys" by R. Lorenz and A. B. Michael (Abstract No. 125)
2:50 P.M.—"Diffusion Coatings of Refractory Metals on Steel" by R. E. Bessey and W. M. Kisner (Abstract No. 126)
3:15 P.M.—"Industrial Aspects of Vapor-Deposited Coatings" by H. W. Schultze (Abstract No. 127)
3:45 P.M.—"Testing of Vapor-Plated Aluminum Films" by F. V. Schossberger and K. D. Franson (Abstract No. 128)

ELECTRONICS—SEMICONDUCTORS (Cont'd)

Compound Semiconductors, with W. J. Turner presiding

(EMERALD ROOM, Shamrock Hilton, off main Lobby)

2:00 P.M.—"Synthesis and Crystal Pulling of Gallium Arsenide in a Magnetic Crystal Puller" by K. Weiser and S. Blum (Abstract No. 135)
2:20 P.M.—"Graded Energy Gap Alloy Semiconductor—$GaAs_xP_{1-x}$" by R. E. Johnson and George Towns (Abstract No. 136)
2:40 P.M.—"Preparation of Gallium Phosphide under Moderate Pressures of Phosphorus Vapor" by J. F. Miller, R. C. Himes, and H. L. Goering (Abstract No. 137)
3:00 P.M.—"Direct Recombination in GaAs" by S. Mayburg (Abstract No. 138)
3:20 P.M.—"Reactions between Gallium and Quartz" by L. M. Foster and R. A. Kramer (Abstract No. 139)
3:40 P.M.—"Analysis of Impurities in Compound Semiconductors" by G. D. Perkins, C. F. Robinson, and R. K. Willardson (Abstract No. 140)
4:00 P.M.—Recent News Papers. Titles and Short Abstracts will be available at the registration desk.

TUESDAY A.M., Oct. 11, 1960

BATTERY (Cont'd)

Lead-Acid Storage Batteries. 100th Anniversary Plante Session, with E. J. Ritchie presiding

(AZALEA ROOM, Exhibit Hall, entrance on Holcombe Blvd.)

9:00 A.M.—Introductory remarks by G. W. Vinal.
9:10 A.M.—"Is the Lead-Acid Battery Obsolete?" by Paul Ruetschi (Abstract No. 13)
10:00 A.M.—"How Lead Becomes a Battery" by R. Jardine and S. K. Lessey (Abstract No. 14)
10:40 A.M.—"The Anodic Oxidation Rate of Pure Lead in Sulfuric Acid" by R. A. Baker (Abstract No. 15)
11:00 A.M.—"Plante, Pourbaix, and Passivation" by Jeanne Burbank (Abstract No. 16)
11:30 A.M.—"Mechanisms of the Electrode Reactions in Lead Accumulators" by W. F. K. Wynne-Jones (Abstract No. 17)
12:30 P.M.—Battery Division Luncheon and Business Meeting, Terrace, Shamrock Hilton.

CORROSION (Cont'd)

Certain Properties of the Interface Related to Corrosion, with G. H. Cartledge presiding

(CONTINENTAL ROOM, Shamrock Hilton, off main Lobby)

9:00 A.M.—"Adsorption and Ion Exchange at the Corrosion Interface" by G. H. Cartledge (Abstract No. 54)
9:30 A.M.—"Proton Mobility in Liquids and Solids" by B. E. Conway (Abstract No. 55)
10:00 A.M.—"The Structure of the Corroding Interface" by T. P. Copan (Abstract No. 56)
10:30 A.M.—Fifteen-minute intermission
10:45 A.M.—"Effects of Corrosion Films on Cathodic Processes" by R. E. Meyer (Abstract No. 57)
11:15 A.M.—Discussion period. Discussion initiated by Norman Hackerman

ELECTRODEPOSITION

Electroless and Immersion Plating, with Abner Brenner presiding

(GRECIAN ROOM, Shamrock Hilton, take right Promenade, then turn left)

9:00 A.M.—"Chemical Deposition of Palladium and Other Platinum Metals" by R. N. Rhoda (Abstract No. 89)
9:30 A.M.—" 'Electroless' Deposition of Gold from Aqueous Solution on Base Metals of Nickel, Iron-Nickel-Cobalt Alloys and Gold" by R. F. Walton (Abstract No. 90)
10:00 A.M.—"Chemical Plating with Borohydrides" by E. A. Sullivan (Abstract No. 91)
10:30 A.M.—"An Electroless Copper Plating System for 'Pure' Aluminum" by S. L. Matlow (Abstract No. 92)
11:00 A.M.—"Mechanisms of Electroless Deposition of Metals on Silicon" by S. L. Matlow (Abstract No. 93)
11:30 A.M.—"Immersion Coatings of the Platinum Metals" by R. W. Johnson (Abstract No. 94)

ELECTRONICS—SEMICONDUCTORS (Cont'd)

Compound Semiconductors (Cont'd) with R. Sangster presiding

(EMERALD ROOM, Shamrock Hilton, off main Lobby)

9:00 A.M.—"Some Comments on the Electronic Structure of Group IV and III-V Semiconductors" by S. L. Matlow (Abstract No. 141)
9:20 A.M.—"Physical Properties of p-Type Zn_3As_2 and n-Type Cd_3As_2" by W. J. Turner, A. S. Fischler, and W. E. Reese (Abstract No. 142)
9:40 A.M.—"Mobility Doping of Semiconducting Compounds" by A. J. Cornish (Abstract No. 143)
10:00 A.M.—"Thermoelectric and Crystalographic Properties of Ag_2Se" by J. B. Conn and R. C. Taylor (Abstract No. 144)
10:20 A.M.—"Properties of HgSe-HgTe Alloys" by T. C. Harman, A. J. Strauss, and L. B. Farrell (Abstract No. 145)
10:40 A.M.—"Crystal Orientation Effects Observed in Tin-Telluride Thin Films" by S. H. Shortes and D. P. Miller (Abstract No. 146)
11:00 A.M.—"The Growth of Single Crystal Iron Ferrites by the Czochralski Method" by F. H. Horn (Abstract No. 147)
11:20 A.M.—"Titanium Thin Film Resistance for Microsystems Electronics" by R. A. Quinn (Abstract No. 148)
11:40 A.M.—Recent News Papers. Titles and Short Abstracts will be available at the Registration Desk.
12:30 P.M.—Electronics—Semiconductor Luncheon, Castillian Room, 3rd floor, Shamrock Hilton.

ELECTROTHERMICS AND METALLURGY

Vacuum-Evaporated Films; Refractory and Reactive Metals, with E. M. Sherwood presiding

(EL SHIRO ROOM, Shamrock Hilton, take right Promenade, then turn left)

9:30 A.M.—"Vacuum-Evaporated Titanium Coatings" by C. Horn and D. K. Wilburn (Abstract No. 169)
9:55 A.M.—"Deposition of InSb Films by Flash Evaporation" by E. H. Layer, F. J. Reid, and A. E. Austin (Abstract No. 170)
10:20 A.M.—"Vacuum Sintering of Tungsten Ingots" by J. W. Pugh and L. H. Amra (Abstract No. 171)
10:45 A.M.—Five-minute intermission
10:50 A.M.—"Reactions in the Niobium-Nitrogen System" by W. M. Albrecht and W. D. Goode (Abstract No. 172)
11:15 A.M.—"Preparation of Rare Earth Master Alloys" by S. J. Morana (Abstract No. 173)

TUESDAY P.M., Oct. 11, 1960

BATTERY (Cont'd)

Lead-Acid Storage Batteries. 100th Anniversary Plante Session (Cont'd), with W. J. Hamer presiding

(AZALEA ROOM, Exhibit Hall, entrance on Holcombe Blvd.)

2:30 P.M.—"Formation Studies of Lead-Acid Battery Plates Using the Electron Microscope" by J. E. Buskirk, P. D. Boyd, and V. V. Smith (Abstract No. 19)
2:55 P.M.—"Electrode Potentials and Thermal Decomposition of α- and β-PbO_2" by R. T. Angstadt and Paul Ruetschi (Abstract No. 20)
3:20 P.M.—"Some Important Factors That Influence the Composition of Positive Plate Material" by V. H. Dodson (Abstract No. 21)
3:50 P.M.—"Composition and Performance of Positive Plate Material" by V. H. Dodson (Abstract No. 22)
4:15 P.M.—"The Next Hundred Years" by E. Willihnganz (Abstract No. 23)

CORROSION (Cont'd)

General Session, with M. A. Streicher presiding

(CONTINENTAL ROOM, Shamrock Hilton, off main Lobby)

2:00 P.M.—"Dissolution of Mild Steel in the System NH_4NO_3-NH_3-H_2O at 30°C" by J. D. Goodrich and Norman Hackerman (Abstract No. 58)
2:30 P.M.—"Corrosion Inhibition and Electronic Configuration at the Amino Nitrogen Atom" by Norman Hackerman, R. R. Annand, and R. M. Hurd (Abstract No. 59)
3:00 P.M.—"Capacitance Studies on Corroding Metal Electrodes" by H. M. Joseph and R. A. Powers (Abstract No. 60)
3:25 P.M.—Ten-minute intermission
3:35 P.M.—"Hydrogen Pickup in Various Zirconium Alloys during Corrosion Exposure in High-Temperature Water and Steam" by Stanley Kass (Abstract No. 61)
4:00 P.M.—"Kinetics of Sulfidization of Copper by Hydrogen Sulfide" by Andrew Dravnieks (Abstract No. 62)
4:30 P.M.—"Copper Sulfide Creep on Porous Electroplate" by M. S. Frant (Abstract No. 63)

ELECTRODEPOSITION (Cont'd)

Electrophoretic Deposition, with A. H. Beebe presiding

(GRECIAN ROOM, Shamrock Hilton, take right Promenade, then turn left)

2:00 P.M.—"Impedance Phenomena in Molten Salts" by G. J. Hills and K. E. Johnson (Abstract No. 95)
2:30 P.M.—"Electrolytic Metallide Coatings in Molten Fluoride" by N. C. Cook (Abstract No. 96)
3:00 P.M.—"Electrophoretic Deposition of Oxidation-Resistant Coatings on Molybdenum and Solid Lubricant Coatings on 304 Stainless Steel" by P. F. Campbell, K. A. Gebler, and S. J. Klack (Abstract No. 97)
3:30 P.M.—"Electrophoretic Deposition: A Versatile Coating Method" by C. P. Gutierrez, J. R. Mosley, and T. C. Wallace (Abstract No. 98)
4:00 P.M.—"Electrophoretic Deposition of Aluminum" by F. Pearlstein, R. Wick, and A. Gallaccio (Abstract No. 99)
4:30 P.M.—"The Electrodeposition of Cermets" by J. C. Withers (Abstract No. 100)

ELECTRONICS—SEMICONDUCTORS (Cont'd)

Technology, with F. Biondi presiding

(EMERALD ROOM, Shamrock Hilton, off main Lobby)

2:00 P.M.—"Some Statistics of Doping Silicon Crystals" by J. W. Brownson and R. Saphir (Abstract No. 149)
2:20 P.M.—"Method of Evaluating Silicon Monocrystals for the Fabrication of Diffused Junction Devices" by A. Ertel (Abstract No. 150)
2:45 P.M.—"A Modified Closed Box System for the Diffusion of Boron in Silicon" by R. S. Yatsko and J. S. Kesperis (Abstract No. 151)
3:05 P.M.—"Some Effects of Paint Strength Variation in Paint-on Diffusion of Silicon" by J. E. Reynolds and W. Gegg (Abstract No. 152)
3:20 P.M.—"Etching Ge with 'Superoxol' " by J. Bloem and J. C. van Vessem (Abstract No. 153)
3:40 P.M.—"Dissolution of Germanium in Hydrogen Peroxide" by Pei Wang and Nino Cerniglia (Abstract No. 154)
4:00 P.M.—"Sizing of Semiconductor Dice by Controlled Chemical Etching" by R. B. Soper (Abstract No. 155)

4:20 P.M.—"A New Technique for the Preparation of Flat Germanium Surfaces" by M. V. Sullivan and R. M. Finne (Abstract No. 156)
4:45 P.M.—"The Wetting of Germanium by Molten Indium" by A. A. Bergh and L. H. Holschwandner (Abstract No. 157)

WEDNESDAY A.M., Oct. 12, 1960

BATTERY (Cont'd)

Solid Electrolyte, Secondary Battery Characteristics, and Silver/Silver Oxide Electrodes, with U. B. Thomas presiding

(AZALEA ROOM, Exhibit Hall, entrance on Holcombe Blvd.)

9:00 A.M.—"Ionic Conductivity of Silver Iodide Pellets for Solid Electrolyte Batteries" by L. N. Mrgudich (Abstract No. 24)
9:30 A.M.—"The Ag/AgCl/ICl Solid Electrolyte Cell System" by D. M. Smyth and C. H. Tompkins (Abstract No. 25)
10:00 A.M.—"An Analytical Representation of the Characteristics of Commercial Secondary Batteries" by S. M. Selis and C. R. Russell (Abstract No. 26)
10:30 A.M.—"Float Characteristics of the Lead-Calcium Cell" by Jeanne Burbank and C. P. Wales (Abstract No. 27)
11:00 A.M.—"The Silver-Silver Oxide Electrode, I. Anodic Oxidation in Alkaline Solutions" by C. P. Wales (Abstract No. 28)
11:30 A.M.—"Electrode Phenomena of the Silver-Silver Oxide System in the Alkaline Battery" by Shiro Yoshizawa and Zenichiro Takehara (Abstract No. 29)

CORROSION (Cont'd)

Passivity, with Norman Hackerman presiding

(CONTINENTAL ROOM, Shamrock Hilton, off Main Lobby)

9:00 A.M.—"Anode Polarization Effects" by O. L. Riggs, Jr., J. D. Sudbury, and D. A. Shock (Abstract No. 64)
9:30 A.M.—"Anodic Behavior of Austenitic Stainless Steels and Susceptibility to Stress Corrosion Cracking" by S. Barnartt and D. van Rooyen (Abstract No. 65)
10:00 A.M.—"The Volatilization of Chromium Oxide" by D. Caplan and M. Cohen (Abstract No. 66)
10:25 A.M.—Ten-minute intermission
10:35 A.M.—"The Passivity of Austenitic Stainless Steels in Sulfuric Acid" by N. D. Greene (Abstract No. 67)
11:00 A.M.—"Effect of Oxygen on the Active-Passive Behavior of Stainless Steel" by N. D. Greene (Abstract No. 68)
11:30 A.M.—"Kinetics of Redox Reactions on Passive Electrodes" by A. C. Makrides (Abstract No. 69)
12:30 P.M.—Corrosion Division Luncheon and Business Meeting, Castillian Room, Shamrock Hilton

ELECTRODEPOSITION (Cont'd)

Metal Deposition, with D. G. Foulke presiding

(GRECIAN ROOM, Shamrock Hilton, take right Promenade, then turn left)

9:00 A.M.—"Effect of Organic Compounds on the Codeposition of Hydrogen with Nickel" by J. R. Goodwyn and T. C. Franklin (Abstract No. 101)
9:30 A.M.—"Mechanism of Addition Agent Reaction in Bright Nickel Deposition" by S. E. Beacom and B. J. Riley (Abstract No. 102)
10:00 A.M.—"Electrodeposition of Iridium" by E. L. MacNamara (Abstract No. 103)
10:30 A.M.—"Electrodeposition of Pure Copper" by Sidney Barnartt (Abstract No. 104)
11:00 A.M.—"Electrodeposition of High-Purity Chromium from Electrolytes Containing Fluoride or Fluosilicate" by N. E. Ryan (Abstract No. 105)
11:30 A.M.—"Measurement of Stress in Very Thin Electrodeposits" by H. Watkins and A. J. Kolk (Abstract No. 106)
12:30 P.M.—Electrodeposition Luncheon and Business Meeting, Terrace, Shamrock Hilton.

ELECTRONICS—SEMICONDUCTORS (Cont'd)

Surfaces, with R. Hurd presiding

(EMERALD ROOM, Shamrock Hilton, off main Lobby)

9:00 A.M.—"Nuclear Magnetic Resonance of Water Adsorbed on Silicon" by C. G. McCormick and G. K. Walters (Abstract No. 158)
9:20 A.M.—"The Retention of Water by the Real Silicon Surface" by S. S. Baird (Abstract No. 159)
9:40 A.M.—"D-C Field and Noise Measurements on Silicon" by B. R. Pagel (Abstract No. 160)
10:00 A.M.—"Variation with Frequency of the Transverse Impedance of Semiconductor Surfaces" by F. Berz (Abstract No. 161)
10:20 A.M.—"Differential Capacity and Surface Conductivity of the Silicon Electrolyte Phase Boundary" by R. M. Hurd, P. T. Wrotenbery, and Don Arnold (Abstract No. 162)
10:40 A.M.—Recent News Papers. Titles and Short Abstracts will be available at the Registration Desk.

WEDNESDAY P.M., Oct. 12, 1960

BATTERY (Cont'd)

Nickel-Cadmium, with J. C. White presiding

(AZALEA ROOM, Exhibit Hall, entrance on Holcombe Blvd.)

2:00 P.M.—"High Energy: Weight Ratio, Nickel Cadmium Cells" by J. C. Duddy and A. J. Salkind (Abstract No. 30)
2:30 P.M.—"Formation of Porous Metal Plates by Electrolytic Reduction under Controlled Pressures" by C. M. Shepherd and H. C. Langelan (Abstract No. 31)
3:00 P.M.—"The Forming Process in Nickel Positive Electrodes" by Donald Tuomi (Abstract No. 32)
3:40 P.M.—"Electrochemical Behavior of the Semi-charged Nickel Oxide Electrode" by B. E. Conway and P. L. Bourgault (Abstract No. 33)

CORROSION (Cont'd)

Passivity (Cont'd), with M. Stern presiding

(CONTINENTAL ROOM, Shamrock Hilton, off Main Lobby)

2:00 P.M.—"Critical pH and Critical Current Density for Passivity in Metals" by H. H. Uhlig (Abstract No. 70)
2:30 P.M.—"Anodic Polarization and Passivity of Ni and Ni-Cu Alloys in Sulfuric Acid" by J. Osterwald and H. H. Uhlig (Abstract No. 71)
3:00 P.M.—"Corrosion Behavior and Passivity of Nickel-Chromium and Cobalt-Chromium Alloys" by A. P. Bond and H. H. Uhlig (Abstract No. 72)
3:25 P.M.—Ten-minute intermission
3:35 P.M.—"Relation of Electron Configuration to Passivity in Cr-Ni-Fe Alloys" by H. G. Feller and H. H. Uhlig (Abstract No. 73)
4:00 P.M.—"Formation and Breakdown of Passive Films on Iron Single Crystal Surfaces" by Jerome Kruger (Abstract No. 74)
4:30 P.M.—"Anodic Polarization Behavior of Iron-Nickel Alloys in Sulfuric Acid Solutions" by George Economy, Rudolph Speiser, F. H. Beck, and M. G. Fontana (Abstract No. 75)

ELECTRODEPOSITION (Cont'd)

Alloy Plating, with D. R. Turner presiding

(GRECIAN ROOM, Shamrock Hilton, take right Promenade, then turn left)

2:00 P.M.—"Influence of Thiourea on the Deposition of Iron-Nickel Films" by R. D. DeMars (Abstract No. 107)
2:30 P.M.—"Influence of Substrates on Thin Magnetic Films Electrodeposited in a Magnetic Field" by M. Lauriente and F. X. McNally (Abstract No. 108)
3:00 P.M.—"Electrodeposition of Cobalt-Molybdenum Alloys" by Albertine Krohn and T. M. Brown (Abstract No. 109)
3:30 P.M.—"Composition and Thickness Effects on Magnetic Properties of Electrodeposited Thin Nickel-Iron Films" by Irving Wolf (Abstract No. 110)
4:00 P.M.—"Effect of Plating Parameters on the Structure and Magnetic Properties of Co and Co-Ni Alloys" by I. M. Croll and H. F. Quinn (Abstract No. 111)
4:30 P.M.—"Electrodeposition of Nickel-Cobalt Alloys from the Pyrophosphate Bath" by Vasanta Sree and T. L. Rama Char (Abstract No. 112)

ELECTRONICS—SEMICONDUCTORS (Cont'd)

Surfaces (Cont'd), with P. H. Keck presiding

(EMERALD ROOM, Shamrock Hilton, off main Lobby)

2:00 P.M.—"Characteristics of the {111} Surfaces of the III-V Intermetallic Compounds, II. Effect of Surface Active Agents" by M. C. Lavine, M. C. Finn, and H. C. Gatos (Abstract No. 163)
2:20 P.M.—"High-Temperature Oxidation Studies on the (111) and the (111) Surfaces of InSb and GaAs" by T. R. Perry, J. G. Harper, and D. P. Miller (Abstract No. 164)
2:40 P.M.—"Properties and Reactions of Stain Films on Silicon" by Allen Gee (Abstract No. 165)
2:55 P.M.—"The Study of Surface Contamination of Semiconductors by Radiochemical Techniques" by G. B. Larrabee (Abstract No. 166)
3:15 P.M.—"Encapsulation of Silicon Diodes in Low Melting Glass, I. Materials and Processes" by I. L. Kalnin and A. P. Pisarchik (Abstract No. 167)
3:40 P.M.—"Encapsulation of Silicon Diodes in Low Melting Glasses, II. Electrical Characteristics" by W. F. J.

Hare (Abstract No. 168)
4:05 P.M.—Recent News Papers. Titles and Short Abstracts will be available at the Registration Desk.

THURSDAY A.M., Oct. 13, 1960

CORROSION (Cont'd)

Dissolution of Metals and Semiconductors, with C. V. King presiding

(CONTINENTAL ROOM, Shamrock Hilton, off Main Lobby)

9:00 A.M.—"Factors Influencing the Rates of Surface Processes" by A. C. Riddiford (Abstract No. 76)
9:50 A.M.—"Dissolution of Copper in Sulfuric Acid Solutions" by D. P. Gregory and A. C. Riddiford (Abstract No. 77)
10:20 A.M.—Ten-minute intermission
10:30 A.M.—"Kinetics of the Reaction between Copper and Aqueous Ammonia" by J. S. Stanley and J. A. Radley (Abstract No. 78)
11:00 A.M.—"Dissolution of Copper in Ferric Chloride Solutions" by H. M. Ferrari and M. J. Sinnott (Abstract No. 79)
11:30 A.M.—"Characteristics of the {111} Surfaces of the III-V Intermetallic Compounds, III. Effect of Cold Work on Dissolution" by H. C. Gatos and M. C. Lavine (Abstract No. 80)

THURSDAY P.M., Oct. 13, 1960

CORROSION (Cont'd)

Dissolution of Metals and Semiconductors (Cont'd), with C. V. King presiding

(CONTINENTAL ROOM, Shamrock Hilton, off Main Lobby)

2:00 P.M.—"A Simple Method for Monitoring the Chemical Etching Rate of Germanium and Silicon" by D. R. Turner (Abstract No. 81)
2:30 P.M.—"Chemical Etching of Germanium, I. Comparison of the Etching of Germanium and Silicon in Solutions of HF-HNO_3" by B. Schwartz and H. Robbins (Abstract No. 82)
3:00 P.M.—"Chemical Etching of Germanium, II. The System HF, H_2O_2, H_2O" by H. Robbins and B. Schwartz (Abstract No. 83)
3:30 P.M.—"Steady-State Liquid-Solid Interface Reactions as Applied to Silicon Etching by HNO_3-HF-H_2O" by J. J. Grossman (Abstract No. 84)
4:00 P.M.—"Magnitude of IR-drop Corrections in Electrode Polarization Measurements Made with a Luggin-Haber Capillary" by Sidney Barnartt (Abstract No. 85)

ELECTRODEPOSITION (Cont'd)

General Session, with D. Trivich presiding

(GRECIAN ROOM, Shamrock Hilton, take right Promenade, then turn left)

9:00 A.M.—"Electrical Behavior of Passive Iron" by J. L. Ord and J. H. Bartlett (Abstract No. 113)
9:30 A.M.—"Anodic Properties of Nickel under Nonpassivating Conditions" by Marvin Kronenberg, Ernest Yeager, and Frank Hovorka (Abstract No. 114)
10:00 A.M.—"Effect of Cathode Vibration on Overpotential of Lead in $NaHPbO_2$ and in Alkaline Lead Tartrate Solutions" by J. L. Griffin and L. O. Case (Abstract No. 115)
10:30 A.M.—"Some Observations of Copper Deposits on Single Crystals of Copper" by I. B. Giron and Fielding Ogburn (Abstract No. 116)
11:00 A.M.—"Electroplating of Silver onto Aluminum" by V. A. Nelson (Abstract No. 117)
11:30 A.M.—"Porosity Measurements on Gold-Plated Copper" by M. S. Frant (Abstract No. 118)

Abstracts

BATTERY

Abstract No. 1

Ambient Temperature Fuel Cells

H. F. Hunger, U.S. Army Signal Research and Development Lab., Ft. Monmouth, N. J.

Fuel cells operating on hydrogen or partially oxygenated organic compounds at room temperature and close to atmospheric pressure, utilizing alkaline electrolytes in the form of aqueous solutions or anion exchange membranes, and reaction mechanisms are discussed. The methods to achieve good electrode performance by proper selection of electrode carriers and preparation of catalysts are shown. Advantages and disadvantages observed with ion exchange membrane electrolytes are described. Special emphasis is given to cells operating on liquid fuels.

Abstract No. 2

Electrode Kinetics of Various Redox Couples for Fuel Cell Use

A. P. Bond and **D. Singman,** Diamond Ordnance Fuze Labs., Ordnance Corps, Washington 25, D. C.

Electrode kinetics of several oxidation-reduction couples of possible use in a redox fuel cell were investigated by means of polarization measurements at platinum, carbon, titanium, and tantalum electrodes. The Ti^{+++}-TiO^{++} and Br_2-Br^- couples appear most suitable from the electrochemical standpoint for use at the anode and cathode, respectively, of a redox fuel cell.

Abstract No. 3

Investigation of the Electrochemical Characteristics of Organic Compounds, VIII. Hydrazine and Hydroxylamine Compounds

R. Glicksman, Semiconductor and Materials Div., Radio Corp. of America, Somerville, N. J.

The electrochemical characteristics of various organic hydrazine and hydroxylamine derivatives are presented, and their use as anode materials in galvanic cells is considered. The anode potential of these compounds is dependent on the type and position of substituent groups in the molecule as well as the pH of the electrolyte. The effect of the first two factors on the anode potential is interpreted in terms of the electron density distribution in the molecule.

Abstract No. 4

Factors Affecting the Discharge Characteristics of Thermal Cells

C. W. Jennings, Sandia Corp., Sandia Base, Albuquerque, N. Mex.

Mechanisms contributing to the voltage decrease under load of thermal cell systems of the type Ca/LiCl, KCl/$CaCrO_4$/Ni at 425°-550°C are discussed. An explanation is given for the variation in cell life to a given cut off voltage with amount and composition of electrolyte.

Abstract No. 5

Recent Studies on Ammonia Battery Systems

Otto Adlhart and **H. R. Knapp,** U.S. Army Signal Research and Development Lab., Ft. Monmouth, N. J.

Electrochemical studies on ammonia battery systems are described. Properties of several ammonia electrolytes are characterized and compared to aqueous and other nonaqueous electrolytes. Polarization curves for several metallic anodes in suitable electrolytes are presented. Construction details for high and low rate structures are presented, and typical cell discharge data are discussed.

Abstract No. 6

The Photogalvanic Effect in Inorganic Oxidation-Reduction Systems, I. The Iodine-Iodide System

H. N. Seiger (present address: R&D Lab., Alkaline Battery Div., Gulton Industries, Inc., Metuchen, N. J.) and **R. A. Marcus,** Polytechnic Institute of Brooklyn, 333 Jay St., Brooklyn 1, N. Y.

The photopotential of an iodide-iodine-platinum electrode half-cell was investigated in the linear current-potential region for various intensities, concentrations, wave lengths, and window-electrode distances. The effect was proportional to light intensity at low intensities and roughly paralleled the absorption spectrum of the electrolyte. The slopes of the i-E plots were substantially increased by illumination. These and other facts are explained here in terms of an enhanced convection. The sign of the small photopotential at $i = 0$ is consistent with the observed temperature increase which accompanied the irradiation.

Abstract No. 7

Investigation of the Electrochemical Characteristics of Organic Compounds, VII. Organic Positive Iodine and Aliphatic Azo Compounds

R. Glicksman and **C. K. Morehouse,** Semiconductor and Materials Div., Radio Corp. of America, Somerville, N. J.

The electrochemical characteristics of organic positive iodine compounds such as iodosobenzene and iodoxybenzene, and aliphatic azo compounds such as azodicarbonamide and N,N'-dichloro-azodicarbonamidine in various electrolytes are presented. Perform-

ance characteristics of magnesium and aluminum dry cells containing these organic oxidizing agents as cathode materials are also presented.

Abstract No. 8

Stability and Solubility of Silver Oxide Electrodes in Alkaline Electrolytes

R. F. Amlie and **Paul Ruetschi,** Carl F. Norberg Research Center, Electric Storage Battery Co., Yardley, Pa.

The decomposition reaction $2AgO \rightarrow Ag_2O + \frac{1}{2} O_2$ in alkaline electrolytes was investigated using a microvolumetric technique. The decomposition rate increases with increasing hydroxyl ion concentration. The solubilities of Ag_2O and AgO in alkaline electrolyte were studied with a polarographic technique using a rotating platinum microelectrode. Evidence is presented that AgO does not produce soluble divalent silver species in contact with alkaline electrolytes. However, AgO slowly self-discharges or decomposes to Ag_2O, and it is the latter which is slightly soluble.

Abstract No. 9

The Magnesium-m-Dinitrobenzene Cell

G. S. Lozier, R. Glicksman, and **J. B. Eisen,** Semiconductor and Materials Div., Radio Corp. of America, Somerville, N. J.

m-Dinitrobenzene was selected from the many possible organic materials for a detailed study as the cathode in magnesium primary cells because of its availability and favorable electrochemical properties. An analysis of the cell reaction has shown that for optimum cell performance a carbon with a very high water retention which maintains a high electrical conductivity is required. The impedance and delayed action characteristics of Mg-m-dinitrobenzene cells are due primarily to the magnesium anode and are similar to comparable size Mg-MnO_2 cells. The magnesium-m-dinitrobenzene cell has a capacity over 90 whr/lb at practical discharge rates.

Abstract No. 10

The Influence of the Active Surface on the Cathodic Reduction of MnO_2

N. C. Cahoon, Battery Development Lab., Union Carbide Consumer Products Co., Cleveland, Ohio, and **M. P. Korver,** Research Lab., Union Carbide Consumer Products Co., Parma, Ohio

The surface area of samples of manganese dioxide is shown to be an important factor in influencing its behavior. Four samples of MnO_2 of widely different origins— electrolytic, activated, natural ore, and synthetic pyrolusite—are used as examples. The rates of the recuperation reaction at temperatures of 21°-50°C are shown to be related to the total surface area of the oxides by a complex relation, dependent on the temperature and other factors. The product of the reaction MnOOH develops on the surface and in the pores of the original MnO_2 particle, thus increasing the diameter and resulting in reduced pore volume, respectively. The MnOOH made under these conditions from all four starting materials appears as rod-shaped units in electron micrographs.

Abstract No. 11

Impedance of Dry Cells and Batteries

R. J. Brodd, National Bureau of Standards, Washington, D. C.

The impedance of Lechanché, mercury, alkaline MnO_2, nickel cadmium, and lead acid cells was measured between 50 cps and 50 kps. The impedance of several Leclanché batteries was also measured between 50 cps and 50 kps. Results are interpreted based on the assumption that the electrode reactions are relaxation processes.

Abstract No. 12

Recharging of Leclanché Dry Cells

W. S. Herbert, Research Center, Electric Storage Battery Co., Yardley, Pa.

The recharging of Leclanché dry cells was studied from the standpoint of the reactions occurring in the cell during both the discharge and charging operations. It was found that constant potential charging in the range of 1.7-2.1 v was most satisfactory. Constant current charging can result in damage to the cells and is to be avoided especially for cells arranged in series. Suitable constant potential charging circuits were developed. Recharging can extend the useful life of dry cells if the conditions are selected carefully.

Abstract No. 13

Is the Lead-Acid Battery Obsolete?

Paul Ruetschi, Carl F. Norberg Research Center, Electric Storage Battery Co., Yardley, Pa.

A brief history of the lead-acid battery from its invention by Planté in 1860 to the present time, including a discussion of major advances in technology, is outlined. Today U.S. production figures for different battery systems are given, and the various systems are compared with regard to availability of raw materials, economy, and specific application. The possible replacement of lead-acid batteries by new portable power sources such as fuel cells, thermoelectric generators, and solar cells is discussed, and the conclusion is drawn that the lead-acid battery will be used for years to come wherever cheap packaged power is required.

Abstract No. 14

How Lead Becomes a Battery

R. Jardine and **S. K. Lessey,** Electric Storage Battery Co., Rising Sun and Adams Ave., Philadelphia 20, Pa.

The paper presents the basic principles of the conversion of lead into Planté storage battery plates. The fact that many methods have been used is stated, and a few commercially used methods are described. The large variety of plate types that have been used is mentioned, and the ones now manufactured are discussed. Commercial battery types and their service abilities and records are illustrated by the use of slides.

Abstract No. 15

The Anodic Oxidation Rate of Pure Lead in Sulfuric Acid

R. A. Baker, Bell Telephone Lab., Inc., Murray Hill, N. J.

The oxidation rate of lead in sulfuric acid solution at polarizations above the $PbO_2/PbSO_4$ potential has been measured at 15°, 30°, and 45°C by a new, nondestructive technique. The rate, at constant temperature, depends exponentially on the polarization. Following an initial transient, the rate at constant temperature and polarization is constant with time. The corrosion product consists of both α- and β-PbO_2 and the attack on the lead is uniform.

Abstract No. 16

Planté, Pourbaix, and Passivation

Jeanne Burbank, U.S. Naval Research Lab., Washington 25, D. C.

Planté plate formation is discussed from the viewpoint of corrosion vs. passivation. The experimental observations of passivation phenomena of pure lead metal under anodic polarization in acid solutions are summarized. The Planté formation techniques are related to these studies and the practical application of the Pourbaix electrochemical phase diagrams to Planté formation is outlined.

Abstract No. 17

Mechanisms of the Electrode Reactions in Lead Accumulators

W. F. K. Wynne-Jones, Chemistry Bldg., King's College, University of Durham, Newcastle-upon-Tyne, England

The over-all reaction of the lead accumulator is given uniquely by the equation: $Pb + PbO_2 + 2H_2SO_4 = 2PbSO_4 + 2H_2O$. Intermediate nonequilibrium, nonelectrochemical steps cannot participate in the electrode re-

actions which are therefore restricted to: formation of $PbSO_4$ on Pb, oxidation of $PbSO_4$ to PbO_2, reduction of $PbSO_4$ to Pb, reduction of PbO_2 to $PbSO_4$, evolution of O_2 on PbO_2, and the evolution of H_2 on Pb. Constant current and constant potential methods have yielded important information on the detailed mechanisms. The exchange between plumbous ions in solution and plumbic ions in the solid phase has shown the importance of diffusion in the solid phase. The rate of exchange is controlled by conditions of preparation, and the more reactive α-PbO_2 is found to exchange more rapidly than the normal β-PbO_2.

Abstract No. 18

(There is no Abstract No. 18)

Abstract No. 19

Formation Studies of Lead-Acid Battery Plates Using the Electron Microscope

J. E. Buskirk, P. D. Boyd, and **V. V. Smith,** Delco-Remy Div., General Motors Corp., Muncie, Ind.

Micrographs to be shown include lead oxide and the surfaces of cured plates, plates soaked in sulfuric acid solutions, and plates formed at two different rates. The electron microscope has promise of becoming a useful tool for battery research.

Abstract No. 20

Electrode Potentials and Thermal Decomposition of α- and β-PbO_2

R. T. Angstadt and **Paul Ruetschi,** Carl F. Norberg Research Center, Electric Storage Battery Co., Yardley, Pa.

Samples of α- and β-PbO_2 were subjected to thermal decomposition in the temperature range from 100° to 580°C. The two modifications of PbO_2 have different thermal stability and decompose into different intermediate materials. The crystal structures of the intermediate products have been studied. Electrode potentials of α- and β-PbO_2 were measured in sulfuric acid and perchloric acid solutions. At pH values below 3 the potentials in solution containing $SO_4^{=}$ ion correspond to the equation

$$PbO_2 + H_2SO_4 + 2H^+ + 2e \rightarrow PbSO_4 + 2H_2O$$

However, at higher pH values the experimental values differ greatly from the ones derived theoretically.

Abstract No. 21

Some Important Factors That Influence the Composition of Positive Plate Material

V. H. Dodson, Electric Autolite Co., Toledo, Ohio

The composition of positive plate material formed (*a*) from positive pastes of various densities, (*b*) in aqueous sulfuric acid solutions of various specific gravities, (*c*) at various rates (current densities), and (*d*) at various temperatures has been studied. Variations in these conditions not only influence the total PbO_2 content of the formed material but also the ratio of α-PbO_2 to β-PbO_2 in the formed material.

Abstract No. 22

Composition and Performance of Positive Plate Material

V. H. Dodson, Electric Autolite Co., Toledo, Ohio

The change in the composition of the positive material during (*a*) initial 20-hr discharge test, (*b*) successive 20-hr tests, (*c*) high rate discharge at 80° and 0°F, and (*d*) stand at room temperature has been studied. The performance of the positive plate under the conditions of these tests can be related to the total PbO_2 and α-PbO_2 content of the positive material.

Abstract No. 23

The Next Hundred Years

E. Willihnganz, C&D Div., Electric Autolite Co., Conshohocken, Pa.

The next hundred years of the storage battery can be predicted only in a general way. A review of the course of development of other inventions compared with a history of the storage battery up to the present indicates what is liable to occur. A review of the field of electrochemical power sources tells in which direction progress might be made. This also helps predict what the future may hold and is valid if nothing unforeseen develops.

Abstract No. 24

Ionic Conductivity of Silver Iodide Pellets for Solid Electrolyte Batteries

L. N. Mrgudich (present address: U.S. Army Signal R&D Lab., Ft. Monmouth, N. J.), Lab. for Insulation Research, Massachusetts Institute of Technology, Cambridge, Mass.

Silver amalgam electrodes were found to provide polarization-free contacts for the measurement of the ionic conductivity of compressed AgI powder pellets. Correlation of the conductivity data with x-ray diffraction studies established the presence of a deformed hexagonal phase as an important factor in determining pellet conductivity. Deformation can be induced by compression, but care must be taken to avoid transformation into the face-centered cubic phase with some resultant decrease in conductivity. Preliminary evidence is presented that hexagonal deformation can be induced by proper control of preparation or by suitable thermal or mechanical pretreatment of the AgI powder.

Abstract No. 25

The Ag/AgCl/ICl Solid Electrolyte Cell System

D. M. Smyth and **C. H. Tompkins,** Sprague Electric Co., North Adams, Mass.

Solid electrolyte batteries based on the Ag/AgCl/ICl system can sustain higher current drains and have improved high-temperature stability compared with batteries based on the Ag/AgCl/Cl_2 system previously described. In these systems the iodine monochloride and chlorine cathode vapors are furnished by the dissociation of $KICl_2$ and $KICl_4$, respectively. High-temperature aging of the ICl system eventually results in a stable voltage plateau indicative of an iodine vapor cathode.

Abstract No. 26

An Analytical Representation of the Characteristics of Commercial Secondary Batteries

S. M. Selis and **C. R. Russell,** Research Labs., General Motors Corp., Warren, Mich.

In 1897 Peukert presented an analytical function which related the constant discharge current of lead-acid batteries to the time actually required for this discharge. It has been found that this function will describe the discharge of modern commercial lead-acid batteries as well as batteries with alkaline electrolytes. In addition, an algebraic relationship is presented which describes battery capacity as a function of the constant discharge current (or discharge time). Modifications to include a term for ambient temperature are also considered.

Abstract No. 27

Float Characteristics of the Lead-Calcium Cell

Jeanne Burbank and **C. P. Wales,** U.S. Naval Research Lab., Washington 25, D. C.

An analysis of the factors determining successful float of lead-calcium cells is presented. True float op-

eration is described, and the individual plate behavior is analyzed. Polarization curves of the individual plates at various states of charge have been determined. It has been observed that a successfully floating cell has a characteristic excess of positive plate capacity, that the positive "floats" on the overvoltage curve of its charging reaction, and the negative floats on its hydrogen overvoltage curve. The developed plate areas must be such that these requirements are met simultaneously by the plates of a given cell if it is to perform satisfactorily in float service.

Abstract No. 28

The Silver-Silver Oxide Electrode, I. Anodic Oxidation in Alkaline Solutions

C. P. Wales, U.S. Naval Research Lab., Washington 25, D. C.

Silver electrodes were oxidized anodically in KOH at various charging currents. The electrodes were given both partial and complete charges. Oxidation was highly efficient. Discharge of partially charged electrodes often showed a potential plateau intermediate between the AgO/Ag_2O and Ag_2O/Ag plateaus. The quantity of charge accepted at each potential level was examined, as well as the form of the potential curves. The oxidation and reduction of the electrode is discussed.

Abstract No. 29

Electrode Phenomena of the Silver-Silver Oxide System in the Alkaline Battery

Shiro Yoshizawa and **Zenichiro Takehara,** Dept. of Industrial Chemistry, Faculty of Engineering, Kyoto University, Kyoto, Japan

Electrode phenomena of the silver-silver oxide system in an alkaline battery and effects of small quantities of various cations when added to the silver electrode were examined by means of the electron-microscope, x-ray diffraction, oscilloscopic determination of the decay and growth of overpotential, and current potential relationships. Results show that, in the case of the charge, Ag_2O and then AgO form, and the underlying Ag crystals expand owing to diffusion of oxygen anion; on discharge, the reverse reaction may occur.

Abstract No. 30

High Energy: Weight Ratio, Nickel Cadmium Cells

J. C. Duddy and **A. J. Salkind,** Carl F. Norberg Research Center, Electric Storage Battery Co., Yardley, Pa.

Conventional nickel cadmium cells contain the active materials in either porous sintered nickel plaques or in nickel or nickel-plated steel pockets or tubes. A new process, adaptable to continuous methods of production, has been developed in which the active and conductive materials are dispersed in a microporous plastic structure. Cells with the high energy to weight ratio of 40 whr/kg have been constructed. Cell volumes are equal to those of the sintered plate design for equivalent capacities.

Abstract No. 31

Formation of Porous Metal Plates by Electrolytic Reduction under Controlled Pressures

C. M. Shepherd and **H. C. Langelan,** U.S. Naval Research Lab., Washington 25, D. C.

Metal plates having porosities from 40 to 90% were produced by the reduction of pasted metal compounds in an electrolytic cell. The porosity was a function of the physical pressure applied to the plate assembly during reduction. Successful formation depended on effective pasting and the proper selection of compound and electrolyte. Nearly all metals that electroplate at high efficiencies can be formed in this manner. The relationships between particle size, water content, tap density, and pasting conditions have been studied.

Abstract No. 32

The Forming Process in Nickel Positive Electrodes

Donald Tuomi, Thomas A. Edison Research Lab. Div., McGraw-Edison Co., West Orange, N. J.

The formation of nickel positive electrodes has been studied by a combination of x-ray diffraction and microscopy techniques. The distinct chemical phases encountered are described. The complexity of the process is illustrated.

Abstract No. 33

Electrochemical Behavior of the Semi-charged Nickel Oxide Electrode

B. E. Conway and **P. L. Bourgault,** Dept. of Chemistry, University of Ottawa, Ottawa, Ont., Canada

The kinetic behavior of semi-charged "$NiO_{1.5}$" electrodes has been studied by emf decay measurements which enable a mechanism of charging and oxygen evolution to be formulated. Optimum charging is shown to occur at high rates on the $NiO_{1.5}$ electrode, oxygen evolution being preferred at low potentials. Reversible and mixed potentials of the nickel oxide electrode are distinguished, and it is shown that previous data refer to mixed potentials. A kinetic analysis enables the true reversible potentials to be evaluated.

CORROSION

Abstract No. 34

A Hypothesis for the Uncoupling Shift Observed in the Iron-Tin System in Citric Acid

W. R. Buck, III, A. N. J. Heyn, and **Henry Leidheiser, Jr.,** Virginia Institute for Scientific Research, Richmond, Va.

When electrical contact is broken between electrodes of iron and tin in citric acid containing dissolved tin, the potential of the iron moves in the noble direction for a short time and then in the active direction for a long time. This phenomenon, first observed by Koehler, is given the name "uncoupling shift." It has been studied with pure iron in boiling 0.2M citric acid. Potential measurements, chemical studies, and electron microscope and electron diffraction observations relating to the effect have been made.

Abstract No. 35

Effect of Tin Ion Complexing Substances on the Relative Potentials of Tin and Steel in Oxygen Free Acid Media

A. R. Willey, Research and Technical Dept., American Can Co., Barrington, Ill.

Half-cell potentials of tin and steel have been measured in a variety of organic and inorganic acids in the absence of oxygen. Tin ion was varied from 0 to 1M and pH from zero to about 6.0. Similar measurements were made in a number of fruit juices. Only in the presence of a strong complexing substance is tin anodic or protective to steel. The data are helpful in studying corrosion problems connected with the tin-plate container.

Abstract No. 36

Oxide Films on Tin Plate

M. Falkenhagen and **J. D. Bode,** Graham Research Lab., Jones & Laughlin Steel Corp., Pittsburgh 30, Pa.

The nature of oxide films on tin plate is revealed by electron micrographic, x-ray and electron diffraction, and spectrographic investigations. Details of the film stripping technique and microscopic examination are described. These studies indicate changes in film characteristics with time, including auxiliary and overgrowths, and different shadowing techniques reveal the microstructure.

Abstract No. 37

Some Factors Affecting the Surface Chromium Content of Electrochemically Treated Tin Plate

P. R. Carter, U.S. Steel Corp., Monroeville, Pa.

The relation among current density, total coulombs, solution temperature and pH, and chromium content of the treatment film for the cathodic and the cathodic-anodic dichromate electrochemical treatments is dis-

cussed as well as the relation between film stability and the chromium content. The previous theory of what occurs during cathodic treatment in sodium dichromate solutions is modified to conform to the new data.

Abstract No. 38

Use of Polarization Methods in the Determination of the Rate of Corrosion of 3003 Aluminum in Anaerobic Acid Media

S. Evans and **E. L. Koehler**, Central Research and Engineering Div., Continental Can Co., Chicago, Ill.

The variation of the corrosion potential of aluminum with pH in citrate buffer solutions in the pH range 2.5-6.4 was found to be analogous to that for hydrogen electrode. The rate of corrosion over this pH interval was practically constant. It was found that the overvoltage-intercept method could be used to determine accurately the rate of corrosion of the aluminum from cathodic polarization data in the citrate buffer solutions and in a variety of other acid media. The polarization resistance method was equally applicable when using an experimentally determined value for the cathodic Tafel-slope and assuming an identical anodic Tafel-slope.

Abstract No. 39

Use of Polarization Methods in the Determination of the Rate of Corrosion of Aluminum Alloys in Anaerobic Food Media

E. L. Koehler and **S. Evans**, Central Research and Engineering Div., Continental Can Co., Chicago, Ill.

The corrosion rate of aluminum in food media is generally too low to be determined accurately by methods such as measurement of weight loss and hydrogen evolution rates. The use of polarization methods has been investigated and has been found to be particularly valuable. In media of very low corrosiveness, Tafel-type anodic curves are obtained which can be used successfully both to determine corrosion rates by the overvoltage-intercept method and to give a slope which is useful in the polarization resistance method. Where an anodic Tafel-type curve cannot be determined experimentally a calculated anodic curve can be used successfully. In all cases investigated, the slope was found to have a numerical value approximately equal to that for the cathodic curve.

Abstract No. 40

The Oxidation of Tin, II. Morphology and Mode of Growth of Oxide Films on Pure Tin

W. E. Boggs, P. S. Trozzo, and **G. E. Pellissier**, Applied Research Lab., U.S. Steel Corp., Monroeville, Pa.

The oxide films formed during a study of tin oxidation kinetics were examined with an electron microscope. The oxide nucleates at numerous sites on the tin surface and grows laterally. The morphology and mode of growth of the oxide crystallites are dependent upon the oxygen pressure. During the growth of oxide platelets, cavities are observed developing at the oxide-metal interface. These cavities eventually reduce the area of contact between oxide and metal by as much as one-third.

Abstract No. 41

The Oxidation of Tin, I. Kinetics of Oxidation of Pure Tin and the Effects of Temperature and Oxygen Pressure

W. E. Boggs, R. H. Kachik, and **G. E. Pellissier**, Applied Research Lab., U.S. Steel Corp., Monroeville, Pa.

The rates of oxidation of pure tin foil have been determined over a range of temperatures and oxygen pressures. At pressures over 1 mm, the oxidation proceeds in three stages: at first, the rate is low, but increases rapidly to a maximum; then it begins to decrease, following a direct logarithmic rate law; and finally, it becomes erratic, either increasing or leveling off. At pressures under 1 mm, the oxidation rate appears to be controlled initially by the dissociation of oxygen at the metal surface.

Abstract No. 42

The Oxidation of Tin, III. Mechanisms of Oxidation of Pure Tin

W. E. Boggs, Applied Research Lab., U.S. Steel Corp., Monroeville, Pa.

During the growth of tin oxide at oxygen pressures over 1 mm, the initial, increasing rate of oxidation is a result of the nucleation and lateral growth of oxide platelets. The subsequent logarithmic rate is believed to be caused by the growth of cavities at the oxide metal interface. The eventual erratic and nonreproducible behavior may be caused by the occasional collapse of the oxide skin over the cavities.

Abstract No. 43

Microtopography of Oxide Films Formed on Tantalum

R. E. Pawel, J. V. Cathcart, and **J. J. Campbell**, Metallurgy Div., Oak Ridge National Lab., Oak Ridge, Tenn.

Optical and electron microscopy were used to characterize the surface of tantalum specimens oxidized at temperatures ranging from 300° to 700°C. Oxide platelets grow during initial oxidation and not during cooling from the reaction temperature. At higher temperatures, both platelets and nodules serve as preferred sites for blister and crack formation in the oxide and thus play an important role in the transition from the protective to the nonprotective stage of oxidation of tantalum.

Abstract No. 44

Interaction between Copper and Gas Discharge Products Condensed at Very Low Temperatures

Jerome Kruger and **W. J. Ambs**, National Bureau of Standards, Washington 25, D. C.

The reaction between oxygen and oxygen-nitrogen mixtures passed through a 2450 mc electrodeless discharge and copper was studied with the ellipsometer. The free radicals or other active species produced by the discharge were trapped out on the copper surface at 4.2°K and allowed to react upon warming. Reaction at 77° and 300°K was also studied. The influence of the addition of varying amounts of nitrogen, condensation temperature, and crystallographic orientation of the copper surface was studied.

Abstract No. 45

Copper Oxides on the Surface of Gold Plate

M. S. Frant and **R. Rajaraman**, Research Division, AMP Inc., Harrisburg, Pa.

Significant quantities of copper oxides were found on the surface of electroplated gold specimens after relatively short heating times at temperatures as low as 125°. Both cuprous and cupric oxides were measured using coulometric reduction techniques. Data are given on the effect of gold thickness, temperature, and type of deposit. The results are shown to be consistent with a mechanism involving diffusion of the copper to the surface, followed by oxidation.

Abstract No. 46

Oxidation of Copper between 250° and 450°C and the Growth of CuO "Whiskers"

E. A. Gulbransen, T. P. Copan, and **K. F. Andrew**, Research Labs., Westinghouse Electric Corp., Pittsburgh 35, Pa.

The results suggest that the oxidation of copper follows the cubic rate law between 250° and 450°C. Small embryonic whiskers of CuO were formed at 250°C after 6 hr of reaction. At 450°C, after 6 hr of reaction, a surface density of $10^6/cm^2$ of long, thin oxide whiskers was found. Calculations show that less than 1% of the oxygen reacted at 450°C resulted in the growth of oxide whiskers. It was concluded that the formation of oxide whiskers had no appreciable effect on the over-all kinetics of the oxidation of copper.

Abstract No. 47

Corrosion Rate of Fe in High-Temperature H_2O by an Electrical Resistance Method

A. J. Panson, Research Labs., Westinghouse Electric Corp., Pittsburgh 35, Pa.

The kinetics of the reaction between pure iron and water has been studied at temperatures up to 365°C. The reaction was followed by determining the increase in electrical resistance with time of corroding samples. The resistance measurements were made while the samples were being reacted in a gold-plated autoclave. A sensitivity of about 70Å of film was achieved. Two hundred-hour experiments at 365°C resulted in reaction of 4000 to 7000Å of metal. The data fit the logarithmic rate law over the entire period at temperature.

Abstract No. 47A

Unusual Oxidation States Encountered in Corrosion Processes

E. C. Pitzer, Knolls Atomic Power Lab., General Electric Co., Schenectady, N. Y.

The industrially important metals are closely grouped near the center of a modified Meggers periodic table. Most of these metals are of variable valence. The end products of corrosion of most metals have been well characterized, but more information is needed on intermediate stages of oxidation. Examples of unusual oxidation states resulting from impressed voltages high enough to overcome the passive films on certain metals are discussed.

Abstract No. 48

Evidence for One-Electron Oxidation as Primary Electrode Reaction in Anodic Dissolution of Bivalent Metals

A. W. Davidson, University of Kansas, Lawrence, Kans.

The amount of metal that dissolves electrolytically from an anode of beryllium, magnesium, zinc, or cadmium in an aqueous electrolyte is usually considerably in excess of that predicted on the basis of Faraday's law. Whenever this is the case, a product of reduction can be found in the anolyte after electrolysis. These facts may be most readily explained in terms of the hypothesis that the primary anode reaction is oxidation of the metal to a unipositive ion with strong reducing properties.

Abstract No. 49

The Relative Stabilities of Oxidation States of Transitional Metals

G. W. Watt, Dept. of Chemistry, University of Texas, Austin, Texas

The stabilities of ionic species that participate in electrochemical and related processes are dependent on several characteristics including (*a*) properties of a specific metal ion, (*b*) nature of the bonded ligands, and (*c*) character of the metal-ligand bonds. The conditions under which one may produce, characterize, and stabilize oxidation states that are unusual in the sense that they are either higher or lower than those normally encountered are discussed. The character of the metal-ligand bond is believed to control the mechanism of electrode reactions of metal ions.

Abstract No. 50

Valency of Ions Formed during Anodic Dissolution of Metals in Acids

M. E. Straumanis, Dept. of Metallurgical Engineering, University of Missouri, School of Mines and Metallurgy, Rolla, Mo.

The apparent valence of ions of active metals, going into solution anodically (in an acid as electrolyte) can be determined from the Faradaic current after the initial, self-dissolution rate has been subtracted from the total rate. However, this apparent valence corresponds to the true valence only in cases when the self-dissolution rate does not change while the anodic current is applied. Usually the rate decreases or increases during the flow of the current (diffusion effect). If this factor is disregarded, ion valencies of lower or higher value than the normal are calculated. Examples involving Zn, Al, Zr, Ti, and TiO_x alloys as dissolving anodes are discussed.

Abstract No. 51

The Difference Effect and Anodic Behavior of Zirconium Dissolving in Hydrofluoric Acid

M. E. Straumanis, W. J. James, and **W. C. Custead,** Depts. of Metallurgical and Chemical Engineering, University of Missouri, School of Mines and Metallurgy, Rolla, Mo.

Zirconium dissolving in hydrofluoric acid exhibited a positive difference effect of such an efficiency that the hydrogen volume developed by the internal polarization current was completely annihilated by the effect. The effect was independent of the concentration of the acid and was accompanied by a strong shift in potential of the Zr electrode toward noble values (passivation). The same occurred in the presence of salts of more noble metals: the rate of dissolution of Zr dropped (nearly to zero with Pt^{++} additions): the black hydride surface film disappeared and the Zr turned bright and shiny (passive Zr). The activity of Zr returned when the anodic current was cut off.

Abstract No. 52

The Difference Effect and the Chunk Effect

G. A. Marsh and **E. Schaschl,** Pure Oil Co. Research Center, Crystal Lake, Ill.

The corrosion rate of a metal such as steel varies as a function of current applied from an external source. An analysis of this corrosion-applied current relationship leads to a new theory on the mechanism of corrosion. By this theory, corrosion proceeds partly by the removal of "chunks" of metal rather than by the removal of one atom at a time. The phenomenon on which the theory is based is called the "chunk effect." In certain acidic solutions the chunk effect accounts for over 50% of the loss of metal. This report also considers the relationship between the chunk effect and the positive and negative difference effects. The positive difference effect is known to be related to anodic polarization of a corroding metal. The negative difference effect, on the other hand, has not previously been adequately explained, and is shown here to be a manifestation of the chunk effect.

Abstract No. 53

(There is no Abstract No. 53.)

Abstract No. 54

Adsorption and Ion Exchange at the Corrosion Interface

G. H. Cartledge, Chemistry Div., Oak Ridge National Lab., Oak Ridge, Tenn.

To introduce the Symposium, consideration is directed to a number of problems connected with the interface between a metal and its environment that have, or may have, relevance to the corrosion process. Among these, adsorption obviously has an important role. It is discussed on the basis of experiments on the influence of adsorbed iodide ions or carbon monoxide on the polarization of iron in acidic solutions in the active region of potentials. Other data to be discussed derive from the cathodic polarization of passive iron in the presence of several inhibitors and in different atmospheres. From these measurements, electrochemical evidence for some new conceptions of the nature of the passive interface was obtained. Finally, it is shown that the passive film may exhibit ion-exchange properties toward certain ions.

Abstract No. 55

Proton Mobility in Liquids and Solids

B. E. Conway, Dept. of Chemistry, University of Ottawa, Ottawa, Ont., Canada

Rates of proton migration in liquids and solids can be determined from conductance and transference ex-

periments. In certain solids, e.g., ice and hydrated nickelic oxide, there is evidence that proton transfer plays an important role in determining the conductivity of the solid. In metallic corrosion under conditions where hydrous oxide surface films are formed, the conductivity of the surface layer can be important in determining the corrosion rate and the onset of passivity. Investigation of the role of proton transfer processes (other than in hydrogen evolution) in electrochemical corrosion is therefore of importance.

Abstract No. 56

The Structure of the Corroding Interface

T. P. Copan, Research Labs., Westinghouse Electric Corp., Pittsburgh 35, Pa.

The structure of the corroding interface can be determined by an electron microscopic study of the crystal habit of the corrosion products formed in vapor phase chemical reactions. Three factors are important in determining the structure of the corroding interface on pure iron, two of which are related to the interface itself: (*a*) nature and activity of the corroding environment, (*b*) nature of the metal structure including impurities, defects, dislocations, precipitates, etc., and (*c*) stress pattern of the metal. Three types of nucleation centers are found in the corroding interface of iron: (*a*) point sources, 150-200Å in diameter of random distribution and a surface density up to $10^9/cm^2$; (*b*) small line sources, 100-200Å wide, up to 15,000Å long and a surface density up to $10^7/cm^2$; and (*c*) large line sources, 100-200Å wide, up to 100,000Å long and an undetermined surface density. The implications of the three types of corroding interfaces are discussed.

Abstract No. 57

Effects of Corrosion Films on Cathodic Processes

R. E. Meyer, Chemistry Div., Oak Ridge National Lab., Oak Ridge, Tenn.

An oxide film on a metal influences reduction processes at the surface in a number of ways which depend on the properties of the film. Three cases may be distinguished according to whether the film has low conductivity, high conductivity, or gross structural defects. Particular attention is paid to the first case, and the influence of film-thickness and inhomogeneities on the steady-state current is included. Expressions for the current as a function of potential and solution activity are given, again with particular attention to films of low conductivity. Transient effects are discussed briefly.

Abstract No. 58

Dissolution of Mild Steel in the System NH_4NO_3-HN_3-H_2O at 30°C

J. D. Goodrich and **Norman Hackerman,** Dept. of Chemistry, University of Texas, Austin 12, Texas

Rates ranged from near zero to almost 30,000 mdd, but the variation did not correlate effectively with metal composition or with grain size. Mechanical stress or quenching from 1000°C increased the rate of those metals corroding slowly, the relationship between stress and rate being discontinuous. Solution composition had a mild effect on the rates. No cracking or pitting was observed. The reduction reaction was in part, if not wholly, nitrate to nitrite. The corrosion product was nonprotective and often nonadherent and appears to be a hydrated or ammoniated iron (II) hydroxide.

Abstract No. 59

Corrosion Inhibition and Electronic Configuration at the Amino Nitrogen Atom

Norman Hackerman, Dept. of Chemistry, University of Texas, Austin 12, Texas, and **R. R. Annand** and **R. M. Hurd,** Texas Research Associates, Austin, Texas

The effect of varying the electron density around the amino nitrogen atom on the efficiency of the amines as inhibitors for mild steel in air-free, acid solutions for a series of *para* substituted *N*-methylanilines is discussed. Estimates of relative electron densities were made from measurements of base strengths and shifts in the absorption spectra. Base strengths and relative strains in a homologous series of polymethylene imines have also been compared to inhibitor efficiencies. Explanation of these effects is given in terms of the type of bond formed between the amino nitrogen and the metal substrate.

Abstract No. 60

Capacitance Studies on Corroding Metal Electrodes

H. M. Joseph and **R. A. Powers,** Research Lab., Union Carbide Consumer Products Co., Parma, Ohio

Behavior associated with the electrical double layer at metal surfaces immersed in concentrated electrolytes has been investigated. Large capacitance values observed are "pseudocapacities" arising from reversible metal-metal ion equilibria rather than true double layer capacities. Certain limited, but apparently real, relationships have been noted between observed "pseudocapacity" and corrosion phenomena under the same conditions. Under ideal conditions, capacitance data may be used to estimate corrosion rates and degree of corrosion inhibition as well as to indicate mechanisms of inhibition. Illustrative data are presented for zinc in NH_4Cl and KOH solutions.

Abstract No. 61

Hydrogen Pickup in Various Zirconium Alloys during Corrosion Exposure in High-Temperature Water and Steam

Stanley Kass, Bettis Atomic Power Div., Westinghouse Electric Corp., Pittsburgh, Pa.

The hydrogen pickup during corrosion in high-temperature water and steam of various binary and ternary alloys of zirconium with iron and tin has been studied. The total hydrogen content of specimens exposed to 750°F steam was found to be greater than that of specimens exposed to 680°F water. Furthermore, the per cent of theoretical hydrogen absorbed in the various alloys was markedly affected by the binary or ternary alloy addition. The per cent theoretical hydrogen absorbed by binary zirconium-iron alloys increased as the iron content was increased from 0.3 to 1.5 w/o and the value for zirconium-tin alloys increased slightly as tin was increased from 0.5 to 0.9 w/o. The hydrogen pickup behavior of ternary zirconium-tin-iron alloys reflected the behavior of zirconium-iron binary alloys.

Abstract No. 62

Kinetics of Sulfidization of Copper by Hydrogen Sulfide

Andrew Dravnieks, R&D Dept., Whiting Research Lab., Standard Oil Co. (Indiana), P. O. Box 431, Whiting, Ind.

The formation of cuprous sulfide scale on copper in hydrogen sulfide at 90°-250°C follows a novel scale-growth law: thin scale grows slowly, but the rate accelerates toward a limiting value as the scale thickens. The kinetics of the sulfidization of wires, Tubandt-Wagner-diffusion experiments, and *in situ* observations on growing scales indicate that the rate is controlled by a slow surface reaction occurring on exposed and inner surfaces of porous scale.

Abstract No. 63

Copper Sulfide Creep on Porous Electroplate

M. S. Frant, Research Div., AMP Inc., Harrisburg, Pa.

Creepage of copper sulfide out from pore sites on tin electroplate on copper has been found in samples returned from field use. Similar creepage has been observed in the laboratory for tin plate on copper and copper-silver alloy, for nickel and for gold on copper, for electroless palladium over nickel and brass, and for lacquered copper specimens. Moisture accelerates the growth of sulfide films in sulfur vapor at 60°.

Abstract No. 64

Anode Polarization Effects

O. L. Riggs, Jr., J. D. Sudbury, and **D. A. Shock,** Continental Oil Co., Ponca City, Okla.

Results were presented of an investigation of the polarization of steel and stainless steel anodes. The

effect of halogen ions and temperature on the energy required to establish, maintain, and remove passivity was shown. Stress-corrosion cracking experiments were conducted to determine the effect of anodic currents on the tendency of stainless steel to crack. Several experiments were carried out to better define the nature of the passive layer. These include measurements of the impedance of the film, electron microscope studies, and a summary of properties usually considered in characterizing semiconductors. Emphasis was made on the relation between impedance of the anode and the throwing power of the electrochemical cell.

Abstract No. 65

Anodic Behavior of Austenitic Stainless Steels and Susceptibility to Stress Corrosion Cracking

S. Barnartt and **D. van Rooyen**, Research Labs, Westinghouse Electric Corp., Pittsburgh 35, Pa.

The corrosion in boiling 42% $MgCl_2$ of a purified 16 Cr-20 Ni stainless steel was compared with that of a commercial 18 Cr-8 Ni alloy. Potential-time curves were compared with those of the pure metals Fe, Cr, and Ni, and the effect of stress and other variables determined. A potentiostatic method was used to follow corrosion currents at elevated potentials and to obtain potential-current curves. Cracking of the 18-8 alloy was greatly accelerated by HCl addition and by a relatively small rise in potential, through elimination of the crack-initiation period. The purified 16-20 steel was unsusceptible to stress corrosion cracking, even under conditions of relatively rapid anodic dissolution. Results were consistent with a purely electrochemical mechanism of crack propagation.

Abstract No. 66

The Volatilization of Chromium Oxide

D. Caplan and **M. Cohen**, Div. of Applied Chemistry, National Research Council, Ottawa, Ont., Canada

The phenomenon of evaporation of chromium oxide from chromium alloys oxidized at high temperatures was investigated by observing the loss in weight when Cr_2O_3 pellets were heated at 1000°-1200°C in various atmospheres. Appreciable volatilization occurred in oxygen, more in wet oxygen, but none in argon or wet argon. Fe_2O_3 specimens showed volatilization in none of these atmospheres. The results indicate that evaporation occurs by oxidation of Cr_2O_3 to gaseous CrO_3.

Abstract No. 67

The Passivity of Austenitic Stainless Steels in Sulfuric Acid

N. D. Greene, Metals Research Labs., Union Carbide Metals Co., Niagara Falls, N. Y. (Present address: Dept. of Metallurgical Engineering, Rensselaer Polytechnic Institute, Troy, N. Y.)

A potentiostatic anodic polarization technique was utilized in an electrochemical study of the passivity of several austenitic stainless steels. The influence of alloy composition, acid concentration, and temperature on active-passive transition characteristics was determined. Eighteen per cent chromium-8% nickel stainless steel exhibited four passive regions in sulfuric acid, and two of these regions were found to be important factors in its corrosion resistance. Active-passive transitions and passive dissolution rates were observed to be markedly time-dependent. The usefulness of potentiostatic polarization techniques as a method for predicting corrosion behavior was demonstrated.

Abstract No. 68

Effect of Oxygen on the Active-Passive Behavior of Stainless Steel

N. D. Greene, Metals Research Lab., Union Carbide Metals Co., Niagara Falls, N. Y. (Present address: Dept. of Metallurgical Engineering, Rensselaer Polytechnic Institute, Troy, N. Y.)

Potentiostatic anodic polarization techniques were used to determine whether dissolved oxygen has any effect on the active-passive behavior of Type 430 stainless steel. Oxygen does not affect the anodic dissolution kinetics of this alloy significantly. This result is contrary to adsorbed oxygen theories of passivity.

Abstract No. 69

Kinetics of Redox Reactions on Passive Electrodes

A. C. Makrides, Metals Research Labs., Union Carbide Metals Co., Niagara Falls, N. Y.

Anodic and cathodic overpotentials for redox reactions on passive electrodes follow Tafel's relation. Exchange current densities are smaller and both Tafel coefficients larger than generally found on active electrodes. A detailed study of redox reactions on a passive iron-chromium alloy is reported, and an attempt is made to account for the Tafel coefficients, kinetic order, temperature dependence, and salt effects observed.

Abstract No. 70

Critical pH and Critical Current Density for Passivity in Metals

H. H. Uhlig, Corrosion Lab., Dept. of Metallurgy, Massachusetts Institute of Technology, Cambridge, Mass.

Equations are derived for the relation of Flade potential to critical pH for passivity, and for critical current density as a function of H^+. For metals passivated by O_2, e.g. Fe, the critical pH is proportional to the negative logarithm of O_2 concentration. For metals passivated by acids, e.g. Mo, Ti, Ta, Zr, the Flade potential must be more active than the hydrogen electrode potential in the same solution, and critical pH is lower the smaller the value of H_2 overvoltage.

Abstract No. 71

Anodic Polarization and Passivity of Ni and Ni-Cu Alloys in Sulfuric Acid

J. Osterwald and **H. H. Uhlig**, Corrosion Lab., Dept. of Metallurgy, Massachusetts Institute of Technology, Cambridge 39, Mass.

Potentiostatic anodic polarization curves were obtained for Ni, Cu, and Ni-Cu alloys in 1*N* H_2SO_4. Critical current density for passivity increases with Cu content as does current required to maintain passivity. Characteristics of passivity in alloys disappear below 30% Ni. The potential of Ni corresponding to critical current density for passivity approximates the most active critical potential in self-activation curves and is linear with pH. The results are related to structure of the passive film and interpreted on thermodynamic grounds.

Abstract No. 72

Corrosion Behavior and Passivity of Nickel-Chromium and Cobalt-Chromium Alloys

A. P. Bond and **H. H. Uhlig**, Corrosion Lab., Dept. of Metallurgy, Massachusetts Institute of Technology, Cambridge 39, Mass.

Pure Ni-Cr alloys containing up to 29% Cr and Co-Cr alloys containing up to 23% Cr were prepared in vacuum. Corrosion rates in sulfuric and nitric acids, corrosion potentials, and critical current densities for passivity were determined at 25°C. The critical minimum Cr content for passivity depended on the environment. It is concluded that specific alloying proportions of passive compositions are better evaluated in relation to electron configuration of the alloy system by critical current densities than by potential or corrosion rate measurements.

Abstract No. 73

Relation of Electron Configuration to Passivity in Cr-Ni-Fe Alloys

H. G. Feller and **H. H. Uhlig**, Corrosion Lab., Dept. of Metallurgy, Massachusetts Institute of Technology, Cambridge 39, Mass.

Critical current densities for passivity, and Flade potentials were measured for ternary Cr-Ni-Fe alloys. Two discontinuities of slope for critical current plotted with % Cr are found for the 50% and 60% Ni alloy

series. These occur close to the ratio 12/88 for Cr to Fe, and 14/86 for Cr to Ni as found in the binary systems. The results are interpreted in terms of separate electron interaction in the ternary system between Cr and Fe distinct from interaction between Cr and Ni.

Abstract No. 74

Formation and Breakdown of Passive Films on Iron Single Crystal Surfaces

Jerome Kruger, National Bureau of Standards, Washington 25, D. C.

The thickness of films found on pure ion surfaces immersed in concentrated HNO_3, chromate and nitrite solutions was studied using the ellipsometer. Potential measurements made at the same time as ellipsometric measurements indicate that a film of 15-30A is responsible for passivity. A logarithmic rate law was found to govern film formation in the passivating solutions. Optical and electron microscopy studies using a decoration technique revealed the influence of crystallographic orientation on film breakdown processes.

Abstract No. 75

Anodic Polarization Behavior of Iron-Nickel Alloys in Sulfuric Acid Solutions

George Economy, (present address: Aluminum Co. of America, New Kensington, Pa.) **Rudolph Speiser, F. H. Beck,** and **M. G. Fontana,** Dept. of Metallurgical Engineering, Ohio State University, Columbus, Ohio

The anodic behavior of twelve annealed iron-nickel alloys in hydrogen saturated H_2SO_4 solutions at 25° ±1°C was investigated by galvanostatic and potentiostatic techniques. The anodic behavior was correlated with the metallurgical structure and electrochemical environment. Particular emphasis was placed on the interpretation of corrosion potential, passivation current, passive current, and the passive-active transition. All the alloys became passive at noble potentials. In general the behavior of the alloys was intermediate to the behavior of iron and nickel.

Abstract No. 76

Factors Influencing the Rates of Surface Processes

A. C. Riddiford, Dept. of Chemistry, University of Southhampton, U. K.

In common with other branches of science, our knowledge of the general field of surface phenomena has developed through the study of at first sight seemingly diverse topics. The fascination and difficulty of such studies stem directly from the number of variables with which workers in any given field may have to contend. In the case of a simple model corrosion system, for example, there are at least ten factors which may influence the observed rate. Nevertheless, progress is now so rapid as to render periodic general surveys of these factors both desirable and practicable.

Abstract No. 77

Dissolution of Copper in Sulfuric Acid Solutions

D. P. Gregory and **A. C. Riddiford,** Dept. of Chemistry, University of Southhampton, U. K.

When copper disks rotate in sulfuric acid solutions, the observed rate of dissolution is first order with respect to the concentration of dichromate ion used as a depolarizer. By studying the effect of temperature and stirring speed at high and low acid concentrations, the process is shown to be completely determined by the rate of transport of dichromate ion to the reacting surface. This has been confirmed by studying the effect of different surface preparations, by measuring the rate of reaction of other metals with these solutions, and by comparing the observed rates with the theoretical values. The effect of blocking off progressively larger areas of the working surface is reported.

Abstract No. 78

Kinetics of the Reaction between Copper and Aqueous Ammonia

J. S. Stanley and **J. A. Radley,** Industrial Research and Development Labs., 220-222 Elgar Rd., Reading, Berks., U. K.

Copper reacts with aqueous ammonia in the presence of oxygen as follows:

$$Cu + \tfrac{1}{2} O_2 + 4NH_3\ (aq) + H_2O \rightarrow Cu(NH_3)_4^{++} + 2\ OH^-$$

The kinetics of this reaction were studied by varying the concentration of ammonia, the partial pressure of oxygen, and the stirring velocity over wide ranges. The rate-determining step is diffusion of one of the reactants to the metal surface, and the course of the reaction depends on the relative concentrations of oxygen, cuprammonium ion, and ammonia in the solution. When cuprammonium ions are reduced by metallic copper, the rate is determined by the transport of the cuprammonium ions to the metal surface.

Abstract No. 79

Dissolution of Copper in Ferric Chloride Solutions

H. M. Ferrari, Metallurgical Advisor, Euratom, Paris, France, and **M. J. Sinnott,** Dept. of Metallurgical Engineering, University of Michigan, Ann Arbor, Mich.

The kinetics of the dissolution of copper in ferric chloride solutions has been studied as a function of the solution and metallic variables. The rate of dissolution of copper single crystals as a function of the ferric chloride concentration; ion contents of chloride, ferric, cupric, ferrous and hydrogen; dissolved oxygen content; and metallic variables of crystallographic orientation and surface finish were studied. Mechanisms which describe the reactions in terms of the kinetic data are presented.

Abstract No. 80

Characteristics of the {111} Surfaces of the III-V Intermetallic Compounds, III. Effect of Cold Work on Dissolution

H. C. Gatos and **M. C. Lavine,** Lincoln Lab., Massachusetts Institute of Technology, Lexington, Mass.

The dissolution rate of the {111} surfaces of the III-V intermetallic compounds increases sharply as a result of surface damage introduced by abrasion. This increase in rate is employed for determining the depth of surface damage. In the present case the observed increase in rate is not due to the higher reactivity of the cold worked surface since the dissolution processes studied are under diffusion control. The experimental results are interpreted on the basis of the surface roughness as affected by the presence of cold work.

Abstract No. 81

A Simple Method for Monitoring the Chemical Etching Rate of Germanium and Silicon

D. R. Turner, Bell Telephone Labs., Inc., Murray Hill, N. J.

The excess holes and electrons produced at the surface of germanium or silicon during chemical etching can be used to monitor the dissolution rate. When an n-type semiconductor electrode is biased anodically or a p-type electrode is made the cathode of an electrolytic cell in the etching solution, the saturation current density is proportional to the rate of etching the semiconductor. The technique also provides a convenient means of determining the fluoride ion concentration in HNO_3-HF mixtures.

Abstract No. 82

Chemical Etching of Germanium, I. Comparison of the Etching of Germanium and Silicon in Solutions of HF-HNO_3

B. Schwartz and **H. Robbins,** Semiconductor Div., Hughes Aircraft Co., P. O. Box 278, Newport Beach, Calif.

The kinetics of the dissolution of germanium and silicon in solutions of nitric acid and hydrofluoric acid is discussed. The etching of germanium is in general more difficult than that of silicon. The etch rates of the latter are reproducible and constant in time, whereas the etch rates of germanium are extremely erratic. In addition, the etch rates of silicon are independent of crystallographic orientation, whereas those of germanium are strongly affected by the crystal orientation over large ranges of composition of etchant. There are also significant differences between the two elements in the temperature dependence of the etch rates.

Abstract No. 83

Chemical Etching of Germanium, II. The System HF, H_2O_2, H_2O

H. Robbins and **B. Schwartz,** Semiconductor Div., Hughes Aircraft Co., P. O. Box 278, Newport Beach, Calif.

The kinetics of the reaction of germanium with solutions of HF and H_2O_2 has been investigated as a function of the composition and temperature of the etchant. The effect of conductivity type and surface orientation on the kinetics has been studied. At low weight ratios of HF to H_2O_2 the etch rates are linearly dependent on the HF concentration, and at high ratios the rates are linearly dependent on the H_2O_2 concentration. The activation energy goes through a maximum at a composition of about 1 H_2O_2 to 1 HF.

Abstract No. 84

Steady-State Liquid-Solid Interface Reactions as Applied to Silicon Etching by HNO_2-HF-H_2O

J. J. Grossman, Semiconductor Div., Hughes Products, Hughes Aircraft Co., P. O. Box 278, Newport Beach, Calif.

Phenomenological equations for steady-state etching of silicon surfaces by diffusion across a bounding liquid film are written using the known homogeneous phase reaction mechanism of HNO_2 with HNO_3, NO_2, and NO. Minimal sets of measurements required to define, unambiguously, the solid-liquid interface reaction are discussed including contributions from semiconductor properties and oxide films. Finally it is shown that activation energies measured in terms of bulk solution concentrations can be misleading.

Abstract No. 85

Magnitude of *IR*-drop Corrections in Electrode Polarization Measurements Made with a Luggin-Haber Capillary

Sidney Barnartt, Research Labs., Westinghouse Electric Corp., Pittsburgh 35, Pa.

Measurement of electrode polarization by the direct method, using a Luggin-Haber capillary, may involve errors resulting from shielding of the electrode surface and from the *IR* drop included in the measurement. When shielding errors are eliminated, accurate corrections for the *IR* drops are readily calculated for planar electrodes. The magnitudes of these corrections are presented. The assumption involved in making similar calculations for cylindrical and spherical electrodes, and the effect of electrode radius on the magnitude of the *IR* drops, are discussed.

Abstract No. 86

(There is no Abstract No. 86)

Abstract No. 87

(There is no Abstract No. 87)

Abstract No. 88

(There is no Abstract No. 88)

ELECTRODEPOSITION

Abstract No. 89

Chemical Deposition of Palladium and Other Platinum Metals

R. N. Rhoda, Research Lab., International Nickel Co., Inc., Bayonne, N. J.

Ductile and adherent palladium may now be deposited reproducibly on a number of catalytic surfaces with ease. The development of this process is reviewed and recent work involving operating conditions and stabilizing of baths is discussed. Advantages of this method as weighed against its present limitations indicate early commercial adoption. Attempts to extend this method to other platinum metals are discussed briefly.

Abstract No. 90

'Electroless' Deposition of Gold from Aqueous Solution on Base Metals of Nickel, Iron-Nickel-Cobalt Alloys, and Gold

R. F. Walton, Glass to Metal Seals Dept., Semiconductor-Components Div., Texas Instruments, Inc., Dallas, Texas

A new solution formulation for the chemical (electroless) deposition of gold is proposed. The main constituents of this solution are potassium gold cyanide, citric acid or tartaric acid, tungstic acid, and N, N-diethylglycine sodium salt. Optimum concentrations of these constituents were determined by a statistical evaluation of the solution at four concentration levels. Investigation of such variables as immersion time, solution temperature, and pH, which affect the chemical deposition of gold from solution, enabled determination of the optimum operating conditions.

Abstract No. 91

Chemical Plating with Borohydrides

E. A. Sullivan, Research and Development Labs., Metal Hydrides Inc., Beverly, Mass.

Essentially pure nickel and cobalt have been plated on both metals and nonmetals by chemical deposition with borohydrides. The aqueous plating baths are maintained strongly alkaline (pH~12) to prevent the usual formation of transition metal borides. Deposition is initiated by warming the baths to 40°-50°C. Smooth, adherent, continuous plates of nickel and cobalt have been formed by this method, particularly on nonmetals such as ceramics, plastics, and glass.

Abstract No. 92

An Electroless Copper Plating System for 'Pure' Aluminum

S. L. Matlow, Hoffman Electronics Corp., 1001 Arden Drive, El Monte, Calif.

A method has been found for displacement plating copper onto "pure" aluminum. The aluminum is first cleaned in perchlorethylene and NaOH baths, then given a sensitizing dip in acidic $CuCl_2$. The plating, done in an ammoniacal solution of $CuCl_2$, adheres quite well and is self-fluxing on soldering. The solder bond formed by this process is found to be stronger than the aluminum itself as determined by soldering two B&S gauge No. 14 aluminum wires together with a ¼ in. overlap. When placed under tension, the solder-copper and the copper-aluminum bonds do not fail; the wire breaks instead.

Abstract No. 93

Mechanisms of Electroless Deposition of Metals on Silicon

S. L. Matlow, Hoffman Electronics Corp., 1001 Arden Drive, El Monte, Calif.

Studies on the electroless deposition of metals onto silicon indicate that there are at least four independent mechanisms by which the deposition can occur. These are (*a*) displacement plating, (*b*) displacement-replacement plating, (*c*) autocatalytic, homogeneous, and (*d*) autocatalytic-heterogeneous. These mechanisms can be distinguished by the apparent rate laws which are obeyed and by the nature of the metallic deposit. Examples of each case are discussed. Except for case (*c*) details of the mechanisms and the experimental data on which they are based are discussed.

Abstract No. 94

Immersion Coatings of the Platinum Metals

R. W. Johnson, Precious Metals Research Lab., Mond Nickel Co., Ltd., Thameshouse, Millbank, London, S.W. 1, England

(No abstract received)

Abstract No. 95

Impedance Phenomena in Molten Salts

G. J. Hills and **K. E. Johnson** (present address: University of Illinois, 314 Noyes Lab., Urbana, Ill.), Dept. of Chemistry, Imperial College, London S.W. 7, England

Impedances at polarized platinum microelectrodes in various molten salt systems (LiCl-KCl, NaBr-$AlBr_3$, $PbCl_2$, and $NaNO_3$-KNO_3) have been measured. A frequency dispersion of both resistance and capacitance was observed in all cases, but apparent double layer capacities obtained by extrapolation to infinite frequency were in agreement with some previously reported data, and of magnitudes consistent with a simple Helmholtz model. The potential dependence of capacity for NaBr-$AlBr_3$ eutectic at 225°C was also consistent with this model but that for LiCl-KCl eutectic at 400°C could only be interpreted in terms of the specific adsorption of chloride ions.

Abstract No. 96

Electrolytic Metallide Coatings in Molten Fluoride

N. C. Cook, Research Lab., General Electric Co., Schenectady, N. Y.

(No abstract received)

Abstract No. 97

Electrophoretic Deposition of Oxidation-Resistant Coatings on Molybdenum and Solid Lubricant Coatings on 304 Stainless Steel

P. F. Campbell, K. A. Gebler, and **S. J. Klack,** Vitro Labs., Div. of Vitro Corp. of America, 200 Pleasant Valley Way, West Orange, N. J.

Molybdenum disilicide-6% nickel coatings were electrophoretically deposited on molybdenum test coupons and molybdenum-0.5% titanium alloy tensile specimens. The coupons resisted oxidation in static air at temperatures up to 2600°F. The tensile specimens were thermally cycled under load at 1800°F for 67 hr before failure. Failures of the coatings at 1800°F is attributed to poor ductility, and a program is described for improving the ductility. A test apparatus is described, and results are given for the evaluation of solid lubricants, electrophoretically deposited and diffusion bonded to 304 stainless steel.

Abstract No. 98

Electrophoretic Deposition: A Versatile Coating Method

C. P. Gutierrez, J. R. Mosley, and **T. C. Wallace,** University of California, Los Alamos Scientific Lab., Los Alamos, N. M.

The technique of electrophoretic deposition has been investigated as a method for the formation of coats of various metals, oxides, carbides, and metal plus oxide composites. Comminution of powders for optimum particle size distribution and the choice of suspension medium are discussed. The importance of purity in all components is stressed in the preparation of stable suspensions with satisfactory plating characteristics. The deposition of the following materials is described in detail as examples of the versatility of the electrophoretic coating method: Re, Zr, Nb, Mo, UO_2, Nb-UO_2, Mo-UO_2, and ZrC-UC.

Abstract No. 99

Electrophoretic Deposition of Aluminum

F. Pearlstein, R. Wick, and **A. Gallaccio,** U. S. Army Ordnance, Frankford, Arsenal, Philadelphia 37, Pa.

Suspensions of aluminum flake in various organic solvents were prepared from which electrophoretic deposits were made. The best results were obtained from stable metal suspensions in acetone, chloroform, or methyl acetate. Additives were found to be effective for improving suspension stability, electrophoretic deposition rates, deposit cohesion, and throwing power. Preliminary work on the diffusion of electrophoretic deposits on steel is described.

Abstract No. 100

The Electrodeposition of Cermets

J. C. Withers, Chemistry Dept., American and Foundry Co., 1025 N. Royal St., Alexandria, Va.

Cermets can be electrodeposited by suspension of the ceramic particles in a conventional electroplating bath. The amount of ceramic codeposited is strongly dependent on the ceramic particle size, method of suspension, and the cathode current density. Cermets of chromium, nickel, cobalt, tungsten, platinum, and rhodium with Al_2O_3, $MoSi_2$, ZrO_2, and SiO_2 have been prepared for use as high-temperature materials such as coating and structural bodies.

Abstract No. 101

Effect of Organic Compounds on the Codeposition of Hydrogen with Nickel

J. R. Goodwyn (present address: Texas Eastman Co., Longview, Texas) and **T. C. Franklin,** Chemistry Dept., Baylor University, Waco, Texas

The codeposition of hydrogen with nickel has been studied in a Watts bath to which various organic compounds were added. Using a coulometric method to measure the amount of hydrogen codeposited, it has been shown that generally the concentration of additive which produced the brightest deposit also produced the deposit containing the least amount of hydrogen. A possible explanation for the curves relating the hydrogen content and the additive concentration is provided by electrode potential data.

Abstract No. 102

Mechanism of Addition Agent Reaction in Bright Nickel Deposition

S. E. Beacom and **B. J. Riley,** Research Labs., General Motors Corp., 12 Mile and Round Rds., Warren, Mich.

Organic addition agents synthesized with C-14 as well as S-35 have been used in a continuing study of the leveling phenomenon associated with the deposition of bright nickel. Analysis of deposits and the gaseous products of deposition have led to speculations concerning the breakdown of addition agents and the possible interactions which may account for the synergistic effect on leveling brought about by combinations of addition agents. Studies have shown that the amount of breakdown products is related to current density and polarization.

Abstract No. 103

Electrodeposition of Iridium

E. L. MacNamara, Pitman-Dunn Labs., U. S. Army Ordnance Arsenal, Frankford, Philadelphia 37, Pa.

The requirement of high-temperature stable protective coatings in certain military applications has focused attention on the Platinum Group Metals. The properties of iridium are of particular interest. Procedures for the aqueous deposition of rhodium, palladium, and platinum are fairly well established. The only successful method reported for the deposition of iridium utilizes molten salts. Experiments at this laboratory have demonstrated that iridium can be plated from aqueous solution containing quadrivalent iridium. Bright, tenacious deposits are obtained with a cathode efficiency of 12% at these optimum conditions; metal content, 10 g/l; current density, 20 amp/ft²; temperature, 60°C.

Abstract No. 104

Electrodeposition of Pure Copper

Sidney Barnartt, Research Labs., Westinghouse Electric Corp., Pittsburgh 35, Pa.

Previous methods of purifying copper by electrodeposition have involved alternate electroplating and melting steps. A highly simplified procedure consisting of electrodeposition from an acid sulfate solution pretreated with sodium sulfide is described. Analytical data and residual resistivity measurements at liquid helium temperatures are presented.

Abstract No. 105

Electrodeposition of High-Purity Chromium from Electrolytes Containing Fluoride or Fluosilicate

N. E. Ryan, Aeronautical Research Labs., Australian Defence Scientific Service, Dept. of Supply, Melbourne, Australia

Investigation of the variables affecting the laboratory scale deposition of chromium from chromic acid electrolytes containing fluoride or fluosilicate has enabled the optimum conditions for the production of high purity chromium (0.03-0.04 wt% oxygen, 0.0008-0.0002 wt% nitrogen) at the highest current efficiency (38-45%) to be determined. This current efficiency is much higher than the 8-10% in the chromic acid-sulfate electrolyte in which chromium of a similar grade can be produced. Continuous electrodeposition in a larger cell showed that the current efficiency in fluoride-containing electrolytes decreased progressively with time to a steady 25-30%. No explanation has been found for this decrease. After steady conditions have been achieved the advantages in current efficiency of the fluoride over the sulfate bath remains substantial.

Abstract No. 106

Measurement of Stress in Very Thin Electrodeposits

H. Watkins and **A. J. Kolk,** Electronics Div., National Cash Register Co., Hawthorne, Calif.

A modified form of the Brenner-Senderoff contractometer is described. Greater sensitivity is achieved by using jewel bearings and optical read-out. The sensitivity is sufficient to determine a 10 KSI stress in a 200A film. This instrument has been used to study the initial growth of the plating in thin electrodeposited films of iron-nickel alloys. Electron micrographs of the films were made to help in interpreting the stress data.

Abstract No. 107

Influence of Thiourea on the Deposition of Iron-Nickel Films

R. D. DeMars, IBM, Research Center, Poughkeepsie Lab., P. O. Box 390, Poughkeepsie, N. Y.

The deposition reactions of iron and nickel were studied polarographically in solutions containing the metal ion and potassium chloride and the metal ion, potassium chloride and thiourea. Analysis of the polarographic waves using Koutecky's method yielded values for the kinetic parameters, αn_a and $k^\circ_{f.b.}$, for the reduction reactions. The affect of temperature and thiourea concentration on these parameters was studied. These results can lead to predictions about the composition of films plated from similar solutions. The predictions are substantiated by a series of plated iron-nickel films.

Abstract No. 108

Influence of Substrates on Thin Magnetic Films Electrodeposited in a Magnetic Field

M. Lauriente and **F. X. McNally,** Air Arm Div., Westinghouse Electric Corp., Baltimore 3, Md.

An investigation was made of the influence that various substrates have on the magnetic properties of thin magnetic films of nominal composition 80Ni-20Fe, electrodeposited in a magnetic field. Included in the study were chemically reduced silver, copper-clad laminate, and sputtered, vacuum evaporated and fired gold. Electron micrographs and magnetic measurements were used to explain some of the unusual magnetic characteristics which were found.

Abstract No. 109

Electrodeposition of Cobalt-Molybdenum Alloys

Albertine Krohn and **T. M. Brown,** University of Toledo, Toledo, Ohio

Previous studies showed that iron-molybdenum alloys could be deposited from pyrophosphate solutions. This investigation shows that a similar bath can be used to deposit cobalt-molybdenum alloys. The addition of hydrazine sulfate to the plating bath prevents anodic oxidation of Co(II) to Co(III). It also causes an increase in the cathode current efficiency and an increase in the molybdenum content of the deposits. Efficiency is further increased by wiping the cathode during plating.

Abstract No. 110

Composition and Thickness Effects on Magnetic Properties of Electrodeposited Thin Nickel-Iron Films

Irving Wolf, Electronics Lab., General Electric Co., P. O. Box 1122, Syracuse, N. Y.

Thin films of nickel-iron have found use in the fabrication of magnetic memories for information storage in computers. These memories have the advantage of very high speed switching. Use is made of a magnetic field during deposition to align the magnetic axes in the film in one direction so that the film exhibits a single "easy" axis of magnetization. Thus an "induced" anisotropy is established. In this work, effects of thickness (500-6000Å) and composition (~60%Ni-100% Ni) on the anisotropy field, H_k, as well as on wall coercive force, H_c, and easy direction disturb, H_r, are presented. Evidence for stress interaction with magnetization and some data on substrate roughness are given.

Abstract No. 111

Effect of Plating Parameters on the Structure and Magnetic Properties of Co and Co-Ni Alloys

I. M. Croll and **H. F. Quinn,** IBM Federal System Div., Owego, N. Y.

Electrodeposited Co and Co-Ni alloys have been prepared under a wide range of plating conditions in an attempt to correlate specific bath conditions with grain orientation, grain size, and microstrain in the deposits. Striking changes in the texture of deposits prepared from simple baths have been found to occur in a critical pH region (3.5-4.0). Extreme preferred orientation has been obtained in deposits plated under combination a-c and d-c conditions. Specific ferromagnetic properties of the deposits are correlated with their structure.

Abstract No. 112

Electrodeposition of Nickel-Cobalt Alloys from the Pyrophosphate Bath

Vasanta Sree and **T. L. Rama Char,** Electrochemistry Lab., Dept. of Inorganic and Physical Chemistry, Indian Institute of Science, Bangalore, India

Nickel has been codeposited with cobalt from the pyrophosphate bath. Detailed studies on alloy composition, cathode efficiency, and potential have led to the optimum conditions for obtaining satisfactory alloy plates with 10-91% nickel. The efficiency of cast alloy anodes is quite high. X-ray patterns of the deposits show the existence of fcc and hexagonal structures. The deposit composition could be altered appreciably only by varying the metal content of the bath.

Abstract No. 113

Electrical Behavior of Passive Iron

J. L. Ord and **J. H. Bartlett,** University of Illinois, Urbana, Ill.

Make and break transients have been recorded for passive iron anodes in sulfuric acid. Capacitative effects are very important, especially when the steady state has been interrupted and the initial part of the open-circuit potential decay curve is examined. To a good approximation, the iron anode may then be represented by an equivalent circuit consisting of a large capacity shunted by a steep Tafel element. On the second portion of the decay curve, the potential decreases in an approximately linear fashion for about 100 mv to a value (Flade potential) where activation ensues.

Abstract No. 114

Anodic Properties of Nickel under Nonpassivating Conditions

Marvin Kronenberg (present address; Union Carbide Research Center, Parma, Ohio), **Ernest Yeager,** and

Frank Hovorka, Dept. of Chemistry, Western Reserve University, Cleveland, Ohio.

Anodic polarization measurements have been made on single crystal and polycrystal nickel in aqueous chloride, perchlorate, and sulfate solutions under non-passivating conditions with an electronic commutator. In the presence of a large excess of a neutral salt, the activation polarization has been found to be strongly dependent on the type of anion but substantially independent of the pH, concentration of nickel ions, and macro orientation of the electrode surface. Energies of activation have been evaluated from the temperature dependence.

Abstract No. 115

Effect of Cathode Vibration on Overpotential of Lead in $NaHPbO_2$ and in Alkaline Lead Tartrate Solutions

J. L. Griffin, Research Labs., General Motors Corp., Warren, Mich., and **L. O. Case,** University of Michigan, Ann Arbor, Mich.

Tartrate ion concentration and pH have marked, opposing effects on the overpotential at a lead cathode in alkaline lead tartrate solutions. Vibrating the lead cathode normal to its surface at 8 kc/sec generally reduced overpotentials by a greater magnitude than that calculated from the relation,

$$E_c = 2.303 \frac{RT}{zF} \ln \frac{{}^{i}L^{-i}}{{}^{i}L}$$

at apparent current densities less than limiting. Depolarization by vibration of the cathode was not complete at currents less than limiting.

Abstract No. 116

Some Observations of Copper Deposits on Single Crystals of Copper

I. B. Giron (Guest Worker from Lima, Peru) and **Fielding Ogburn,** National Bureau of Standards, Washington, D. C.

Isolated faces of copper single crystals were plated with copper from sulfuric acid-copper sulfate solutions. Metal distribution and topography of the deposits were observed, cross sections were examined microscopically, and x-ray diffraction patterns were obtained. Topography was characteristic of crystallographic plane. Deposits giving diffraction patterns showing uniform orientation were found to contain grain boundaries associated with topographic features. Over-all metal distribution showed a tendency to deviate from normal current distribution toward establishment of a more closely packed plane.

Abstract No. 117

Electroplating of Silver onto Aluminum

V. A. Nelson, Research Labs., Allis-Chalmers Manufacturing Co., Milwaukee, Wis.

A method for plating silver onto aluminum by means of a mercury immersion coating has been developed and can be used with conventional plating equipment. Corrosion, mechanical, and electrical tests show that the resulting plates are of comparative quality to present commercial plates. Aside from conventional cleaning, the new plating procedure requires only two chemical baths and one electrochemical operation. The new plating procedure permits aluminum to be silver-plated even more conveniently than copper.

Abstract No. 118

Porosity Measurements on Gold-Plated Copper

M. S. Frant, Research Div., AMP Inc., Harrisburg, Pa.

Using a chemical porosity test (in which the specimen is exposed to an ammonia-ammonium persulfate solution which attacks copper but not gold, so that the amount of copper dissolved is a measure of the porosity of the coating), the conventional cyanide gold bath and 6 proprietary baths were compared for porosity. The relationship between porosity and thickness was found to be $P = at^{-n}$, where P is chemical porosity, a varies for each bath, t is gold thickness, and n generally varies between 1.3 and 2. A linear relationship, with a slope close to 1, was found for the variation of porosity with current density in both alkaline and acid baths.

ELECTRODEPOSITION—ELECTROTHERMICS AND METALLURGY

Abstract No. 119

Prepurification Techniques: Their Role in Metal Production

R. G. Bourdeau and **E. Rose,** The Alloyd Corp., 35 Cambridge Pkwy., Cambridge 42, Mass.

The hydrogen reduction of metal halides was investigated as a technique for the production of high-purity tungsten and molybdenum. The approach used relied on the degree of purity which could be achieved in the starting materials. Particular emphasis was placed on zone refining of the metal chlorides as a means of achieving low impurity levels in the metals produced. The techniques developed, as well as the results obtained during this investigation, are presented.

Abstract No. 120

Mass and Heat Transfer during the Vapor Deposition of Metals

J. H. Oxley and **J. M. Blocher, Jr.,** Battelle Memorial Institute, Columbus 1, Ohio

A general mathematical treatment of the mass and heat transfer rates in a de Boer-Van Arkel refining cell is presented. This treatment covers one of the more practical process situations wherein the change in dimensions of the deposition surface, as a result of metal deposition, significantly affects the diffusion path between the deposit and feed and the heat lost by the deposition surface. A steady-state, counter-diffusion, nonconvective system is assumed.

Abstract No. 121

Mechanism of Hydrogen Reduction of Cuprous Iodide Vapor

C. R. Morelock and **G. W. Sears,** Research Lab., General Electric Co., Schenectady, N. Y.

A study has been made of the growth of copper whiskers by the hydrogen reduction of cuprous iodide vapor. Alternative mechanisms have been proposed involving a homogeneous vapor phase reduction and a surface catalyzed reduction at the whisker tip. A necessary consequence of the homogeneous vapor phase reaction is the existence of a highly supersaturated copper vapor. It is shown that the vapor was not appreciably supersaturated in copper vapor and that the catalytic site is probably the step associated with an axial screw dislocation in the growing whisker.

Abstract No. 122

Tungsten Coatings by Gas Phase Deposition

W. E. Reid, Jr., and **Abner Brenner,** National Bureau of Standards, Washington, D. C.

Thick, dense coatings of tungsten were obtained by passing a mixture of tungsten hexafluoride and hydrogen over an object heated to 650°C. The reaction is heterogeneous and the operating conditions are uncritical over a wide range of temperature, pressure, flow rate, and substrate materials. Plating rates of 1 mil/min have been obtained. The investigation included a study of the variation in the properties of the coating with the operating conditions.

Abstract No. 123

Fluidized-Bed Coating of Uranium Dioxide Powder Particles with Niobium and Other Elements

J. M. Blocher, Jr., N. D. Veigel, J. H. Oxley, V. M. Secrest, and **E. E. Rose,** Battelle Memorial Institute. Columbus 1, Ohio

Conditions have been established for applying uniform coatings of niobium to UO_2 powder particles by

the hydrogen reduction of $NbCl_5$ vapor in a fluidized bed of the particles. Particle size has ranged from 40 to 200 μ with coating thicknesses of from 1 to 50 μ. Factors involved in maintaining bed fluidity are discussed and preliminary data are given on the coating of UO_2 particles for pyrolytic carbon, chromium, molybdenum, tungsten, and niobium-vanadium alloys.

Abstract No. 124

Vapor Deposition of Carbon onto Sintered UO_2 Reactor Fuel

E. G. Wintucky and **E. H. Layer,** Battelle Memorial Institute, Columbus 1, Ohio

Strongly adhesive carbon coatings have been vapor deposited onto sintered UO_2 platelets by a process involving the thermal decomposition of methane gas at 1025°C. The vapor deposition is carried out in a nitrogen atmosphere at atmospheric pressure. Although the coatings are relatively thin, they are apparently nonporous as evidenced by the prevention of a UO_2-Zircaloy reaction at 862°C. The coatings are currently being used to prevent this reaction during the gas-pressure bonding of PWR-type fuel plates.

Abstract No. 125

Oxidation Resistant Silicide Coatings for Columbium and Tantalum Alloys

R. Lorenz and **A. B. Michael,** Fansteel Metallurgical Corp., North Chicago, Ill.

Two types of oxidation resistant silicide coatings on substrates of columbium and tantalum alloys were investigated. In one case, a thin layer of the alloy substrate is converted to the silicides of the alloy. For the other coating, a molybdenum-rich layer is vapor deposited on the substrate and converted to molybdenum disilicide. The silicides are formed by vapor phase reactions with silicon tetrachloride and hydrogen. The vapor phase techniques, oxidation resistances, mechanical properties, and structures are discussed.

Abstract No. 126

Diffusion Coatings of Refractory Metals on Steel

R. E. Bessey and **W. M. Kisner,** Ordnance Corps, Springfield Armory, Springfield 1, Mass.

Preliminary results of a study to determine the properties of coatings produced on steel by diffusion of refractory metals are presented. Metallic coatings of W, Ta, Mo, Nb, V, Cr, and Ti were applied by vapor deposition, the plasmarc process, or electrodeposition, and were diffused at temperatures of 900°-1100°C. The apparatus for and the method of application of niobium plate by hydrogen reduction of the pentachloride are described. Results are discussed, and photomicrographs of the diffusion layers are presented.

Abstract No. 127

Industrial Aspects of Vapor-Deposited Coatings

H. W. Schultze, The Alloyd Corp., Cambridge, Mass.

Vapor phase techniques are being investigated and utilized more widely because of recent advances in the technology and ready availability of plating compounds. Fluorides, chlorides, carbonyls and organometallics are making possible the coating of missiles components, electronic parts, nuclear fuel materials, automotive parts, and other products requiring wear resistant or high-temperature coatings. Deposition of composite parts, alloys, and semiconductor alloys is opening up new areas of utility and providing new properties for investigation.

Abstract No. 128

Testing of Vapor-Plated Aluminum Films

F. V. Schossberger and **K. D. Franson,** Armour Research Foundation, Illinois Institute of Technology, Technology Center, 10 W. 35 St., Chicago 16, Ill.

An abrasion-resistivity test was developed to study the uniformity and adhesion of vapor-deposited aluminum films. The essential idea of the abrasion resistivity test is the measurement of resistance of the metal film while its thickness is being reduced in a uniform manner. (The variation of resistance with time between two contacts on unmasked areas can be derived for an ideal model, and the effect of a number of possible departures from the ideal can be shown.) Differences in plating and annealing conditions of evaporated films were detected by this test. Experiments were performed to determine the uniformity of platings by using abrasion time as the criterion. Electron micrographs and electron diffraction diagrams were taken of the surface of the annealed metal film and of the surface of the substrate after dissolving the aluminum film. The pitted substrate surface was observed where the aluminum or the aluminum oxides reacted with the silica of the substrate.

ELECTRONICS—SEMICONDUCTORS

Abstract No. 129

Growth Steps on the Surfaces of Germanium, Silicon, and III-V Compound Dendrites

G. R. Booker, Research Labs., Westinghouse Electric Corp., Beulah Rd., Churchill Boro., Pittsburgh 35, Pa.

The methods of optical, interference, and electron microscopy have been used to study the growth steps occurring on the "flat" surfaces of germanium, silicon, and III-V compound dendrites. Variations in height, slope, form, and distribution of the steps have been observed. The role of the steps in increasing the thickness of the dendrites is discussed.

Abstract No. 130

Silicon Dendrite Studies

S. N. Dermatis, Semiconductor Dept., Westinghouse Electric Corp., Youngwood, Pa., and **J. W. Faust, Jr.,** Research Labs., Westinghouse Electric Corp., Beulah Rd., Churchill Boro., Pittsburgh 35, Pa.

Dendrites of silicon have been grown and evaluated. Some of the problems of growing silicon dendrites are discussed. Pertinent information of growth processes, segregation, and crystal perfection is given.

Abstract No. 131

Investigations of Crystal Perfection of Semiconductor Crystals by X-Ray Diffraction Microscopy

G. H. Schwuttke, General Telephone & Electronics Labs. Inc., Bayside Labs., Bayside, N. Y.

The application of x-ray diffraction microscopy to semiconductor crystals is discussed. This technique has been used successfully to reveal dislocation structures in single crystals. Now its application to detect impurities in the semiconductor lattice is described. Segregation, cluster formation, and precipitated second phases can be revealed in the diffraction image. The sensitivity of this method makes possible, for instance, the detection of oxygen concentrations in silicon as small as $10^{17}/cm^3$.

Abstract No. 132

Germanium Structural Defects—Their Cause and Effect

D. H. Lyon, Semiconductor Product Dept., General Electric Co., Syracuse, N. Y.

Line defects and point defects found in germanium single crystals are discussed. The line defects are dislocations, and the point defects are believed to be a precipitated phase. Etching methods are used to detect each type of defect by the production of characteristic etch pits, called dislocation pits and saucers. Several observations have been made regarding the origin and control of the default during crystal growth as well as possible effects on device performance.

Abstract No. 133

Horizontal Growth of Germanium Single Crystals Using a Silicon Nitride Receptacle

J. L. Porter, Sylvania Electric Products Inc., Woburn, Mass.

The use of silicon nitride as a replacement for quartz in the horizontal formation of germanium single crys-

tals is described. The complete nonwettability of the silicon nitride offers a distinct advantage and thus facilitates the formation of large cross-sectional ingots of high crystallographic perfection.

Abstract No. 134

Simple Method of Determining Crystal Perfection, II

H. K. Herglotz, Pigments Dept., E. I. du Pont de Nemours & Co., Inc., Newport, Del. (present address: Oesterreichische Stickstoffwerke, Linz/Donau, Austria)

Additional experimental results demonstrate the usefulness of the semi-quantitative scale for crystal perfection suggested in Part I of this paper. Quantitative investigations make use of the close resemblance of single crystal perfection and orientation in rolled sheets. These quantitative evaluations also show a method of increasing the reliability of the semi-quantitative scale by use of alloyed x-ray tube targets.

Abstract No. 135

Synthesis and Crystal Pulling of Gallium Arsenide in a Magnetic Crystal Puller

K. Weiser and **S. Blum,** International Business Machines Corp., Poughkeepsie, N. Y.

An all-quartz magnetic crystal puller is described in which GaAs is synthesized *in situ* and then pulled from the melt. Details of the puller are given, and the preparation of both doped and undoped material is described. Some electrical properties in the temperature range from 4° to 750°K of n- and p-type single crystals prepared in this manner are reported.

Abstract No. 136

Graded Energy Gap Alloy Semiconductor—$GaAs_xP_{1-x}$

R. E. Johnson and **George Towns,** Central Research Labs., Texas Instruments, Inc., Box 1079, Dallas, Texas

Alloy semiconductors have been prepared for possible use in thermoelectric devices. This study describes the preparation of a graded energy gap alloy semiconductor, $GaAs_xP_{1-x}$, where x varies with position along the bar. For use in high-temperature thermoelectric applications, it is possible to match the composition gradient of the alloy to the thermal gradient of the element for maximum efficiency. Evaluation results at various selenium doping levels are described.

Abstract No. 137

Preparation of Gallium Phosphide under Moderate Pressures of Phosphorus Vapor

J. F. Miller, R. C. Himes, and **H. L. Goering,** Battelle Memorial Institute, Columbus 1, Ohio

Results of experiments on the crystallization of GaP under moderate pressures of phosphorus vapor (1-5 atm) are presented. Sound transparent ingots of the compound have been prepared by the Bridgman method (2-5 atm) and by the Czochralski technique (1-3 atm). Apparatus and procedures used are described in some detail. Exploratory work on other "low-pressure" preparation methods and results of recent experiments are also discussed briefly.

Abstract No. 138

Direct Recombination in GaAs

S. Mayburg, Bayside Labs., General Telephone and Electronics Labs. Inc., Bayside, N. Y.

Experimental evidence for direct recombination in GaAs is obtained by showing a decrease in lifetime with injection level in contrast to indirect semiconductors like Ge where lifetime stays constant or increases with injection level. Stimulated emissions of electrons from the conduction to the valence band with photons of energy of the band gap have also been observed. Some consequences of direct recombination on GaAs device characteristics are discussed.

Abstract No. 139

Reactions between Gallium and Quartz

L. M. Foster and **R. A. Kramer,** Alcoa Research Labs., Aluminum Co. of America, New Kensington, Pa.

From simple thermodynamic considerations, gallium metal cannot react with silica. For the reaction $SiO_2 + Ga \rightarrow Si + Ga_2O$, the free energy change at 1273°K is +136 kcal. Because of the considerable solubility of silicon in gallium at high temperatures, however, this reaction can proceed until the silicon content reaches 1×10^{-7} atom % in the gallium. Vacuum heating experiments in all quartz environments have shown that attack on the quartz is much greater than this. The findings can be explained by the reaction $SiO_2 + Ga \rightarrow Si + Ga_2O$ and the volatilization of the gallium suboxide.

Abstract No. 140

Analysis of Impurities in Compound Semiconductors

G. D. Perkins, C. F. Robinson, and **R. K. Willardson,** Research Div., Consolidated Electrodynamics Corp., Pasadena, Calif.

Problems involved in the application of mass spectrometry to the detection and identification of impurities in compound semiconductors are discussed. A typical problem is the detection of silicon in InSb, AlSb, GaAs, or in fact any other matrix. At mass $28^{\pm 0.05}$ a quadruplet consisting of Si, Co, N_2, and C_2H_4 is usually found, and a resolution of at least 1:1600 is required. Mass spectrographic analyses are compared with impurity concentrations expected from controlled impurity additions and electrical analysis.

Abstract No. 141

Some Comments on the Electronic Structure of Group IV and III-V Semiconductors

S. L. Matlow, Hoffman Electronics Corp., El Monte, Calif.

The evidence for the structure of the valence band of the elements and intermetallics which crystallize in the diamond-cubic, zinc blend, or wurtzite structures being the $\sigma(sp^3)$ band is so extensive that the model is almost universally accepted. Except for the C and BN systems it is not clear whether the conduction band is the $\sigma^*(sp^3)$ band or the $\pi(d)$ band. Chemical, crystallographic, spectroscopic, and electrical data are presented which indicate that $\pi(d)$ model is the more accurate.

Abstract No. 142

Physical Properties of p-Type Zn_3As_2 and n-Type Cd_3As_2

W. J. Turner, A. S. Fischler, and **W. E. Reese,** Research Lab., International Business Machines Corp., Poughkeepsie, N. Y.

Zn_3As_2 and Cd_3As_2 are II-V semiconductors which obey normal valence rules. Both compounds are tetragonal with solid-solid phase transitions at elevated temperatures. The single crystals reported on were prepared in this laboratory. In general, p-type Zn_3As_2 has a room-temperature hole mobility of less than 30 cm^2 v sec. From Hall data the carrier concentration in undoped material was approximately 5×10^{17} cm^{-3} in the range 77°-300°K. Selenium appears to act as a deep level compensator when added to the melt. The intrinsic optical gap of Zn_3As_2 at 300°K is 0.93 ev. Electron Hall mobilities as high as 15,000 cm^2/v sec have been observed in n-type Cd_3As_2 with net carrier concentration of 3×10^{18} cm^{-3}. The Hall coefficient remains constant from 4° to 300°K. The room-temperature optical gap obtained from absorption measurements is 0.13 ev.

Abstract No. 143

Mobility Doping of Semiconducting Compounds

A. J. Cornish, Solid State Physics Dept., Westinghouse Research Labs., Beulah Rd., Churchill Boro., Pittsburgh 35, Pa.

Doping of semiconducting compounds is normally accomplished by adjusting carrier densities. In many

applications it appears advantageous to be able to control the mobilities of the carriers as well as the densities. Mobility doping, the adjustment of the mobilities of the carriers, is explained and illustrated.

Abstract No. 144

Thermoelectric and Crystallographic Properties of Ag_2Se

J. B. Conn and **R. C. Taylor,** Merck Sharp and Dohme Research Labs., Rahway, N. J.

Silver selenide has been prepared by fusion techniques and found to be an excellent thermoelectric material. The Seebeck coefficient, resistivity, and thermal conductivity have been measured as a function of temperature. The effect of doping with 30 different elements and compounds at different doping concentrations has been studied. The inter-relationships between the thermoelectric properties have been examined and are discussed. The crystal lattice of silver selenide has been determined, and the subcell and superstructure are elucidated.

Abstract No. 145

Properties of HgSe-HgTe Alloys

T. C. Harman, A. J. Strauss, and **L. B. Farrell,** Lincoln Lab., Massachusetts Institute of Technology, Lexington 73, Mass.

The phase diagram for the pseudo-binary system HgSe-HgTe has been determined by differential thermal analysis and x-ray diffraction techniques. Melting points measured for HgSe and HgTe are 799° and 670°C, respectively. Continuous solid solution occurs over the whole range of composition. Large single crystals of the alloys have been prepared by the Bridgman method, and data are presented on the electrical properties of the alloys as a function of composition, impurity concentration, and temperature.

Abstract No. 146

Crystal Orientation Effects Observed in Tin-Telluride Thin Films

S. H. Shortes and **D. P. Miller,** Texas Instruments Inc., P. O. Box 312, Dallas, Texas

Tin-telluride thin films may be oriented crystallographically to certain preferred directions either during evaporation or during subsequent annealment. Degree of orientation has been studied for different evaporation pressures and for effects of annealment ambient. X-ray diffraction measurements reveal either 111 or 110 crystal planes may be preferentially aligned parallel to the evaporation substrate. The results indicate that variations from stoichiometry of the film is sufficient for orientation. A tin-rich film orients to the 111 direction while a tellurium-rich film orients to the 110 direction.

Abstract No. 147

The Growth of Single Crystal Iron Ferrites by the Czochralski Method

F. H. Horn, Research Lab., General Electric Co., Schenectady, N. Y.

A procedure is described for growing iron ferrites into single crystals by pulling from the melt. An iridium crucible is used which, unlike platinum or platinum-rhodium alloys, does not react with ferrites. The melting and growing is performed in a carbon dioxide atmosphere. Problems attending this method of growth, such as the maintaining of stoichiometry and purity, are discussed.

Abstract No. 148

Titanium Thin Film Resistance for Microsystems Electronics

R. A. Quinn, Lockheed Missiles and Space Div., Lockheed Aircraft Corp., Palo Alto, Calif.

The material requirements of the MSE Program at LMSD have resulted in the development of chemical processes for the fabrication of a stable thin film resistance material. Titanium is deposited on a ceramic substrate using a fused-salt technique and then electrochemically processed to produce a thin film with stable resistance values up to 2000 ohms per square and useful from —65° to 250°C. The resistance is monitored during the conversion process so that exact values may be made. The dependency of resistance characteristics on the process control parameters is discussed.

Abstract No. 149

Some Statistics of Doping Silicon Crystals

J. W. Brownson and **R. Saphir,** Semiconductor Div., Raytheon Manufacturing Co., 150 California St., Newton 58, Mass.

The application of statistical techniques to crystal doping problems has yielded several valuable process techniques as well as improved understanding of impurity variations in silicon material. Some of the techniques which have been evolved are evaluation of raw silicon, optimization of doping, doping process control, analysis of scrap and its recovery, and the detection of unsuspected contaminants in the material. Those new techniques have quantified analytically the variations of impurity levels within and among samples of the various forms of silicon. The causes of these variations have been analyzed partially.

Abstract No. 150

Method of Evaluating Silicon Monocrystals for the Fabrication of Diffused Junction Devices

A. Ertel, ITT Components Div., International Telephone and Telegraph Corp., Clifton, N. J.

During the manufacture of silicon diffused junction devices, such as rectifiers and zener voltage regulators, changes in resistivity during high-temperature diffusion operations along with initial crystal imperfections may result in devices having reverse voltage characteristics other than those desired. A method of predetermining the quality of devices which may be expected from a given monocrystal is described. Characterization is made immediately after diffusion and prior to device fabrication. Some typical evaluations are described and discussed in detail.

Abstract No. 151

A Modified Closed Box System for the Diffusion of Boron in Silicon

R. S. Yatsko and **J. S. Kesperis,** U. S. Army Signal Research and Development Lab., Fort Monmouth, N. J.

A modified closed box diffusion system has been investigated over a wide range of conditions. Boron layers have been diffused in silicon from B_2O_3-SiO_2 sources ranging from concentrations of 0.2% B by weight to pure B_2O_3. Nonmelting source conditions have been varied to melting source conditions yielding surface concentrations ranging from 10^{19} to 10^{20} carriers/cc. Some effects of environmental atmospheres and materials are discussed. Applications to photovoltaic devices and double diffused transistors are described.

Abstract No. 152

Some Effects of Paint Strength Variation in Paint-on Diffusion of Silicon

J. E. Reynolds and **W. Gegg,** Semiconductor Products Div., Motorola Inc., 5005 E. McDowell Rd., Phoenix, Ariz.

Control of impurity diffusion of phosphorus and boron into silicon by the paint-on procedure has been investigated. Concentrations of P_2O_5 and B_2O_3 were varied over a range of 16-fold in di-methoxyethanol as the solvent. Evaluation of surface concentration, sheet resistance, and electrical parameters of assembled devices were made involving double anode diffusions of N- and P-type silicon for resistivities ranging from 0.001 to 15 ohm-cm. Several different diffusion atmospheres involving N_2, O_2, and H_2O were used. Results are given, and it is concluded that paint composition can be used for limited control of surface concentration and hence electrical parameters.

Abstract No. 153

Etching Ge with "Superoxol"

J. Bloem and **J. C. van Vessem**, Semiconductor Development Lab., N. V. Philips' Gloeilampenfabrieken, Nijmegen, Netherlands

$Hf—H_2O_2—H_2O$ is a widely used etchant for germanium single crystals. A survey is given of the influence of etch rate on the composition of the etchant and surface structures after etching (which may be important in device fabrication) are studied. A quantitative description of the experimental results is presented whereupon correlations and differences between etching and alloying can be explained.

Abstract No. 154

Dissolution of Germanium in Hydrogen Peroxide

Pei Wang and **Nino Cerniglia**, Semiconductor Div., Sylvania Electric Products Inc., Woburn, Mass.

The dissolution rate of germanium in aqueous hydrogen peroxide solution has been studied in relation to hydrogen peroxide concentration, pH, and temperature of the solution. The dissolution rate has been found independent of the hydrogen peroxide concentration, etching time, and pH of the solution over a wide range. It is strongly pH dependent above pH 5.5 at the temperature investigated (25°-70°). The reaction mechanism, which seems to have a pH dependence, is discussed.

Abstract No. 155

Sizing of Semiconductor Dice by Controlled Chemical Etching

R. B. Soper, Sylvania Electric Products Inc., Woburn, Mass.

A controlled chemical etching process by which semiconductor dice may be reduced uniformly in thickness is described. The process is particularly effective because uniformity of temperature, concentration of the etchant, and interfacial relationship are maintained. Etching so controlled yields high-quality dice of predictable thickness. An etching apparatus satisfying these conditions and capable of etching production quantities of germanium dice also is discussed.

Abstract No. 156

A New Technique for the Preparation of Flat Germanium Surfaces

M. V. Sullivan and **R. M. Finne**, Bell Telephone Labs., Inc., Murray Hill, N. J.

A new electropolishing technique has been developed which employs the gentle stirring of the electrolyte near the germanium surface being electropolished. With a "flat" stirring surface, etching on the high points is accelerated, and the germanium can be electropolished to a scratch-free mirror finish at rates of 0.02-2 mm/hr. Germanium polished in this manner has a surface roughness of less than 5×10^{-7} cm and an over all flatness of 2×10^{-4} cm over a 1 in.^{2} area.

Abstract No. 157

The Wetting of Germanium by Molten Indium

A. A. Bergh and **L. H. Holschwandner**, Bell Telephone Labs., Inc., Allentown, Pa.

Different types of unwetted areas on germanium-indium alloy junction transistors are revealed by methods of etching and sectioning for microscopic examination. Among the factors influencing wetting, the roles of indium and germanium oxides and of occluded gases are discussed. The mechanism of the formation of the different unwetted areas and ways to achieve good wetting are shown. Finally, some correlation is presented between wetting and electrical characteristics.

Abstract No. 158

Nuclear Magnetic Resonance of Water Adsorbed on Silicon

C. G. McCormick and **G. K. Walters**, Central Research Labs, Texas Instruments Inc., P. O. Box 1079, Dallas, Texas

Using the spin-echo technique, preliminary measurements have been made of the spin-lattice and spin-spin relaxation times, T_1 and T_2, of protons in water adsorbed on finely powdered silicon. For coverages up to five monolayers the values of T_1 and T_2 are found to be considerably shorter than those reported for water adsorbed on silica gel and titanium dioxide. A time dependent increase in T_2 is observed for a coverage of approximately one monolayer.

Abstract No. 159

The Retention of Water by the Real Silicon Surface

S. S. Baird, Central Research Labs., Texas Instruments Inc., P. O. Box 1079, Dallas, Texas

Crushed, low resistivity, n-type silicon was treated with various reagents, washed, and dried by several techniques. The water remaining on the surface after drying was determined titrimetrically with Karl Fisher reagent. Results are presented for surfaces prepared by treatment with various reagents commonly used in the manufacture of silicon devices, and a model of the real silicon surface is proposed to explain the observed results.

Abstract No. 160

D-C Field and Noise Measurements on Silicon

B. R. Pagel, Central Research Labs., Texas Instruments Inc., P. O. Box 1079, Dallas, Texas

D-C field and noise measurements have been made on single-type crystals of silicon. The material was high resistivity p-type, with two types of surfaces: a hydrophobic surface, freshly etched, and a hydrophilic surface, prepared by soaking in HF. The surface potential was changed with the d-c field in the presence of several ambient gases and vacuum. The results of this experiment are reported showing the variation of the excess noise generated in connection to the surface as the surface states and surface potential are changed.

Abstract No. 161

Variation with Frequency of the Transverse Impedance of Semiconductor Surfaces

F. Berz, Mullard Research Labs., Cross Oak Lane, Salfords, nr. Redhill, Surrey, England

A theoretical investigation is carried out on the variation with frequency of the transverse impedance of surface layers in semiconductors. This variation shows two main relaxation times corresponding to the filament lifetime and to the relaxation time of the fast states. Numerical examples illustrate the results. Some factors affecting the validity of the linear treatment are discussed briefly.

Abstract No. 162

Differential Capacity and Surface Conductivity of the Silicon Electrolyte Phase Boundary

R. M. Hurd and **P. T. Wrotenbery**, Texas Research Associates, 1701 Guadalupe St., Austin 1, Texas, and **Don Arnold**, Texas Instruments Inc., P. O. Box 312, Dallas, Texas

Results of measurements of the differential capacity and surface conductivity of silicon surfaces in contact with both acidic and basic electrolytes have been compared to values calculated from space charge theory. Deviations between theory and experiment have been used to draw some tentative conclusions as to the distribution of the potential drop across the space charge and through the phase boundary, and to the nature of possible surface states.

Abstract No. 163

Characteristics of the {111} Surfaces of the III-V Intermetallic Compounds, II. Effect of Surface Active Agents

M. C. Lavine, M. C. Finn, and **H. C. Gatos,** Lincoln Lab., Massachusetts Institute of Technology, Lexington 73, Mass.

Certain surface active agents (organic or inorganic) act preferentially on either the {111} surfaces terminating with group III atoms or the {111} surfaces terminating with group V atoms. The preferential action is reflected not only in the appreciable decrease of the dissolution rates of these surfaces but also in the size and geometric shape of the resulting etch figures and dislocation pits. The role of the surface active agents in the dissolution and etching behavior of the III-V intermetallic compounds is interpreted on the basis of specific adsorption and the resulting changes in the rate components parallel and vertical to the surface.

Abstract No. 164

High-Temperature Oxidation Studies on the (111) and the (111) Surfaces of InSb and GaAs

T. R. Perry, J. G. Harper, and **D. P. Miller,** Texas Instruments Inc., P. O. Box 312, Dallas, Texas

Gatos and Lavine have indicated the effect of polarity on the (111) surfaces in the etching behavior of III-V compounds. This phenomenon has been measured semi-quantitatively in InSb and GaAs. Oxidation reactions are performed in oxygen and in air and the relative reaction rates are measured by differential thermal analysis (DTA). The data indicate qualitative agreement with Gatos and Lavine. The A faces begin to oxidize at a lower temperature, but the oxidation of the B faces soon becomes the predominate one and proceeds at a much faster rate.

Abstract No. 165

Properties and Reactions of Stain Films on Silicon

Allen Gee, Semiconductor-Components Div., Texas Instruments Inc., P. O. Box 312, Dallas, Texas

Silicon when etched with certain mixtures of nitric and hydrofluoric acids is frequently stained. Such stains, consisting essentially of amorphous silicon, have been avoided in fabrication of semiconductor devices. When subjected to controlled chemical or anodic oxidation, these stain films manifest some interesting properties. Electrode potential, electrical characteristics, and luminescence associated with film-covered silicon are discussed.

Abstract No. 166

The Study of Surface Contamination of Semiconductors by Radiochemical Techniques

G. B. Larrabee, Central Research Labs., Texas Instruments Inc., P. O. Box 1079, Dallas Texas

This paper describes a recent study of the adsorption of metallic ion impurities from solution by intermetallic semiconductors. A mechanism for this adsorption is presented and an attempt is made to correlate this mechanism with silicon surface adsorption studies.

Abstract No. 167

Encapsulation of Silicon Diodes in Low Melting Glass, I. Materials and Processes

I. L. Kalnin and **A. P. Pisarchik,** Bell Telephone Labs., Inc., Murray Hill, N. J.

The dip encapsulation of diffused silicon diodes in low melting, that is below 350°C, arsenic-sulfur-thallium and arsenic-sulfur-iodine glasses is described. Glass properties, processing techniques, and encapsulation results are discussed. Limitations of this type of encapsulation depend on the flow temperature of the glass and the difference in the thermal expansivities of the materials involved. The useful temperature range of the encapsulated diodes in the particular glasses used is approximately −40° to +100°C. Glass dip encapsulation is shown to improve diode characteristics.

Abstract No. 168

Encapsulation of Silicon Diodes in Low Melting Glasses, II. Electrical Characteristics

W. F. J. Hare, Bell Telephone Labs., Inc., Murray Hill, N. J.

The initial values and the stability of the electrical characteristics of silicon diodes encapsulated in low melting arsenic-thallium-sulfur glasses has been investigated. Three hundred diodes have been monitored while under forward or reverse bias, at various temperatures, for 3000 hr. The reverse current of diodes drifts consistently upward when aged under reverse bias and downward when aged under forward bias, reaching an equilibrium in about 1000 hr. Both the initial reverse currents and these equilibria are at low values, of the order of 10^{-6} amp, as compared with values of 10^{-4} for conventional production devices. These aging characteristics are adequately explained by an ion-migration model.

ELECTROTHERMICS AND METALLURGY

Abstract No. 169

Vacuum-Evaporated Titanium Coatings

C. Horn, Materials Branch, and **D. K. Wilburn,** Physical Sciences Labs., U. S. Army Ordnance Tank-Automotive Command, 1501 Beard, Detroit 9, Mich.

Thick titanium films have been successfully vacuum evaporated on low alloy steels as corrosion resistant coatings. Typical metallized films when properly treated exhibit excellent corrosion resistant properties. Coating thicknesses in the range 0.02-1.2 mils can be achieved by means of multiple boat evaporations. Excellent coating adhesion is accomplished by means of a vacuum diffusion technique, and basis metal degassing. A photomicrographic and x-ray diffraction study of laboratory produced coatings provides supplementary information on the metallurgical and crystallographic nature of the thick evaporated titanium coatings.

Abstract No. 170

Deposition of InSb Films by Flash Evaporation

E. H. Layer, F. J. Reid, and **A. E. Austin,** Battelle Memorial Institute, Columbus 1, Ohio

A method of preparing films of InSb is described. It depends on the evaporation and condensation of indium and antimony in equal proportions by the creation of "instantaneous" evaporation conditions. These conditions were created by feeding granular InSb onto a preheated evaporation strip in vacuum. X-ray diffraction, resistivity, and Hall coefficient data show that (*a*) major phase was InSb, (*b*) crystallite sizes ranged up to approximately several thousand angstroms, and (*c*) crystallites were less pure than the single crystal material which was granulated for the evaporant.

Abstract No. 171

Vacuum Sintering of Tungsten Ingots

J. W. Pugh and **L. H. Amra,** Refractory Metals Lab., General Electric Co., Cleveland, Ohio

A furnace for vacuum sintering tungsten is described and results obtained from tungsten sintering experiments are discussed. The rate of densification at various temperatures is given special emphasis, but microstructure, hardness, fabricability and purity are also examined. Temperatures from 1800° to 3100°C and times from 0.25 to 8.00 hours were employed. Results indicate that sintered densities at least as high as 82.5% of theoretical density are necessary for successful fabrication, and that densities as high as 97.0 have structures which are readily fabricable. High temperature vacuum sintering is found to produce very pure tungsten, commensurate in this respect with the best arc cast tungsten.

Abstract No. 172

Reactions in the Niobium-Nitrogen System

W. M. Albrecht (present address: Glendale Lab., International Business Machines, Endicott, N. Y.) and **W. D. Goode,** (present address: Gaseous Diffusion Plant, Union Carbide Nuclear Co., Oak Ridge, Tenn.) Battelle Memorial Institute, Columbus 1, Ohio

The rates of the reactions of nitrogen with niobium were studied at 200°-1600°C. The reaction was found to follow a logarithmic rate law below 600°C. Above this temperature, the reaction followed a parabolic rate law with a change in mechanism between 975° and 1100°C. The diffusion coefficients and terminal solubilities of nitrogen in niobium were determined at 800°-1600°C.

Abstract No. 173

Preparation of Rare Earth Master Alloys

S. J. Morana, The Beryllium Corp., Hazleton, Pa.

A new and improved method of preparing rare earth master alloys directly from the rare earth halide salt results in the production of a rare earth master alloy comprised of the rare earth metal, the base metal, and a small percentage of magnesium. Base metal produced has included nickel, aluminum, manganese-aluminum, titanium-aluminum, copper, etc., containing 10-30% rare earth metal. Base metal selected is dependent on metal to be treated with rare earth.

INDEX TO AUTHORS

(The number in the right hand column is the abstract number used in the Technical Program and in the Abstracts)

	Abstract No.
Adlhart, Otto	5
Albrecht, W. M.	172
Ambs, W. J.	44
Amlie, R. F.	8
Amra, L. H.	171
Andrew, K. F.	46
Angstadt, R. T.	20
Annand, R. R.	59
Arnold, Don	162
Austin, A. E.	170
Baird, S. S.	159
Baker, R. A.	15
Barnartt, Sidney	65, 85, 104
Bartlett, J. H.	113
Beacom, S. E.	102
Beck, F. H.	75
Bergh, A. A.	157
Berz, F.	161
Bessey, R. E.	126
Bloem, J.	153
Blocher, J. M., Jr.	120, 123
Blum S.	135
Bode, J. D.	36
Boggs, W. E.	40, 41, 42
Bond, A. P.	2, 72
Booker, G. R.	129
Bourdeau, R. G.	119
Bourgault, P. L.	33
Boyd, P. D.	19
Brenner, Abner	122
Brodd, R. J.	11
Brown, T. M.	109
Brownson, J. W.	149
Buck, W. R., III	34
Burbank, Jeanne	16, 27
Buskirk, J. E.	19
Cahoon, N. C.	10
Campbell, J. J.	43
Campbell, P. F.	97
Caplan, D.	66
Carter, P. R.	37
Cartledge, G. H.	54
Case, L. O.	115
Cathcart, J. V.	43
Cerniglia, Nino	154
Cohen, M.	66
Conn, J. B.	144
Conway, B. E.	33, 55
Cook, N. C.	96
Copan, T. P.	46, 56
Cornish, A. J.	143
Croll, I. M.	111
Custead, W. C.	51
Davidson, A. W.	48
DeMars, R. D.	107
Dermatis, S. N.	130
Dodson, V. H.	21, 22
Dravenieks, Andrew	62
Duddy, J. C.	30
Economy, George	75
Eisen, J. B.	9
Ertel, A.	150
Evans, S.	38, 39
Falkenhagen, M.	36
Farrell, L. B.	145
Faust, J. W., Jr.	130
Feller, H. G.	73
Ferrari, H. M.	79
Finn, M. C.	163
Finne, R. M.	156
Fischler, A. S.	142
Fontana, M. G.	75
Foster, L. M.	139
Franklin, T. C.	101
Franson, K. D.	128
Frant, M. S.	45, 63, 118
Gallaccio, A.	99
Gatos, H. C.	80, 163
Gebler, K. A.	97
Gee, Allen	165
Gegg, W.	152
Giron, I. B.	116
Glicksman, R.	3, 7, 9
Goering, H. L.	137
Goode, W. D.	172
Goodrich, J. D.	58
Goodwyn, J. R.	101
Greene, N. D.	67, 68
Gregory, D. P.	77
Griffin, J. L.	115
Grossman, J. J.	84
Gulbransen, E. A.	46
Gutierrez, C. P.	98
Hackerman, Norman	58, 59
Hare, W. F. J.	168
Harman, T. C.	145
Harper, J. G.	164
Herbert, W. S.	12
Herglotz, H. K.	134
Heyn, A. N. J.	34
Hills, G. J.	95
Himes, R. C.	137
Holschwandner, L. H.	157
Horn, C.	169
Horn, F. H.	147
Hovorka, Frank	114
Hunger, H. F.	1
Hurd, R. M.	59, 162
James, W. J.	51
Jardine, R.	14
Jennings, C. W.	4
Johnson, K. E.	95
Johnson, R. E.	136
Johnson, R. W.	94
Joseph, H. M.	60
Kachik, R. H.	41
Kalnin, I. L.	167
Kass, Stanley	61
Kesperis, J. S.	151
Kisner, W. M.	126
Klack, S. J.	97
Knapp, H. R.	5
Koehler, E. L.	38, 39
Kolk, A. J.	106
Korver, M. P.	10
Kramer, R. A.	139
Krohn, Albertine	109
Kronenberg, Marvin	114
Kruger, Jerome	44, 74
Langelan, H. C.	31
Larrabee, G. B.	166
Lauriente, M.	108
Lavine, M. C.	80, 163
Layer, E. H.	124, 170
Leidheiser, Henry, Jr.	34
Lessey, S. K.	14
Lorenz, R.	125

	Abstract No.
Lozier, G. S.	9
Lyon, D. H.	132
MacNamara, E. L.	103
Makrides, A. C.	69
Marcus, R. A.	6
Marsh, G. A.	52
Matlow, S. L.	92, 93, 141
Mayburg, S.	138
McCormick, C. G.	158
McNally, F. X.	108
Meyer, R. E.	57
Michael, A. B.	125
Miller, D. P.	146, 164
Miller, J. F.	137
Morana, S. J.	173
Morehouse, C. K.	7
Morelock, C. R.	121
Mosley, J. R.	98
Mrgudich, L. N.	24
Nelson, V. A.	117
Ogburn, Fielding	116
Ord, J. L.	113
Osterwald, J.	71
Oxley, J. H.	120, 123
Pagel, B. R.	160
Panson, A. J.	47
Pawel, R. E.	43
Pearlstein, F.	99
Pellissier, G. E.	40, 41
Perkins, G. D.	140
Perry, T. R.	164
Pisarchik, A. P.	167
Pitzer, E. C.	47A
Porter, J. L.	133
Powers, R. A.	60
Pugh, J. W.	171
Quinn, H. F.	111
Quinn, R. A.	148
Radley, J. A.	78
Rajaraman, R.	45
Rama Char, T. L.	112
Reese, W. E.	142
Reid, F. J.	170
Reid, W. E., Jr.	122
Reynolds, J. E.	152
Rhoda, R. N.	89
Riddiford, A. C.	76, 77
Riggs, O. L., Jr.	64
Riley, B. J.	102
Robbins, H.	82, 83
Robinson, C. F.	140
Rose, E.	119
Rose, E. E.	123
Ruetschi, Paul	8, 13, 20
Russell, C. R.	26
Ryan, N. E.	105
Salkind, A. J.	30
Saphir, R.	149
Schaschl, E.	52
Schossberger, F. V.	128
Schultze, H. W.	127
Schwartz, B.	82, 83
Schwuttke, G. H.	131
Sears, G. W.	121
Secrest, V. M.	123
Seiger, H. N.	6
Selis, S. M.	26
Shepherd, C. M.	31
Shock, D. A.	64
Shortes, S. H.	146
Singman, D.	2
Sinnott, M. J.	79
Smith, V. V.	19
Smyth, D. M.	25
Soper, R. B.	155
Speiser, Rudolph	75
Sree, Vasanta	112
Stanley, J. S.	78
Straumanis, M. E.	50, 51
Strauss, A. J.	145
Sudbury, J. D.	64
Sullivan, E. A.	91
Sullivan, M. V.	156
Takehara, Zenichiro	29
Taylor, R. C.	144
Tompkins, C. H.	25
Towns, George	136
Trozzo, P. S.	40
Tuomi, Donald	32
Turner, D. R.	81
Turner, W. J.	142
Uhlig, H. H.	70, 71, 72, 73
van Rooyen, D.	65
van Vessem, J. C.	153
Veigel, N. D.	123
Wales, C. P.	27, 28
Wallace, T. C.	98
Walters, G. K.	158
Walton, R. F.	90
Wang, Pei	154
Watkins, H.	106
Watt, G. W.	49
Weiser, K.	135
Wick, R.	99
Wilburn, D. K.	169
Willardson, R. K.	140
Willey, A. R.	35
Willihnganz, E.	23
Wintucky, E. G.	124
Withers, J. C.	100
Wolf, Irving	110
Wrotenbery, P. T.	162
Wynne-Jones, W. F. K.	17
Yatsko, R. S.	151
Yeager, Ernest	114
Yoshizawa, Shiro	29

Guide for the Preparation and Publication of Synopses

Provided by United Nations Educational, Scientific, and Cultural Organization (UNESCO)

1. "Synopsis" is a term adopted by the Royal Society of London (in fulfillment of a recommendation of the Scientific Information Conference sponsored by the Society in 1948) and by the Unesco International Conference on Science Abstracting, 1949, to describe an author's summary of a scientific paper which is published simultaneously with the paper itself after editorial scrutiny by the editor of the journal in which it is published.

2. The purpose of a synopsis is not only to convenience the readers of the journal in which it is published, but also to reduce the cost and to expedite the work of the abstracting journals, and thus to contribute to the general improvement of informational services in the scientific field.

3. The synopsis should comprise a brief and factual summary of the contents and conclusions of the paper, a pointer to any new information which it may contain, and an indication of its relevance. It should enable the busy reader to decide more surely than he can from the mere title of the paper whether it merits his reading it.

4. The author of every paper is consequently requested to provide also a synopsis of it, in accordance with the following suggestions.

Style of Writing

5. Use complete sentences rather than a mere list of headings. Any reference to the author of the article should be in the third person. Standard rather than proprietary terms should be used. Unnecessary contractions should be avoided. It should be presumed that the reader has some knowledge of the subject but has not read the paper. The synopsis should therefore be intelligible in itself without reference to the paper. (For example, it should not cite sections or illustrations by their numerical references in the text.)

Content

6. As the title of the paper is usually read as part of the synopsis, the opening sentence should be framed accordingly so as to avoid repetition of the title. If, however, the title is not sufficiently indicative, the opening sentence should indicate the subjects covered. Usually, the beginning of a synopsis should state the objects of the investigation.

7. It is sometimes valuable to indicate the treatment of the subject by words such as: brief, exhaustive, theoretical, etc.

8. The synopsis should indicate newly observed facts, conclusions of an experiment or argument, and, if possible, the essential parts of any new theory, treatment, apparatus, technique, etc.

9. It should contain the names of any new compound, mineral species, etc., and any new numerical data such as physical constants; if this is not possible, it should draw attention to them. It is important to refer to new items and observations, even though some may be incidental to the main purpose of the paper; such information may otherwise be hidden although in fact it might be very useful.

10. When giving experimental results the synopsis should indicate the methods used; for new methods the basic principle, range of operation, and degree of accuracy should be given.

References, Citations

11. If it is necessary to refer in the synopsis to earlier work, the reference should always be given in the same form as in the paper; otherwise, references should be omitted.

12. Citations to scientific journals should be made in conformity with the standard practice of the journal for which the paper is written. (The International Conference on Science Abstracting has recommended the standard proposed by the International Organization for Standardization, Technical Committee 46, names of journals being abbreviated as in the *World List of Scientific Periodicals*.)

Length

13. The synopsis should be as concise as possible. It should only in exceptional cases exceed 200 words, so as—among other things—to permit it, when printed, to be cut out and mounted on a 3 × 5 inch card.

Publication—Language and Format

14. The International Conference on Science Abstracting has recommended that synopses be published in one of the more widely used languages, no matter what the original language of the paper, in order to facilitate its international usefulness.

15. The International Conference on Science Abstracting also commended the practice of certain journals in which all the synopses appearing in a single issue are printed together either inside the cover or with advertisments on the back in such a way that they can be cut out and mounted on index cards for reference without mutilating pages of the journal itself. For this purpose the synopses should be not more than about 4 inches wide so as to be mounted on 3 × 5 inch cards.

Current Affairs

Candidates for Society Offices, 1961

H. B. Linford

John Convey

L. I. Gilbertson

E. G. Enck

The Board of Directors of The Electrochemical Society, in accordance with the provisions of our Constitution, has approved the following Report of the Nominating Committee.

Report of Nominating Committee

The Nominating Committee takes pleasure in submitting the following nominees for election to the offices to be filled for the term starting in May 1961:

For President to Serve One Year (1961-1962)—

Henry B. Linford

For third Vice-President to Serve Three Years (1961-1964)—

John Convey
Lyle I. Gilbertson

For Treasurer to Serve Three Years (1961-1964)—

Ernest G. Enck

Each of the above candidates has been notified of his selection and has expressed his willingness to run for office and to serve if elected.

The two other Vice-Presidents, Frank L. LaQue and Walter J. Hamer, since they were elected for a three-year term, will automatically become first and second Vice-President, respectively.

(Signed)

Norman Hackerman, Chairman
F. W. Fink
A. C. Haskell
M. F. Quaely
E. M. Sherwood

The above slate will be voted on in the fall ballot-by-mail election, and the successful candidates will assume office in the spring of 1961 at the Indianapolis Meeting of the Society.

Henry B. Linford

Presidential Candidate

Henry B. Linford, professor of chemical engineering, Columbia University, New York City, was born in Logan, Utah, in 1911. He received his undergraduate training at Utah University and his graduate training at Washington State University, receiving the Ph.D. degree in physical chemistry in 1936. In 1936, he was awarded the Weston Fellowship by The Electrochemical Society and worked under the direction of Dr. Colin G. Fink at Columbia University during the school year 1936-1937. He then served as a research electrochemist at the American Smelting & Refining Co. in New Jersey.

Dr. Linford joined the staff of Columbia University as an instructor in 1941. He became an assistant professor in 1946, an associate professor in 1949, and a professor in 1952. His research interests deal principally with the field of electrochemical engineering. He and his students have published numerous articles on preparation of metal surfaces for electroplating, on electroplating, and corrosion.

A member of The Electrochemical Society since 1936, Dr. Linford served as Chairman of the New York Section in 1942 and Chairman of the Electrodeposition Division in 1948. He was National Secretary of the Society from the spring of 1949 to the spring of 1958, when he took office as Vice-President, and served concurrently as Vice-President and Interim Secretary from May 1958 to January 1959. In 1959, he was presented with a Certificate of Appreciation for his many years of distinguished service to the Society. This October, at the Houston Meeting, he will be awarded the Edward Goodrich Acheson Medal and Prize of The Electrochemical Society.

He belongs to the American Electroplaters' Society, of which he has been Director of Research Project No. 12, "Cleaning and Preparation of Metals for Electroplating," since 1949. He also is a member of Alpha Chi Sigma, Phi Lambda Upsilon, Sigma Xi, the American Chemical Society, the American Institute of Chemical Engineers, the National

Association of Corrosion Engineers, the Chemists' Club, and is a Fellow of the New York Academy of Sciences.

John Convey

Vice-Presidential Candidate

John Convey was born in 1910 in County Durham, England, the son of a coal miner, and spent the first 18 years of his life in coal-field areas. He completed his secondary school education in England, then emigrated to Canada in 1929, where his family settled in Clandonald, Alberta.

He graduated from the University of Alberta with a degree in honor physics and later obtained an M.Sc. degree in physics from the same university. After a short time as lecturer in physics on the University of Alberta staff, he proceeded to the University of Toronto, earning a doctorate degree in atomic physics in 1940.

In March 1940, Dr. Convey joined the R.C.N.V.R. and immediately was posted to Britain on loan to the Royal Navy. After Dunkirk, he was shore based and served with Scientific Research Dept. of the R.N. The next six years were spent in the Sheffield laboratories where he worked on a wide variety of problems pertaining to operational research. He was awarded the Sorby Prize in 1942 for original work in metallurgical research.

He returned to Canada in June 1946 to become associate professor of physics at the University of Toronto where he remained until 1948, when he joined the Mines Branch as chief of the Physical Metallurgy Division. Three years later, he became director of the Mines Branch.

Dr. Convey received the Blaylock Medal in 1956 from the Canadian Institute of Mining and Metallurgy for his contribution to the development of controlled atomic energy in Canada. He was honored by McMaster University at its convocation in October 1959 when he received an honorary Doctor of Science degree in recognition of his contribution to the development of metallurgy in Canada.

Since joining The Electrochemical Society in 1954, Dr. Convey has been active in its affairs. He served as Chairman of the Ontario-Quebec Section in 1954-1955 and was Honorary Chairman in 1958-1959. He was General Chairman of the Society's Fall 1958 Meeting in Otttawa.

In addition, he is a member of the American Institute of Mining and Metallurgy, and is a Fellow of the American Institute of Physics and of the Institute of Physics of Great Britain. He is Chairman of the Non-Ferrous Metals Division of the Canadian Standards Association and of the Canadian Zinc Research and Development Committee. He also is Chairman of the Materials Research Panel of the Defence Research Board and a member of the Advisory Board of the Faculty of Science at the University of Ottawa.

Lyle I. Gilbertson

Vice-Presidential Candidate

Lyle I. Gilbertson, administrative director of the Central Research Laboratories, Air Reduction Co., Inc., Murray Hill, N. J., was born in Beloit, Wis., in 1903.

He received his undergraduate training in chemistry at Augustana College in Sioux Falls, S. Dak. He obtained his Master's degree in inorganic chemistry at the University of Wisconsin and the Ph.D. degree in inorganic electrochemistry at Indiana University where as American Silver Producers Research Fellow he contributed to the development of electrodeposited silver bearings for aircraft engines.

From Carleton College, where he was instructor in chemistry, he went in 1927 to Washington State University as a member of the instructional staff of the Chemistry Dept. Until 1942, he and his students published in the general fields of electrodeposition and inorganic chemistry. In 1942, he joined the Division of War Research of Columbia University. During the war years, he was associated with the work of the Manhattan Project. He joined Air Reduction Co. in 1946 and subsequently has served as administrative manager of the Research and Engineering Dept., and director of the Murray Hill Laboratories.

Dr. Gilbertson has been active as a member of The Electrochemical Society since 1938. He was a member of the Executive Committee of the New York Metropolitan Section for a number of years, and was Chairman of the Section in 1950. He has served the Society in many capacities: as Chairman of the Membership Committee from the spring of 1950 to 1955; as a member of the Admissions Committee since the spring of 1954 (term expires 1962); and briefly as a member of the Publication Committee. On completion (in 1961) of his second term of office as Society Treasurer, he will have served on the Board of Directors for 12 years. Currently, in addition to being Treasurer, he is a member of the Electrothermics and Metallurgy Division, Chairman of the Finance Committee, a member of the Convention Advisory Committee, and of the Admissions Committee. Other memberships include the American Chemical Society, Alpha Chi Sigma, Sigma Xi, Phi Lambda Upsilon, Research Society of America, Fellow of the American Institute of Chemists, Fellow of the New York Academy of Sciences. He also is a member of the Rotary Club of Summit, N. J., and the Chemists' Club of New York.

Ernest G. Enck

Candidate for Treasurer

Ernest G. Enck was born in Lititz, Pa., in 1907. He attended Drexel Institute in Philadelphia, specializing in chemical engineering.

Mr. Enck's entire professional career until 1957 was with Foote Mineral Co. of Philadelphia, Pa. He joined the company in 1926 as chemist and became its chemical director in 1934. In 1936, he was elected a member of the Board of Directors and secretary of the company in 1942, serving in these two capacities until 1957. In 1947, he became director of procurement and, in this capacity, traveled extensively in foreign countries, especially throughout Africa.

Mr. Enck was, and still is, interested in the chemistry and metallurgy of zirconium, lithium, tungsten, strontium, and cesium, and was responsible for the development, and later production, of these products at Foote until 1947. He is the author or coauthor of numerous technical papers and articles including the chapters on Hafnium in the "Encyclopaedia of Chemical Technology" and Strontium in the latest edition of "Industrial Minerals."

He joined The Electrochemical Society in 1939. He has served the Philadelphia Section as Treasurer, Vice-Chairman, and, later, Chairman, and is a member of its Executive Committee. He was General Convention Chairman for the National Meetings held in Philadelphia in 1949 and 1959, and Finance Chairman for the 1952 Meeting. He was a member and Chairman of the Society's Acheson Award Committee, and represented his Section on the Council of Local Sections. At present, he is a member of the Investment Advisory Panel and Chairman of the Convention Advisory Committee.

Other society memberships in-

clude the American Chemical Society, American Institute of Chemical Engineers, American Institute of Mining, Metallurgical, and Petroleum Engineers, and the Canadian Institute of Mining and Metallurgy.

Currently, Mr. Enck is consulting in long-range planning and general management, and is actively interested in Boy Scouts, community planning, and conservation programs.

Abstracts of "Recent News" Papers

Presented at Electronics Division Semiconductor Symposia

Chicago Meeting
May 2-4, 1960

Effect of p-Type Germanium Arsenide Occlusions on the Resistivity of Heavily Doped n-Type Germanium

F. A. Trumbore, Bell Telephone Labs., Inc., Murray Hill, N. J.

Optical examination and thermal probing has revealed the presence of occlusions of p-type germanium arsenide in low-resistivity arsenic-doped germanium. The presence of such occlusions leads to measured resistivities which are lower than the true resistivity of the bulk germanium. It is postulated that these occlusions are the cause of the difficulties encountered in obtaining material of resistivities lower than 0.0006—0.0007 ohm-cm, thus explaining the anomalous results of five different types of crystal growth experiments.

Gallium-Arsenide Dendrites*

R. H. Moss and H. C. Nicholson, Materials Engineering Depts., Westinghouse Electric Co.

Sustained and controlled dendritic growth in gallium arsenide has been investigated. Dendrites have been reproducibly pulled from the melt using a syringe-type furnace in which the composition of the melt is determined by means of a controlled vapor pressure. Under both macroscopic and microscopic examination, the gallium-arsenide dendrites have the salient characteristics of dendrites as reported by Longini, Bennet, *et al.*

* This work was supported in part by Wright Air Development Division, U. S. Air Force.

Solubility Enhancement in GaP-Si Alloys

E. E. Loebner and I. J. Hegyi, RCA Labs., Princeton, N. J.

According to the literature, the mutual solubility of III-V compounds and elements IV is limited to about 1%.* A theory has been proposed to explain this in terms of incompatible lattice polarizations.† We have been able to grow single mixed crystals of a sphalerite structure which contain GaP and Si in amounts varying from 0 to 100 mole % provided that they were also heavily zinc doped. Zinc appears to function as a *differential charge compensator*. It seems necessary, since the amphoteric silicon self-compensates in GaP only incompletely while the solubility of P in Si somewhat exceeds that of the partly compensating Ga. Evidence for complex compound formation is discussed.

* E. Schillmann, *Z. Naturforsch.*, **11a**, 463 (1956); **12a**, 943 (1957. C. Kolm, *et al.*, *Phys. Rev.*, **108**, 965 (1957). D. A. Jenny, *et al.*, *J. Appl. Phys.*, **29**, 596 (1958).
† O. G. Folberth, *Z. Naturforsch.*, **13a**, 856 (1958).

Diffusion of Zinc, Manganese, and Sulfur in Gallium Arsenide, and a Method for Controlling the Surface Concentration

M. E. Jones and D. L. Kendall, Texas Instruments Inc., Dallas, Texas

Data and comments on the diffusion of zinc, manganese, and sulfur in gallium arsenide are presented. The unusual properties of zinc diffusion in gallium arsenide* are enlarged upon. A method for controlling the surface concentration of the diffusant using an alloy source also is presented.

* J. W. Allen and F. A. Cunnell, *Nature*, **182**, 1185 (1958).

Diffusion of Zinc in Indium Antimonide and a Novel Method of Determining Acceptor Surface Concentration

D. L. Kendall, Texas Instruments Inc., Dallas, Texas

The unusual diffusion properties of zinc in gallium arsenide* are also noted in indium antimonide. Methods for reducing these effects are reported. Comments on the diffusion mechanism are presented, which indicate the difficulty of attaining an accurate activation energy on high-surface concentration samples. A novel method of estimating acceptor surface concentration, which makes use of the temperature at which a p-type layer becomes n-type by thermal probing, is presented.

* J. W. Allen and F. A. Cunnell, *Nature*, **182**, 1185 (1958).

Low-Temperature Photoconductivity in Crystalline Boron

J. T. Breslin and G. K. Gaulé, U. S. Army Signal Research and Development Lab., Fort Monmouth, N. J.

At room temperature, crystalline B (β-rhombohedral form) shows photoconductivity from 0.45 to at least 2.4μ with a sharp peak near 0.8μ*). The spectral response does not change significantly as the material is cooled to 200°K, only rise and decay times become longer. At 80°K, however, the behavior is completely changed; sensitivity for the infrared is not present unless the material was previously illuminated with visible light. The photoconductivity caused by visible light at 80°K has an exceedingly long decay time, but it can be "quenched" by a slight temporary warm-up. A model explaining the phenomena in terms of Bube's† formulas is proposed.

* G. K. Gaulé, J. T. Breslin, J. R. Pastore, and R. A. Shuttleworth, "Proceedings of the USASRDL Conference on Boron," Plenum Press, New York, Being published.
† R. H. Bube, *J. Appl. Phys.*, **31**, 315 (1960).

Silicon Etching in the HNO_2-Rich Phase of the HF-HNO_2 System

D. L. Klein and D. J. D'Stefan, Bell Telephone Labs., Inc., Murray Hill, N. J.

The etching rate of single-crystal silicon in HF-HNO_2 was studied as a function of the ratio of the concentrated acids, stirring rate, and temperature. Over the ranges studied, the rates were proportional to these functions. For N, P, and junction samples, ranging in resistivity from 0.05 to 78 ohm-cm, no difference in etch-rate was observed. Etch-rate appears to be dependent on diffusion of the fluoride ion to the silicon surface for HF-$HNO_2 < 1$.

Capacities of the Silicon-Electrolyte Phase Boundary*

R. M. Hurd and P. T. Wrotenbery, Texas Research Associates, Austin, Texas

Capacities of the silicon-electrolyte phase boundary were measured using an impedance bridge. Both n- and p-type silicon samples of about 10 ohm-cm resistivity were studied in solutions of H_2SO_4 and KOH, with K_2SO_4 added to maintain constant ionic strength over the pH range 0-14.

In the region of minimum capacity, the experimental curves show good agreement with theoretical curves calculated on the assumption that the measured capacity corresponds entirely to the capacity of the space-charge regions. However, they show a marked deviation at positive surface potentials for p-type silicon and at negative surface potentials for n-type silicon. There is also a frequency variation associated either with the densities and time constants of surface states, or with the Helmholtz layer.

Measurements of this type on the silicon-electrolyte interface were found to be considerably more difficult than similar measurements on

the germanium-electrolyte interface. Reasons for this greater difficulty in the case of silicon arise both from the chemistry of the surface and from the semiconductor properties of the space charge region.

* Work done at Texas Research Associates under a research contract with Texas Instruments, Inc.

Surface Damage in III-V Compounds: {111} Surfaces

E. P. Warekois, M. C. Lavine, and H. C. Gatos, Lincoln Lab.,* Massachusetts Institute of Technology, Lexington 73, Mass.

It was observed that for a given cold-working treatment the depth of damage in the GaAs and In-Sb {111} surfaces terminating with group V atoms is greater than the corresponding depth of damage in the {111} surfaces terminating with group III atoms. In the absence of cold-work, the group V surfaces exhibit a somewhat greater degree of perfection than the group III surfaces. The experimental methods employed included etching and x-ray diffraction techniques.

* Operated with support from the United States Army, Navy, and Air Force.

Preparation and Properties of Silicon Films

W. J. McAleer, P. I. Pollak, and H. Kallmann, Joint Contribution from the Physics Dept. of New York University and the Electronic Chemicals Dept. of the Merck Sharp & Dohme Research Labs., Div. of Merck & Co., Inc., Rahway, N. J.

A vacuum-evaporation method for the preparation of silicon thin films from single-crystal silicon emitters of known type and resistivity is described. These films exhibit larger than band gap photovoltages which vary markedly with the wave length of the incident light and the temperature at which the measurements are made. Electron microscopic and x-ray diffraction examinations have been made in an effort to elucidate the mechanism by which these photovoltages are created.

Silicon P-N Junctions for Device Applications by Direct Deposition from a Vapor Phase

J. E. Allegretti and D. J. Shombert, Merck Sharp & Dohme Research Labs., Div. of Merck & Co., Inc., Rahway, N. J.

Large single crystals of silicon of good perfection have been grown by vapor deposition. The deposit is so pure (impurities on the order of 1 ppb) that material of a specified type and resistivity can be produced, without compensation, by controlled doping during the deposition. Thus P-N junctions can be produced containing very large electrically perfect areas.

The profiles of the type of the deposit across the junctions were studied with a one-point probe. Resistivities and resistivity gradients at the junctions were determined by measuring the capacitance of the junctions under reverse bias. Lifetimes of the deposits at the junctions were over 30 μsec.

The electrical quality of the junctions and their potential usefulness for device applications have been studied by making rectifiers from the deposited crystals. Reverse breakdown voltages above 2000 v, at reverse leakage currents of less than 5 μa, were consistently obtained; forward currents from 50 to 250 amp/cm^2 at 1 v were obtained. Demonstration rectifiers were made with 10-amp, 2000-v ratings.

Semiconductor Thin Wafer Techniques

G. W. Reutlinger, J. J. Kleimack, and C. A. Bittmann, Bell Telephone Labs., Inc., Murray Hill, N. J.

A technique has been developed to produce thin semiconductor wafers; for example, germanium wafers of 0.3 mil thickness. This is accomplished by masking and etching plateaus on one side of a semiconductor slice with the plateau diameter equal to the desired wafer diameter and the etch depth greater than the desired wafer thickness. The opposite side of the slice is then etched to reduce the wafer thickness to that desired, simultaneously separating the individual wafers.

This technique has been used to reduce the collector series resistance of microwave germanium transistors and silicon switching transistors, and to reduce the storage time of germanium switching transistors.

Anomalous Resistivity Measurements on Tunnel Diode Materials

B. Selikson, Raytheon Manufacturing Corp., Newton, Mass.

Four-point-probe resistivity measurements have been made on a number of germanium single crystal slices. Samples chosen had resistivities ranging from 2 ohm-cm to 0.0006 ohm-cm. It was observed that while the apparent resistivities rose while the slice was lapped down, the corrected resistivity held constant until a certain thickness was reached. On further reduction of thickness the corrected resistivity started to increase. The percentage increase of resistivity and the thickness at which the thickness was initiated is resistivity dependent.

Division News

E & M Symposium on Ultrafine Particles, Spring 1961

A Symposium on Ultrafine Particles is being planned by the Electrothermics and Metallurgy Division for the Spring Meeting of The Electrochemical Society to be held in Indianapolis, Ind., April 30, May 1, 2, 3, and 4, 1961.

A comprehensive program is planned with emphasis on submicron materials prepared by vaporization and condensation techniques and reactions in the vapor state.

A thorough treatment of the subject and eventual publication of the papers are the goals of the symposium. It is hoped to solicit sufficient papers for a three-day program of both invited and contributed papers. Topics on which contributions will be welcomed include:

1. Methods and techniques for the production of ultrafine particles. The mechanism of nucleation and growth of particles from the vapor state produced in various ways, including arc plasmas, amalgam techniques, shock tubes, vacuum evaporation and condensation, etc. Also, a comprehensive review paper on other methods of producing submicron powders or individual papers on comminution and chemical precipitation methods.

2. The nature of fine particles as they approach molecular dimensions. An imaginative, speculative paper would be welcomed on this subject.

3. The behavior of ultrafine particles in processes involving sintering, hot pressing, dispersion strengthening of metals, intimate blending, surface chemistry, etc.

4. Physical measurements including electron microscopy and electron diffraction techniques, particle size, surface area, and particle size distribution, chemical activity, electrical properties.

5. The properties of submicron powders of specific materials, including metals, oxides, carbides, borides, nitrides, etc.

6. Special subjects that do not fit into the above categories are also welcome.

Only those papers concerned with particles preponderantly less than 1 micron and preferably less than 0.1 micron will be considered. Papers on colloid chemistry will not be considered for this symposium.

Mr. W. E. Kuhn, Program Chairman, Research and Development Division, Carborundum Co., Niagara Falls, N. Y., would appreciate suggestions as to subjects which should be covered in the formal papers, and specialists who would be willing to submit papers.

Titles, authors' names, and abstracts in triplicate (*not exceeding*

75 words) should be sent to Mr. W. E. Kuhn and must be received at Society Headquarters, 1860 Broadway, New York 23, N. Y., *by January 2, 1961*. Abstracts should bear the notation "For Ultrafine Particle Symposium, Spring 1961," and the name of the author who will present the paper should be underlined. A complete manuscript ready for publication in all details must be given to the session chairman immediately following presentation.

An announcement and progress report will appear later in the JOURNAL, naming the session chairmen and topics to be covered by each session.

Section News

Washington-Baltimore Section

At the April meeting of the Section, the following officers were elected for the ensuing year (spring 1960-1961):

Chairman—Jerome Kruger, National Bureau of Standards, 101 N.W. Bldg., Washington 25, D. C.

Vice-Chairman—Ralph J. Brodd, National Bureau of Standards, Sec. 1.8, Washington 25, D. C.

Secretary—Sigmund Schuldiner, 3101 "P" St., S.E., Washington 20, D. C.

Treasurer—Vernon A. Lamb, National Bureau of Standards, Electrodeposition Section, Washington 25, D. C.

Councilor (2 years)—David Schlain, P. O. Box 348, College Park, Md.

Each year, the Washington-Baltimore Section awards a prize in each of the local science fairs to the best project in the field of interest of The Electrochemical Society. These awards are given to stimulate interest in electrochemistry. At the May meeting, the 1960 winners and their teachers were honored. A "Handbook of Physics and Chemistry" was presented to each of the winners: Michael Brenner, Ralph C. Spilsbury, Robert Young, Robert Ewing, Stanley J. Shapiro, and Ane Karen Olsen.

The 1959-1960 Technical Calendar of the Section was as follows:

Oct. 15, 1959—I. I. Sochard, "Thermoelectric Cooling"; R. J. Labrie, "Transference Numbers in Molten Salts."

Nov. 19, 1959—Margaret A. Reed, "Electromotive Forces and Activities in the Fused Lead Bromide-Potassium Bromide System"; C. P. Wales, "Oxide in the Silver Electrode."

Jan. 21, 1960—Bell Telephone Laboratory Films: (*a*) "Semiconductor Physics," (*b*) "The Formation of Ferromagnetic Domains." Discussion led by James H. Becker.

Feb. 18, 1960—Hugh L. Logan, "Mechanism of Stress Corrosion."

Mar. 17, 1960—Louis J. Frisco, "Effects of Tropical Exposure on the Electrical Properties of Insulating Materials"; Kurt O. Otley, "The Controlled Breakdown of Oxide Films."

Apr. 21, 1960—John K. Taylor, "Electroanalytical Chemistry."

May 19, 1960—Herman S. Preiser, "Some Studies of Cathodic Protection on Cavitation Damage"; Blanton C. Duncan, "The Permeability Characteristics of a Boundary-0.1*N* NaCl: Cellophane: 0.1*N* NaCl."

Detroit Section

The Detroit Section held its annual business meeting on May 19 at the Wayne State University Student Center. The following officials were elected for the coming year (July 1960-June 1961):

Chairman—James P. Hoare, Scientific Labs., Ford Motor Co., P. O. Box 2053, Dearborn, Mich.

1st Vice-Chairman—Seward E. Beacom, Research Labs., General Motors Corp., 12 Mile & Mound Rds., Warren, Mich.

2nd Vice-Chairman—A. Albert Johnson, Metal & Thermit Corp., 1700 E. 9 Mile Rd., Detroit 20, Mich.

Secretary-Treasurer—Ann Piken, Bendix Corp., Research Labs. Div., Southfield (Detroit), Mich.

Councilor—Frank Passal, 19757 Edinborough, Detroit 19, Mich. (Dr. Henry Brown continues as the other Councilor.)

The program consisted of a Panel Discussion on the topic "Experimental Techniques for the Measurement of Electrochemical Parameters." The participants, all members of the Detroit Section, were: John L. Griffin, Research Labs., General Motors Corp., who discussed "Ultrasonics in Electrode Processes"; A. Edward Remick, Wayne State University, who spoke on "A-C Bridge Techniques"; Seward E. Beacom, General Motors Corp., who talked on "Radiotracer Studies of Electrodeposition"; and James P. Hoare, Ford Motor Co., who explained "Electronic Current Interruption Technique."

S. E. Beacom, *Secretary-Treasurer*

Science Fair winners, left to right—Michael Brenner, Ralph C. Spilsbury, Robert Young, Robert Ewing, Stanley J. Shapiro, and Ane Karen Olsen.

Correction
Ontario-Quebec Section

In the June JOURNAL, page 135C, in the list of new officers of the Ontario-Quebec Section, the *Vice-Chairman (Membership)* was incorrectly shown as P. G. Walker, Electro Metallurgical Industries Ltd., Ottawa. This should read R. P. Bailey, Quebec Metallurgical Industries Ltd., Ottawa.

Also, under *Committeemen*, R. C. Jacobson should read R. C. Jacobsen.

News Items

A. C. Riddiford to Attend ECS Houston Meeting

A keynote speaker at the Corrosion Division's Houston Symposium on Dissolution of Metals and Semiconductors will be A. C. Riddiford of the University of Southampton, England. He will speak on the topic "Factors Influencing the Rates of Surface Processes" and also will present experimental studies of the dissolution of copper. He will attend the Fall 1960 Houston Meeting of The Electrochemical Society as guest of American Gas and Chemicals, Inc.,

manufacturers and distributors of leak-detecting fluids and devices.

A. C. Riddiford

Dr. Riddiford will remain in this country for about a month, and will visit a number of university, industrial, and Government laboratories. He will speak on various occasions on the topics. "The Rotating Disk as a Research Tool"; "Kinetics of Electrode Processes"; and "Measurement and Significance of Contact Angles."

Dr. Riddiford received the B.Sc. degree in 1948 and the Ph.D. degree in 1950, both at the University of Birmingham. Since 1951, he has been Lecturer in Physical Chemistry at the University of Southampton. His publications on metal dissolution include a critical examination of the Levich application of hydrodynamic theory to the rotating disk. He was co-editor and co-author of the monograph "Surface Phenomena in Chemistry and Biology"; more recently, he has turned to the study of electrode kinetics.

Sheriff's Mounted Posse to Perform at ECS Houston Meeting

Ballads are sung and stories are told to immortalize the hard-bitten riders who kept the peace in the early days of Texas.

Those heroes of the frontier were ordinary citizens—cowboys and storekeepers and doctors—who swung into the saddle at the sheriff's call whenever he needed a posse. The Sheriff's Mounted Posse, Inc., of Harris County is a modern replica available to the sheriff whenever help is needed. It is a nonpolitical organization composed of qualified business and professional men, citizens of Harris County, who are bound together by their common interest, horses.

The Posse is composed of about 100 members, out of which the 21-man drill team stems. The team is on a highly competitive basis and a rider must be in perfect physical condition because sharp reflexes are needed to make the fast maneuvers in the drill. Months and months of hard practice drilling are what it takes to condition both horse and rider. What started out to be a way of amusing themselves on horseback has become a very successful endeavor. The Sheriff's Mounted Posse of Harris County has performed before one-quarter of a million people in the past two years and is recognized as one of the top drill teams in the country. The fast precision exhibition and torch ride with the arena in total darkness is a feat seldom duplicated in any rodeo arena. The horses, all top quarter type, and the trailers, some of which would do justice to a caravan of a modern-day Arabian sheik, are opened and maintained personally by each of the men. Besides appearing at rodeos, the Posse has paraded on many of the main streets within a hundred-mile radius of Houston, and is always available for a civic function.

The Posse will be part of the entertainment at the Society's Fall Meeting, October 9-13, in Houston, Texas. It will perform at the Texas-Style Barbecue on Monday, October 10.

The specialty food to be served at the Barbecue will be chicken, pork ribs, and cowboy beef stew.

Newark College of Engineering Dedicates Weston Hall

Newark College of Engineering dedicated its new $1,500,000 Weston Hall on May 26 at 4:30 P.M. in special ceremonies honoring the Edward Westons, father and son, whose relationships with the 75-year-old institution date from 1885 to the present.

The seven-story building, which replaces an earlier Weston Hall built in 1893, contains 15 laboratory areas, a 417-seat lecture hall, a new library, gymnasium, and bookstore, and several offices. It is located at 367 High St., Newark.

The building is named jointly for Edward Weston, inventor, and founder of the Weston Electrical Instrument Corp., now Daystrom Inc., Weston Instruments Division, who was the first trustee to be appointed for the original Newark Technical School, and for Dr. Edward F. Weston, his son, who succeeded his father as president and later as board chairman of Weston, and who has been chairman of the NCE board since 1946.

Dr. Edward Weston, who was a Charter Member and later was elected an Honorary Member of The Electrochemical Society, was the founder, in 1928, of the Society's Weston Fellowship in Electrochemistry.

The dedicatory plaque was unveiled after Dr. Weston's response by Miss Edith Ann Hoyt, 15, a granddaughter. A reception and tour of the building closed the ceremonies.

New ECS Sustaining Members

The following recently became Sustaining Members of The Electrochemical Society:

Industro Transistor Corp., Long Island City, N. Y.

Ovitron Corp., Long Island City, N. Y.

Conference on Magnetism and Magnetic Materials, November 1960

The Sixth Annual Conference on Magnetism and Magnetic Materials will be held in New York City, November 14-17, at the New Yorker Hotel. This conference is sponsored

The Sheriff's Mounted Posse, Inc., of Harris County in action

jointly by the American Institute of Electrical Engineers and the American Institute of Physics, in cooperation with the Office of Naval Research, the Institute of Radio Engineers, and the Metallurgical Society of the A.I.M.E.

Authors should submit titles and abstracts of proposed papers by August 26 to A. M. Clogston or R. C. Fletcher, Program Chairmen, Bell Telephone Labs., Inc., Murray Hill, N. J. Further conference details can be obtained from the Local Chairman, L. R. Bickford, Jr., IBM Research Center, Yorktown Heights, N. Y.

Seminar on Rare Earth Research, Fall 1960

A seminar on "Rare Earth Research" is being planned for the fall of 1960, to be sponsored jointly by the University of California, the Dept. of Defense, and Research Chemicals. Reservations have been made for the Arrowhead Center of the University of California for October 23-26.

The program is planned as a series of five seminars. Invited papers in selected research areas are to be preprinted and distributed to all attendees. Each session will consist of a brief summary by the authors, followed by a general discussion period. Sessions are being planned for discussions in the areas of solution chemistry, ceramic systems, and metals, alloys, and intermetallics.

Because of the limited facilities, attendance will be restricted to scientists actively interested in research with the rare earth elements. Requests for information should be directed to Dr. E. V. Kleber, Research Chemicals, Burbank, Calif., or Mr. Harry Tallman, University of California, Los Angeles 24, Calif.

Boston Semiconductors Conference, August 1960

A program of 34 technical papers has been announced for the Conference on "Metallurgy of Elemental and Compound Semiconductors," to be held in the Statler Hotel, Boston, Mass., August 29-31.

The conference is sponsored by the Semiconductors Committee, Institute of Metals Division of The Metallurgical Society, and the Boston Section of the American Institute of Mining, Metallurgical, and Petroleum Engineers. The society is a constituent organization of the Institute.

Sessions will be as follows: August 29, morning and afternoon, "Esaki-Tunnel Diodes"; August 30, morning, "Dendritic Growth"; August 30, afternoon, "Vapor Growth"; August 31, morning, "Growth of Other Materials."

A bound Proceedings of the conference, including both papers and discussions, will be published with the cooperation of Interscience Publishers, Inc., New York City.

Techno Fund, Inc.

Techno Fund, Inc., a small business investment company, has been organized under the Small Business Investment Act of 1958 to serve technically based industries throughout the country.

Established under the leadership of Clyde Williams, president of Clyde Williams and Co., 50 W. Gay St., Columbus, Ohio, Techno Fund will specialize in financial aid to promising young companies and new enterprises based primarily on technology. These will include the fields of electronics, chemicals, the "new" metals, nuclear energy, instruments, and unusual mechanical products. Investments also will be made in companies engaging in real estate and land development.

In addition to supplying capital, Techno Fund will make available to small businesses a wide variety of special advisory and technical services in organization, management, finance, research programing, new product development, etc. These services will be provided through Clyde Williams and Co. which has been retained to manage Techno Fund, Inc.

Precious Metals Refining Corp. Formed by Sel-Rex

The formation of Precious Metals Refining Corp. by the principals of Sel-Rex Corp., Nutley, N. J., has been announced by Morris M. Messing, president. The new company has been situated in a separate building encompassing nearly 10,000 square feet, immediately adjacent to Sel-Rex's Executive Offices.

Notice to Members and Subscribers
(Re Changes of Address)

To insure receipt of each issue of the JOURNAL, please be sure to give us your old address, as well as your new one, when you move. Our records are filed by states and cities, not by individual names. The Post Office does not forward magazines.

A brochure listing details of the refining service, as well as a Precious Metals Refining Schedule of prices, has been prepared and may be requested directly from Precious Metals Refining Corp., 85 River Rd., Nutley 10, N. J.

New Alcoa Aluminum Smelter

The nation's newest source of primary aluminum began operations in May when Aluminum Co. of America started up its ultramodern $80,000,000 Warrick (Ind.) smelter.

The works, located 18 miles above Evansville on the Ohio River, initially is operating one of five potlines, with a capacity to produce 35,000 tons of aluminum annually. Total capacity of the facility will be 175,000 tons of metal a year, but Alcoa will not complete construction of the remaining four potlines until market demand appears likely to require the additional output.

Electric power for the Warrick works is being produced by one of three generating units at Alcoa's new 375,000-kw steam plants, fired by coal, and adjacent to the smelter. The power plant, now utilizing but one of its units at partial capacity, is being operated by the Southern Indiana Gas & Electric Co.

Squaw Creek Coal Co., which eventually will supply the power plant's fuel requirements from nearby Alcoa mining properties, is not activating its facilities while the Warrick works is at its present minimal operating rate. Interim fuel needs are being supplied on a contract basis by another area source.

The smelter, Alcoa's first in Indiana and its eighth U.S. facility for producing basic aluminum, will serve to further integrate the company's operations in that state.

Advisory Committee Recommends Expansion in Commerce Dept. Science and Technology Programs

Secretary of Commerce Frederick H. Mueller recently released the report of a Special Advisory Committee of the National Academy of Sciences on "The Role of the Department of Commerce in Science and Technology."

"Science and technology," the Committee asserts, "are playing an increasingly larger part in the industrial and business activities of the nation." The report affirms the importance and relevance of the Dept. in this modern role and appraises its programs to insure that the Dept. fulfills "its responsibilities in the

progress of the nation's science and technology."

The Committee recommends the establishment of an Office of Assistant Secretary for Science and Technology to be filled by an official "with professional and management experience in science and technology," and specific expansions of agency programs in science and technology.

Secretary Mueller designated Under Secretary of Commerce Philip A. Ray, Dept. representative on the Federal Council for Science and Technology, to initiate prompt measures for appraisal of the report and to propose plans for a course of appropriate implementation.

The ten-member committee with Dr. Mervin J. Kelly, recently retired president of the Bell Laboratories, chairman, was appointed in 1958 by Dr. Detlev W. Bronk, National Academy president, at the request of Commerce Secretary Sinclair Weeks "to evaluate the functions and operations of the Dept. of Commerce in relation to present national needs." Final examining work was completed in September 1959.

The agencies examined were: the National Bureau of Standards, the Patent Office, the Coast and Geodetic Survey, the Weather Bureau, the Office of Technical Services, the Maritime Administration, and the Bureau of Public Roads.

Seven special panels, each concentrating on one of these specific agencies, contributed recommendations. They came under five classifications summarized by the Committee as follows:

"1. Enlarged programs in science and technology. (Requiring major increases in operating budgets.)

"2. New and modern functional space equipped with adequate modern facilities. (Requiring large capital expenditures.)

"3. Increase in size of professional staffs to implement the enlarged programs.

"4. A larger fraction of professional staffs in the higher compensation grades. (To meet competition and to provide adequate incentive for attracting and holding scientists and engineers of high quality.)

"5. Creation of standing advisory committees and special study of ad hoc committees (all of great value to department operations and programs)."

The Committee also recommended:

"1. The Office of Assistant Secretary of Commerce for Science and Technology be established. The Assistant Secretary shall have professional competence in science and technology and administrative experience.

"2. The Office be provided with a small professional staff with its two senior members selected from among the Government administrative staffs in science and technology.

"3. The Assistant Secretary for Science and Technology have responsibility for the Bureau of Standards, the Patent Office, the Coast and Geodetic Survey, the Weather Bureau, the Office of Technical Services, and cognizance of the science and technology activities of the Maritime Administration and the Bureau of Public Roads."

The Committee's objectives were defined to include the study of all major elements "(1) of the needs of science and industry for services of the type the Dept. should provide, (2) of new or improved means to enable the Dept. effectively to meet these needs, and (3) of improved methods of relating the Dept.'s program on a continuing basis to dominant and changing needs of science and industry."

News from the National Bureau of Standards

Effect of Organic Compounds on Metal Fatigue

Coatings of certain polar organic compounds on specimens of steel, magnesium, and copper-beryllium alloys markedly increase fatigue strength, according to recent National Bureau of Standards experiments. The compounds found most beneficial have a carbon chain of at least 12 with a polar group at one end. Apparently, the polar group attaches to a metal surface in such a way that a tightly packed monomolecular film is formed which acts as a barrier to water and oxygen molecules.

References

1. For further technical details, *see* "The Effects of Oleophobic Films on Metal Fatigue," by H. E. Frankel, J. A. Bennett, and W. L. Holshouser, *J. Research NBS*, Sec. C (In press).
2. "Some Further Experiments on Atmospheric Action in Fatigue," by H. J. Gough and D. G. Sopwith, *J. Inst. of Metals*, **56**, 55 (1935).
3. "Hydrophobic Monolayers Adsorbed from Aqueous Solutions," by E. G. Shafrin and W. A. Zisman, *J. Colloid Sci.*, **4**, 571 (1949).

Improved Method for Measuring Abrasion Resistance of Coatings

Improvements made in a National Bureau of Standards method of measuring abrasion resistance of protective coatings have significantly increased the speed, ease, and precision of the measurements.

References

1. For further details, *see* "Improved NBS Abrasive Jet Method for Measuring Abrasion Resistance of Coatings," by A. G. Roberts, ASTM Bul. No. 244, p. 48 (1960).
2. "Abrasive Jet Method for Measuring Resistance of Organic Coatings," by A. G. Roberts, W. A. Crouse, and R. S. Pizer, ASTM Bul. No. 208, p. 36 (1955); and *NBS Tech. News Bul.*, **39**, 33 (1955). Apparatus for Measuring Abrasion Resistance, U. S. Patent No. 2,907,200, Oct. 1959.

Nitriding Phenomena in Titanium and a Titanium Alloy

In a recent National Bureau of Standards study of the effects of nitriding titanium, it was found that the nitride case continues to increase in thickness following a parabolic relationship with prolonged treatment. Nitriding a Ti-6Al-4V alloy, however, results in elongated grains extending down into the core that cause a significant reduction in impact strength. Results of this study have been applied to naval aircraft engine components.

References

1. For further technical details, *see* "Nitriding Phenomena in Titanium and the 6Al-4V Titanium Alloy," by J. R. Cuthill, W. D. Hayes, and R. E. Seebold, *J. Research NBS*, **64A**, 119 (1960).
2. "Surface Hardening of Titanium with Metalloid Elements," by R. W. Hanzel and V. Pulsifer, Armour Research Foundation Report to Watertown Arsenal, June 1, 1952 to May 31, 1953.
3. "Nitriding of Titanium with Ammonia," by J. L. Wyatt and N. J. Grant, *ASM Trans.*, **46**, 540 (1954).

Book Reviews

Gmelin's Handbuch der Anorganischen Chemie. 8th Edition. Silicon, Part B: The Element. Inorganic Compounds. System Number 15. Published by Verlag Chemie, GmbH., Weinheim/Bergstrasse, Germany, 1959. IV + LX + 923 pages, 154 figures; $135.50 paperbound, $137.00 clothbound.

The LX pages of this volume consist of the Table of Contents, with parallel columns in German and English; throughout the book, headings and subheadings are given in English in the margins. This is an extremely useful feature for many of us who read German slowly, since the paragraphs of immediate interest can be found quickly.

The preparation and properties of the element silicon occupy 226 pages. The literature is covered thoroughly only up to 1950, which may disappoint those interested in Si as a semiconductor. However, the section on preparation of extremely pure Si is carefully done, and there is an 18-page section on electrical properties of the element. Some references later than 1950 are given in the text, and a 3-page Appendix to the volume gives many book and literature references appearing from 1950-1959, dealing with Si and SiC as semiconductors, in transistors, solid-state physics, and the like. In addition, semiconductors were reviewed more thoroughly in a recent Gmelin volume on germanium.

Oxygen compounds are treated in 376 pages, with much detail about quartz and the properties which make it useful commercially. Silicic acids, silica gels, and alkali silicates are included in this section, but there is not much about the mineral silicates. Silicon halides occupy 132 pages; there has been considerable literature because of the importance of these compounds in silicone chemistry and in preparation of the pure element. Carbon compounds occupy 103 pages, much of which is devoted to the commercially important SiC. Organic compounds are deferred to Part C of the series, which contains 400 pages and describes some 9600 compounds.

Glass is not taken up in detail, but the last part of the book consists of a 55-page monograph on the glass electrode. In the earlier section on quartz, the glass and quartz electrodes are compared briefly.

In the Handbuch Volumes, of which the present one is typical, the space assigned to each topic corresponds fairly closely to the technical importance and the amount of literature extant. The books are not, however, mere reference compilations; the literature pertaining to the subject is arranged carefully, analyzed, and evaluated as critically as the necessary brevity warrants.

C. V. King

Les Réactions Electrochimiques (Les Méthodes Electrochimiques D'Analyse), by G. Charlot, J. Badoz-Lambling, and B. Tremillon. Published by Masson and Co., 120 Boulevard Saint-Germain, Paris 6, France, 1959. 396 pages, 407 figures; 6.000 fr. paperbound, 6.800 fr. clothbound.

This book is concerned with a systematic presentation of electrochemical reactions (at electrodes) and the electrochemical measurements related to chemical reactions, particularly those of interest to analytical chemists. Derivations are kept to a minimum but the text contains a large number of figures which illustrate the electrochemical phenomena.

After an introductory qualitative discussion of electrochemical reactions, five chapters are devoted to current-potential curves, including their experimental determination, and how influenced by the rate of reaction and physical factors.

In individual chapters, the authors discuss: potentiometry; amperometry; relations between potentiometry and amperometry; coulometry. Applications of current-potential curves to studies of corrosion, reduction by metals and amalgams, electrochemical catalysis, electrolytic separations, and electrochemical preparations are treated in a single chapter.

Recent electrochemical methods such as chronoamperometry, chronopotentiometry, and modifications of polarography are considered, briefly. The text concludes with an excellent chapter on solvents and their relation to electrochemical reactions.

While principles rather than analytical procedures are stressed, most chapters contain sufficient examples to illustrate the methods. Extensive references to the literature are provided.

This book supplements rather than duplicates the several excellent electroanalytical books now available. It should be of special interest to those chemists who are interested in the interpretation of electrochemical measurements and the development of analytical methods based on their utilization.

John K. Taylor

Progress in Inorganic Chemistry. Vol. I. Edited by F. Albert Cotton. Published by Interscience Publishers, Inc., New York City, 1959. 566 + IX pages; $14.50.

For a quarter of a century, inorganic chemists have been referring to the renaissance of inorganic chemistry but, until very recent years, such talk has been based more on faith and hope than on accomplished fact. No one now can deny, however, that the renaissance has taken place, and that inorganic chemistry again has become one of the major branches of the science. Evidences for this are many and varied—for example, the demand for inorganic chemists continues to far exceed the supply, even though the number of students specializing in inorganic has increased severalfold in the past decade. Courses in advanced inorganic chemistry, which a few years ago were elected by only a small handful of students, are now a "must" in every chemistry curriculum. New research areas in inorganic chemistry are being explored in both industrial and academic circles, and this activity is reflected in a rapidly increasing number of publications. Even as recently as five years ago, the appearance of a book on inorganic chemistry was a rare event which excited much comment but, within the last twelve months, at least six such books have been published in the English language. A good many more are in preparation.

There is need, in such a vigorously growing field, for a periodical publication to review the developments and present them in critical summary. Professor Cotton and the distinguished advisory board which he has assembled have undertaken the task of providing such a publication and, if the first volume can be taken as representative of what is to follow, the series "Progress in Inorganic Chemistry" will become one of great distinction. The seven topics chosen for review have been well selected, and each is discussed by a leading authority. In most cases, the authors have clearly delineated the research results which are solidly established from those which are still uncertain; here and there, a research problem is proposed. The latter, while interesting, is not necessary, for the imaginative reader

will ask himself a host of questions for which, as yet, there are no answers. Every chapter is well written and can be read with understanding (though, as Dr. Cotton points out in the introduction, not necessarily easily) by any well-trained inorganic chemist. He who has allowed his German to become rusty will have a chance to brush up on it here, for Professor Becke-Goehring's chapter "Uber Schwefel-Stickstoff Verbindungen" is written in that language. The inclusion of chapters on "Cyclopentadienyl and Arene Metal Compounds" (Wilkinson and Cotton) and "Isocyanide Complexes of Metals" (Malatesta) show how closely inorganic and organic chemistry have become intertwined; the chapter on "The Effect of Inner Orbital Splitting on the Thermodynamic Properties of Transition Metal Compounds and Coordination Complexes" (George and McClure) similarly illustrates the overlap between inorganic and theoretical chemistry. Progress in inorganic chemistry has, of course, become heavily dependent upon the use of physical methods, as is particularly illustrated by the remaining chapters "Interstitial Compounds of Graphite" (Hennig), "Metal-Ammonia Solutions" (Jolly), and "The Structure and Properties of Mixed Metal Oxides" (Ward).

The authors, as well as the editor, are to be commended upon a fine piece of work. Inorganic chemists everywhere look forward to the appearance of Vol. II.

John C. Bailar, Jr.

Electrolyte Solutions: The Measurement and Interpretation of Conductance, Chemical Potential and Diffusion in Solutions of Simple Electrolytes (Second Edition), by R. A. Robinson and R. H. Stokes. Published by Academic Press, Inc., New York City, 1959. XV + 559 pages; $11.50.

The second edition of this useful monograph contains 47 more pages than the first (1955) edition. The reader cannot fail to be impressed by the authors' success in keeping abreast of recent developments in the physical chemistry of electrolytic solutions. Two pages of the appendix, for example, present the elements of Fuoss' new treatment of ion pair formation, even though the original paper appeared only nine months before the publication date of this revised edition.

Other welcome evidence of the desire for modernization which motivated the authors in the preparation of this new edition can be found. To name a few examples: new values of the dielectric constants and viscosities of water originating recently at the National Bureau of Standards have been adopted, and the constants of the Debye-Hückel and Debye-Hückel-Onsager equations have been recalculated with their aid. The Nernst "theoretical slopes" are now given only in absolute volts, although the international ohm is retained in the listing of conductance data. The extensive tables of ionization constants are, in this reviewer's opinion, the most reliable and useful summaries available. They have been expanded considerable in the new edition by adding newly published data.

Another major change is the transfer of the discussion on the conductance of concentrated solutions to Chapter 11, whereas the treatment of dilute solutions remains in Chapter 7. This separation finds justification in the rather anomalous position of conductance theory today. We now have at our disposal a rigid theory valid for the conductance of 1:1 electrolytes up to about 0.04M, as the recent book by Fuoss and Ac-

FUNDAMENTAL RESEARCH OPPORTUNITIES

For

Physicists Chemists Metallurgists

Offered by Our

METALLURGICAL LABORATORIES

A multi-million-dollar facility new and fully equipped, Affording Challenging Opportunities in ALUMINUM, COPPER, AND BRASS

SURFACE CHEMISTS—5 positions.

Fundamental surface chemical investigations involving application of electron-optics, ellipsometry, infra-red reflectance, and other appropriate aids. Applicants should be interested in research rather than engineering approach, and should have a Ph.D. or equivalent experience.

1. Surface chemistry and physics of oxide films, including adsorption, electrochemical kinetics, electrical and optical structure, and mechanistic studies of surface film formation processes involved in finishing of metals.
2. A second position is in the same technical area, but requires less academic training and experience.
3. Investigation of chemical, electrochemical, and metallurgical factors affecting kinetics of general, localized and stress corrosion processes for aluminum and brass alloys for various environment.
4. Surface chemistry of inter-action of metal and metal oxide surfaces with organic materials. Approach is mechanistic, aimed at optimizing interactions to achieve optimum adhesion in adhesive bonding and organic coatings.
5. Surface chemistry of reactions involving molten salt and molten metals with metal and metal oxide surfaces. Objective is thorough understanding of phenomena involved in wetting and adhesion of high energy surfaces.

WELDING ENGINEER

Welding or metallurgical degree and at least 5 years experience in welding research. Will be responsible for planning, supervising, and reporting on metallurgical and physical phenomena involved in welding processes for aluminum and copper alloys. Applicants should have research rather than engineering attitude.

PHYSICISTS OR METALLURGISTS

Ph.D's or equivalent, for fundamental studies of oxidation of aluminum and copper alloys. Good background in semi-conductor technology or metal physics required, together with good first-hand knowledge of the applicable experimental techniques. Some familiarity with aluminum or brass metallurgy is desirable. Previous industrial research experience is not mandatory.

Send resume in confidence to:
E. R. PATTERSON, Salaried Employment Administrator

OLIN MATHIESON CHEMICAL CORP.

275 Winchester Ave. New Haven 4, Conn.

cascina ("Electrolytic Conductance," Interscience Publishers, Inc., New York, 1959) makes clear. There are, however, difficulties in using the Fuoss equation as a guide to conductance behavior in concentrated solutions, and it is therefore necessary to resort to an empirical approach. That this empirical approach can be not only remarkably successful but also instructive is amply evident in Chapters 7 and 11.

The new edition contains a brief discussion of Glueckauf's treatment of ionic hydration. It also presents in useful form the equations for the distribution of hydrogen ion among several bases, as, for example, the anions of a polybasic acid or amino acid complicated by "overlapping" effects.

Happily, all of the best features of the first edition, which made this monograph not only authoritative but also highly readable, have been retained.

Roger G. Bates

Properties of Matter, Third Edition, by F. C. Champion and N. Davy. Published by Philosophical Library, Inc., New York City, 1959. 336 pages; $10.00.

This book is a very valuable one to have on one's library shelf. It contains a great number of topics not usually treated within the covers of one volume. Among the major topics are Acceleration Due to Gravity, Newton's Gravitation, Elasticity, Seismic Waves, Capillarity, Surface Films, Osmotic Pressure, Diffusion, Viscosity, Kinetic Theory of Matter, and Problems of Measurement, not necessarily in this order.

The treatment of topics is mostly classical with a few minor applications of quantum theory. The treatment of the subject matter is very detailed and mathematically rigorous, although the level of mathematics is kept within the confines of a knowledge of differential equations.

Most of the topics are discussed in very great detail and include descriptions of a variety of experimental methods. To locate all of the topics that are contained in this one convenient volume, one would have to look through a great deal of literature. A few more modern topics are included in this third edition. For example, there is a section on Relativity and Gravitation and the last chapter has, in addition to a treatment of Errors of Measurement, a discussion of many topics normally considered branches of modern physics. For example, under Methods of Determining the Planck Constant, a large variety of different methods are discussed, such as the continuous x-ray spectrum method, electron diffraction method, Compton shift method, and so forth. There is also a table of the present values of atomic constants. This reviewer believes that this book will be of greater value as a reference book for the topics included, than as a text on the structure of matter.

Henry Semat

Personals

Charles A. Escoffery represented the United States in a World Symposium on Solar Energy in Rome, June 15-29, by invitation of Italy. The solar scientist is employed by International Rectifier Corp., El Segundo, Calif., as technical assistant to president Eric Lidow. The meeting of leading solar technologists of the world was sponsored by

electrochemical engineer

Excellent opportunity for man with experience in primary battery research and development to work as Assistant to Vice-President for Research and Development. Old company with new young management, expanding in sales and new development. Opportunity to work with top management with real advancement potential.

Robert Whitehill, Inc.
37 West 57th Street • NY 19

FUEL CELL RESEARCH

We have immediate openings for physical or electro chemists with experience in FUEL CELLS. Work consists of laboratory research and development on FUEL CELLS.

Recognition of achievement is readily attained in our small development group of 20 men. New air-conditioned laboratories will be ready in September of this year. Location is in Minnesota, famous for its year-round beauty and recreational opportunities.

Résumé should include educational background and complete details of fuel cell experience.

Reply to Box A-284,
c/o The Electrochemical Society, Inc.,
1860 Broadway, New York 23, N. Y.

the Italian Government during the Seventh International Conference on Electronics, Nuclear Energy, and Teleradiocinematography. Dr. Escoffery, who received his Ph.D. degree in physical chemistry from M.I.T., recently led the research team that applied photovoltaic conversion of solar energy to the world's first solar automobile for the 1960 Institute of Radio Engineers Show in New York City.

William C. Gardiner, formerly manager of research engineering, has been named manager, electrochemicals section, development department, industrial chemicals, of Olin Mathieson Chemical Corp., Niagara Falls, N. Y.

N. D. Greene, Jr., recently was presented with the 1959 Young Author Award during the 16th Annual Conference of the National Association of Corrosion Engineers in Dallas, Texas. The award is given annually for the best technical paper published during the year in the association's journal. The winning paper, "Unveiling New Concepts Concerning the Mechanism of Pitting Corrosion," summarized the results of the Corrosion Research Program conducted by the Alloy Casting Institute at Ohio State University. Dr. Greene at present is assistant professor of metallurgical engineering at Rensselaer Polytechnic Institute. **Mars G. Fontana,** professor of metallurgical engineering and research, and supervisor of the ACI research program at Ohio State University, is coauthor of the paper.

CHEMICAL ENGINEER and/or PHYSICAL CHEMIST

Electrochemical research and development in fuel cells. Ph.D. or lesser degree with equivalent experience. Send résumé to D. L. SMELSER Professional Placement Coordinator

ELECTRO-OPTICAL SYSTEMS, INC.

126 North Vinedo Avenue
Pasadena, California
MUrray 1-4671

B. H. Nicolaisen has been named director of the new development department, industrial chemicals, Olin Mathieson Chemical Corp., Niagara Falls, N. Y.

Announcements from Publishers

"Russian Journal of Physical Chemistry." Edited by R. P. Bell. Published in a cover-to-cover translation by the Chemical Society of London. Available from Cleaver-Hume Press Ltd., 31 Wright's Lane, London W.8. Price, $90.00 per year (12 monthly issues) with a 25% reduction for educational institutions.

Each number is about 112 pages in length and contains about 20 illustrated papers and many shorter notes. The English versions appear about three months after the Russian.

"International Rectifier Corporation Zener Diode Handbook," No. 2 of a series of technical handbooks. Published by International Rectifier Corp., El Segundo, Calif. 96 pages; $2.00.

"Marine Atmosphere Exposure of Galvanic Couples Involving Magnesium—STP 255." Published by American Society for Testing Materials, 1916 Race St., Philadelphia 3, Pa. 28 pages, heavy paper cover; $2.25.

"Fundamental Investigations of Electrical Power Sources, Vol. 2—Batteries," E. J. Hellund, Plasmadyne Corp., for U. S. Air Force, April 1959. Report PB 161262,* 97 pages; $2.25.

A survey of performance data, structure, power-weight ratio, and power-volume ratio of fuel cells and nuclear batteries.

"A Survey of Organic Solvents for the Electrodeposition of Plutonium," July 1959. AEC Report DP-389,* 12 pages; 50 cents.

"Metal-Water Reactions: 4—Heat Transfer Conditions During Severe Nuclear Excursions in Water Cooled Reactors," Sept. 1959. AEC Report GEAP-3204,* 19 pages; 75 cents.

* Order from Office of Technical Services, U. S. Dept. of Commerce, Washington 25, D. C.

PHYSICAL CHEMISTS

ELECTRO-CHEMISTS

CHEMICAL ENGINEERS

Important research positions are available in the Electrochemistry Laboratory at Lockheed Missiles and Space Division, located 40 miles south of San Francisco.

The laboratory is engaged in the field of electrochemical energy conversion such as fuel cell systems, and requires outstanding personnel qualified by extensive experience or academic background in the following areas:

CHEMICAL ENGINEERS
PROCESS & EQUIPMENT DESIGN
MASS TRANSFER
PILOT OPERATIONS

CHEMISTS
SOLID STATE CHEMISTRY
SURFACE CHEMISTRY
HETEROGENEOUS KINETICS
CATALYSIS
ELECTROCHEMISTRY
PHOTOCHEMISTRY

These positions provide an excellent opportunity in a young and growing new technology with an assured future. If you are experienced in work related to the above areas, you are invited to write: Research and Development Staff, Dept. H-26, 962 W. El Camino Real, Sunnyvale, Calif. U.S. citizenship or existing Department of Defense industrial security clearance required.

Lockheed
MISSILES AND SPACE DIVISION

Sunnyvale, Palo Alto,
Van Nuys, Santa Cruz,
Santa Maria, California
Cape Canaveral, Florida
Alamogordo, New Mexico
Hawaii

"Effects of Nuclear Radiation on Magnetic and Ferroelectric Materials and Quartz: A Literature Survey," S. I. Taimuty, Sanford Research Institute, for U. S. Air Force, July 1959. Report PB 161115,* 22 pages; 75 cents.

"Elevated-Temperature Mechanical Properties and Oxidation Resistance of Columbium and Its Alloys," (DMIC Memo 8), Feb. 1959. Report PB 161159,* 12 pages; 50 cents.

"Glass-Bonded Refractory Coatings for Iron- or Nickel-Base Alloys," (DMIC Memo 16), April 1959. Report PB 161166,* 19 pages; 50 cents.

"Procedures for Electroplating Coatings on Refractory Metals," (DMIC Memo 35), Oct. 1959. Report PB 161185,* 26 pages; 50 cents.

"An Investigation of Impulse-Voltage Breakdown in Polyethylene," C. R. Vail, U. S. Naval Research Lab., Dec. 1959. Report PB 151955,* 58 pages; $1.50.

"Calculation of Transient Discharges between Separating Contacts," H. E. Stauss and C. W. Klee, U. S. Naval Research Lab., Jan. 1960. Report PB 161024,* 16 pages; 50 cents.

Translation of "Fourth Soviet Conference on Electrochemistry"

A comprehensive review of progress in the field of electrochemistry in the Soviet Union was the object of the Fourth Soviet Conference on Electrochemistry. Abstracts of all the papers presented at this important conference by the most eminent Russian electrochemists were translated and published in one volume by Consultants Bureau, Inc., New York City, as soon as they were made available by the U.S.S.R. Academy of Sciences.

These abstracts were reviewed in several technical journals, and the overwhelming reaction was that they "give a fascinating and tantalizing glimpse into what is being done in Russia . . . it is obvious that the articles themselves when released and translated will be of immense value."[1]

In 1959, the U.S.S.R. Academy of Sciences published the complete texts of all the most important reports given at the Fourth Soviet Conference on Electrochemistry. The book contains over 800 pages and may well be too large and too expensive to publish under one cover. However, because of the excellence of these papers, and the necessity for English-speaking scientists to become aware of the achievements of their Russian counterparts, Consultants Bureau is making every effort to publish this volume.

The "Proceedings of the Fourth Soviet Conference on Electrochemistry" are divided into ten sections, as follows: The Electrical Double Layer. Adsorption at a Metal-Solution Boundary. General Questions on Electrochemical Kinetics and the Theory of Hydrogen Overvoltage: 16 papers; Electrolytic Reduction: 15 papers; The Mechanism of Electrochemical Oxidation Processes: 10 papers; Electrode Processes in Melts: 11 papers; The Electrodeposition of Metals: 33 papers; Metal Passivity and Chemisorbed Layers: 9 papers; Diffusion Kinetics: 7 papers; Electrochemical Processes in Non-Ferrous Metallurgy: 7 papers; Chemical Sources of Current: 13 papers; Electrolysis in the Chemical Industry: 6 papers. Each section is followed by a discussion. The reports by well-known veterans of Russian electrochemistry, such as the introductory paper by A. N. Frumkin, "Some Results of Developments in the Study of Electrochemical Reaction Mechanisms in the Last Five Years", assure the reader of the high quality of the entire collection.

Until such time as publication of the complete Proceedings becomes feasible, translations of individual papers are being offered at the rate of $4.00 per Russian page (about half the normal cost for such custom translation). All diagrams and tables are integrated with the text, and the translation is done by bilingual scientists. The complete table of contents is available from Consultants Bureau on request, and the translated and typed articles are supplied with a minimum of delay.

[1] *This Journal*, **106**, 35C (1959).

* Order from Office of Technical Services, U. S. Dept. of Commerce, Washington 25, D. C.

Employment Situations

Positions Wanted

Metallurgist—B.S. degree in mathematics, physics, chemistry. Graduate work in mathematics and spectrographic analysis. Three and one half years' experience in spectrographic, metallographic, physical controls of transistor, die cast, and punch press parts. Desires responsible position in production or research. *Reply to Box 368, c/o The Electrochemical Society, 1860 Broadway, New York 23, N. Y.*

Electrochemical Engineer—12 years' R & D experience in almost all phases of electrochemical processes. Extensive theoretical knowledge with ability in practical application. Combine the above with curiosity, resourcefulness, and creativity. Highly adaptable and capable. Supervisory experience. Desires position of considerable responsibility where experience and abilities will be most valuable. Prefers West Coast location, but will go anywhere. Salary, $11-12,000. *Reply to Box 369, c/o The Electrochemical Society, 1860 Broadway, New York 23, N. Y.*

Positions Available

Chemists and Chemical Engineers—We need physical, organic, and inorganic chemists and chemical engineers to carry out Engineering and development work in the rapidly growing power sources field. Research & Development center located in Minneapolis near University of Minnesota. Battery experience preferred but not required.

Send résumés to: J. W. Baxter, Employee & Labor Relations, Gould-National Batteries, Inc., E. 1326 First National Bank Bldg., St. Paul 1, Minnesota.

Physicists—Energy conversion (fuel cells, etc.) enterprise forming. If you have Ph.D. and related experience and seek association with equity in a new enterprise (no investment), write history of education and experience to *Box A-285, c/o The Electrochemical Society, 1860 Broadway, New York 23, N. Y.*

Advertiser's Index

E. I. du Pont de Nemours & Company (Inc.) 162C-163C
Eagle-Picher Company 165C
Electro-Optical Systems, Inc. 207C
Great Lakes Carbon Corp., Electrode Division ..... Cover 2
Lockheed Missiles & Space Division 207C
Olin Mathieson Chemical Corporation 205C
E. H. Sargent & Company 168C
Stackpole Carbon Company 167C
Robert Whitehill, Inc. 206C

The Electrochemical Society

Patron Members

Aluminum Co. of Canada, Ltd., Montreal, Que., Canada

International Nickel Co., Inc., New York, N. Y.

Olin Mathieson Chemical Corp., Niagara Falls, N. Y.
- Industrial Chemicals Div., Research and Development Dept.

Union Carbide Corp.
- Divisions:
  - Union Carbide Metals Co., New York, N. Y.
  - National Carbon Co., New York, N. Y.

Westinghouse Electric Corp., Pittsburgh, Pa.

Sustaining Members

Air Reduction Co., Inc., New York, N. Y.

Ajax Electro Metallurgical Corp., Philadelphia, Pa.

Allen-Bradley Co., Milwaukee, Wis.

Allied Chemical & Dye Corp.
- General Chemical Div., Morristown, N. J.
- Solvay Process Div., Syracuse, N. Y. (3 memberships)

Allied Research Products, Inc., Detroit, Mich.

Alloy Steel Products Co., Inc., Linden, N. J.

Aluminum Co. of America, New Kensington, Pa.

American Metal Climax, Inc., New York, N. Y.

American Potash & Chemical Corp., Los Angeles, Calif. (2 memberships)

American Smelting and Refining Co., South Plainfield, N. J.

American Zinc Co. of Illinois, East St. Louis, Ill.

American Zinc, Lead & Smelting Co., St. Louis, Mo.

American Zinc Oxide Co., Columbus, Ohio

M. Ames Chemical Works, Inc., Glens Falls, N. Y.

Auto City Plating Company Foundation, Detroit, Mich.

Basic Inc., Maple Grove, Ohio

Bell Telephone Laboratories, Inc., New York, N. Y. (2 memberships)

Bethlehem Steel Co., Bethlehem, Pa. (2 memberships)

Boeing Airplane Co., Seattle, Wash.

Burgess Battery Co., Freeport, Ill. (4 memberships)

Canadian Industries Ltd., Montreal, Que., Canada

Carborundum Co., Niagara Falls, N. Y.

Catalyst Research Corp., Baltimore, Md.

Ciba Pharmaceutical Products, Inc., Summit, N. J.

Columbian Carbon Co., New York, N. Y.

Columbia-Southern Chemical Corp., Pittsburgh, Pa.

Consolidated Mining & Smelting Co. of Canada, Ltd., Trail, B. C., Canada (2 memberships)

Continental Can Co., Inc., Chicago, Ill.

Cooper Metallurgical Associates, Cleveland, Ohio

Corning Glass Works, Corning, N. Y.

Diamond Alkali Co., Painesville, Ohio (2 memberships)

Dow Chemical Co., Midland, Mich.

Wilbur B. Driver Co., Newark, N. J. (2 memberships)

E. I. du Pont de Nemours & Co., Inc., Wilmington, Del.

Eagle-Picher Co., Chemical Div., Joplin, Mo.

Eastman Kodak Co., Rochester, N. Y.

Thomas A. Edison Research Laboratory, Div. of McGraw-Edison Co., West Orange, N. J.

Electric Auto-Lite Co., Toledo, Ohio
- C & D Division, Conshohocken, Pa.

Electric Storage Battery Co., Yardley, Pa.

Englehard Industries, Inc., Newark, N. J. (2 memberships)

The Eppley Laboratory, Inc., Newport, R. I. (2 memberships)

Erie Resistor Corp., Erie, Pa.

Exmet Corp., Tuckahoe, N. Y.

Fairchild Semiconductor Corp., Palo Alto, Calif.

Food Machinery & Chemical Corp.
- Becco Chemical Div., Buffalo, N. Y.
- Westvaco Chlor-Alkali Div., South Charleston, W. Va.

Foote Mineral Co., Paoli, Pa.

Ford Motor Co., Dearborn, Mich.

General Electric Co., Schenectady, N. Y.
- Chemistry & Chemical Engineering Component, General Engineering Laboratory
- Chemistry Research Dept.
- General Physics Research Dept.
- Metallurgy & Ceramics Research Dept.
- Aircraft Accessory Turbine Dept., West Lynn, Mass.

General Instrument Corp., Newark, N. J.

(Sustaining Members cont'd)

General Motors Corp.
Delco-Remy Div., Anderson, Ind.
Guide Lamp Div., Anderson, Ind.
Research Laboratories Div., Detroit, Mich.
General Transistor Corp., Jamaica, N. Y.
Gillette Safety Razor Co., Boston, Mass.
Globe-Union, Inc., Milwaukee, Wis.
Gould-National Batteries, Inc.,
Minneapolis, Minn.
Grace Electronic Chemicals, Inc.,
Baltimore, Md.
Great Lakes Carbon Corp., New York, N. Y.
Hanson-Van Winkle-Munning Co.,
Matawan, N. J. (2 memberships)
Harshaw Chemical Co., Cleveland, Ohio
(2 memberships)
Hercules Powder Co., Wilmington, Del.
Hill Cross Co., Inc., New York, N. Y.
Hoffman Electronics Corp., El Monte, Calif.
Hooker Chemical Corp., Niagara
Falls, N. Y. (3 memberships)
Hughes Aircraft Co., Culver City, Calif.
Industro Transistor Corp.,
Long Island City, N. Y.
International Business Machines Corp.,
Poughkeepsie, N. Y.
International Minerals & Chemical
Corp., Skokie, Ill.
ITT Laboratories, Nutley, N. J.
Jones & Laughlin Steel Corp.,
Pittsburgh, Pa.
K. W. Battery Co., Skokie, Ill.
Kaiser Aluminum & Chemical Corp.
Div. of Chemical Research,
Permanente, Calif.
Div. of Metallurgical Research,
Spokane, Wash.
Kennecott Copper Corp., New York, N. Y.
Keokuk Electro-Metals Co., Keokuk, Iowa
Libbey-Owens-Ford Glass Co., Toledo, Ohio
M. & C. Nuclear, Inc., Attleboro, Mass.
Mallinckrodt Chemical Works, St. Louis, Mo.
P. R. Mallory & Co., Indianapolis, Ind.
McGean Chemical Co., Cleveland, Ohio
Merck & Co., Inc., Rahway, N. J.
Metal & Thermit Corp., Detroit, Mich.
Minnesota Mining & Manufacturing Co.,
St. Paul, Minn.
Monsanto Chemical Co., St. Louis, Mo.
Motorola, Inc., Chicago, Ill.
National Cash Register Co., Dayton, Ohio
National Lead Co., New York, N. Y.
National Research Corp., Cambridge, Mass.
National Steel Corp., Weirton, W. Va.
New York Air Brake Co., Kinney Vacuum
Div., Boston, Mass.
Northern Electric Co., Montreal, Que.,
Canada
Norton Co., Worcester, Mass.
Olin Mathieson Chemical Corp.,
Research & Engineering Operations,
Energy Div., New Haven, Conn.
Ovitron Corp., Long Island City, N. Y.
Peerless Roll Leaf Co., Inc., Union City, N. J.
Pennsalt Chemicals Corp.,
Philadelphia, Pa.
Phelps Dodge Refining Corp., Maspeth, N. Y.
Philco Corp., Philadelphia, Pa.
Philips Laboratories, Inc., Irvington-on-
Hudson, N. Y.
Pittsburgh Metallurgical Co., Inc.,
Niagara Falls, N. Y.
Poor & Co., Promat Div., Waukegan, Ill.
Potash Co. of America,
Carlsbad, N. Mex.
Radio Corp. of America
Tube Div., Harrison, N. J.
RCA Victor Record Div., Indianapolis,
Ind.
Ray-O-Vac Co., Madison, Wis.
Raytheon Manufacturing Co.,
Waltham, Mass.
Reynolds Metals Co., Richmond, Va.
(2 memberships)
Rheem Semiconductor Corp.,
Mountain View, Calif.
Schering Corporation, Bloomfield, N. J.
Shawinigan Chemicals Ltd., Montreal, Que.,
Canada
Speer Carbon Co.
International Graphite & Electrode
Div., St. Marys, Pa. (2 memberships)
Sprague Electric Co., North Adams, Mass.
Stackpole Carbon Co., St. Marys, Pa.
Stauffer Chemical Co., New York, N. Y.
Sumner Chemical Co., Div. of
Miles Laboratories, Inc., Elkhart, Ind.
Sylvania Electric Products Inc., Bayside,
N. Y. (2 memberships)
Tennessee Products & Chemical Corp.,
Nashville, Tenn.
Texas Instruments, Inc., Dallas, Texas
Three Point Four Corp., Yonkers, N. Y.
Titanium Metals Corp. of America,
Henderson, Nev.
Tung-Sol Electric Inc.,
Newark, N. J.
Udylite Corp., Detroit, Mich.
(4 memberships)
Universal-Cyclops Steel Corp.,
Bridgeville, Pa.
Upjohn Co., Kalamazoo, Mich.
Victor Chemical Works, Chicago, Ill.
Western Electric Co., Inc., Chicago, Ill.
Wyandotte Chemicals Corp.,
Wyandotte, Mich.
Yardney Electric Corp., New York, N. Y.